# Binding partners of histone H2A variant and their molecular implications in carcinogenesis

**By**

**Divya Reddy Velga**

[LIFE09201104011]

**Tata Memorial Centre**

**Mumbai**

*A thesis submitted to the*

*Board of Studies in Life Sciences*

*In partial fulfillment of requirements*

*for the Degree of*

## DOCTOR OF PHILOSOPHY
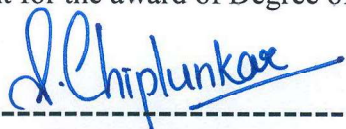
*of*

## HOMI BHABHA NATIONAL INSTITUTE

**September, 2017**

# Homi Bhabha National Institute
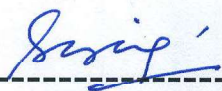
## Recommendations of the Viva Voce Committee

As members of the Viva Voce Committee, we certify that we have read the dissertation prepared by Ms. Divya Reddy Velga entitled "Binding partner of histone H2A variant and its molecular implications in carcinogenesis" and recommend that it may be accepted as fulfilling the thesis requirement for the award of Degree of Doctor of Philosophy.

_____ 18/9/17 _____

Chairman – Dr. S.V. Chiplunkar                    Date:

_____ 18/9/17 _____

Guide/Convener – Dr. Sanjay Gupta                    Date:

_____ 18/9/17 _____

External Examiner – Dr. M.K. Thakur                    Date:

_____ 18/9/17. _____

Member – Dr. Rukmini Govekar                    Date:

_____ 18/9/17 _____

Member – Dr. Sanjeev Waghmare                    Date:

_____ 18/9/17 _____

Invitee – Dr. Sanjeev Galande                    Date:

---

Final approval and acceptance of this thesis is contingent upon the candidate's submission of the final copies of the thesis to HBNI.

I hereby certify that I have read this thesis prepared under my direction and recommend that it may be accepted as fulfilling the thesis requirement.

Date:
Place: Navi Mumbai                                   Dr. Sanjay Gupta   18/9/17
                                                     Guide

# STATEMENT BY AUTHOR

This dissertation has been submitted in partial fulfillment of requirements for an advanced degree at Homi Bhabha National Institute (HBNI) and is deposited in the Library to be made available to borrowers under rules of the HBNI.

Brief quotations from this dissertation are allowable without special permission, provided that accurate acknowledgement of source is made. Requests for permission for extended quotation from or reproduction of this manuscript in whole or in part may be granted by the Competent Authority of HBNI when in his or her judgment the proposed use of the material is in the interests of scholarship. In all other instances, however, permission must be obtained from the author.

Divya Reddy Velga

# DECLARATION

I, hereby declare that the investigation presented in the thesis has been carried out by me. This work is original and has not been submitted earlier as a whole or in part for a degree/ diploma at this or any other Institution / University.

Divya Reddy Velga

# LIST OF PUBLICATIONS ARISING FROM THE THESIS

## Journal

1. Divya Reddy, Bharat Khade, Riddhi Pandya and Sanjay Gupta. A novel method for isolation of histones from serum and its implications in therapeutics and prognosis of solid tumors. Clinical Epigenetics (2017), 9:30

2. Monica Tyagi*, Divya Reddy*, and Sanjay Gupta. Genomic characterization and dynamic methylation of promoter facilitates transcriptional regulation of H2A variants, H2A.1 and H2A.2 in various pathophysiological states of hepatocyte. The International Journal of Biochemistry & Cell Biology. (2017), 85:15-24. * equal contribution.

3. Divya Reddy and Sanjay Gupta. Histone variant H3.3 and its future prospects in cancer clinic. Journal of Radiation and Cancer Research. (2017) 8:77-81

4. Divya Reddy, Saikat Bhattacharya and Sanjay Gupta. Histone Chaperones: Functions beyond Nucleosome Deposition. Advances in Biosciences and Biotechnology, 2014, May, 5, 546-556.

5. Divya Reddy, Saikat Bhattacharya, Vinod Jani, Riddhi Pandya, Uddhavesh Sonavane, Rajendra Joshi and Sanjay Gupta. Biochemical and Biophysical Characterization of higher oligomeric structure of Rat Nucleosome Assembly Protein 1. **(Manuscript Communicated)**.

6. Divya Reddy, Saikat Bhattacharya, Sanjay Gupta. Downregulation of Histone H3 Variant H3.3 Contributes to the Development of Hepatocellular Carcinoma. **(Manuscript Communicated)**.

## Chapter in books

1. Monica Tyagi, Shafqat A Khan, Saikat Bhattacharya, Divya Reddy, Ajit K Sharma, Bharat Khade, Sanjay Gupta. Techniques to Access Histone Modifications and Variants in Cancer. 'Cancer Epigenetics: Risk Assessment, Diagnosis, Treatment, and Prognosis', *Methods in Molecular Biology Series* (Humana Press/Springer) 2015. 251-272.

# Conferences

1. Presented poster entitled "Histone H3 variants and their respective chaperones regulate cancer specific phenotypic changes" at the 6$^{th}$ Meeting of the Asian Forum of Chromosome and Chromatin Biology held at CCMB, Hyderabad, India, 2017.

2. Presented poster entitled "Histone H3 Variants: Regulators of Cancer Epigenome?" at the Gordon Research conference "Chromatin Structure and Function" held at Les Diablerets, Switzerland, 2016

3. Presented poster entitled "Histone H3 Variants: Determinants of Cancer Epigenome?" at the TMC platinum jubilee conference 2016 held at NCPA, Mumbai, India, 2016

4. Presented poster entitled "Epigenetic Landscape of Cancer: Role of H2A Isoforms and H3 Variants" at Carcinogenesis conference held at ACTREC, Navi Mumbai, India, 2015.

5. Presented poster entitled "Epigenetic Landscape of Cancer: H2A Isoforms and H3 Variants determinants?" at the 5$^{th}$ Meeting of the Asian Forum of Chromosome and Chromatin Biology held at JNCASR, Bangalore, India, 2015.

6. Presented a poster entitled "Deciphering the Molecular Role of Histone H2A Variants, H2A.1 and H2A.2" at the Frontiers in Modern Biology conference organized at Indian Institute of Science, Bangalore, India in 2013.

Divya Reddy Velga

*Dedicated to my Dad……..*

# ACKNOWLEDGEMENTS

*"It is good to have an end to journey towards; but it is the journey that matters in the end."*

- *Ursula K. Legun*

First of all, I express my deep sense of gratitude and sincere thanks to my mentor, Dr. Sanjay Gupta for his guidance, valuable suggestions, intellectual support and encouragement. He nurtured my thought process to adopt a socio-scientific temperament, which enabled the development of my raw skills into scientific expertise. It was his able supervision as well as giving me extraordinary experiences throughout the work, which has resulted in fruitful outcome. He has been a mentor in the true sense from whom I have learnt a lot both professionally and personally. I really hope I put all the things I learnt from you to use in my career ahead sir.

PhD is a very long and a lonely journey which is made tolerable only due to some exceptional people you meet. One person who has been my strength and voice of wisdom is Saikat. In him I found a friend for life whom I can trust blindly. His words 'If you understand a concept completely you should be able to convey to any person and make him understand' has driven me to work hard on my communication and presentation skills. The patience he showed in helping me learn most of the things shows he is going to be an exceptional mentor.

I am thankful to Dr. S.V.Chiplunkar (Director, ACTREC), Dr. R. Sarin (Ex-Director, ACTREC) and Dr. S. Zingde (Ex-Deputy Director, ACTREC) for providing the infrastructure and necessary to carry out research in ACTREC. I would like to thank my present Doctoral Committee Members, Dr. S.V.Chiplunkar, Dr. Rukmini Govekar, Dr. Sanjeev Waghmare, Dr. Sanjeev Galande and earlier members, Late Dr. R. Kalraiya and Dr. G. B. Maru for their critical comments on data, helpful suggestions and cooperativity towards the progress of work. Special thanks to Mr. Nikhil Gadewal, BTIS, ACTREC and Vinod from CDAC, Pune for their

Divya Reddy Velga

# Table of Contents

6

# *Synopsis*

## Homi Bhabha National Institute

### SYNOPSIS OF PhD THESIS

1. **Name of the Student: Divya Reddy Velga**

2. **Name of the Constituent Institution:  Tata Memorial Centre, ACTREC**

3. **Enrolment No.: LIFE09201104011, 1st September 2011.**

4. **Title of the Thesis: Binding partners of histone H2A variant and their molecular implications in carcinogenesis**

5. **Board of Studies: Life Sciences**

## SYNOPSIS

### 1. Introduction

Epigenetics is the study of the change in gene expression pattern which does not involve change in the nucleotide sequence of DNA. The term epigenetics was coined by Waddington in 1942 and was derived from the Greek word "epigenesis" which originally described the influence of genetic processes on development. Epigenetic studies were initially focused on DNA methylation; however, subsequent studies elucidated the role of histones in regulating gene expression pattern [1].

Histones are a class of highly conserved basic proteins and packaging the genome was the primary function previously attributed to them. The core histones comprise of H2A, H2B, H3 and H4, form an octameric protein core around which ~147bp of DNA is wrapped to form the nucleosome core particle (NCP) [2]. Further compaction is achieved with the aid of linker histone H1 [3]. The canonical histone genes are synthesized during the S-phase and to meet up

with their high demand during DNA replication, their encoding genes are present in clusters. There exists other class of histones known as 'Histone variants', which are non-allelic isoforms of canonical histones, synthesized throughout cell cycle and exist as individual genes. The histone variants owing to their sequence dissimilarities undergo unique post translational modifications and thus may bring about the change in chromatin organization by influencing the histone-DNA interactions [4].

Earlier studies from our lab have shown the differential expression of two major H2A variants, H2A.1 and H2A.2 further, these variants were found to be associated with undifferentiated hepatocyte. The two variants differ in their identity by only three residues: T16S, L51M and R99K. These observations were found in liver tissues of normal and hepatocellular carcinoma (HCC) induced by N-nitrosodiethylamine (NDEA) in Sprague Dawley rats. Also, similar results were obtained in cell lines CL44 (pre-neoplastic) and CL38 (neoplastic) derived from the same animal model system.

*In the current study, we aim to understand the differential binding partners of histones H2A variants at chromatin (histones within the nucleosome) and nucleosolic (histone chaperones) level. The study is essential because the biochemical properties of hetero-nucleosomes and homo-nucleosomes are different and can potentially influence the stability of the nucleosomes, global chromatin architecture and gene transcription. Also, histone assembly onto DNA is brought about by histone chaperones, which guide the gene-specific deposition/eviction of histones. Hence, study on nucleosolic binding partners will provide the information of any possible differential histone chaperone association with histone H2A variants.*

## 2. Objectives

In the light of the above hypothesis the following objectives were laid down;

    I.     Identification of the binding partners of H2A.1 and H2A.2

    II.    To understand the role of binding partners in chromatin mediated processes.

## 3. Work Plan

To answer the above objectives, we raised the following questions and employed the below detailed work plan.

### *3.1. Identification and characterization of the nucleosolic binding partners of H2A.1 and H2A.2*

1. Immunoprecipitation using nucleosolic fractions to identify the specific association of histone chaperone, nucleosome assembly protein (NAP1) with H2A.1 and H2A.2.

2. Biophysical characterization of rat NAP1 by using gel filtration chromatography, circular dichroism (CD spectroscopy) and Dynamic light scattering (DLS).

3. Biochemical characterization of casein kinase-2 (CK2) phosphorylated NAP1 using native PAGE and histone binding assays.

### *3.2. Identification of the chromatin binding partners of H2A.1 and H2A.2 and their effect on nucleosomal organization*

1. Global expression profiling of H3 variants in rat liver normal, HCC and cell lines at transcript (Real time PCR) and protein level [Acetic acid-Urea-triton - PAGE and reverse phase coupled high pressure liquid chromatography (RP-HPLC)].

2. Mononucleosomal immunoprecipitations and molecular dynamic simulations (MDS) for analysis of nucleosomes - H2A.1/H3.2, H2A.1/H3.3, H2A.2/H3.2 and H2A.2/H3.3 to understand their relative association and stability.

3. Global profiling of H3 PTMs followed by mononucleosomal immunoprecipitation and western blotting of various H3 variants separated by RP-HPLC for identification of alterations in specific PTMs with emphasis on 'activation' and 'repressive' marks.

4. Micrococcal nuclease assay and pulse chase *in vitro* transcription assay for assessing the global changes in chromatin organization and gene transcription in HCC.

### 3.3. Delineating the transcriptional regulatory mechanisms governing the differential expression of H2A and H3 variants.

1.  Effect of DNA methyl transferase (DNMT) - 5Aza-C and histone deacetylase (HDAC) - Trichostatin A (TSA) inhibitors on H2A and H3 variant expression.

2.  Methyl DNA (MeDIP) and Hydroxyl-methyl DNA immunoprecipitation (hMeDIP) assays to delineate the methylation pattern on H2A.1, H2A.2, H3.2 and H3.3 promoters in normal liver tissue, HCC and cell lines.

### 3.4. Understanding the importance of H3 variants on cell physiology

1.  Cell proliferation and colony formation assay to study the effect of ectopic overexpression of H3.2 and H3.3 variants.

2.  shRNA mediated knock down of H3.3 and its effect on cell proliferation, cell cycle analysis, microccocal nuclease assay and *in vitro* transcription assay.

3.  Chromatin immunoprecipitation (ChIP) followed by qPCR to monitor the association of H3.3 and H3.2 with tumor suppressor genes.

### 3.5. Delineating the significance of H3 chaperones in cellular processes

1.  Global expression changes in H3.2 and H3.3 specific histone chaperones in normal liver and HCC.

2.  Cell proliferation, cell cycle analysis, microccocal nuclease assay and *in vitro* transcription assay to understand the effect of knock down of P150.

### 3.6. Expression profiling of H3 variants in human cancer cell lines

Monitoring the expression status of H3 variants, H3.2, H3.3 and H3.1 by real time PCR in various human cancer cell lines (Liver, Skin and Breast) in comparison to their immortalized counter parts.

*3.7. Profiling of histone PTM marks and modifiers by liquid biopsy and their potential in clinics*

1. Development of protocol for isolation of serum histones.

2. Comparative analysis of changes in histone PTMs profile of serum with paired HCC and other non-target organs.

3. HDAC assay on paired rat tumor tissue lysate and serum samples.

## 4. Results

### 4.1. NAP1 interacts with both histone variants H2A.1 and H2A.2

Nucleosolic immunoprecipitation of histone variants, H2A.1 and H2A.2 revealed NAP1 as an interacting partner for both. However, MDS analysis suggests, H2A.1/H2B/NAP1 is more stable than H2A.2/H2B NAP1 complex. Interestingly, bacterially purified rat NAP1 (rNAP1) showed a tendency to form higher oligomeric species in comparison to yeast NAP1 (yNAP1). Gel filtration chromatography and DLS of rNAP1 indicate that the protein exists as a complex mixture of multimeric species even at 500mM ionic strength. The solution-state complexity remains unchanged even at higher ionic strength. Equilibrium unfolding ($\Delta G$ 14.6 kcal mol$^{-1}$) shows that rNAP1, both dimeric and oligomeric species, follow two-state model of unfolding with no detectable intermediates. MDS analysis of the two structures also reveals that rNAP1 dimer is more stable owing to extensive hydrogen bonding compared to yNAP1. *In vitro* kinase assay using CK2 show that phosphorylation of rNAP1 favors its oligomerization with no effect on histone variants, H2A.1 and H2A.2 binding capacity.

### 4.2. Global changes in H3 variant profile correlates with change in gene transcription in hepatocellular carcinoma

Histone profiling in rat liver normal and HCC revealed a decrease in H3.3 and increase in H3.2 respectively at both protein and transcript level. These changes were further validated and

quantified at protein level through separation of H3 variants by RP-HPLC. Western blot analysis for global changes in H3 PTMs with site-specific antibodies revealed an increase in 'repressive' marks and decrease of 'activation' marks. Further, mononucleosomal immunoprecipitations and western blot analysis of H3 variants, separated by HPLC confirmed that H3.2 is enriched with 'repressive' marks whereas H3.3 with 'activation' marks. These changes also bring about of global chromatin compaction with a decrease in global gene transcription. Interestingly, immunoprecipitation analysis revealed that H2A.1/H3.2, H2A.1/H3.3, H2A.2/H3.2 and H2A.2/H3.3 combinatorial nucleosomes exists in cellular system. However, these nucleosomes differ in their stability, with H2A.1/H3.2 being the most stable and H2A.2/H3.3 least stable as observed by MDS analysis.

**4.3. DNA methylation, a key epigenetic component governs the expression changes of H2A and H3 variants**

Differential expression of H2A variants, H2A.1 and H2A.2 have been associated with HCC and also in maintenance of undifferentiated state of hepatocyte [5][6]. Also, we observe an increased expression of H3.2 and subsequent decrease of H3.3 in HCC. Together, the data suggests a possibility of an overlapping mechanism of transcription regulation of H2A and H3 variants. Moreover, *in silico* analysis of the promoters have shown that H2A.1 and H3.2 contain multiple CpG sites whereas, H2A.2 and H3.3 contain CpG island, suggesting these might be epigenetically regulated. Indeed, treatment with 5-Aza-C and TSA increased the expression of H2A.2 and H3.3 with no significant change in H2A.1 and H3.2 levels in CL38 cell line. Further, MeDIP and hMeDIP coupled with qPCR of specific CpG regions near transcriptional start site revealed hypo-methylation and hyper-methylation of H2A.1, H3.2 and H2A.2, H3.3 respectively in HCC compared to normal liver tissue.

## 4.4. Histone H3 variant specific chaperones are dysregulated in HCC

The increased expression of H3.2 and downregulation of H3.3 correlates with levels of their respective histone chaperones, in HCC and cancer cell lines compared to normal. The expression of H3.2 associated chaperone complex components - P150 and P60 increases, whereas a decrease in H3.3 chaperone -HIRA complex was observed, concomitant to the expression changes in H3.2 and H3.3. In addition, the expression status of these chaperones correlated well with expression of H3 variants in various rat normal tissues. In accordance, ectopic overexpression of H3 variants does not have any phenotypic or PTM changes, suggesting that the balance between levels of variants and their respective chaperones is important for their enrichment onto chromatin.

Inducible knockdown of P150 in CL38 cell line leads to arrest of cells in S-phase after 72h of doxycycline treatment. This affects the cell proliferation and decreases the clonogenic potential of the cells. Interestingly, P150 knock down led to increase in H3.3 transcript, histone 'activation' PTM marks and global gene transcription. However, the elevated transcriptional activity of P150 knock down cells can also be partly attributed to their increased residence in S-phase of cell cycle.

## 4.5. shRNA mediated knock down of H3.3 leads to decrease in tumor suppressor gene expression

H3.3 knock down increased cell proliferation, with no major changes in cell cycle progression. Further, an increase of H3.2 and H3.1 was observed at both transcript and protein level which compensates for the knock down of H3.3. The deposition of H3.2 increased chromatin compaction thus leading to global transcriptional repression. Further, ChIP-qPCR analysis revealed the enrichment of H3.3 to be more than H3.2 on tumor suppressor genes. Thus, tumor suppressor gene expression was severely hampered owing to loss of H3.3 in HCC and knock

down cell line. Conclusively, H3.3 knock down recapitulates the similar phenotype as of cancer cells.

**4.6. Differential expression of H3.2 and H3.3 in human cancer cell lines**

Our observations in rat hepatocellular carcinoma prompted us to investigate the expression of H3 variants - H3.2, H3.3 and H3.1 in human cell lines. The expression profiling on cell lines of liver (HepG2), breast (MCF7) and Skin (A431) origin and their immortalized untransformed counterparts, that is, HHL5 (liver), MCF10A (breast) and HACAT (skin) suggests an increase in the relative expression of H3.2 in all transformed cell lines with decrease of H3.3.

**4.7. Serum histone PTM matches with paired tumor tissue pattern**

A cost-effective and time-efficient protocol for isolation of circulating histones from serum was developed. Their identity was confirmed by mass spectrometry and western blotting. Profiling of PTMs on serum purified histones showed a comparable pattern of modifications like acetylation (H4K16Ac), methylation (H4K20Me3) and phosphorylation (γ-H2AX and H3S10P) to paired HCC and is different with respect to non-target organs. Further, the observed hypo-acetylation of histone H4 in tissue and serum samples of tumor bearing animals corroborated with the elevated HDAC activity in both samples compared to normal. Interestingly, human normal and tumor serum samples also showed elevated HDAC activity with no significant changes in HAT activity.

**5. Summary**

✓ Histone H2A/H2B chaperone, NAP1 follows a two-state model of unfolding. CK2 mediated phosphorylation governs its oligomerization potential. Further, rNAP1/H2A.1/H2B complex is more stable than rNAP1/H2A.2/H2B complex.

✓ Histone H3 variants, the nucleosomal binding partners of H2A show significant changes in their expression profile in cancer cells. The levels of H3.2 increases with decrease of H3.3

in HCC compared to normal liver tissues. Similar changes in expression profile are also observed in human cancer cell lines of liver, breast and skin.

✓ The dynamic alterations of DNA methylation govern the expression changes of the histone H2A and H3 variants - H2A.1, H2A.2 and H3.2, H3.3 respectively in HCC. This coordinated regulation of expression leads to increase in quantity of nucleosomes containing H2A.1/H3.2, the most stable nucleosome, thus may contribute towards the changes in chromatin organization and influencing the transcriptional status of genes.

✓ Expression changes of histone H3 variants H3.2 and H3.3 correlated with the increase in 'repressive' and decrease in 'activating' PTM marks respectively. Interestingly, the levels of H3 variants specific chaperones – CAF-1 and HIRA show a direct correlation with expression of H3.2 and H3.3 respectively. All these changes contribute to an attainment of condensed chromatin architecture and thus a global suppression of gene transcription in HCC.

✓ H3.3 is associated with many tumor suppressor genes and its knock down decreases the expression of these genes, elevates cell proliferation and recapitulates the similar changes as observed in HCC.

✓ The changes in histone PTMs and modifier seen in tumor tissue can also be observed in paired serum samples and hence can be used for determining epi-drug based patient treatment regime and thus contributing to disease prognosis.

*Conclusively, the DNA methylation mediated deregulation of histone H2A and its binding partner H3 variants, in association with their respective chaperones aids in acquirement of unique 'chromatin signature' which brings a decrease in expression of tumor suppressor genes. These changes affect the proliferative potential of cells and thus contributes to carcinogenesis. Further, 'real time' monitoring of serum based 'cancer specific epigenetic*

Thesis | Divya Reddy Velga

*marks' can be used for prognostication, also aid in sub-grouping of patients for targeting by*

*DNMT & HDAC inhibitors and thus assisting in better clinical management of cancer.*



GRAPHICAL ABSTRACT: H3 variants, a nucleosomal binding partner of H2A A master regulators of altered tumor suppressors gene expression.
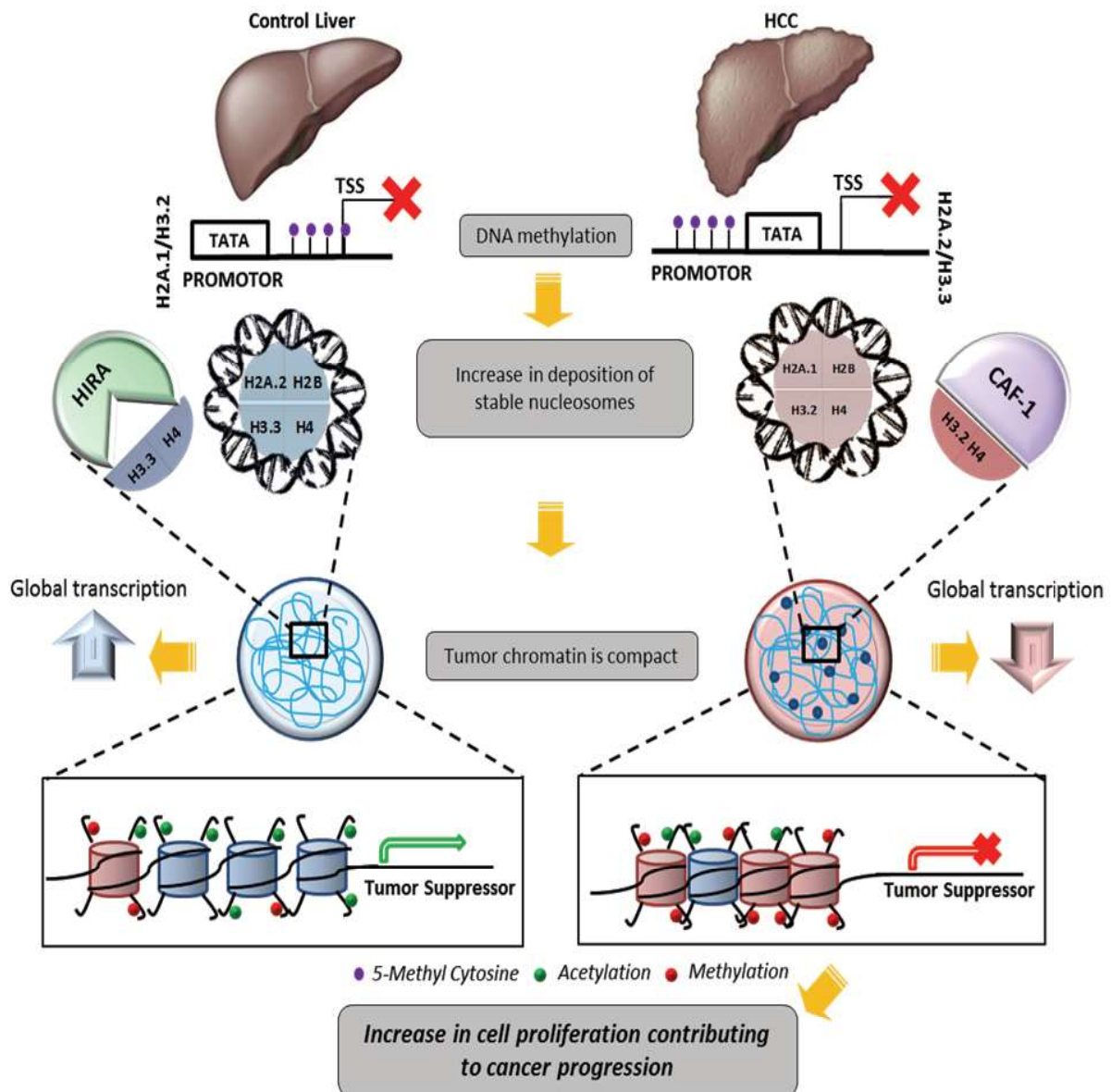
## 6. REFERENCES

[1]   Tessarz, P. & Kouzarides, T. Histone core modifications regulating nucleosome structure and dynamics. Nat. Rev. Mol. Cell Biol. (2014) 15, 703–708

[2]   K. Luger,  a W. Mäder, R.K. Richmond, D.F. Sargent, T.J. Richmond, Crystal structure of the nucleosome core particle at 2.8 A resolution, Nature. 389 (1997) 251–260.

[3]   J.T. Finch, A. Klug, Solenoidal model for superstructure in chromatin, Proc. Natl. Acad. Sci. U. S. A. 73 (1976) 1897–1901.

[4]   C.M. Weber, S. Henikoff, Histone variants : dynamic punctuation in transcription, (2014) 672–682.

[5]   S.P. Khare, A. Sharma, K.K. Deodhar, S. Gupta, Brief Communication Overexpression of histone variant H2A . 1 and cellular transformation are related in N-nitrosodiethylamine-induced sequential hepatocarcinogenesis, (2011) 30–35.

[6]   M. Tyagi, B. Khade, S.A. Khan, A. Ingle, S. Gupta, Expression of histone variant, H2A.1 is associated with the undifferentiated state of hepatocyte, Exp. Biol. Med. (Maywood). (2014) 1535370214531869.

## PUBLICATIONS IN REFFERED JOURNAL:

### a. Published:

- **Divya Reddy**, Bharat Khade, Riddhi Pandya and Sanjay Gupta. A novel method for isolation of histones from serum and its implications in therapeutics and prognosis of solid tumors. Clinical epigenetics. (2017), 9:30

- Monica Tyagi*, **Divya Reddy**\*, and Sanjay Gupta. Genomic characterization and dynamic methylation of promoter facilitates transcriptional regulation of H2A variants, H2A.1 and H2A.2 in various pathophysiological states of hepatocyte. The International Journal of Biochemistry & Cell Biology. (2017), 85:15-24.

  *  *equal contribution*

- **Divya Reddy** and Sanjay Gupta. Histone variant H3.3 and its future prospects in cancer clinic. Journal of Radiation and Cancer Research. (2017) 8:77-81

- **Divya Reddy**, Saikat Bhattacharya and Sanjay Gupta. Histone Chaperones : Functions beyond Nucleosome Deposition. Advances in Biosciences and Biotechnology, 2014, May, 5, 546-556.

**b. Accepted:** -

**c. Communicated:**

- **Divya Reddy**, Saikat Bhattacharya, Vinod Jani, Riddhi Pandya, Uddhavesh Sonavane, Rajendra Joshi and Sanjay Gupta. Biochemical and Biophysical Characterization of higher oligomeric structure of Rat Nucleosome Assembly Protein 1.
- **Divya Reddy**, Saikat Bhattacharya, Sanjay Gupta. Downregulation of Histone H3 Variant H3.3 Contributes to the Development of Hepatocellular Carcinoma.

**d. Other Publications:**

*Research Papers:*

- Monica Tyagi, Shafqat A Khan, Saikat Bhattacharya, **Divya Reddy**, Ajit K Sharma, Bharat Khade, Sanjay Gupta. Techniques to Access Histone Modifications and Variants in Cancer. 'Cancer Epigenetics: Risk Assessment, Diagnosis, Treatment, and Prognosis', Methods in Molecular Biology Series (Humana Press/Springer) 2015.
- Ajit K. Sharma, Shafqat A. Khan, Asmita Sharda, **Divya V Reddy**, Sanjay Gupta. MKP1 phosphatase mediates G1-specific dephosphorylation of H3Serine10P in response to DNA damage. Mutation Research. (2015), 778 71–79.
- Shafqat Ali Khan, **Divya Reddy**, Sanjay Gupta. Global histone post-translational modifications and cancer: Biomarkers for diagnosis, prognosis and treatment. World J Biol Chem. (2015), 6(4): 333-345.
- Saikat Bhattacharya, **Divya Reddy**, Arvind Ingle, Bharat Khade, and Sanjay Gupta. Histone H2A mono-ubiquitination and cellular transformation are inversely related in N nitrosodiethylamine-induced hepatocellular carcinoma. Exp Biol Med (Maywood). (2016), 241(16): 1739-44
- Saikat Bhattacharya, **Divya Reddy**, Raja Reddy, Asmita Sharda, Kakoli Bose, Sanjay Gupta. Incorporation of a tag helps to overcome expression variability in a recombinant host. Biotechnology Reports. (2016) 62–69.

## Conference Abstracts:

- Presented poster entitled "Epigenetic Landscape of Cancer: H2A Isoforms and H3 Variants determinants?" at the 5th Meeting of the Asian Forum of Chromosome and Chromatin Biology held at JNCASR, Bangalore, India, 2015.

- Presented poster entitled "Epigenetic Landscape of Cancer: Role of H2A Isoforms and H3 Variants" at Carcinogenesis conference held at ACTREC, Navi Mumbai, India, 2015.

- Presented poster entitled "Histone H3 Variants: Determinants of Cancer Epigenome?" at the TMC platinum jubilee conference 2016 held at NCPA, Mumbai, India, 2016.

- Presented poster entitled "Histone H3 Variants: Regulators of Cancer Epigenome?" at the Gordon Research conference "Chromatin Structure and Function" held at Les Diablerets, Switzerland, 2016.

Signature of Student: V. Dimya

Date: 27|02|17

## Doctoral committee

| S. No. | Name | Designation | Signature | Date |
|--------|------|-------------|-----------|------|
| 1. | Dr. S.V. Chiplunkar | Chairman | *V. Chiplunkar* | 16/3/17 |
| 2. | Dr. Sanjay Gupta | Guide & Convener | *signature* | 27/02/17 |
| 3. | Dr. Rukmini Govekar | Member | *signature* | 27/02/17 |
| 4. | Dr. Sanjeev Waghmare | Member | *signature* | 27/02/17 |
| 5. | Dr. Sanjeev Galande | Invitee | *signature* | 27/02/17 |

Forwarded Through:

Dr. S.V. Chiplunkar 16/3/17
Director, ACTREC
Chairperson,
Academic & training Program, ACTREC

Prof. K. Sharma
Director, Academics
T.M.C.

Dr. S. V. Chiplunkar
Director
Advanced Centre for Treatment, Research &
Education in Cancer (ACTREC)
Tata Memorial Centre
Kharghar, Navi Mumbai 410210.

# *List of Abbreviations*

| | |
|---|---|
| **APS** | *A*mmonium *Per*sulfate |
| **ATM** | *A*taxia *T*elangiectasia *M*utated |
| **ATR** | *A*taxia *T*elangiectasia and *R*ad3-related |
| **ATRX** | *A*lpha *T*halassemia/Mental *R*etardation Syndrome *X*-Linked |
| **AUT** | *A*cetic Acid, *U*rea, *T*riton-X |
| **BPB** | *B*romo*p*henol *B*lue |
| **CD** | *C*ircular *D*ichroism |
| **CLL** | *C*hronic *L*ymphocytic *L*eukemia |
| **CTCF** | CC*CTC*-binding *F*actor |
| **DAXX** | Death-Domain Associated Protein |
| **DDR** | *D*NA-*D*amage *R*esponse |
| **DNMT** | *D*NA *M*ethyl*t*ransferase |
| **DTT** | *Di*thio*t*hreitol |
| **ERE** | *E*strogen *R*esponsive *E*lement |
| **DUSP1** | *D*ual *S*pecificity *P*hosphatase *1* |
| **ES Cells** | *E*mbryonic *S*tem *C*ells |
| **GFP** | *G*reen *F*luorescent *P*rotein |
| **GST** | *G*lutathione-*S-T*ransferase |
| **H2ABbd** | *H2A B*arr *B*ody *D*eficient |
| **HAR Domain** | *H*istone H2*A R*epression *D*omain |
| **HAT** | *H*istone *A*cetyl*t*ransferase |
| **HCC** | *H*epato*c*ellular *C*arcinoma |
| **HDAC** | *H*istone *D*e*ac*etylase |
| **HMG** | *H*igh *M*obility *G*roup |
| **IPTG** | *I*so*p*ropyl β-D-1-*t*hio*g*alactopyranoside |
| **MALDI** | *M*atrix-*A*ssisted *L*aser *D*esorption/*I*onization |
| **MDS** | *M*olecular *D*ynamic *S*imulation |
| **MNase** | *M*icrococcal *N*uclease |
| **MSK1** | *M*itogen and *S*tress *A*ctivated *K*inase *1* |
| **MTT** | 3-(4,5-Dimethylthiazol-2-yl)-2,5-Diphenyltetrazolium Bromide |
| **NAP1** | *N*ucleosome *A*ssembly *P*rotein *1* |
| **NCBI** | *N*ational *C*entre for *B*iotechnology *I*nformation |
| **NCP** | *N*ucleosome *C*ore *P*article |
| **NDEA** | *N*itroso*di*ethyl*a*mine |
| **NTA** | *N*itrilo*t*riacetic *A*cid |
| **PBS** | *P*hosphate *B*uffered *S*aline |
| **PCNA** | *P*roliferating *C*ell *N*uclear *A*ntigen |
| **PMSF** | *P*henyl*m*ethyl*s*ulfonyl *f*luoride |
| **PP1** | *P*rotein *P*hosphatase *1* |
| **PRC1** | *P*olycomb *R*epressive *C*omplex *1* |
| **Pre-RC** | *Pre-R*eplication *C*omplex |
| **PTM** | *P*ost *T*ranslational *M*odification |
| **PVDF** | *P*oly*v*inyli*d*ene *F*luoride |
| **RBS** | *R*ibosome-*B*inding *S*ite |
| **RMSD** | *R*oot *M*ean *S*quare *D*eviation |
| **RT-PCR** | *R*everse *T*ranscriptase - *P*olymerase *C*hain *R*eaction |
| **SAM** | *S-A*denosyl *M*ethionine |
| **SDS** | *S*odium *D*odeocyl *S*ulfate |
| **SET** | *S*u(var)3-9, *E*nhancer of Zeste, *T*rithorax |

| | |
|---|---|
| TEMED | *Te*tra*me*thylethylene*d*iamine |
| TEV | *T*obacco *E*tch *V*irus |
| TFA | *T*ri*f*luoroacetic *A*cid |
| TSA | *T*richo*s*tatin *A* |
| TSS | *T*ranscription *S*tart *S*ite |
| VPA | *Val*proic *A*cid |
| NAP1 | *N*ucleosome *A*ssembly *P*rotien *1* |
| NLS | *N*uclear *L*ocalisation *S*ignal |
| CK 2 | *C*asein *K*inase *2* |
| GFC | *G*el *F*ilteration *Ch*romatography |
| RP-HPLC | *R*everse *P*hase *H*igh *P*erformance *L*iquid *C*hromatography |
| PAGE | *P*oly *A*crylamide *G*el *E*lectrophoresis |
| DAE | *D*ual *A*cid *E*xtraction |

## *List of Tables*

## *List of Figures*

| 4.13 | Effect of H3.3 knockdown on chromatin structure and global gene expression. | 139 |
|---|---|---|
| 4.14 | H3.3 association with tumor suppressor gene expression | 140 |
| 4.15 | Effect of H3.3 knockdown on tumor suppressor gene expression | 141 |
| 4.16 | DNA methylation governs expression changes of H2A isoforms and H3 variants | 142 |
| 4.17 | H3 variant expression changes in human cell lines | 144 |
| 4.18 | Probable Scenario in HCC | 149 |
| 5.1 | Origins and Characteristics of circulating nucleosomes in plasma | 153 |
| 5.2 | Diagrammatic representation of protocol for isolation of histones from blood | 158 |
| 5.3 | Resolution and identification of purified histones from paired serum and liver tissue of normal and tumor | 159 |
| 5.4 | Profiling of site-specific histone modifications and modifiers in paired serum and liver tissue of normal and tumor | 162 |
| 5.5 | Profiling of histone modifiers in human serum samples | 164 |
| 5.6 | Schematic representation of Liquid biopsy as tool for better clinical management of cancer patients. | 170 |
| 6 | Schematic representation of the conclusions of the work done | 179 |
| S1 | Biophysical characterisation of rNAP1 Oligomer | 205 |
| S2 | In vitro phosphorylation of rNAP1 with PKC | 205 |
| S3 | H3 variants differences and similarities | 206 |
| S4 | RP-HPLC chromatogram of histones isolated from rat | 206 |

24

Chapter 1

# 1. Introduction

## 1.1. Overview

The primary function of histone proteins is compaction of DNA. This is achieved by formation of nucleosomes that are the basic repeating units of the chromatin and consists of a protein component, comprised of an octameric core of histones and a nucleic acid component, which is ~147bp of DNA[1]. Histone genes, though are highly conserved, sequence divergence is observed within them. Broadly owing to these dissimilarities they can be classified into two groups, histone isoforms and histone variants. Histone isoforms constitute the group of histones synthesised and deposited in a replication dependent manner and are present in clusters [2] whereas histone variants are dispersed across the genome and are synthesised in a replication independent manner [3].

Epigenetic changes are present in all human cancers and are now known to cooperate with genetic alterations to drive the cancer phenotype. These changes involve DNA methylation, histone modifiers and readers, chromatin remodelers, microRNAs, and other components of chromatin. Cancer genetics and epigenetics are inextricably linked in generating the malignant phenotype; epigenetic changes can cause mutations in genes, and, conversely, mutations are frequently observed in genes that modify the epigenome. Especially, histone PTMs and/or isoforms, variants - all components are now established to be deregulated in cancer. Over the past decade accumulated evidences indicate towards the strong association of aberrant histone variant mutations termed as 'oncohistones' and histone PTMs, termed as 'histone onco-modifications' with cancer. Further, available literature has suggested that the alteration in the global histone variant and PTMs in multiple cancers can be explored as prognostic markers for better management of cancer patients. However, many studies have emphasised individual role of these components and a unified study connecting these all is lacking.

Histone isoforms have been reported to be differentially expressed in various patho-physiological states [2,4,5,6]. The distinct functional effects of replication-dependent histone H2A

isoforms have been demonstrated [27], and their mechanistic basis of the non-redundancy in part is attributed to their property to confer differential nucleosome stability[7]. However, it is still not clearly understood, whether the deposition of these isoforms is brought about by the same histone chaperones and whether they show any differential interaction with other histones. The work done in this dissertation investigated the interaction of H2A.1 and H2A.2 isoforms, which differs from each other by only three amino acids. **The results obtained have been divided into three chapters.**

**Chapter 3** entitled *'Nucleosolic binding partners of histones H2A.1 and H2A.2'* discusses the possibility of differential chaperones for H2A isoforms. NAP1 (Nucleosome assembly protein 1), a major H2A/H2B histone chaperone interacts with both H2A.1 and H2A.2 enabling us to conclude that histone isoforms may have a similar set of chaperones aimed for their chromatin deposition. Further, the work done elucidates that the inherent stability of histone chaperone NAP1 is different between yeast and higher vertebrate species rat NAP1, highlighting that primary sequence differences contribute to significant changes in protein stability. Another interesting observation that emerged from this study is that phosphorylation favors oligomerization of NAP1 proteins. Further, the implications of PTMs occurring on chaperone complexes in terms of effecting their distribution inside the cell has been discussed.

The work done in the context of understanding the other histone binding partners of H2A.1 and H2A.2 have been highlighted in **Chapter 4** entitled '*Chromatin binding partners of histones H2A.1 and H2A.2'*. Profiling for global alterations of other histones revealed changes in H3 variants, H3.2 and H3.3 with former being upregulated and later downregulated in tumor samples similar to H2A.1 and H2A.2 respectively. Further, the work done shows that both H2A isoforms interact with these H3 variants thus, indicating for a similar transcriptional regulation of histones. Indeed, DNA methylation pattern at promoters of H2A isoforms and H3 variants was seen to be regulating their coordinated expression pattern as seen in HCC. Interestingly,

any alterations in H3 variant levels and their chaperones can modulate chromatin dynamics by undergoing differential 'active' and 'inactive' PTMs thus influencing global transcription profile. In addition, on attempting to understand the role of H3 variants in cancer progression we discover, they regulate tumor suppressor gene expression.

**Chapter 5** entitled *'Identification of epigenetic alterations in serum and its clinical implications'* emphasizes the importance of histone PTM changes in terms of biomarkers. A novel, simple and robust protocol to purify histones from serum has been developed to explore histone PTM changes for their value as tumor liquid biopsy markers. Our study for the first time also provides a basis for patient sub grouping by measuring HDAC (Histone deacetylase) activity in serum. Further, the correlation of HDAC activity values with established serum biomarkers has been discussed.

## 1.2. Epigenetics

The genetic information combined in the zygote after fertilization is transmitted to every single somatic cell within an organism. Still, the dramatic morphological, cytological and physiological differences that evolve during development cannot be attributed alone to information embedded in the DNA sequence. Conrad Waddington coined the term 'epigenetic landscape' in 1953 to describe this process of cellular differentiation during embryogenesis[8]. A more recent definition considers all mitotically and/or meiotically heritable changes in phenotype and gene expression that occur without an apparent change in DNA sequence as 'epigenetics'[9]. Research over a last few decades has shown that the molecular basis of these heritable changes lies within the chromatin.

DNA methylation is perhaps the best characterized chemical modification of chromatin. In mammals, nearly all DNA methylation occurs on cytosine residues of CpG dinucleotides. Regions of the genome that have a high density of CpGs are referred to as CpG islands, and

DNA methylation of these islands correlates with transcriptional repression[10]. DNA methylation was soon studied in context of disease as well and it was unraveled that in many cancers global hypo-methylation and the hyper-methylation of tumor suppressor genes occurs[11]. In fact, cancer was the first human disease to be linked to epigenetics. Studies performed by Feinberg and Vogelstein in 1983, using primary human tumor tissues, uncovered that genes of colorectal cancer cells were substantially hypomethylated compared with normal tissues[12]. However now the contribution of other epigenetic components is well appreciated [**Figure 1.1**].
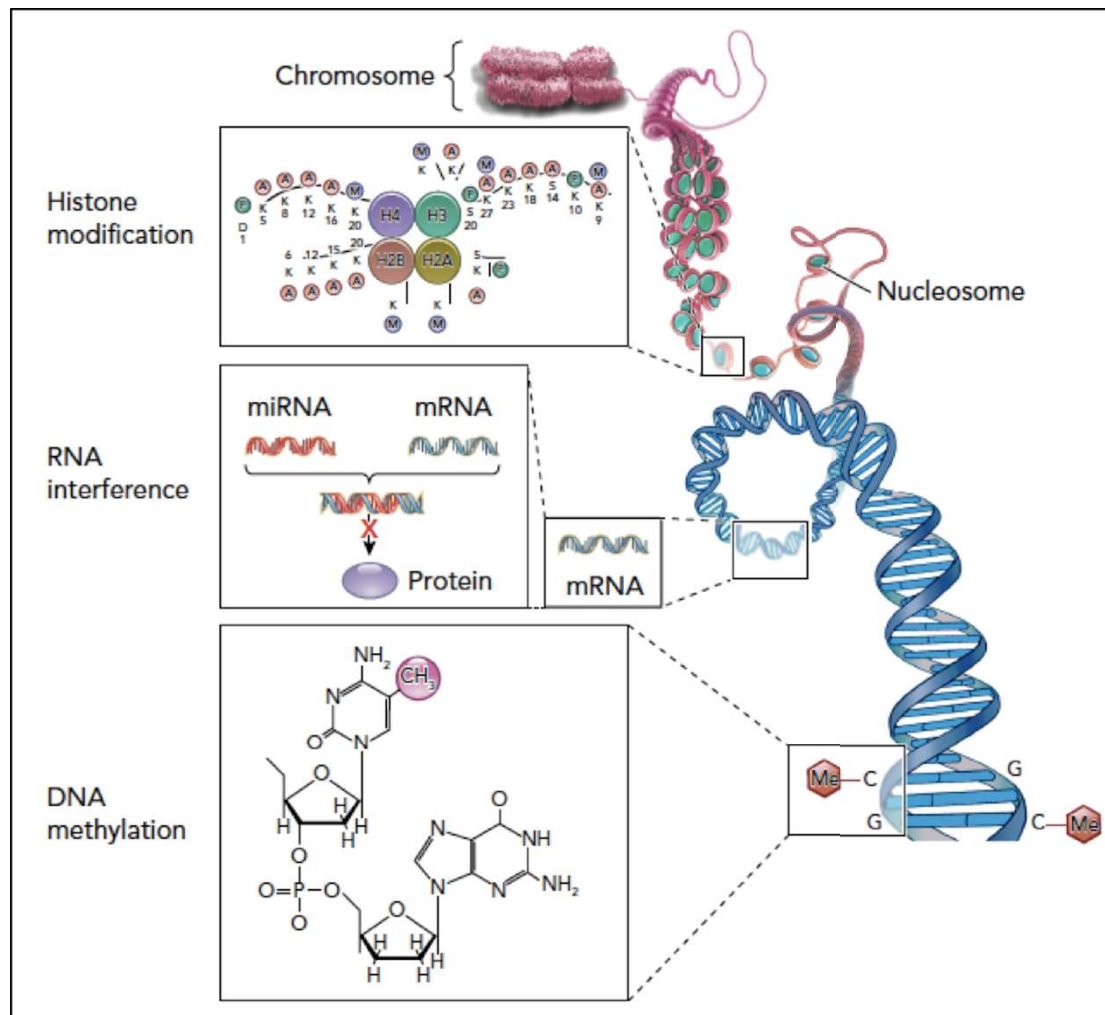


**Figure 1.1. Epigenetic Regulators.** Covalent modifications of DNA (e.g. cytosine methylation) or of histone proteins (e.g. lysine acetylation, lysine and arginine methylation, serine and threonine phosphorylation, and lysine ubiquitination) and miRNAs of RNAi machinery play central roles in epigenetic regulation.
*Adapted from:*
*James S. Hagood. (2014). Beyond the Genome: Epigenetic Mechanisms in Lung Remodeling. Physiology (Bethesda), 29(3):177-185. DOI: 10.1152/physiol.00048.2013*

For many decades, DNA methylation was the focus of investigators to uncover the epigenetic regulatory mechanisms used by cells. However, it was suspected that the condensation of DNA by histones may result in repression of processes such as DNA replication, transcription and repair by limiting access of the underlying DNA sequence to the cellular apparatus. This idea was proved correct by *in vitro* experiments demonstrating that transcription was inhibited with nucleosomal DNA templates but not naked DNA[9]. This, along with the identification of various post translational modifications (PTMs) that histones undergo, ignited the investigation of histones as influential players in contributing to epigenetic regulation of chromatin mediated processes. Continued research has advanced our knowledge of the role of epigenetic regulators like DNA methylation and histone PTMs in governing cellular phenotypes in different contexts. Additionally, it also has led to the identification of new epigenetic regulators like the sequence divergent form of the canonical histones, referred to as histone variants and also microRNAs.

## 1.3. Histones and chromatin structure

Eukaryotic organisms package nearly two metres of DNA into a small nuclear compartment using a series of hierarchical layers. The lowest layer of compaction occurs through the wrapping of DNA into a nucleosome, which is formed from ~146 base pairs (bp) of DNA wrapped around a histone octamer composed of two units each of core histones viz H2A, H2B, H3 and H4. This nucleosome core particle (NCP) forms the basic repeating structural unit of chromatin[13]. The repeating units of NCPs joined by linker DNA forms a 'beads on a string' model structure or a 11nm fibre[14]. Linker histones (H1 and H5) bind to the DNA linker regions in close proximity to the sites of DNA entry and exit to the NCP, and organize the nucleosomal arrays into a more condensed 30-nm chromatin fibre, regarded as the second level of DNA compaction[15,16]. The association of non-histone proteins like HMGs further compact this

chromatin fibre, and finally by association of various protein factors during metaphase of cell cycle the most compact form of DNA, chromosome is seen [**Figure 1.2**].
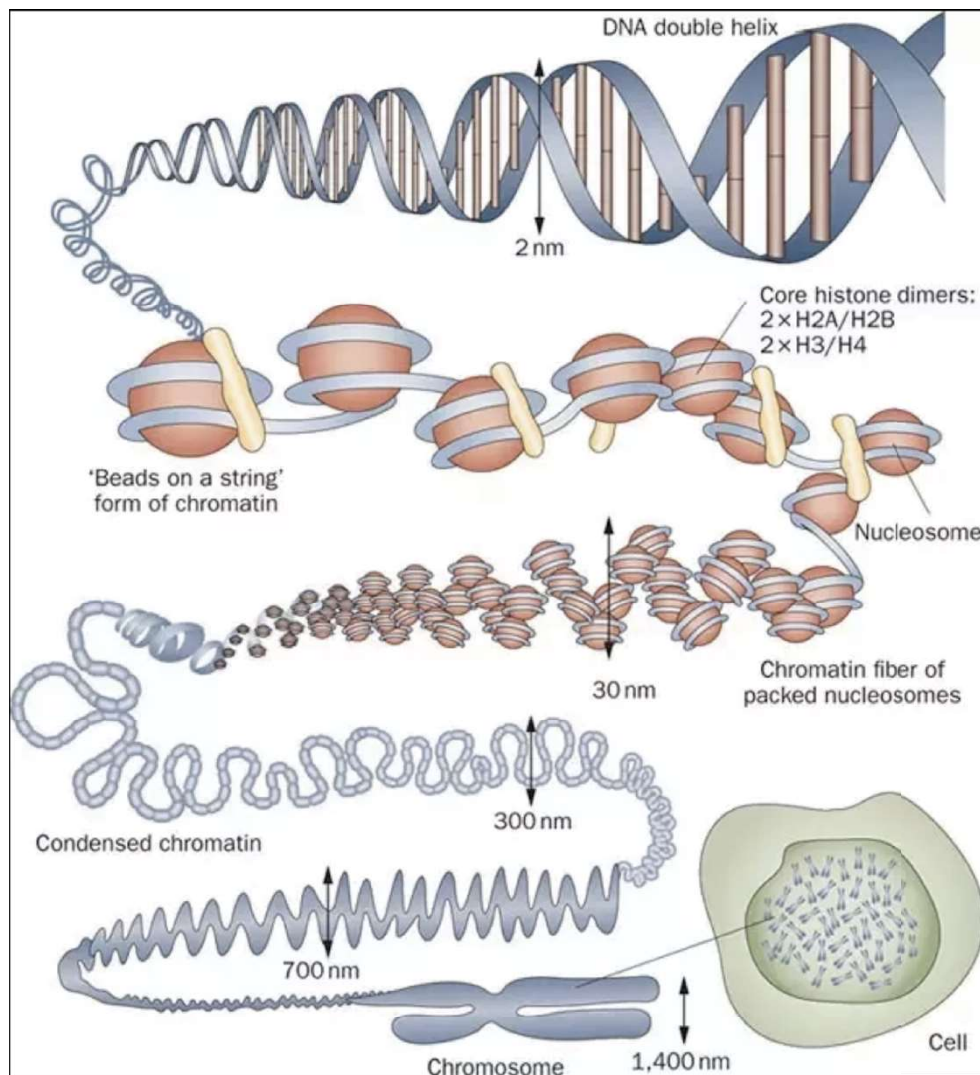


**Figure 1.2. Hierarchical organisation of DNA inside nucleus.** Chromosomal DNA that is more than 6 feet in length is packaged inside a nucleus which is only a few microns in diameter. This is brought about with the aid of highly basic proteins called histones. With the aid of histones, the naked DNA is organized in form of nucleosome which is the fundamental repeating unit of the chromatin. Nucleosomes further fold to form a 30-nanometer chromatin fibre, which forms loops averaging 300 nanometres in length. The 300 nm fibres are compressed and folded to produce a 700 nm-wide fibre, which is tightly coiled into the chromatid of a 1400nm wide chromosome.
*Adapted from: https://www.quora.com/What-is-the-basic-difference-between-bacterial-DNA-and-human-DNA*

The extent of global chromatin condensation varies during the life cycle of a cell. In interphase cells, most of the chromatin is relatively decondensed and is called euchromatin/open chromatin[17]. This is consistent with the fact that during this period of the cell cycle, genes are

transcribed and the DNA is replicated in preparation for cell division. Most of the euchromatin in interphase nuclei appears to be in the form of 30-nm fibers, organized into large loops containing approximately 50 to 100 kb of DNA. About 10% of interphase chromatin is in a very highly condensed state called heterochromatin that is transcriptionally inactive and contains highly repeated DNA sequences[18]. Conclusively, the temporal, structural and chemical alteration of these various layers of DNA compaction influence gene activity and various cellular programs.

## 1.4. Nucleosome assembly and disassembly

The assembly of histone to form nucleosomes is very well regulated and occurs in an orderly fashion, to facilitate proper formation of chromatin fibre [**Figure 1.3**].
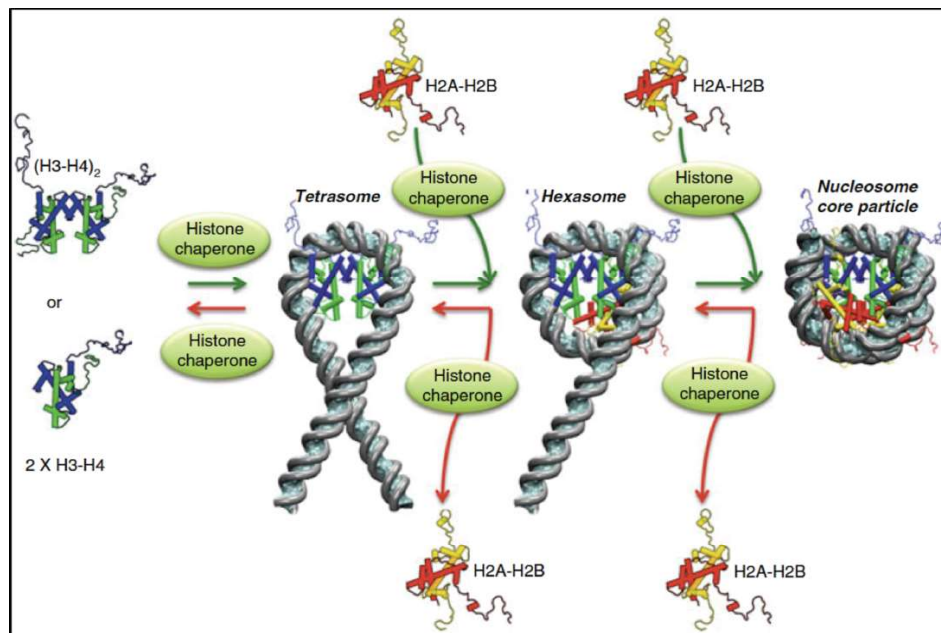


**Figure 1.3. Assembly and disassembly of nucleosome.** Stepwise assembly and disassembly of nucleosomes is mediated by histone chaperones. Green arrows represent steps in chromatin assembly and the red arrows indicate steps in chromatin disassembly. DNA is wrapped around two H3–H4 dimers and two H2A–H2B dimers to form the nucleosome core particle. The stepwise assembly, along with the different possible intermediates including the tetrasome and hexasome, are represented here. Histone chaperones mediate each step of the assembly/disassembly process. Histone H2A is depicted in yellow, H2B in red, H3 in blue, and H4 in green.
*Adapted from: Briana K. Dennehey and Jessica Tyler. (2014). Histone Chaperones in the Assembly and Disassembly of Chromatin. Fundamentals of Chromatin, Springer books. DOI: 10.1007/978-1-4614-8624.4-2.*

This process is mediated by specialised set of proteins known as histone chaperones[19]. First H3/H4 tetramers are deposited on DNA, thus marking the site for NCP formation (nucleosome positioning) followed by deposition of two H2A/H2B dimers[20]. The disassembly of nucleosome follows the same events in a reverse order.

## 1.5. Histone post translational modifications

Each of the histone proteins possesses a characteristic side chain, or tail, which is densely populated with basic lysine and arginine residues. These histone tails are subject to extensive covalent posttranslational modifications (PTMs) that cooperate to govern the chromatin state[21]. Some PTMs can alter the charge density between histones and DNA, impacting chromatin organization and underlying transcriptional processes, but they can also serve as recognition modules for specific binding proteins that, when bound, may then signal for alterations in
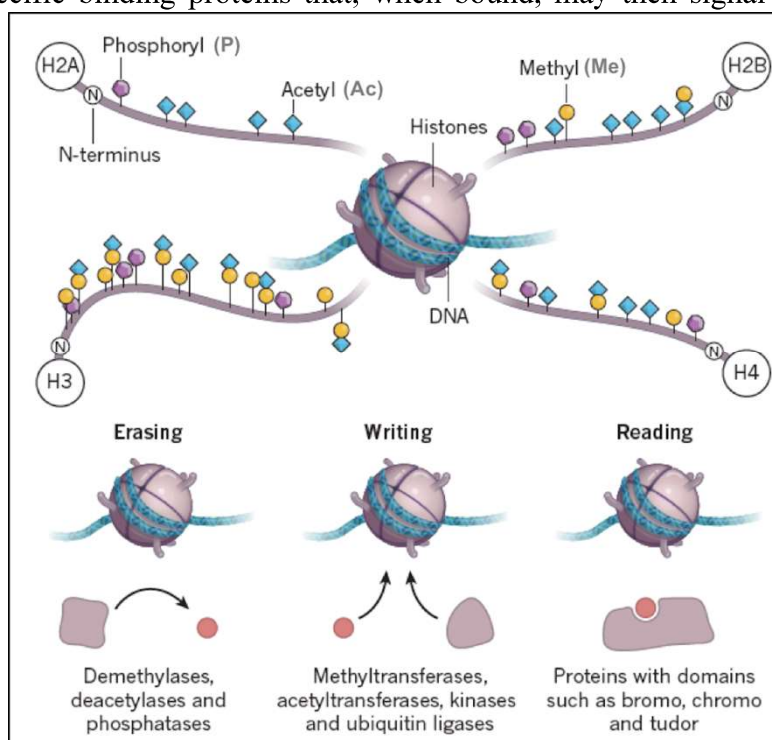


**Figure 1.4. Histone post-translational modifications.** Schematic drawing of a nucleosome with the four canonical core histones (H2A, H2B, H3 and H4). The covalent PTMs [methylation (Me), acetylation (Ac), and phosphorylation (P)] are highlighted on the N- and C-terminal tails of each histone. The modifications which occur in the core body of histones like H3K56Ac are not depicted in the drawing. The enzymes which add and remove these modifications are known as writers and erasers respectively . The proteins which bind to these modifications are readers.
*Adapted from: Kristian Helin & Dashyant Dhanak. (2013). Chromatin proteins and modifications as drug targets. Nature. 502, 480–488. DOI:10.1038/nature12751.*

chromatin structure or function[22][**Figure 1.4**]. The site-specific modification on different histones depends on the signalling and physiological condition within the cell[21]. These multiple independent modifications enable combinatorial complexity; resulting in a large variety of functionally distinct nucleosomes. Some of the major histone modifications influencing gene transcription are tabulated in **Table 1.1**.

| Modification | Position | Writers | Function in transcription |
|---|---|---|---|
| **Methylation** | H3K4 | MLL,SETD1A,SETD1B,SETD7 and ASH1L | Activation |
| | H3K9 | SUV39H1, G9a and SETDB1 | Repression |
| | H3K27 | EZH1 and EZH2 | Repression |
| | H3K36 | SETD2, ASH1L and NSD1 | Activation |
| | H3K79 | DOT1L | Activation |
| | H3R2,H3R17 and H3R26 | PRMT4 | Activation |
| | H3R8 | PRMT5 | Repression |
| | H2AR3 | PRMT1 and PRMT5 | Activation and/or repression |
| | H4K20 | SETD8,SUV4-20H1 and SUV4-20H2 | Repression |
| | H4R3 | PRMT1 and PRMT5 | Activation and/or repression |
| **Acetylation** | H3K9,H3K14,H3K18,H3K23 and H3K27 | GCN5,PCAF,p300 and CBP | Activation |
| | H4K5,H4K8,H4K12 and H4K16 | TIP60,KAT7,p300,CBP and ATF2 | Activation |
| Ubiquitylation | H2AK119 | RNF2 | Repression |
| | H2BK120 | UBE2E1,RNF20 and RNF40 | Activation and/or repression |

**Table 1.1. Major histone modifications and their functions in transcriptional regulation along with the writers.** ASH1L, (absent, small or homeotic)-like; CBP, CREB binding protein; DOT1L, DOT1-like; EZH, enhancer of zeste homologue; KAT, lysine acetyltransferase; MLL, mixed lineage leukaemia; NSD1, nuclear receptor binding SET domain protein 1; PRMT, protein arginine methyltransferase; RNF, ring finger protein; SETD, SET domain-containing protein; SUV, suppressor of variegation; UBE2E1, ubiquitin conjugating enzyme E2 E1. *Adapted from: Fan Liu (2016). Beyond transcription factors: how oncogenic signalling reshapes the epigenetic landscape. Nature Reviews Cancer 16, 359–372. DOI:10.1038/nrc.2016.41*

Many of the modifications can interact together or affect others, collectively constituting the 'histone code'[23], which states that:

- Distinct modifications on core and tail regions of histone proteins generate docking sites for a large number of non-histone chromatin-associated proteins,

- Modifications on the same or different histone tails may be inter-dependent and generate various combinations and 'cross-talk' within themselves to perform different function,

- Distinct regions of higher order chromatin, such as euchromatic or heterochromatic domains, are largely depend on the local concentration and combination of differentially modified nucleosomes,

- 'Binary switches 'represent the differential readout of distinct combinations of marks on two neighbouring residues, where one modification influence the binding of an effector protein onto another modification on an adjacent or nearby residue

- 'Modification cassettes' signifies combinations of modifications on adjacent sites within these short clusters lead to distinct biological readouts.

Addition, removal and identification of these post-translational modifications on histone tails is brought about by 'writers', 'erasers' and 'reader' proteins, which together regulate various biological processes, including transcription, DNA replication and DNA repair[21]. It is now well established that there is an intense cross-talk between histone modifications to drive distinct downstream functions[21].

## 1.5.1. Histone Acetylation

Histone acetylation is a reversible modification that occurs on the ε-amino groups of lysine residues generally at the N-terminal tails of core histones. Allfrey *et al.,* first reported histone acetylation in 1964. This modification is almost invariably associated with activation of transcription. Acetylation removes the positive charge on the histones, thereby decreasing the

interaction of the N termini of histones with the negatively charged phosphate groups of DNA. As a consequence, the condensed chromatin is transformed into a more relaxed structure that is associated with greater levels of gene transcription. This relaxation can be reversed by HDAC activity. Relaxed, transcriptionally active DNA is referred to as euchromatin. More condensed (tightly packed) DNA is referred to as heterochromatin. These reactions are typically catalyzed by enzymes with "histone acetyltransferase" (HAT) or "histone deacetylase" (HDAC) activity[24][**Figure 1.5**].
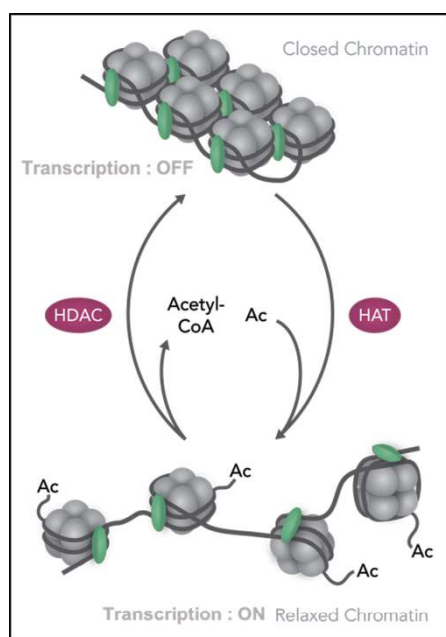


**Figure 1.5. Histone acetylation.** Shown in this illustration, the dynamic state of histone acetylation/deacetylation regulated by HAT and HDAC enzymes. Acetylation of histones increases accessibility of chromatin and gene transcription. *Adapted from: https://www.horizondiscovery.com/cell-lines/all-products/explore-by-your-research-area/epigenetics*

## 1.5.2. Histone Methylation

Histone methylation is a process by which methyl groups are transferred to lysine or arginine residues of histone proteins[25]. Histone methyltransferases (HMT) catalyze the transfer of one, two, or three methyl groups to lysine and arginine residues of histone proteins. Two major types of histone methyltransferases exist, lysine-specific (which can be SET (Su(var)3-9, Enhancer of Zeste, Trithorax) domain containing or non-SET domain containing) and arginine-specific[26,27]. In both types of histone methyltransferases, S-Adenosyl methionine (SAM) serves as a cofactor and methyl donor group[25].

**Lysine methylation:** They usually modify one single lysine on a single histone and their output can be either activation or repression of transcription. Three methylation sites on histones are implicated in activation of transcription: H3K4, H3K36, and H3K79. Three lysine methylation sites are connected to transcriptional repression: H3K9, H3K27, and H4K20[28].

**Arginine methylation:** Like lysine methylation, arginine methylation can be either activate or repress the transcription. There are two classes of arginine methyltransferases, the type I and typeII enzymes. The two types of arginine methyltransferases form a relatively large protein family (11 members), the members of which are referred to as Protein Arginine Methyltransferases (PRMTs). All of these enzymes transfer a methyl group from SAM (S-adenosyl methionine) to the ω- guanidine group of arginine within a variety of substrates[29].

Methylation of histones can either increase or decrease transcription of genes, depending on which amino acids in the histones are methylated, and how many methyl groups are attached. For example, trimethylation of histone H3 at lysine 4 (H3K4Me3) is an active mark for transcription whereas, trimethylation of histone H3 at lysine 9 (H3K9Me3) is a signal for transcriptional silencing [**Figure 1.6**].
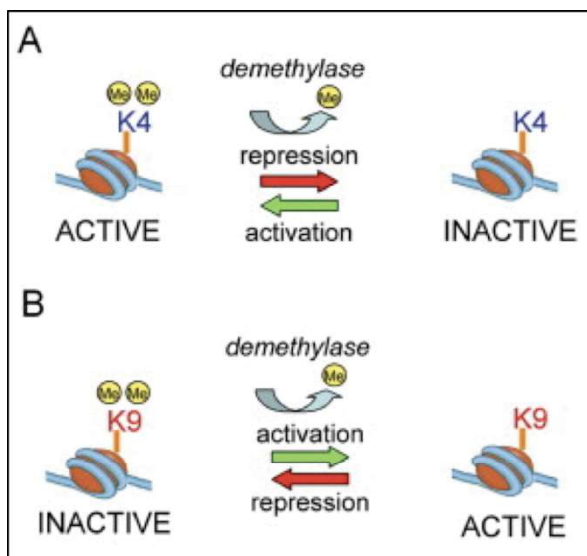


**Figure 1.6. Histone methylation.** The methylation of histone lysines is reversible and regulates gene expression. (A) Methylation of H3K4 is often associated with active genes, and conversely, its demethylation accompanies gene repression. (B) In contrast, methylation of H3K9 is often associated with silenced genes, hence removal of H3K9 methyl marks coincides with gene activation.
*Adapted from:*
*Wysocka J, Milne TA, Allis CD. Taking LSD1 to a new high. Cell. 2005;122(5):654–658.*

## 1.5.3. Histone Phosphorylation

The phosphorylation of histones is highly dynamic. It takes place on serine, threonine and tyrosine, predominantly, but not exclusively, in the N- terminal histone tails. The levels of the modification are controlled by kinases and phosphatases that add and remove the modification, respectively. Histone kinases transfer a phosphate group from ATP to the hydroxyl group of the target amino- acid side chain. In doing so, the modification adds significant negative charge to the histone that undoubtedly influences the chromatin structure[30] [**Figure 1.7**].
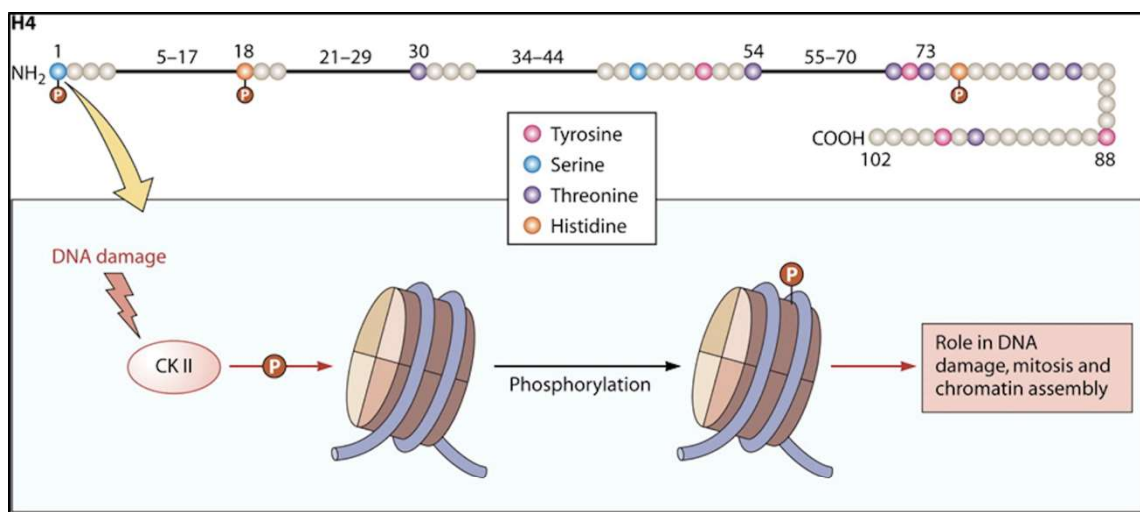


**Figure 1.7. Histone Phosphorylation.** Serine, threonine, tyrosine, and histidine residues of human H4 are known to undergo phosphorylation as shown with a red "P". Schematic of the events occurring at S1 post DNA damage has been pictorial represented.
*Adapted from: Banerjee T, Chakravarti D. A peek into the complex realm of histone phosphorylation. Molecular and cellular biology. 2011;31(24):4858–4873.*

A wide array of kinases (like Aurora B, MSK1, ATM etc.) and phosphatases (like DUSP1, PP1 etc.) participate in modulating the levels of phosphorylation mark on histones in different cell cycle stages and contexts[31]. Characterization of the biological functions of the histone phosphorylation marks is an area of intensive investigation. One well studied phosphorylation mark is the phosphorylation of H2A variant H2AX. This modification demarcates large chromatin domains around the site of DNA breakage is one the earliest events in the DNA damage response pathway[32]. This modification takes place on serine 139 in mammals and serine 129 in yeasts of the variant histone H2AX, and is commonly referred to as γH2AX.

Protein kinases ATM and ATR in mammals carry out this phosphorylation[33]. This wide distribution of γH2AX around the break is thought to create a specific signaling platform for recruitment and/or retention of DNA damage repair and signaling factors[34].

Apart from the role of phosphorylated H2AX, phosphorylated histone residues are associated with gene expression. For example, H3S10P and H2BS32P have been linked to the expression of proto-oncogenes such as c-fos, c-jun and c-myc[35,36,37]. Furthermore, targeting H3S28 phosphorylation to promoters of genes such as c-fos and α-globin was shown to control their activation[38]. Phosphorylation of H3 on T11 and T6 has also been implicated in transcription regulation in response to androgen stimulation[39].

## 1.6. Histone Isoforms and Variants

Histone genes are present in clusters and in multiple copies to facilitate their robust synthesis during the S-phase of cell cycle for proper chromatin packaging after DNA replication [**Figure 1.8**].
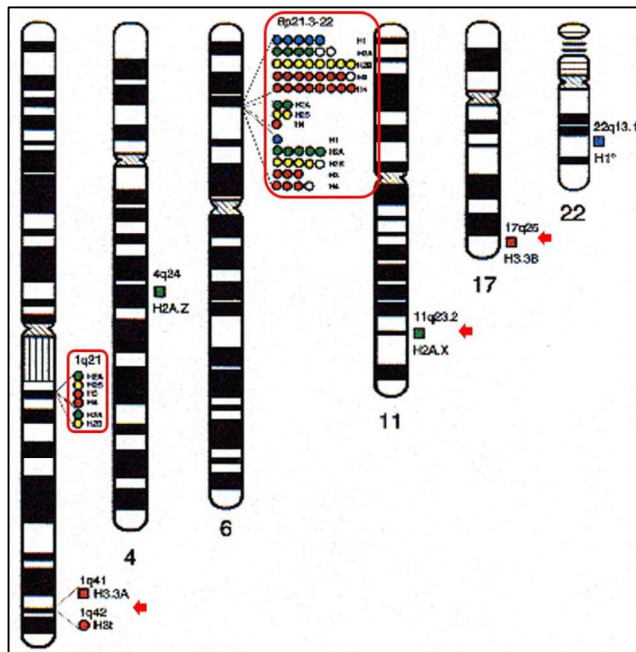


**Figure 1.8. Histone genes in humans.** The ideogram depicts the location of the histone genes in human chromosomes. The clusters indicated in red box shows the location of replication-dependent canonical histone genes. The two major clusters are present on chromosome 1 and 6, with the one on chromosome 6 being the largest one. The genes indicated with red arrows marks the gene for replication-independent histone variants like H3.3, H2A.Z, H2A.X etc. Unlike the genes for canonical histones, genes for variants are not present in multiple copies.

Multiple genes encoding for single subtype of histone (H2A, H2B, H3 and H4) are present in these clusters, however, owing to minor differences in the gene sequence, they encode for

similar histone subtypes differing in few amino acids and are known as 'histone isoforms'. For example a total of 16 histone H2A canonical genes are present in human genome encoding for 12 types of H2A proteins differing in few amino acids. The information regarding histone genes and isoforms has been tabulated in **Table 1.2**. There are three clusters of canonical histone gene present in humans at chromosome number 1 (cluster 2 and 3) and 6 (cluster 1). In rat clusters are on chromosome 2, 10 and 17. Apart from histones present in clusters there are other types of histone genes present as a single copy across the genome and encode of proteins known as 'histone variants'.

| Histone subtype | Genes | Isoforms |
| --- | --- | --- |
| H1 | 6 | 6 |
| H2A | 16 | 12 |
| H2B | 22 | 18 |
| H3 | 14 | 3 |
| H4 | 6 | 3 |

Table 1.2. Histone Isoforms present in human genome.

These proteins are synthesised and deposited in a replication independent manner i.e., in all the phases of cell cycle. Replacement with histone variants/isoforms leads to the formation of a nucleosome having distinct functions compared to existing nucleosome with canonical histones inside the cell. Histone variants have been associated with number of cellular functions such as DNA repair, transcription regulation, and replication thus, presenting their emerging importance in various disease conditions as well, markedly cancer. Investigations into the evolution, structure, and metabolism of histone variants provide a foundation for understanding the participation of chromatin in important cellular processes and in epigenetic memory. The emerging view from these studies is that histone variants and the processes that deposit them into nucleosomes provide a primary differentiation of chromatin that might serve as the basis for epigenetic processes. The four core histones, H2A, H2B, H3, and H4, differ with respect to their propensity to diversify into variants. For example, humans have only one H4 isotype but

several H2A paralogs with different properties and functions. Evidently, the different positions of the core histones within the nucleosome particle have subjected them to different evolutionary forces, leading to important diversifications of H2A and H3 but not to H2B and H4 **[Figure 1.9]**.
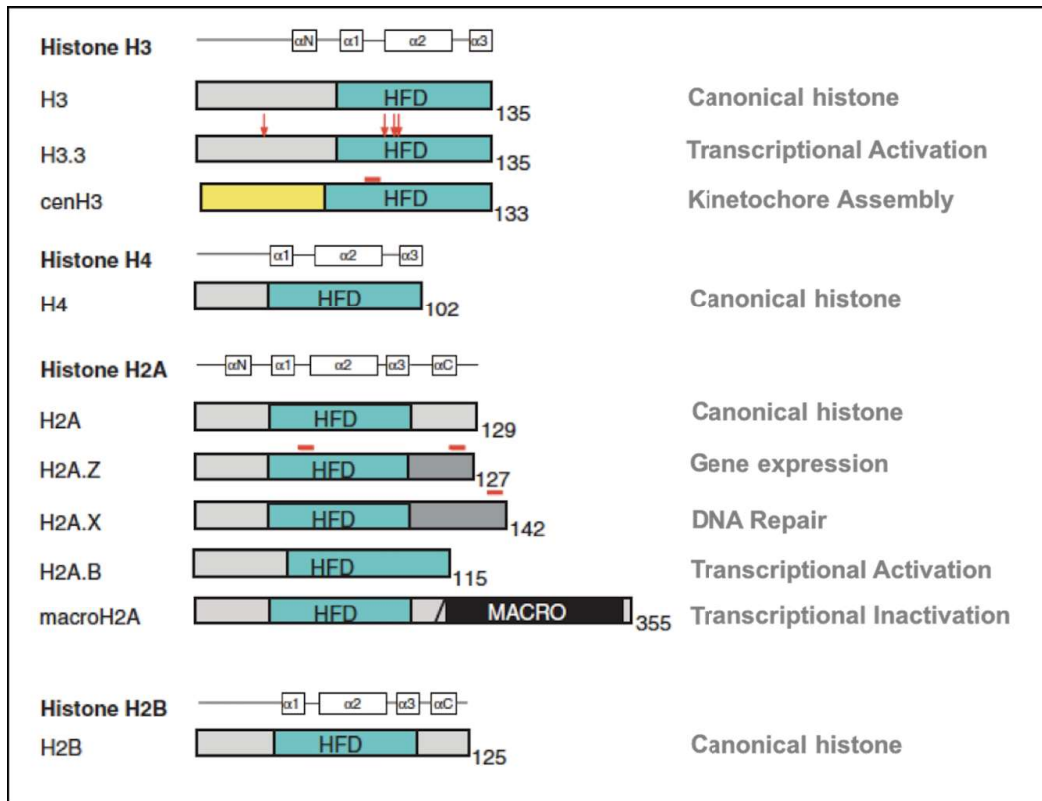


**Figure 1.9. Histone variants and their functions.** Histone variants. Protein domain structure for the core histones (H3, H4, H2A, and H2B), linker histone H1, and variants of histones H3 and H2A. The histone-fold domain (HFD) is where histone dimerization occurs. Regions of sequence variation in histone variants are indicated in red. The respective functions are also depicted for each histone in the diagram.
*Adapted from: Steven Henikoff and M. Mitchell Smith. Histone Variants and Epigenetics. Cold Spring Harb Perspect Biol 2015;7:a019364.*

For example, the histone variants H2A.Z and H3.3 are replication-independent histone variants. In addition, there are variants like H2A.X which exhibit both replication-dependent as well as independent expression. For example, H2A.X nucleosome marks the site for recruitment of DNA damage proteins[34]. Similarly, histone H3 variants (H3.1, H3.2, H3.3 and CENPA) have differential functions with CENPA being centromeric histone enables kinetochore assembly[40].

## 1.7. Histone Chaperones and Cargo selectivity

Histone chaperones can be illustrated on the basis of their histone binding selectivity and thus deposition, using which they can be differentiated into those favourably interacting with H3-H4 from those that prefer H2A-H2B. Some of the histone chaperones along with their specificity and functions are tabulated in **Table 1.3.**

| Histone Chaperone | Histone Selectivity | Functions |
|---|---|---|
| Asf1 | H3/H4 | Histone import, histone transfer to CAF-1 and HIRA, Regulation of H3K56ac |
| CAF-1 | H3.2/H4, H3.2/H4 | H3.1–H4 deposition, Heterochromatin formation, repair |
| Daxx | H3.3/H4 | H3.3–H4 deposition at telomeric heterochromatin |
| DEK | H3.3/H4 | H3.3–H4 deposition, maintenance of heterochromatin |
| NASP | H1, H3/H4 | H1 and H3/H4 supply and turnover |
| NPM | H1, H3/H4 | H1 and H3/H4 deposition, Ribosome assembly, genomic stability |
| NAP1 | H2A/H2B, H1 | Histone H2Avariant exchange, Nucleosome sliding, Histone shuttling |
| FACT | H2A/H2B | H2A/H2B deposition, Transcription |

**Table 1.3. Major histone Chaperones and their functions.** Asf1- Anti silencing factor 1; CAF-1 – Chromatin assembly factor; Daxx-Death domain associated protein; NPM – Nucleplasmin; NAP-1 – Nucleosome assembly protein-1; FACT- Facilitates active transcription.
*Adapted from: Eitoku (2008). Histone Chaperones: 30 years from isolation to elucidation of mechanisms of nucleosome assembly and disassembly. Cell. Mol. Life. Sci. 65(3):414-44DOI: 10.1007/s00018-007-7305-6*

Some of the very well-studied chaperones of H2A/H2B includes NAP1 (nucleosome assembly protein-1), first identified in HeLa cell extracts as an activity that facilitates the in vitro reconstitution of nucleosomes using pure histones in combination with other factors[15]. Another H2A/H2B chaperone is FACT (Facilitates Active Chromatin Transcription) complex composed of two subunits hSpt16 and SSRP1, identified initially as a factor indispensable for transcriptional elongation through chromatin[15]. Later it has been shown to form stable

complexes with the histone H2A-H2B dimer and functions through restructuring of nucleosomes within the ORFs of actively transcribed genes[15]. Examples of H3/H4 chaperones are CAF-1 (Chromatin Assembly Factor) complex consisting of three subunits: p150, p60 and p48, formerly identified by complementation as a factor participating in the assembly of chromatin during SV40 origin-dependent DNA replication in human cell extracts[15]. N1/N2 is also an H3/H4 chaperone, isolated first from oocytes of *X. laevis*[41]. Apart from the core histones, linker histone H1 also has a chaperone- NASP (Nuclear Autoantigenic Sperm Protein), aiding its deposition on to the DNA[42].

Formerly chaperones were thought to be as mere "histone carriers/vehicles" but now with accumulating evidence they are known to be key players at all phases of histone existence. Chaperones interact with histones upon their synthesis thus preventing their aggregation and interaction with other cellular moieties[43]. Also guide them into the nucleus, and help in their specific association with DNA during different processes involving DNA-replication [42,44], repair [44] and transcription [45].

Histone variants do not just have specialized functions but their localization and recruitment onto the chromatin is very specifically regulated by different set of histone chaperones. For example, incorporation of histone H3 variants H3.1 and H3.2 is bought by CAF-1 complex during the S- phase of the cell cycle, whereas for histone variant deposition like, H3.3 - HIRA (Histone Regulator A) and DAXX are responsible.

Other histone variant specific chaperones include Chz1 (Chaperone of H2A.Z/H2B) of yeast[9], ANP32E a specific H2A.Z chaperone in humans[9], and HJURP for chaperoning CENPA histones[9]. These specific chaperones also determine the localization pattern though out the genome. They bring about these varied functions by interacting with many cellular factors like check point proteins, transcription factors, with the help of which they determine the site and

position of nucleosome assembly/disassembly and thus affecting gene regulation [**Figure 1.10**]. Therefore, from being just an observer to an active participant, chaperones have evolved as the crucial component in maintaining chromatin integrity and dynamics.
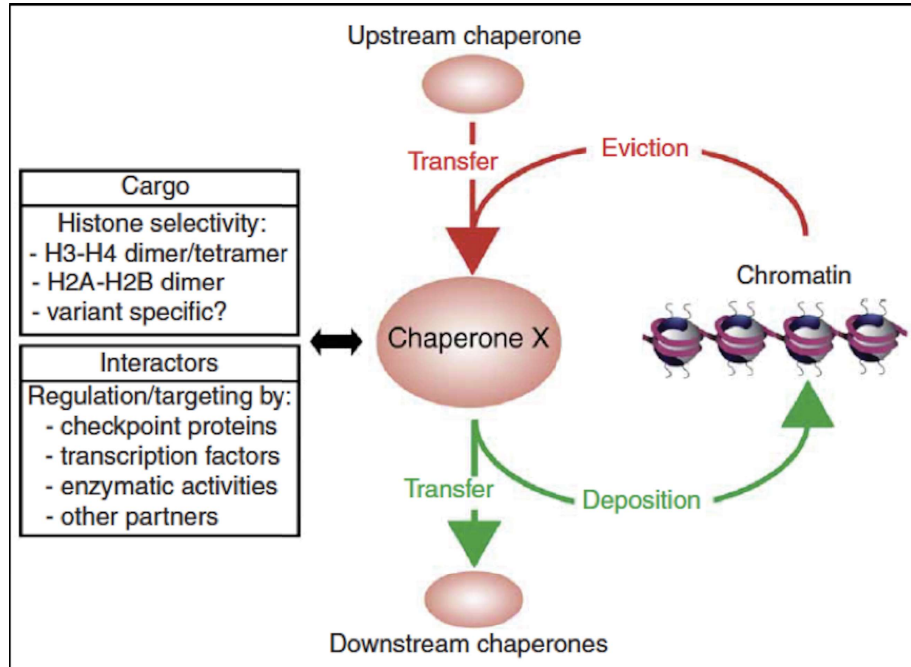


**Figure 1.10. Determinants of chaperone selectivity.** Schematic representation of the relationship of a given histone chaperone to its network of binding partners. The chaperone will have various degrees of selectivity toward specific histone dimers, or possibly tetramers, which it will accept from, or transfer to, other chaperones. Alternatively, the chaperone could also accept histones immediately after their eviction from chromatin or transfer histones directly onto DNA in a deposition reaction. The histone chaperone's function will be regulated and targeted through its binding partners, which are involved in various cellular processes.
*Adapted from: Leanne De Koning, et al. (2007). Histone chaperones: an escort network regulating histone traffic. Nature structural and molecular biology. 14, 997 - 1007. DOI: 10.1038/nsmb1318*

## 1.8. Epigenetics and Cancer

Cancer is ultimately a disease of gene expression in which the complex networks governing homeostasis in multicellular organisms become deranged, allowing cells to grow without reference to the needs of the organism as a whole. Historically, research has focused on the genetic basis of cancer, particularly, in terms of how mutational activation of oncogenes or inactivation of tumor-suppressor genes (TSGs) underpins above pathway changes. However, since the 1990s, a growing research endeavor has centered on the recognition that heritable changes, regulated by epigenetic alterations, may also be critical for the evolution of all human

cancer types. Epigenetic alterations can be observed as abnormal patterns of DNA methylation, disrupted patterns of histone posttranslational modifications (PTMs), and changes in chromatin composition and/or organization. Changes in the epigenome largely occur through disrupting the epigenetic machinery, and the different elements of the epigenetic machinery that are now known to be perturbed in cancer [**Figure 1.11**].
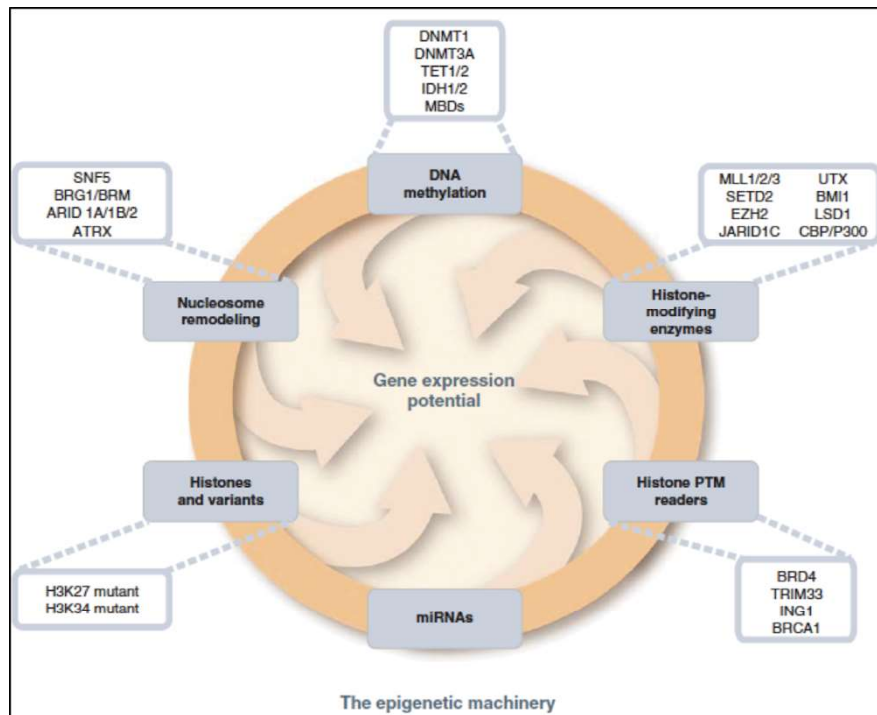


**Figure 1.11. Epigenetic modifiers in cancer.** The drawing shows the input of epigenetic processes in specifying gene expression patterns. Recent whole-exome sequencing studies show that mutations in various classes of epigenetic modifiers are frequently observed in many types of cancers, further highlighting the cross talk between genetics and epigenetics. The mutations of epigenetic modifiers potentially cause genome-wide epigenetic alterations in cancer. MBDs, methylcytosine-binding proteins; PTM, posttranslational modification.
*Adapted from: Stephen B. Baylin and Peter A. Jones. Epigenetic Determinants of Cancer. Cold Spring Harb Perspect Biol 2016;8:a019505.*

These epigenomic changes not only are associated with altered patterns of expression for otherwise wild-type genes, but, in some cases, may also be causal to their changed expression state. The recognition of an epigenetic component in tumorigenesis, or the existence of a cancer "epigenome," has led to new opportunities for the understanding, detection, treatment, and prevention of cancer. The association of histone variants, isoforms, their PTMs and chaperones to cancer has been discussed in detail.

# 1.9. Histone Variants/Isoforms and Cancer

Consistent with their role in governing gene expression and other chromatin mediated processes, some of the histone variants have been found to be aberrantly expressed in cancer [**Table 1.4**]. Emerging evidence points towards the role for histone variants in contributing to tumor progression. This is further emphasized with the recent findings of cancer-associated mutation in H3.3 variant gene. Some of the reports linking histone variants and cancer are discussed below.

| Variant | Cancer type | Dysfunction | Proposed Mechanism |
|---|---|---|---|
| H2A.Z (H2A.Z.1) | Colorectal cancer | Overexpression | N.D. |
| | Undifferentiated cancers | Overexpression | N.D. |
| | Metastatic breast carcinoma | Overexpression | N.D. |
| | Primary breast cancer | Overexpression | ER alpha- and Myc-dependent upregulation |
| | Breast cancer (MCF7 cell line) | Overexpression | Increased proliferation |
| | Breast cancer | Overexpression | H2A.Z recruited at promoters of ER alpha target genes |
| | Prostate cancer (LNCaP cell line) | Overexpression | Myc-mediated H2AFZ upregulation |
| | Prostate cancer (LNCap xenograft) | N.D. | H2A.Zub evicted from PSA promoter/enhancer upon activation |
| | Prostate cancer (LNCaP cell line) | N.D. | H2A.Zac associated with oncogene activation, unmodified H2A.Z with tumor-suppressor silencing |
| H2A.X | B-CLL and T-PLL | Translocations and deletions chr 11q23 | Increased genome instability |
| | Head and neck squamous cell carcinoma | Gene deletion | Increased genome instability |
| | Non-Hodgkin lymphoma | Gene mutation | Increased genome instability |
| | Gastrointestinal stromal tumor | Upregulation | Promote apoptosis upon the treatment with a kinase inhibitor |
| | Breast cancer | Gene deletion | Increased genome instability |
| | Lung cancer | Reduced protein levels/splicing defects | Suppression of cell proliferation via reduced PARP-1 |
| mH2A.1 | Breast cancer | Reduced protein levels/splicing defects | N.D. |
| | Melanoma | Transcriptional downregulation | Upregulation of CDK8 |
| | Testicular, bladder, ovarian, cervical, endometrial cancers | Splicing defects | N.D. |
| | Colon cancer | Reduced protein levels and splicing defects | N.D. |
| mH2A.2 | Lung | Reduced protein levels | N.D. |
| | Melanoma | Transcriptional downregulation | Upregulation of CDK8 |

| | | | |
|---|---|---|---|
| CENP-A | Colorectal cancer | Overexpression | Aneuploidy |
| | Invasive testicular germ cell tumors | Overexpression | N.D. |
| | HCC | Overexpression | Deregulation of cell cycle and apoptotic genes |
| | Breast cancer | Overexpression | N.D. |
| | Lung adenocarcinoma | Overexpression | N.D. |
| H3.3 | Carcinoma of the esophagus | Overexpression | N.D. |
| | Lung | Overexpression | Upregulation of EMT genes |
| | Adult Glioma | Transcriptional downregulation | Promotes differentiation |
| | Pediatric GBM | Mutation (K27M, G34V/R) | N.D. |

**Table 1.4. Histone variants in cancer.** Cancer associated variants and the proposed mechanism. *Adapted from Angelica, M.D., Fong, Y., 2008. NIH Public Access. October 141, 520–529. doi:10.1016/j.surg.2006*

## 1.9.1. H3.3

H3.3 (136 amino acids) has only four amino acid differences with H3.2 (at positions 31, 87, 89 and 90) and five with H3.1 (with an additional difference at amino acid 96). These residues have been proposed to account for particular properties of histone H3.3. The residues 87, 89 and 90 are thought to participate in the regulation of histone-histone interaction stability[46]. In support of this, H3.3 containing nucleosomes are highly sensitive to salt-dependent disruption[47]. Multiple alignment of H3 proteins is shown in **Figure 1.12**



```
                                         31
                                         ⌄
H3.3    MARTKQTARKSTGGKAPRKQLATKAARKSAPSTGGVKKPHRYRPGTVALREIRRYQKSTE
H3.1    MARTKQTARKSTGGKAPRKQLATKAARKSAPATGGVKKPHRYRPGTVALREIRRYQKSTE
H3.2    MARTKQTARKSTGGKAPRKQLATKAARKSAPATGGVKKPHRYRPGTVALREIRRYQKSTE
        *****************************.*****************************
                                     87 8990    96
                                     ⌄ ⌄⌄     ⌄
H3.3    LLIRKLPFQRLVREIAQDFKTDLRFQSAAIGALQEASEAYLVGLFEDTNLCAIHAKRVTI
H3.1    LLIRKLPFQRLVREIAQDFKTDLRFQSSAVMALQEACEAYLVGLFEDTNLCAIHAKRVTI
H3.2    LLIRKLPFQRLVREIAQDFKTDLRFQSSAVMALQEASEAYLVGLFEDTNLCAIHAKRVTI
        *************************:*: *****.*********************

H3.3    MPKDIQLARRIRGERA
H3.1    MPKDIQLARRIRGERA
H3.2    MPKDIQLARRIRGERA
        ****************
```

**Figure 1.12. Multiple alignment of H3 variants.** Red arrows mark the amino acid changes.

Apart from the fact that serine 31, which is specifically found in H3.3, can be phosphorylated[48], H3.3 relate to the increased proportion of PTMs associated with active chromatin such as acetylation and H3K4 methylation[49,50,51]. Consistent with this, chromatin immunoprecipitation has revealed specific enrichment of H3.3 throughout the gene body of transcribed genes as well as at the promoter regions[52,53]. Notably, H3.3 enrichment at promoters has been observed not only at active but also at inactive genes, possibly accounting for a poised state of these genes[54]. As might be expected H3.3 has different set of proteins which deposit it in different chromatin territories. The H3.3 chaperone HIRA is responsible for the deposition of H3.3 at active chromatin regions[55,56] whereas the DAXX/ATRX complex deposits H3.3 at pericentric heterochromatin and telomeric regions[57,58].

A breakthrough finding which reemphasizes the role of histone variants in development of cancer is the driver mutations in H3.3 identified in pediatric gliobastoma[59]. To better describe these H3.3 mutations the word 'Oncohistone' has been coined. Somatic mutations in the H3.3-ATRX-DAXX chromatin remodeling pathway were identified in 44% of tumors (21/48). Recurrent mutations in H3F3A, which encodes the replication-independent histone variant H3.3, were observed in 31% of tumors, and led to amino acid substitutions at two critical positions within the histone tail (K27M, G34R/G34V) involved in key regulatory post-translational modifications[59]. Mutations in ATRX and DAXX, encoding two subunits of a chromatin remodeling complex required for H3.3 incorporation at pericentric heterochromatin and telomeres, were identified in 31% of samples overall, and in 100% of tumors harboring a G34R or G34V H3.3 mutation.

Not only mutations but deregulation of H3.3 levels has also been seen in certain cancers. MLL5 mediated decrease in H3.3 expression favors self-renewal properties of adult glioblastoma (glioblastoma multiforme [GBM]) cells and phenocopies pediatric GBM with H3.3 mutations, indicating potential therapeutic strategies for adult GBM[60]. Furthermore, a recent study has

highlighted overexpression H3.3 is associated with lung cancer progression and promotes lung

cancer cell migration by activating metastasis related genes through the occupation of intronic

regions[61]. H3.3 is incorporated into promoters of developmentally regulated genes, and these

loci bear both H3K27Me3 and H3K4Me3 marks, marking these promoters as bivalent domains

poised for transcriptional induction[62]. H3.3 is required for the establishment of the H3K27Me3

mark in these domains and it is easy to envisage that a switch to K27Ac or possibly K36Me3

either by recruitment of mutated H3.3 or global decrease in H3.3 may tip the balance to

activation of aberrant developmental programs leading to tumorigenesis [**Figure 1.13**].
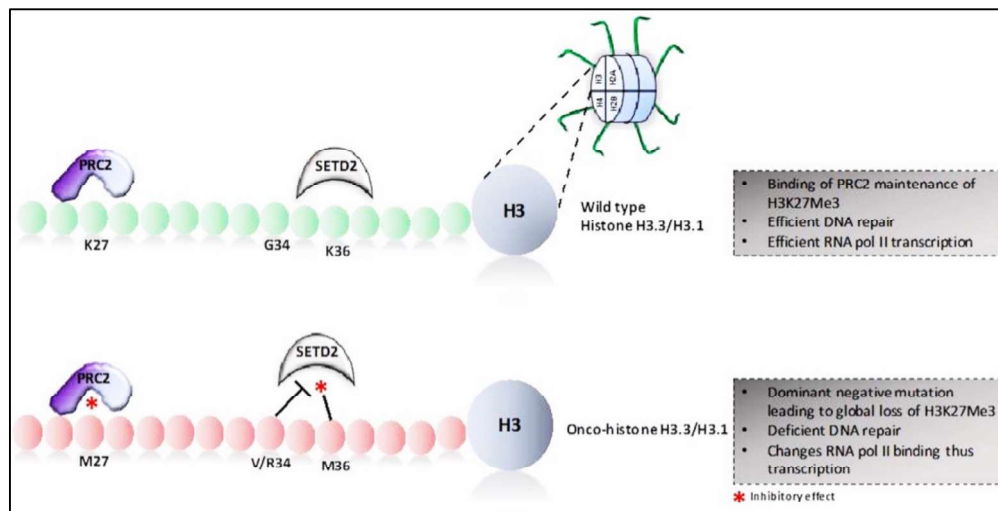


**Figure 1.13. Effect of oncohistone H3 on epigenome of cancer cells.** Replacement of wild-type H3 (harbouring K27, K36, and G34 residues) with oncohistones (harbouring M27, M36, and V/R/W/L34 residues) leads to inhibitory effect on the activity of the writers, polycomb-repressive complex 2 and SETD2 enzymes, thus leading to alteration of epigenome in favor of oncogenesis
*Adapted from: Divya Reddy and Sanjay Gupta. Histone Variant H3.3 and its Future Prospects in Cancer Clinic. J Radiat Cancer Res 2017; 8:77-81. DOI:10.4103/jrcr.jrcr_4_17.*

## 1.9.2. H2A.Z

H2A.Z is essential for early embryonic development and is the only histone variant that has

been shown to be indispensable for survival[63]. It's a 128 amino acid containing protein and its

homology with canonical H2A is less than 60%, however, it is highly conserved from yeast to

human[64,65]. H2A.Z has been implicated to participate in many diverse biological processes such

as transcription regulation[66], DNA repair[67], heterochromatin formation[70] and chromosome

segregation[69]. H2A.Z preferentially localizes at the transcription start site (TSS) where it frequently flanks nucleosome-deficient regions[70,71,66]. Notably, the TSS of an active gene comprises a labile histone H3.3–H2A.Z double-variant nucleosome[72] which could only be purified under conditions of very low ionic strength. These double-variant nucleosomes also marks CTCF insulator binding factor sites[72]. The presence of H2A.Z at the −1 and +1 nucleosomes adjacent to the transcription start site (TSS) has been linked to dynamic changes in gene expression[73,74]. H2A.Z protects euchromatin from the ectopic spread of silent heterochromatin[75]. In H2A.Z$^{-/-}$ cells, Sir2 and Sir3 spread into flanking euchromatic regions, producing changes in histone H4 acetylation and H3 4-methylation indicative of ectopic heterochromatin formation.

Overexpression and redistribution of H2A.Z have been reported in cancer[76,77,78]. H2A.Z is upregulated in bladder cancer and stimulates cell proliferation[79]. Further, H2A.Z redistribution correlates with increased expression of proliferation related genes[79]. In prostate cancer, there is an H2A.Z reorganization that poises the oncogene promoters for activation. Furthermore, the overall levels of H2A.Z decrease at the transcription start sites (TSSs) of such promoters upon activation which is accompanied by a gain of acetylated H2A.Z[80]. In this way, in the presence of androgen H2A.Z operates as a facilitator of transcription that is subject to a rapid dynamic turnover once the gene is undergoing cycles of transcription[81].

High expression of H2A.Z is ubiquitously detected in the progression of breast cancer[78]. Importantly, H2A.Z expression is significantly associated with lymph node metastasis and patient survival. This makes H2A.Z an excellent target for diagnostic and therapeutic interventions. Expression of TFF1 has been used as a marker for breast cancer and ER- positive tumors[82]. Interestingly, H2A.Z is also associated with estrogen responsive element (ERE) of the TFF1 promoter. Upon stimulation by estrogen, H2A.Z disassociates from the ERE regions and deposits at the proximal regions of promoter leading to poising of gene for expression[83].

Similarly, H2A.Z has been shown to incorporate within the promoter of the cathepsin D gene that upregulates its expression upon estrogen stimulation[84]. Further, aberrant expression of H2A.Z facilitates abnormal cellular proliferation through c-Myc, p21/p53, and estrogen target genes expression. Collectively, these findings suggest that H2A.Z overexpression causes increased breast cancer proliferation. To restore H2A.Z function, two potential drug treatments for cancer therapies has been suggested: targeting c-Myc transcription factor (using inhibitor 10058-F4) and the H2A.Z-remodelling enzyme, p400/Tip60 (using anacardic acid)[85].

### 1.9.3. macroH2A

Histone variant macroH2A are characterized by their large size (368 amino acids), which is three times that of canonical histone H2A[86]. There are two macroH2A genes in the mouse[87,86], termed macroH2A.1 and macroH2A.2[88]. MacroH2A is unique among variants in that it possesses multiple domains, including the histone domain, a 38 residue linker sequence, and a large "macro-domain". MacroH2A incorporate into chromatin via their histone H2A- like region. This is attached via a linker region to the macro domain that projects out of the nucleosome[89]. MacroH2A is generally associated with heterochromatin and transcriptional repression[90]. Consistent with this, macroH2A exists in large populations in the inactive X chromosome of females but is scarcely found in active genes[91]. On its own, the histone domain is sufficient for reducing transcriptional activity *in vivo* and increasing the stability of the nucleosome complex[92]. MacroH2A has been demonstrated to interfere with transcription factor binding and SWI/SNF nucleosome remodeling[92].

Evidences suggest that macroH2A acts as a tumor suppressor as it is frequently found to be downregulated in a variety of cancers. First report to suggest involvement of macroH2A in cancer progression came from human breast and lung tumor biopsies where macroH2A1.1 and macroH2A2 expression inversely correlated with proliferation[93]. Subsequently, macroH2A was found to be downregulated in melanoma and acts as a tumor suppressor by binding to

CDK8 promoter and suppresses tumor progression of malignant melanoma[94]. Loss of macroH2A1.2 isoforms positively correlated with increasing malignant phenotype of melanoma cells in culture and human tissue samples. Knockdown of macroH2A isoforms in melanoma cells of low malignancy results in significantly increased proliferation and migration.

However, the role of macroH2A1.2 appears to be more complex than generally being a tumor suppressor. As discussed, in favor of a tumor suppressive function, macroH2A1.2 was found to reduce metastatic potential of melanoma cells[94]. In contrast, in breast cancer cells macroH2A1.2 increased migration, invasion and growth in attachment-free conditions[95]. Thus, macroH2A1.2 function and gene targets may have context dependence or cell type specificity.

## 1.9.4. H2A isoforms and cancer

In cancer, the expression level of H2A isoforms have been reported to alter. Earlier studies from our lab have shown the differential expression of two major H2A isoforms, H2A.1 and H2A.2, in rat hepatocellular carcinoma model system. The study showed for the first-time *in vivo* overexpression of a major histone H2A isoform H2A.1 and a decrease in H2A.2 at protein and mRNA in HCC. H2A.1 and H2A.2 are highly homologous, replication- dependent, non-allelic variants of histone H2A differing at only three amino acid positions[96]. We further showed that these isoforms alter the gene expression pattern by influencing nucleosome stability[7].

In human cancers as well, the expression of H2A1C isoform is downregulated in chronic lymphocytic leukemia and gall bladder cancer[2,97]. In 4 normal individuals and 40 CLL patients, a significant decrease in the relative abundance of histone H2A1C was observed in primary CLL cells as compared to normal B cells[97]. Similar changes in the abundance of H2A isoforms are also associated with the proliferation and tumorigenicity of bladder cancer cells [2]. The

regulation of replication-dependent histone H2A expression was also reported to occur on a gene-specific level[2]. Interestingly, later on with a larger cohort of samples, H2A1C expression was conversely reported to be up regulated in CLL. In breast cancer H2A1C is upregulated and controls ER target genes in ER positive breast cancer cell lines[5].

## 1.10. Histone Chaperones and Cancer

Any mis-positioning of nucleosomes on to a stretch of DNA results in defect in gene expression and at times genome instability and cancer. Therefore, it is not incorrect to assume that mis-regulation of histone chaperones or histone-modifying enzymes regulating nucleosome assembly/disassembly may stimulate development of human disease. Some chaperones associated with cancer are tabulated in **Table 1.5.**

| Histone Chaperone | Histone Selectivity | Dysfunction | Proposed Mechanism |
|---|---|---|---|
| CAF-1 | Breast, Renal, Endometrial and Cervical carcinomas | Upregulated | Maintaining chromatin stability during DNA replication and repair |
| ASF1 | Breast | Upregulated | Increases Cell proliferation and suppresses senescence |
| DEK | Retinoblastoma, Melanoma, Ovarian and Lung cancer | Upregulated | Increases DNA repair and invasiveness |
| DAXX | Pancreatic neuroendocrine tumors, Pediatric glioblastoma and AML | Mutated | Perturbed telomeres and altered transcription profiles |
| NPM1 | AML, Colorectal cancer | Upregulated, Mutated and translocated | Promote tumor growth by inactivation of the tumor suppressor p53/ARF pathway |

**Table 1.5. Histone Chaperones in Cancer.** Cancer associated Chaperones and their proposed function. *Adapted from: Mina Rafaeii et al., (2008). Histone Chaperones, Epigenetics and cancer. Systems Analysis of Chromatin-Related Protein 1 Complexes in Cancer. Springer Books. DOI 10.1007/978-1-4614-7931-4_15*

FACT complex (H2A/H2B chaperone) is expressed at higher levels in tumor cell lines than in normal cells *in vitro* and its knockdown lead to reduced growth and survival of tumor cells[98]. In addition, FACT expression was found to be elevated during the development of mammary carcinomas in transgenic mice expressing the Her2/neu protooncogene[99]. Also, FACT

expression is seen to be elevated upon *in vitro* transformation of fibroblasts and epithelial cells by various agents indicating its requirement for transformation, but its overexpression cannot substitute for the requirement of H-RasV12[100].

Overexpression of the DEK, a histone chaperone for H3.3 has been reported in a number of cancers like glioblastoma, melanoma, colorectal and bladder carcinoma and is known to play major role in promoting epithelial transformation[101,102]. DEK inhibits senescence and apoptosis via the destabilization of p53, hinting its role in carcinogenesis[103]. In human promyelocytic HL-60 cells differentiation led to DEK down regulation[104]. Conversely, upon overexpression of the DEK, differentiation programs can be neutralized, favoring oncogenic transformation. A direct proof of DEK as "oncogene" has developed when it was seen that papilloma formation was significantly decreased in DEK knockout mice compared to wild type animals and heterozygote controls[105]. Amplifications and copy number increase of the DEK gene were also found in a variety of malignancies, particularly in bladder cancer, melanoma and retinoblastoma[106]. Apart from overexpression, certain mutations within chaperones and their associated proteins have also been related to cancer. Mutations in Daxx-ATRX–H3.3 pathway have been observed in pancreatic neuroendocrine tumors[107]. Such mutations have also been identified in pediatric glioblastoma tumor samples. Because of their high incidence these mutations are now called as the "driver mutations" for promoting cancers[108].

## 1.11. Histone PTMs and Cancer

Alterations in the patterns of histone PTMs have been extensively linked to cancer, both at the global level across the genome and at specific gene loci. Global loss of acetylation of histone H4 at lysine 16 (H4K16Ac), together with loss of trimethylation of histone H4 at lysine 20 (H4K20Me3) has been observed along with DNA hypomethylation at repetitive DNA sequences in various primary tumors and were the first histone marks reported to be

deregulated in cancer cells. Unlike most histone modifications, H4K16Ac is unique for regulating higher-order chromatin structures beyond the level of nucleosomes[109]. Loss of this mark may bring a 'compact' chromatin conformation, which might contribute to genome instability[110].Alterations in H3K9 and H3K27 methylation patterns are associated with aberrant gene silencing in various forms of cancer[111,112]. A very important association has been made in terms of phosphorylation of H3S10, as the only histone marks directly associated with cellular transformation[113]. Further, Mitogen- and stress-activated kinase 1 (MSK1) has been shown to phosphorylate H3S10 in TPA and EGF mediated cellular transformation[114]. Some of the established histone PTM deregulation and their role in oncogenesis are highlighted in **Figure 1.14.**



**Figure 1.14. Functional consequences of histone onco-modifications.** Specific histone modifications, which have been shown to occur in cancer cells, are displayed and their implication in cancer associated processes, such as aberrant gene expression (in green), genomic instability (in purple), DNA repair (in orange) and cell cycle checkpoint alterations (in blue). Modification upregulated are in green and downregulated in red.
*Adapted from: J Fullgrabe, et al., Histone onco-modifications. Oncogene. 2011. 30, 3391–3403. DOI:10.1038/onc.2011.121*

## 1.12. Histone PTMs and clinical relevance

Decades of research have identified a battery of histone PTMs to be altered in cancer, however only few have reached clinics owing to the issues of sensitivity and specificity of the antibodies used. The discovery of the presence of DNA and circulating nucleosomes in serum has led to the foundation of identifying epigenetic markers such as DNA methylation and histone post-translational modification for cancer diagnosis[115]. Presence of histone proteins is not known in

fecal and urine samples; therefore, histone post translational modifications have been utilized as cancer diagnostic markers using circulating nucleosomes (cNUCs) in serum samples. Ugur *et al.* investigated the correlation between the H3K9Me3 and H4K20Me3 of cNUCs in healthy subjects and patients with colorectal cancer and multiple myeloma and found low level of these PTMs in cancer[116]. ChIP based analysis of circulating nucleosomes in serum samples has reported a low level of H3K9Me3 and H4K20Me3 in patients with colorectal, pancreatic, breast and lung cancer compared to healthy control[117]. Moreover, H3K9Me3 and H4K20Me3 have been found to be lower at the pericentromeric satellite II repeat in patients with CRC when compared with healthy controls or patients with multiple myeloma[118]. In summary, identification of histone PTMs from serum isolated circulating nucleosomes have open the doors of immense possibility that blood samples collected by cancer patients can also be used for histone PTM based cancer diagnosis.

In cancer, to date, histones PTMs have been mostly studied for their potential as prognostic marker **[Table 1.6]**. The first report in this area which strongly suggested the utility of histone PTMs in cancer diagnosis showed a loss of H4K16Ac and H4K20Me3 in several cancers and established these two marks as a 'epigenetic hallmark of tumor'[119]. A study on prostate cancer showed a positive correlation of H3K18Ac, H4K12Ac and H4R3Me2 with increasing tumor grade[120]. Moreover, independently of other clinical and pathologic parameters, high rate of tumor recurrence in low-grade prostate carcinoma patients is associated with low level of H3K4Me2 [120]. A decrease of H3K4Me2/Me3 is observed in a range of neoplastic tissues such as non-small cell lung cancer[121], breast cancer[122], renal cell carcinoma[123] and pancreatic adenocarcinoma[124] serving as a predictor of clinical outcomes[121]. Acetylation of histone H3K9 has shown ambiguous results with the increase in some and decrease in other cancers. Decrease of H3K9Ac in prostate and ovarian tumors has been linked with tumor progression, histological

grading and clinical stage[124]. In agreement, a decrease in H3K9Ac is coupled with a poor prognosis for these patients.

| Histone PTM | Writer | Eraser | Function | Diagnosis/Prognosis/treatment |
|---|---|---|---|---|
| H3K9Ac | GCN5 | SIRT1, SIRT6 | Transcription initiation | Diagnosis: ? <br><br> Prognosis: Lung, Breast, Ovary <br><br> Treatment: ? |
| H3K18Ac | CBP/P300 | ? | Transcription initiation | Diagnosis: ? <br><br> Prognosis: Lung, Breast, Prostate, Oesophagus <br><br> Treatment: ? |
| H4K5Ac | CBP/P300, HAT1, TIP60, HB01 | ? | Transcription Activation | Diagnosis: ? <br><br> Prognosis: Lung <br><br> Treatment: ? |
| H4K8Ac | TIP60, HB01 | ? | Transcription Activation | Diagnosis: ? <br><br> Prognosis: Lung <br><br> Treatment: ? |
| H4K16Ac | TIP60, hMOF | SIRT1, SIRT2 | Transcription Activation | Diagnosis: Colorectal <br><br> Prognosis: Lung, breast <br><br> Treatment: ? |
| H3K4Me | SETD1A, SETD1B, ASH1L, MLL, MLL2, MLL3, MLL4, SETD7 | KDM1A, KDM1B, KDM5B, NO66 | Transcription Activation | Diagnosis: ? <br><br> Prognosis: Prostate, Kidney <br><br> Treatment: ? |
| H3K4Me2 | SETD1A, SETD1B, MLL, MLL2, MLL3, MLL4, SMYD3 | KDM1A, KDM1B, KDM5A, KDM5B, KDM5C, KDM5D, NO66 | Transcription Activation | Diagnosis: ? <br><br> Prognosis: Prostate, Kidney, Lung, Breast, Pancreatic, Liver <br><br> Treatment: ? |
| H3K4Me3 | SETD1A, SETD1B, ASH1L, MLL, MLL2, MLL3, MLL4, SMYD3, PRDM2 | KDM2B, KDM5A, KDM5B, KDM5C, KDM5D, NO66 | Transcription Elongation | Diagnosis: ? <br><br> Prognosis: Prostate, Kidney, Liver <br><br> Treatment: ? |
| H3K9Me | SETDB1, G9a, EHMT1, PRDM2 | KDM3A, KDM3B, PHF8, JHDM1D | Transcription Initiation | Diagnosis: Myeloma, <br><br> Prognosis: Prostate, Kidney, Pancreatic <br><br> Treatment: ? |
| H3K9Me2 | SUV39H1, SUV39H2, SETDB1, G9a, EHMT1, PRDM2 | KDM3A, KDM3B, KDM4A, KDM4B, KDM4C, KDM4D, PHF8, KDM1A, JHDM1D | Transcription Repression | Diagnosis: ? <br><br> Prognosis: Prostate, Pancreatic <br><br> Treatment: ? |

| | | | | |
|---|---|---|---|---|
| **H3K9Me3** | SUV39H1, SUV39H2, SETDB1, PRDM2 | KDM3B, KDM4A, KDM4C, KDM4D | Transcription Repression | Diagnosis: Colorectal, Myeloma, Prostate, Breast and Lung<br><br>Prognosis: Prostate, Lung, Breast, Leukaemia, Stomach<br><br>Treatment: ? |
| **H3K27Me** | EZH2, EZH1 | JHDM1D | Transcription Activation | Diagnosis: ?<br><br>Prognosis: Kidney<br><br>Treatment: ? |
| **H3K27Me3** | EZH2, EZH1 | KDM6A, KDM6B | Transcription Repression | Diagnosis: ?<br><br>Prognosis: Prostate, Liver, Breast, Leukaemia, Stomach, Oesophagus, Ovarian<br><br>Treatment: ? |
| **H4K20Me3** | SUV420H1, SUV420H2 | ? | Transcription Repression | Diagnosis: Colorectal, Myeloma, Prostate, Breast and Lung<br><br>Prognosis: Breast, Lymphoma, Colon, ovarian<br><br>Treatment: ? |

**Table 1.6. Histone PTMs in clinics.** Association of global histone PTMs with cancer and their current status in clinical applications.
*Adapted from: Shafqat Ali Khan, Divya Reddy, Sanjay Gupta. Global histone post-translational modifications and cancer: Biomarkers for diagnosis, prognosis and treatment? World J Biol Chem. (2015) November 26; 6(4): 333-345. DOI: 10.4331/wjbc.v6.i4.333*

Patients with non-small cell lung adenocarcinoma exhibited better prognosis on the reduction of H3K9Ac expression level[125]. In contrast, in hepatocellular carcinoma an increase in H3K9Ac levels was reported[126]. Methylation of the same residue K9 of histone H3 requires loss of H3K9Ac and is also linked to number of cancers. An increase in H3K9 methylation, leading to aberrant gene silencing, has been found in various forms of cancer and high level of H3K9Me3 were associated with poor prognosis in patients with gastric adenocarcinoma[127]. However, in patients with acute myeloid leukaemia decrease in H3K9Me3 found to be associated with better prognosis[129]. Mass spectrometry based analysis showed high level of H3K27Ac in colorectal cancer than the corresponding normal mucosa[128]. Immunohistochemical analysis on metachronous liver metastasis of colorectal carcinomas has correlated H3K4Me2 and H3K9Ac with the tumor histological type[126]. In addition, lower levels

of H3K4Me2 correlated with a poor survival rate and also found to be an independent prognostic factor.

Another histone mark, H3K27Me3 has been evaluated as a prognostic factor in prostate, breast, ovarian, pancreatic and oesophageal cancers, however, some of the results are perplexing and need further investigation[129]. In oesophageal cancer, high level of H3K27Me3 correlates with poor prognosis, whereas, in case of breast, prostate, ovarian and pancreatic cancers low level of H3K27Me3 had significantly shorter overall survival time when compared with those with high H3K27Me3 expression[130]. This indicates, once again, that one histone modification can predict differential prognosis in different cancer types and that histone marks may possess tissue-specific features.

Recently, a study showed K27M mutations of histone H3.3 variants in 31% paediatric glioblastoma tumors suggesting another level of complexity in alteration of histone PTMs in cancer which is independent of histone modifying enzymes[108]. This highlights that along with monitoring the histone PTM changes it is equally important to monitor the histone variant profile and modifiers, which currently is lacking in most of the studies, such a comprehensive analysis of these components will enable us to properly assess the cancer epigenetic changes and exploit their clinical use.

## 1.13. Targeting histone PTM changes

Reversible nature of histone modifications has drawn major attention of scientific community to study the molecular mechanism regulating the alteration in histone posttranslational modifications. Such efforts have led to the discovery of several histone modifying enzymes and their chemical inhibitors which has emerged as an attractive strategy in cancer treatment. Targeting these enzymes can reactivate epigenetically silenced tumor-suppressor genes by modulating the levels of histone posttranslational modifications. The interaction between different components of the epigenetic machinery has led to the exploration of effective

combinatorial cancer treatment strategies. Indeed, combinations of DNA methyltransferase (DNMT) and histone deacetylase (HDAC) inhibitors appear to synergize effectively in the reactivation of epigenetically silenced genes[131]. Such combination treatment strategies have been found to be more effective than individual treatment approaches. For example, the derepression of certain putative tumor suppressor genes was only seen when 5-Aza-CdR (DNMTi) and trichostatin A (HDACi) were combined[131]. Synergistic activities of DNA methylation and HDAC inhibitors were also demonstrated in a study showing greater reduction of lung tumor formation in mice when treated with phenyl butyrate and 5-Aza-CdR together [131]. Pre-treatment of HDACi, SAHA relaxes the chromatin and sensitizes cells to DNA damage induced by Topoisomerase II inhibitor[131]. Similarly, pretreatment of valproic acid (HDACi) act in synergy with epirubicine and reduces the tumor volume in breast cancer mouse model [131]. The combination of HDACi, entinostat with the DNMTi, azacitidine reduced tumor burden and retarded the growth of orthotopically engrafted K-ras/p53 mutant lung adenocarcinomas in immunocompromised nude rats[131].

Based on these studies an 'epigenetic vulnerability' of tumor cells has been proposed, where in contrast to normal cells that show redundancy in epigenetic regulatory mechanisms – HDACs and or DNMTs may be essential in tumor cells for the maintenance of a set of key genes required for survival and growth. In accordance, a large number of HDAC inhibitors have been synthesized and tested in clinical trials, resulting in the approval of four inhibitors (Vorinostat, Romidepsin, Bellinostat, Panobinostat)[132]. This could be interpreted as a successful history of drug development, with validation of HDACs as important targets in cancer, but the situation is far more complex, and the clinical results do not reflect those expected from the preclinical work, both in terms of efficacy (observed only in selected cancer subtypes, mainly in haematology) and safety (several side effects were observed, among which the most common are fatigue, diarrhea, bone marrow toxicity, thrombocytopenia)[132]. The reasons for this, at least

in part for this disappointing set of clinical results are not clear; one explanation could be that may be only small sub-set of populations respond well with these drugs hence there is a need to envision a smart approach for patient stratification for therapy success.

*Chapter 2*

# II. Aims and Objectives

## 2.1. Statement of the Problem

H2A isoforms, H2A.1 and H2A.2, in rat are known to exhibit altered expression under different physiological conditions and impart differential stability to nucleosomes, thus they may have a potential to influence gene expression patterns. However, it is not known whether the deposition of these isoforms occurs by a similar set of chaperones or there are any differential chaperones attributed for their chromatin assembly. Further, after deposition on to DNA what could be the possible composition of these nucleosomes, under various physiological states, in terms of other histones in the octameric core. This study is essential because the biochemical properties of variant nucleosomes are different and can potentially influence the stability of the nucleosomes, global chromatin architecture and gene transcription. Further, as all the components of the epigenetic machinery like histone chaperones, histone isoforms and their modifiers have a potential to influence gene expression patterns and contribute to global changes in the epigenomic landscape of cancer, it is essential to understand which proteins could be interacting with these histone isoforms.

## 2.2. Hypothesis

We hypothesize that the differential incorporation of H2A.1 and H2A.2 may be brought about by a specific set of proteins and post deposition, they have a differential interaction with other histones in octameric core. Thus, together this interplay may alter chromatin dynamics which in turn may influence the gene expression and phenotypic behaviour of the cell.

## 2.3. Objectives

I.   Identification of the binding partners of H2A.1 and H2A.2

II.  To understand the role of binding partners in chromatin mediated processes.

## 2.4. Experimental Approach

The results obtained using the experiments mentioned in the following sections has been divided in to three chapters. Each of the chapters consists of the subsections *Introduction, Methods, Results, Discussion* and *Conclusion*. **Chapter 3** will discuss the work done regarding the identification of nucleosolic binding partners (Histone chaperones) of H2A.1 and H2A.2. **Chapter 4** relates to the chromatin binding partners of H2A.1 and H2A.2 and emphasizes the importance of Histone H3 variants for cancer progression and also highlights the role of DNA methylation in governing the expression status of H2A isoforms and H3 variants. **Chapter 5** will discuss the similarities between tissue and liquid biopsy in context of histone PTMs and their modifiers and also establishes liquid biopsy as a tool for solid tumor containing patient stratification for epi-drug treatment. This will be followed by a consolidated discussion in **Chapter 6** and **Chapter 7** will emphasize the salient findings and future directions of the work.

The experimental approach used to accomplish the work done has been represented here as per the division of results.

***Chapter 3: Nucleosolic binding partners of histones H2A.1 and H2A.2.***

 - ➢ Nucleosolic Immunoprecipitation of FLAG tagged H2A.1 and H2A.2 followed by SDS PAGE analysis.

 - ➢ Immunoprecipitation of FLAG H2A.1/H2A.2 for assessing their interaction with NAP1.

 - ➢ Chromatin deposition of H2A.1 and H2A.2 upon knock down of NAP1.

 - ➢ Biophysical characterization of rat NAP1 by using gel filtration chromatography, Circular Dichroism (CD spectroscopy) and Dynamic Light Scattering (DLS).

 - ➢ Biochemical characterization of Casein Kinase-2 (CK2) phosphorylated NAP1 using native PAGE and histone binding assays.

### *Chapter 4: Chromatin binding partners of histones H2A.1 and H2A.2.*

➢ Global histone H3 profiling in control and tumor tissues by AUT-PAGE and RP-HPLC.

➢ Relative association and stability of nucleosomes - H2A.1/H3.2, H2A.1/H3.3, H2A.2/H3.2 and H2A.2/H3.3 - Mononucleosomal immunoprecipitations, salt dissociation and molecular dynamic simulations (MDS) analysis were performed.

➢ Methyl DNA (MeDIP) and Hydroxyl-methyl DNA immunoprecipitation (hMeDIP) assays to delineate the methylation pattern on H2A.1, H2A.2, H3.2 and H3.3 promoters in liver tissues and cell lines.

➢ Global profiling of H3 PTMs followed by mononucleosomal immunoprecipitation to assess the variant specific PTM association.

➢ Micrococcal Nuclease assay and pulse chase *in vitro* transcription assay for assessing the global changes in chromatin organization and gene transcription in HCC.

➢ Cell proliferation and colony formation assay to study the effect of ectopic overexpression of H3.2 and H3.3 variants.

➢ Global expression changes in H3.2 and H3.3 specific histone chaperones in normal liver and HCC.

➢ Cell proliferation, cell cycle analysis, microccocal nuclease assay and *in vitro* transcription assay to understand the effect of knock down of P150.

➢ Cell proliferation and colony formation assay to study the effect of ectopic overexpression of H3.2 and H3.3 variants.

➢ shRNA mediated knock down of H3.3 and its effect on cell proliferation, cell cycle analysis, microccocal nuclease assay and *in vitro* transcription assay.

➢ Chromatin immunoprecipitation (ChIP) followed by qPCR to monitor the association of H3.3 and H3.2 with tumor suppressor genes.

➢ Monitoring the expression status of H3 variants, H3.2, H3.3 and H3.1 by real time PCR in various human cancer cell lines (Liver, Skin and Breast) in comparison to their immortalized counter parts.

***Chapter 5: Identification of epigenetic alterations in serum and its clinical implications.***

➢ Development of protocol for isolation of serum histones

➢ Comparative analysis of changes in histone PTMs profile of serum with paired HCC and other non-target organs.

➢ HDAC assay on paired rat tumor tissue lysate and serum samples and in human serum samples.

Chapter 3

# III. Nucleosolic Binding Partners of Histones H2A.1 and H2A.2

# 3.1. Introduction

The deposition of histones on to DNA for the formation of nucleosome occurs in a sequential manner and is brought about by a specialized set of proteins known as 'histone chaperones'. These chaperones associate with histones upon their synthesis, escort them into the nucleus and modulate their association with DNA during essential cellular processes such as DNA replication, repair or transcription. Additionally, they are also involved in histone storage which prevents their non-productive aggregation with DNA[133].

The H2A/H2B chaperones specifically deposit them onto DNA. Based on their nucleosomal positioning, the dynamics of H2A/H2B may play several critical roles, including: (i) octamer nucleosome assembly, (ii) initiation of nucleosome disassembly, (iii) favoring of nucleosome 'breathing' and position sliding via loosening of nucleosomal/inter-nucleosomal histone–histone and histone–DNA interactions, (iv) exchange of nucleosomal H2A/H2B with free histones carrying similar or different modifications or with variant histones. H2A/H2B chaperones include Nucleosome Assembly Protein 1 (NAP1), Facilitates Chromatin Transcription (FACT), NAP1-Related Protien (NRP) **[Figure 3.1].**
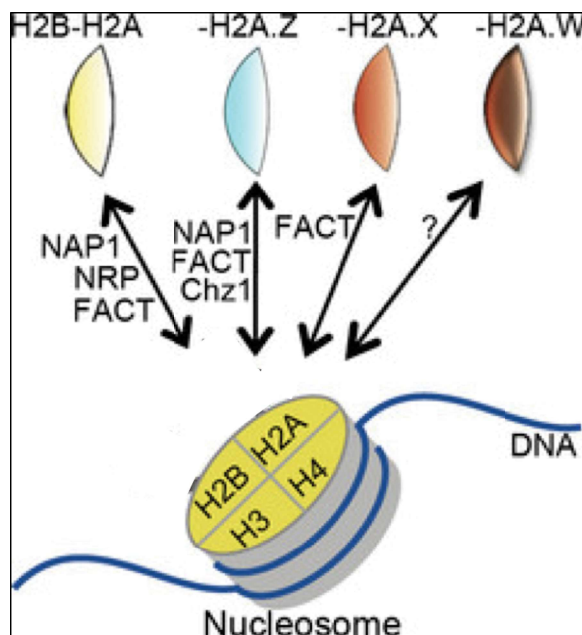


**Figure 3.1. Histone H2A chaperones and their variant selectivity.** The canonical H2B–H2A dimer and variant H2B–H2A.Z, H2B–H2A.X and H2B–H2A.W dimers are indicated by different colours. Double-headed arrows indicate exchange activity mediated by histone chaperones. The question mark indicates involvement of an chaperone of unknown identity.
*Adapted from:*
*Wangbin Zhou et al., (2015). Histone H2A/H2B chaperones: From molecules to chromatin-based functions in plant growth and development. The Plant Journal, 83(1):78-95. DOI: 10.1111/tpj.12830*

Research over few years had helped to understand the molecular basis of function of the histone H2A/H2B chaperones NAP1 and FACT, and to appreciate their critical roles in transcription, DNA replication, repair, development and disease. In conjunction with covalent histone modifications and histone variants, NAP1/FACT-mediated dynamic exchange of H2A–H2B within the nucleosome has great implications with regard to chromatin structure/function and epigenetic reprogramming and inheritance.

NAP1 is one such bonafide and a major chaperone which deposits H2A-H2B onto chromatin [134]. Genome-wide expression analysis in Saccharomyces cerevisiae showed that approximately 10% of genes are regulated by NAP1[135]. NAP1 interacts with all four core histones (H2A/H2B and H3/H4) *in vitro*[136]; however *in vivo* interaction is exclusive to H2A/H2B dimers[137]. Therefore NAP1 is mainly considered a H2A/H2B-specific chaperone and performs a plethora of functions related to this role Apart from histone deposition/eviction, NAP1 is also involved in nuclear import of H2A-H2B dimers by engaging with karyopherin, Kap11[138]. It also has been shown to stimulate replication and transcription by modulating chromatin structure through putative interactions with transcriptional activators and co-activators such as p300[139].

Apart from its role in formation of nucleosomes with canonical histones, it also leads to formation of nucleosomes with variant histones[140], again suggesting its function as a transcriptional regulator. The precise stoichiometry of NAP1 with histone H2A/H2B or H1 remains controversial, as two binding stoichiometries have been proposed. The first postulates that yeast NAP1 (yNAP1) may bind to one histone H2A/H2B heterodimer or one linker histone H1 (1:1)[141,142,143], and the second that yNAP1 may bind two histone H2A/H2B heterodimers or two linker histones H1 (1:2)[144]. Analyses of NAP1 complexes from *Xenopus* were in agreement with a stoichiometry of a single NAP1 dimer bound to one histone H2A/H2B heterodimer[145] or one linker histone B4 monomer[145]. The general consensus of these papers advances a 1:1 stoichiometry, however recent studies of human NAP1 (hNAP1) complexes

reported that both stoichiometries can be detected depending on sample preparation[136]. NAP1 is relatively conserved amongst different species and have high sequence homology. For example, yeast NAP1 (yNAP1) is 36% and 37% identical to human NAP1 (hNAP1) and *Xenopus* NAP1 (xNAP1), respectively[146] **[Figure 3.2]** .



**Figure 3.2: Amino acid sequence alignment of NAP1 across the species.**

Previous biochemical and biophysical experiments done with yNAP1 have demonstrated the existence of higher oligomeric structures of NAP1 which are disrupted at higher ionic strength giving rise to predominantly dimeric species[147]. This oligomerization phenomenon is not unique to yNAP1 and has also been observed in xNAP1 and hNAP1[146]. Structural studies have revealed that the presence of central α-helix and a β-hairpin is essential for the dimerization and oligomerization in yNAP1, respectively[148].

Interestingly, hNAP1 tends to be more in oligomeric form than yNAP1[136]. Notably, the differences in their oligomeric properties are also reflected in the basic interaction of NAP1 with different species with histones. For instance, *in vitro* experiments suggest that hNAP1 binds to H2A-H2B dimer and H3-H4 tetramer with equal propensity unlike yNAP1 which has higher affinity towards H3-H4 tetramer[141]. This difference might be attributed in part, to the differential oligomerization tendencies of hNAP1 and yNAP1 because the self-association states of NAP1 has been linked closely to its stoichiometric association with histones[142]. Interestingly, equilibrium-unfolding studies conducted on oligomeric yNAP1 suggest that it follows a three-state model of unfolding, where it unfolds sequentially from oligomeric form to dimeric and then completely denatures. Despite many efforts by several groups, contradictory reports on the stoichiometry and oligomerization states of NAP1 persist in different species. In addition, casein kinase 2 (CK2) mediated phosphorylation of NAP1 has been correlated with its nuclear localization in *Drosophila*[149]. It is possible that phosphorylation of NAP1 has the potential to favor/disrupt oligomerization, thus affecting histone-binding or deposition properties on chromatin. We hypothesized that the difference in the stability of hNAP1 oligomers is reflected in its unfolding characteristics and further phosphorylation might affect the oligomerization properties of these histone-binding proteins. There is no comprehensive study on these aspects of hNAP1, which are vital for understanding the mechanisms of NAP1-mediated functions in higher vertebrates.

## 3.2. Methods

### *3.2.1  Cell line maintenance*

CL44, a rat liver non-tumorigenic cell line and CL38, a rat liver tumorigenic cell line, *in vivo* transformed by NDEA carcinogenesis, was a kind gift from Dr. H. M. Rabes (University of Munich, Germany).

Sterile techniques were maintained when working with cell-line. Antibiotics were added to culture medium. Reusable glassware, plasticware and solutions were sterilized by suitable means prior to use. Cell culture work was carried out in laminar flow hood. CL44 and CL38 cells were maintained in Earle's Minimum Essential Medium (MEM) supplemented with 6%v/v fetal bovine serum in humidified incubator maintained at 37˚C, 5%$CO_2$. Complete media was prepared by adding 10% FBS and 1% antibiotic.

The frozen vials of cells stored in liquid nitrogen were allowed to thaw at 37˚C water-bath. The thawed cell suspension was transferred to sterile centrifuge tube containing 2ml MEM media and centrifuged for 10min at 1400g at RT. The cell pellet obtained was resuspended in 1ml MEM and transferred to sterile culture plates with sufficient amount of media (2ml media for 35mm dish). Cell condition was tracked after 24h under microscope and media was changed if it turned from red to yellow.

The culture plates were sub cultured by trypsinization. These cells were then counted and transferred into new sterile plates with sufficient media. The numbers of viable cells were determined by adding 20µl of 1mg/ml trypan blue into 180µl of cell suspension. The drop from this mixture was loaded on haemocytometer and viable cells were counted.

Cells/ml = average number of cells per WBC chamber x dilution factor (10) x$10^4$

The details of the cell lines used throughout the work has been included in *Appendix as Annexure III.*

### 3.2.2  Preparation of Competent Cells (Calcium Chloride Method)

The protocol for preparation of competent cells is as described earlier. 100ml of LB media was inoculated with 1ml of overnight grown culture that was obtained by inoculating a single colony of bacteria from streaked plate incubated at $37^0C$ overnight. The cells were grown for approximately 2h ($OD_{600} = 0.4$) in a shaker incubator. The culture was chilled on ice for 30min. The cells were harvested by centrifugation at 10000g for 5min at $4^0C$ and the supernatant was discarded. The cells were washed with chilled 100mM $CaCl_2$ and centrifuged at 8000g for 5min at $4^0C$. The cells were resuspended in 20ml of chilled 100mM $CaCl_2$ and kept on ice for 45min. The cells were again harvested by centrifugation at 8000g for 5min at $4^0C$ and the supernatant was discarded. The cells were resuspended in ice-cold sterile solution of 100mM $CaCl_2$ + 15% glycerol and kept on ice for 10min. 200μl aliquots were made in pre-chilled tubes and stored at $-80^0C$ after freezing in liquid nitrogen.

### 3.2.3  Preparation of Ultra Competent Cells

The protocol for plasmid isolation is as described earlier[150]. *E. Coli*, DH5α was streaked onto LB agar plate and incubated overnight at $37^0C$. 100ml of SOB in 1000ml flask was inoculated with a single colony from the plate. The flask was incubated at $18^0C$ with shaking at 200rpm. Once the $OD_{600}$ reached 0.3- 0.4, the culture was kept on ice for 10min. The cells were harvested by centrifugation at 10000g for 5min at $4^0C$ and the supernatant was discarded. The cell pellet was resuspended in 32ml of ice cold transforming buffer *(composition Annexure V)* and kept on ice for 10min. The cells were harvested by centrifugation at 10000g for 5min at $4^0C$ and the supernatant was discarded. The cell pellet was resuspended in 8ml of ice cold transforming buffer and 600μl DMSO is added. Cells were kept on ice for 10min. 100μl aliquots were made in pre-chilled tubes and stored at $-80^0C$ after freezing in liquid nitrogen. For transformation of a ligation mixture an 100μl aliquot was used.

### 3.2.4 Construct preparation

The coding sequence of NAP1 was amplified using Taq Polymerase (NEB# M0273) from the cDNA synthesised from RNA (treated with DNaseI) isolated from rat cell lines. The amplicon was then cloned into pTZRT57 vector according to manufacturer's (Thermo scientific #K1213) instructions. The cloned fragment was further sequenced. For subsequent cloning into different expression vectors like pCDNA MYC, pET28a and pET3a, the coding sequence were amplified with primers incorporating the appropriate restriction sites (please see *Annexure IV* in *Appendix* for primer sequences) and were sub cloned, maintaining the correct reading frame which was verified by sequencing.

### 3.2.5 Plasmid Isolation (Mini-prep)

The protocol for plasmid isolation is as described earlier[150]. 10ml of LB media, containing suitable antibiotic, was inoculated with single colony from the transformed plate and incubated at $37^0$C overnight. 1.5ml of the overnight grown culture were transferred to an Eppendorf tube and the bacterial cells were pelleted down by centrifuging at 10000g for 5min at $4^0$C. The supernatant was discarded and the pellet was resuspended uniformly without any clumps in 150µl of TELT buffer (*Annexure V*). 5µl of lysozyme (50mg/ml) was added to the tube. The contents were mixed and kept on ice for 1min. The tube was then placed in a boiling water bath for 1min and immediately chilled on ice for 10min. The tube was then centrifuged at 12000g for 10min at $4^0$C. The pellet was discarded with the help of a micro-tip. 330µl of chilled absolute alcohol was added to the supernatant and placed at $-20^0$C for 30min or $-70^0$C for 5min. The tube was then centrifuged at 12000g for 10min at $4^0$C. The supernatant was discarded and the pellet was washed with 70% ethanol. The supernatant was discarded and the pellet was air dried. The air dried pellet was dissolved in 20µl of nuclease free water.

### *3.2.6 Agarose gel electrophoresis*

Agarose gel electrophoresis was carried out to analyse levels of PCR and RT-PCR products in different samples[151]. Adequate 1X TAE electrophoresis buffer (40mM Tris-acetate and 2mM Na$_2$EDTA) was prepared to fill the tank of electrophoresis chamber (Techno Source, India) and to prepare the gel. For preparation of gel, agarose (1.5% w/v in TAE) was melted in a microwave oven. Ethidium bromide at a concentration of 0.5μg/ml was added to melted agarose solution, cooled down to ~55°C. This was then poured into the gel casting platform with prefixed comb. The comb was removed from the hardened gel. Ethidium bromide was added to tank buffer (0.5μg/ml in 1X TAE) and gel casting platform was placed into the electrophoresis chamber. DNA samples were prepared in appropriate amount of 6X loading buffer (12% Ficoll 400, 60mM EDTA pH 8.0, 0.6% w/v SDS, 0.15% w/v bromophenol blue and 0.15% w/v xylene cyanol). Hundred base pair DNA ladder (NEB #3231) was loaded as molecular weight marker. The gel was electrophoresed at 5V/cm of gel and the progress of separation was monitored by migration of dyes in the loading buffer. After separation of tracking dyes, the gel was examined on UV trans-illuminator to visualize DNA.

### *3.2.7 Transfection*

Rat CL38 and CL44 cells grown on 6 well plate to approximately 40% confluence was transfected with eukaryotic plasmids using cation based transfecting reagent, Turbofect (Fermentas #R0531), according to the manufacturer's instructions. Post 48h the media was changed and fresh media with selection marker G418 (Sigma # G9516) or Puromycin (Sigma #P8833) at a concentration of 400μg/ml and 400ng/ml respectively was added. The cells surviving after selection period of 10-15 days for G418 and 4 days for Puromycin where pooled and used for further experiments. Before performing any further experiments, cells were tested by western blotting for successful transfection and clone selection.

### *3.2.8 shRNA cloning*

The complementary A and B oligonucleotides for shRNA were designed to form a secondary structure with XhoI site 'CTCGAG' (can also use PstI site 'CTGCAG' to help screening for positive clones) in the loop as follows to give 5'AgeI and 3'EcoRI overhangs upon annealing:

Oligo A: 5' CCGG (target sequence) CTCGAG (reverse complement of target sequence) TTTTTG 3'

Oligo B: 5' AATTCAAAAA (target sequence) CTCGAG (reverse complement of target sequence) 3'

The oligos used for shRNA has been tabulated in *Annexure IV* in *Appendix.* 5μl each of the oligos were mixed in the NEB polynucleotide kinase buffer and the reaction was made upto 20μl by PCR grade MilliQ. A PCR program ($94^0$C for 4min, $70^0$C for 10min) was used for annealing. The reaction was allowed to cool to RT by switching off the PCR machine. The pLKO.puro vector was then digested with AgeI and EcoRI and ligated with 0.2μl of the annealed shRNA oligonucleotides. Post cloning and sequence verification the plasmids were transfected as previously described.

### *3.2.9 SDS PAGE analysis*

The protocol for SDS PAGE analysis of proteins is as described earlier. In brief, glass plate sandwich was assembled using 0.1cm thick spacers. Resolving gel solution (*Annexure V*) was prepared and poured into the glass plate sandwich and allowed to polymerize for approximately 30min. During the polymerisation process a thin layer of water was overlaid on top of the resolving gel to prevent contact with oxygen. Once the resolving gel polymerised the overlaid water was decanted. Stacking gel solution (*Annexure V*) was prepared and poured into the glass plate sandwich on top of the polymerised resolving gel. in similar manner. A 0.1cm thick Teflon comb was inserted and gel was allowed to polymerize. Protein samples to be analysed were diluted 1:1 (v/v) with 2X SDS sample buffer and incubated for 5min in boiling water.

Teflon comb was removed, sandwich was attached to the electrophoresis chamber and filled with electrophoresis buffer (*Annexure V*). Samples were loaded into the wells formed by comb. The gel was run at 20mA of constant current until the BPB tracking dye entered the separating gel and then at 30mA until the BPB dye reached the bottom of the gel. The power supply was then disconnected and gel was subjected to Coomassie staining or western blot analysis. For Coomassie staining gel was transferred to tray containing Coomassie Brilliant Blue R-250 (CBBR) staining solution (0.1% w/v CBBR, 50% methanol and 10% acetic acid in water). The gel was stained for ~3h on shaker. Gel was then transferred to destaining solution (50% methanol and 10% acetic acid in water). The gel was destained on shaker with several changes in destaining solution until protein bands appeared on clear gel.

### 3.2.10 Western blot analysis

Levels of particular proteins or their post-translational modifications were assessed by western blot analysis using the appropriate antibody. See *Annexure II* in *Appendix* for the details of the antibodies used in the study.

a)      *Electroblotting from SDS-PAGE:* Proteins were electroblotted from SDS-PAGE gels to PVDF membranes for western blot analysis. The transfer tank of electroblotting apparatus (Trans-Blot Cell, Bio-Rad) was filled with 1X transfer buffer (see *Annexure V* for composition). PVDF membrane was activated in 100% methanol for 5sec. The activated membrane and SDS-PAGE gel were equilibrated in 1X transfer buffer. The gel membrane transfer sandwich was prepared and inserted into the transfer tank with gel on cathode side and membrane on anode side. Transfer was conducted at a constant current of 300mA for 200min. Proteins transferred onto the membrane were detected by staining with Ponceau S (0.5% w/v Ponceau S in 1% v/v acetic acid) and destaining with several changes of water.

b)      *Immunoblot detection:* Proteins transferred onto PVDF membrane were probed with antibodies. In general, membrane with transferred proteins was incubated in 'blocking buffer'

i.e. 5% BSA in Tween20/Tris-buffered saline (TTBS, 100mM Tris-Cl pH7.5, 0.9% w/v NaCl and 0.1% v/v Tween20) for 1hr at room temperature on orbital shaker. Blocking buffer was then replaced by recommended dilutions of primary antibodies in TTBS and incubated for 1hr at room temperature in orbital shaker (see *Annexure II*). The membrane was vigorously washed four times with TTBS for 15min each at room temperature. Further the membrane was incubated in recommended concentrations of HRPO labelled secondary antibodies in TTBS for 1hr at room temperature on orbital shaker (see *Annexure II*). The membrane was again washed vigorously four times with TTBS at room temperature and developed using Immobilon Western (Millipore, cat#P90719). The membrane was exposed to X-ray film in dark room and developed using Optimax X-ray film processor (Protec). Band/Lane intensities were analysed using ImageJ and GraphPad prism software.

### 3.2.11 Immunoprecipitation

Nuclear extracts were prepared using a modification of the Dignam protocol[152]. Cells were lysed in hypotonic buffer (10mM Tris-HCl at pH 7.65, 1.5mM $MgCl_2$, 10mM KCl) and disrupted by Dounce homogenizer. The cytosolic fraction was separated from the pellet by centrifugation at 4°C. The nuclear soluble fraction was obtained by incubation of the pellet in high salt buffer (to get a final NaCl concentration of 300mM). Tagged histone proteins were immunoprecipitated with anti-Flag M2-agarose (Sigma #F2426), eluted with Flag peptide (0.5mg/mL), further affinity purified with anti-HA antibody-conjugated agarose, and eluted with HA peptide (1mg/mL). The HA and Flag peptides were first buffered with 50mM Tris-Cl (pH 8.5), then diluted to 4 mg/mL in TGEN 150 buffer (20mM Tris at pH 7.65, 150mM NaCl, 3mM $MgCl_2$, 0.1mM EDTA, 10% glycerol, 0.01% NP40), and stored at 20°C until use. Between each step, beads were washed in TGEN 150 buffer. Complexes were then resolved by 4-20% SDS-PAGE and silver stained. For immunoprecipitation of MYC tagged NAP1,

MYC antibody (Sigma) was used and the similar mentioned steps were followed except for peptide elutions and where then subjected to western blotting.

For silver staining the protocol described earlier was used[153]. The gel was immersed in ten gel volumes of freshly prepared ammonical silver nitrate solution for 30min. The gel was washed thrice with water each time for 2min. The gel was then developed by using developing solution (0.01% w/v citric acid monohydrate and 0.1% w/v formaldehyde). The development was stopped when protein spots appeared on clear gel using stopping solution (40% methanol and 10% acetic acid).

### *3.2.12 Growth and IPTG induction of transformed bacterial expression hosts*

The protocol for recombinant histone expression is as described earlier with slight modifications[154]. The plasmids (100ng) containing the gene of interest was transformed in either competent BL21 (DE3) pLysS and Rosetta (DE3) pLysS and plated onto LB agar plates containing the appropriate antibiotic (ampicillin or kanamycin) for selection of transformed bacteria. In addition, chloramphenicol (25μg/ml) was incorporated into media to maintain selection pressure for the T7 lysozyme-containing phage present in the bacterial strains used for expression studies. The plates were incubated at $37^{o}C$ for 16h in a temperature controlled incubator. A single colony was inoculated from the plates of transformed bacteria in 5ml or 20ml LB media containing the appropriate antibiotic and incubated at $37^{o}C$ with constant shaking until the $OD_{600}$ reached between 0.4 and 0.6. Induction of recombinant protein expression were carried out by adding IPTG to a final concentration of 0.2mM. The cultures were induced for 3h at $37^{o}C$. One tube was kept as uninduced as a negative control.

Post induction the bacteria were harvested by centrifugation at 8000g for 10min at $4^{o}C$ and processed. The soluble and the insoluble fractions of proteins were separated resuspending the cell pellet in 1ml of buffer containing 50mM Tris-Cl pH 8.0, 0.5% Triton X-100 and 100μg/ml lysozyme followed by three rounds of sonication, each for 30 seconds at 10% amplitude. The

lysate was then centrifuged at 27000g for 30min at 4°C. The supernatant and pellet, thus obtained, contains the soluble proteins and the insoluble proteins respectively. Sample was prepared by vortexing followed by boiling the lysate for 10min in a boiling water bath after adding equal amount of 2X loading Dye. The sample was kept on ice for 10min and then the proteins were resolved by loading the samples on 10 or 18% SDS-PAGE followed by Coomassie staining (Brilliant Blue R250).

### *3.2.13 Ni-NTA affinity purification of NAP1*

The protocol for Ni-NTA affinity purification of recombinant NAP1 is as described earlier with certain modifications. The soluble fraction containing recombinant protein was added to 2ml of 50% slurry of nickel–nitrilotriacetic acid (Ni–NTA) agarose beads (Qiagen#30210), equilibrated with buffer containing 50mM Tris-Cl pH 8.0 and 0.5% Triton X-100. The 50% slurry was added onto a PD10 column (GE) with a stopper. Five times bed volume buffer was added and allowed to flow through. This was repeated at least thrice. The stopper was attached to prevent the liquid from flowing through and the supernatant containing the 6xHis-tagged NAP1 were then added onto the column. The column was kept on a rocker at $4^0$C for allowing efficient and uniform binding of the proteins to the beads. After a 60min incubation, the stopper was opened and the flow-through was collected and labelled as unbound fraction. The beads were washed with 50mM Tris–HCl buffer (pH 8.0) containing 500mM NaCl, 5% glycerol, and 10mM imidazole in a way similar to what was described for equilibration. The 6xHis-tagged NAP1 was eluted by a linear gradient of imidazole from 5 to 300mM in buffer containing 500mM NaCl and 5% glycerol. The eluted fractions were analysed by preparing the sample as described earlier and loading on 10% SDS-PAGE. The purified protein was loaded on to a HiLoad 16/60 Superdex-200 gel filtration column (GFC) to identify the oligomeric status. The chromatography was carried out in a buffer containing 500mM NaCl, otherwise mentioned in the results.

### *3.2.14 Ni-NTA affinity purification of Histones*

For purification of histones, similar protocol as above was followed apart from incorporation of 6M urea in the buffer for dissolving insoluble pellet obtained after cell lysis after centrifuged again. The insoluble pellet obtained was again resuspended in 10ml of the same buffer for re-extraction of histones. Samples were again centrifuged at 27,000g for 20min at $4^0$C. The supernatant was pooled with the previously collected supernatant and the insoluble pellet obtained was discarded. Then for bead binding, washing and elution similar protocol was followed expect for incorporation of 6M urea in all the buffers. The histones obtained post purification were dialysed against 2L 10mM HCl to remove urea and salts with the help of D-tube Dialyser 6-8KDa cut-off (Millipore). The histones were processed immediately for reconstitution experiments or were stored at $-80^0$C post lyophilisation.

### *3.2.15 Reconstitution of H2A-H2B dimer*

To reconstitute the H2A-H2B dimer, the His6-tagged histones H2A and H2B or H3 and H4 in 10mM HCl were mixed in 1:1 stoichiometry. The concentration was determined for the histones by using their molar extinction coefficient. Further, the quantification was validated by resolving the histones on an 18% SDS-PAGE followed by coomassie staining. After adding the histones, the mixture was rapidly diluted three folds by adding 50mM Tris–HCl (pH 8.0) containing 10mM DTT and 2mM EDTA with continuous stirring. The diluted mixture was then dialyzed (cut-off 10kDa) against 1L of 50mM Tris–HCl (pH 8.0) containing 10mM DTT, 2mM EDTA and 2M NaCl for 1h at room temperature, and the dialysis was continued overnight at $4^0$C. After an overnight dialysis, the impurities and excess histones precipitated. The insoluble histones were removed by centrifugation at 27,000g for 20min at $4^0$C. The dialysate was then concentrated using a 10kDa cut-off protein concentrator (Amicon Ultra-15, Millipore). The concentrated proteins were loaded onto equilibrated Superdex-200 HiLoad 16/60 (GE) gel filtration column and the peak fractions were collected. The elution of the

protein was monitored by absorbance at 280nm. The salt concentration was reduced by stepwise dialysis for downstream assays.

### *3.2.16 Ion exchange purification of NAP1*

The supernatant containing rNAP1 obtained after cell lysis from above was mixed with 50% slurry of Anion exchange resin (Q sepharose, Pharmacia biotech) pre-equilibrated with buffer and kept on rotator at $4^0$C. After 60min incubation, the column was washed and eluted with a linear NaCl gradient with buffer A containing 20mM Tris, pH 7.6 (4 °C), 0.5mM EDTA, 10% glycerol, 1mM dithiothreitol, 0.1mM phenylmethylsulfonyl fluoride. Fractions were assayed for NAP1 by SDS-PAGE, and peak fractions were pooled. The fractions were diluted with buffer A to a final NaCl concentration of 150mM and applied to a 1ml Mono Q anion exchange column (Amersham Biosciences). The rNAP1 was eluted by buffer containing 500mM NaCl. The eluted proteins were resolved on 10% SDS-PAGE and stained with Brilliant Blue R250. The purified protein was loaded on to a HiLoad 16/60 Superdex-200 gel filtration column (GFC) to identify the oligomeric status. The chromatography was carried out in a buffer containing 500mM NaCl, otherwise mentioned in the results.

### *3.2.17 Equilibrium Unfolding*

Equilibrium unfolding as a function of urea and temperature was monitored by CD spectroscopy. Also, equilibrium unfolding as a function of urea was monitored by change in fluorescence. For CD spectroscopy, the protein (25μg/ml) was incubated in presence of various concentrations of the denaturant at $25^0$C for 24h. In the thermal unfolding experiments, the spectra were recorded 3min after the desired temperature was attained. Spectra were recorded in the temperature range of 20-100$^0$C. The intrinsic tryptophan fluorescence spectra of NAP1 was recorded on a spectrofluorimeter, equipped with water bath. The protein was excited at 280nm using a cell of 1.0 cm path-length and both excitation and emission slit widths were set

at 3nm. CD spectra were recorded on a computer interfaced JASCO spectropolarimeter using a cylindrical quartz cell of 1 mm (190 − 250nm) and 10mm (250 − 300) at a protein concentration of 1μg/ml. For each spectrum, 20 successive scans were collected and the averaged spectra were used for further analysis.

### 3.2.18 Data fitting

The unfolding data was fit into two-state model of unfolding as described previously [155]. The denaturation curves were plotted, with the fluorescence intensities at 305nm of native and denatured NAP1, against denaturant concentration, and further analysis of the data was performed as described by Pace *et al.* [156]. Similar analysis was performed with the denaturation curves plotted with the drop in CD signal at 222nm with increasing temperature or urea concentration. From the denaturation curves, a two state $F \leftrightarrow U$ unfolding mechanism was assumed, and consequently, for any of the points, only the folded and unfolded conformations were present at significant concentrations. Thus, if $f_F$ and $f_U$ represent the fraction of protein present in the folded and unfolded conformations, respectively then

$$f_F + f_U = 1 \qquad (1)$$

$f_U$ was calculated using the following equation

$$f_U = (F_F - F_0) / (F_F - F_U) \qquad (2)$$

where $F_F$ is the fluorescence intensity of completely folded or native protein, $F_0$ is the observed fluorescence intensity at any point of denaturant concentration or temperature, $F_U$ is fluorescence intensity of the completely denatured or unfolded protein.

For a two state $F \leftrightarrow U$ unfolding mechanism, the equilibrium constant $K$ and $\Delta G_U$, the free energy of unfolding was calculated using Equation 4 and 5 respectively.

$$K = f_U / (1 - f_U) \qquad (3)$$

$$\Delta G_U = RT \ln K \qquad (4)$$

where R is the gas constant and T is the absolute temperature. It is assumed that the free energy of unfolding, $\Delta G_U$, has a linear dependence on the concentration of the denaturant [D].

$$\Delta G_U = \Delta G^{H20} + m[D] \qquad (5)$$

$\Delta G^{H20}$ and $m$ are therefore the intercept and the slope respectively, of the plot of $\Delta G_U$ versus [D]. $\Delta G^{H20}$ corresponds to the free energy difference between the folded and unfolded states in the absence of any denaturant and $m$ is a measure of the cooperativity of the unfolding reaction. The concentration of denaturant at which the protein is half unfolded (when $\Delta G_U = 0$) is given by $D_{1/2}$ and from Equation 5, $\Delta G^{H20} = - m\, D_{1/2}$.

The data from the thermal unfolding curves were obtained under the same conditions as those for denaturant unfolding curves. Values of $f_U$, $K$ and $\Delta G_U$ were calculated using Equations 2, 3 and 4. The midpoint of thermal ($T_m$) denaturation was obtained as the temperature at which $\Delta G_U = 0$ from the plot of $\Delta G_U$ versus T. The slope of such a plot at Tm yielded $\Delta S_m$, the change in entropy. The enthalpy change for unfolding at $T_m$, $\Delta H_m$, was calculated using the equation:

$$\Delta H_m = T_m \Delta S_m \qquad (6)$$

$\Delta C_p$, the change in heat capacity that accompanies protein unfolding was obtained from the slope of the plot of $\Delta H_m$ versus $T_m$, where $T_m$ was varied as a function of Gdn-Chl concentration. $\Delta G_U$ at $25^0$C was calculated using equation:

$$\Delta G\ (T) = \Delta H_{\mathrm{m}}\ (1\text{-}\ \mathrm{T}/\ T_{\mathrm{m}}) \text{-} \Delta C_{\mathrm{p}}\ [(T_{\mathrm{m}} \text{-}\ \mathrm{T}) + \mathrm{T}\ \ln\ (\mathrm{T}/\ T_{\mathrm{m}})] \qquad (7)$$

### 3.2.19 Dynamic Light Scattering (DLS)

Different oligomeric complexes obtained post GFC were subjected to DLS. Protein and buffer solution was filtered (0.44μm pore size) and degassed prior to measurement. 1mg/ml protein in 10mM Sodium phosphate buffer (pH 7.5), 100mM NaCl was loaded into a 45μl quartz cuvette. Measurements were performed at temperature 25°C and at least $30 - 40$ measurements each of 12sec duration were collected (DynaPro NanoStar, Wyatt Technology). The refractive index and viscosity values were taken for the water as provided by the software. The translational diffusion coefficient of the protein was calculated from the autocorrelation of scattered light intensity. Histogram analyses of DLS results were carried out using the software DYNAMICS v.6.0

### 3.2.20 Homology Modelling

The homology modelling was carried out due to the unavailability of crystallographic coordinates of *Rattus norvegicus* NAP1. The model of NAP1 was constructed using PDB ID: 2AYU as a template. Homology modeling was carried out using modeller v 9.2, where dimer was used as a template. The modelled structure of NAP1 was cross-validated using multiple tools such as Procheck 22, Verify_3D23 and Errat24 using SAVES server (http://nihserver.mbi.ucla.edu/ SAVES/).

### 3.2.21 Molecular Dynamic Simulations (MDS)

MDS were carried out using GROMACS v 5 with AMBER ff99sb force field for 100ns. For both rNAP1 and yNAP1 the flexible N-terminal and C-terminal residues were not included and therefore total 292 amino acid sequence was used for simulation. Both the systems were solvated in a cubic box with approximately 48300 TIP3P water. The distance between closest protein fragment and edges of the box was kept to be 10Å. Both the systems were neutralized

by adding $Na^+$ ions. The salt concentration of 150mM was kept during molecular simulation. The energy minimization was carried out for 2500 steps. This was followed by two step equilibrations, first position restrained NVT equilibration has been run for 500ps using V-rescale thermostat[157] followed by NPT equilibration for 1nsec using the Berendsen barostat[158]. Long-range electrostatic interactions were calculated using the particle-mesh Ewald (PME) method. The Vander Waal's interactions and Coulomb interactions were cut off at 12Å. Leap frog integrator with the integration time step of 2fsec has been used to solve the Newton's equation of motion. The LINCS algorithm was used to constrain the bond lengths involving in hydrogen atoms[159]. Production runs have been carried out using Parrinello-Rahman barostat[160].

MM-PBSA technique was used for the calculation of free energy of binding yNAP1 and rNAP1[161]. Root Mean Square Deviation (RMSD) and Root Mean Square Fluctuation (RMSF) was calculated using g_rms tool and g_rmsf utility of GROMACS considering all atoms. Further, hydrogen bond was calculated using g_hbond utility of GROMACS where only H-bonds with distance <0.35 nm between cooperated donor and acceptor heavy atoms were considered. VMD was used for visualization and image rendering.

### 3.2.22 In vitro Kinase and Phosphatase Assay

The reaction was carried out in 1X assay buffer (5mg/ml BSA, 150mM Tris pH 8.0, 100mM $MgCl_2$, 2mM ATP) with 2$\mu$g purified rNAP1 and 2$\mu$l Casein kinase 2 (CK2, NEB #P6010) at $30^0C$ for 30, 45, 60, 75 and 90min. Post phosphorylation with CK2 (90min), serine threonine kinase inhibitor PMSF was added. Then calf intestinal phosphatase (CIP, NEB #M0290) treatment for dephosphorylating the phosphorylated rNAP1 was carried out at $37^0C$ for 30, 45, 60, 75 and 90min. Finally, all samples were stored at $-80^0C$ till further use. The un-phosphorylated, phosphorylated and dephosphorylated rNAP1 proteins were analysed by 10% SDS-PAGE followed by western blot with pan-phosphoserine antibody (Abcam, ab# 9332) to

confirm the phosphorylation status, then they were loaded on a 6% Native-PAGE and silver stained.

### 3.2.23 Histone Binding Assay

6X His tag H2A and H2B were purified under denaturing conditions and then the dimers were reconstituted as previously described[154]. The dimers were purified by size-exclusion chromatography using HiLoad 16/60 Superdex-200 gel filtration column (GE). The H2A/H2B dimers were incubated with rNAP1 and Phos-rNAP1 in binding buffer (20mM HEPES pH 8.0, 0.5mM EDTA, 1% Glycerol, 5μM $ZnSO_4$,1mM $MgCl_2$, 25mM KCl, 1mM DTT, 0.1% NP-40) for 1h at $4^0$C. The Ni-NTA beads used were pre-blocked with 10% BSA and each binding assay included a final concentration of 3% BSA. Post incubation the beads were then washed with binding buffer thrice. The bound material was eluted with SDS loading buffer, analysed by 18% SDS-PAGE and stained with Coomassie Brilliant Blue.

## 3.3. Results

### 3.3.1 Immunoprecipitation of histone chaperone identification

The histone isoforms, H2A.1 and H2A.2 were ectopically expressed by cloning in a pcDNA FLAG-HA vector in CL38 cell line. Post stable clone selection, nucleosolic fractions were isolated from the cell lines and where subjected to immunoprecipitation (IP) sequentially by FLAG and then HA. The immunoprecipitate obtained was initially checked by western blotting [Figure 3.3a] and then loaded on to a 4-20% SDS gradient gel and subjected to silver staining [Figure 3.3b]. As seen in the gel image, many differential and significant protein bands were not observed visually for lanes corresponding to H2A.1 and H2A.2. However, the protein eluate obtained post IP was also subjected to LC-MS, nevertheless, significant and consistent differences were clearly not found, thereby making it imperative for us to use a candidate

protein approach. For this we choose NAP1 as it is one of the major histone H2A chaperone in eukaryotic system.
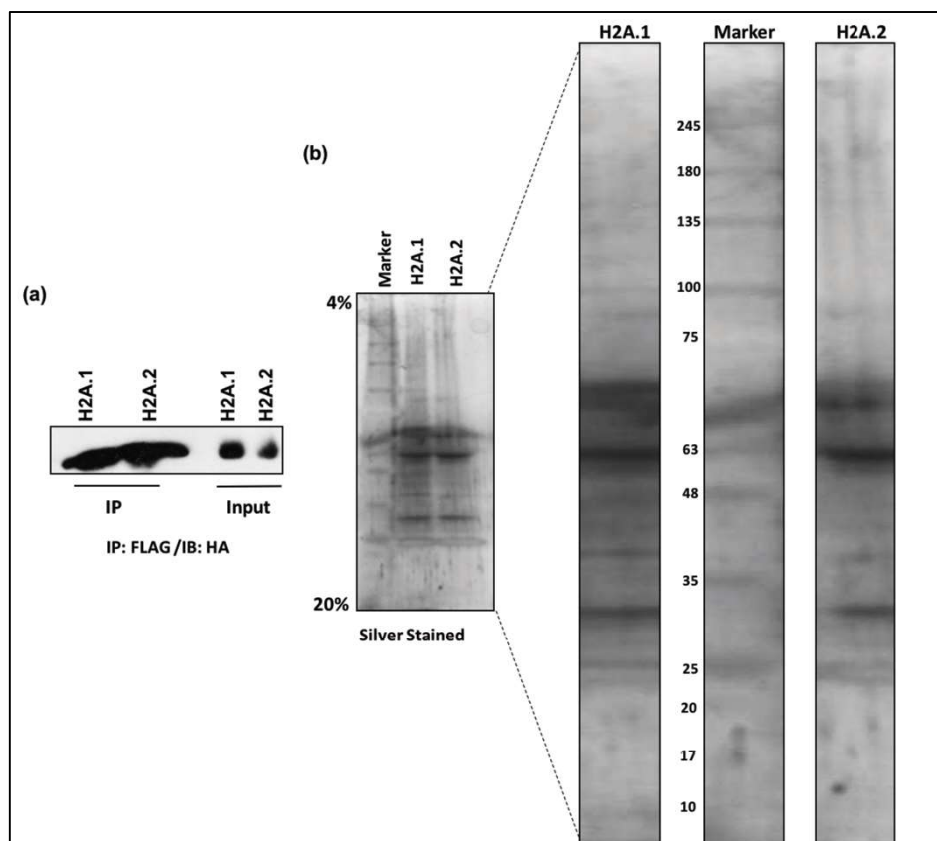


**Figure 3.3. Nucleosolic binding partners of H2A.1 and H2A.2.** (a) Western blotting of immunoprecipitate and input fractions with HA antibody. Immunoprecipitation was done by FLAG antibody. (b) Silver stained gel image of H2A.1 and H2A.2 immunoprecipitate loaded on a 4-20% SDS gradient gel.
IP: Immunoprecipitation; IB: Immunoblotting.

### 3.3.2  NAP1, a histone chaperone for H2A.1 and H2A.2

NAP1 was cloned in a pcDNA MYC vector and transfected into H2A.1 and H2A.2 FLAG-HA expressing CL38 cell lines. Post 72h of transfection, the cells were collected and nucleosolic fraction prepared and IP with MYC was carried out. After verification of IP, by western blotting with MYC antibody, presence of H2A.1 and H2A.2 were detected by immunoblotting with FLAG antibody **[Figure 3.4a]**. As seen by the presence of FLAG signal corresponding to H2A.1 and H2A.2 in IP of NAP1 MYC, both the histone isoforms seem to interact with histone chaperone NAP1.
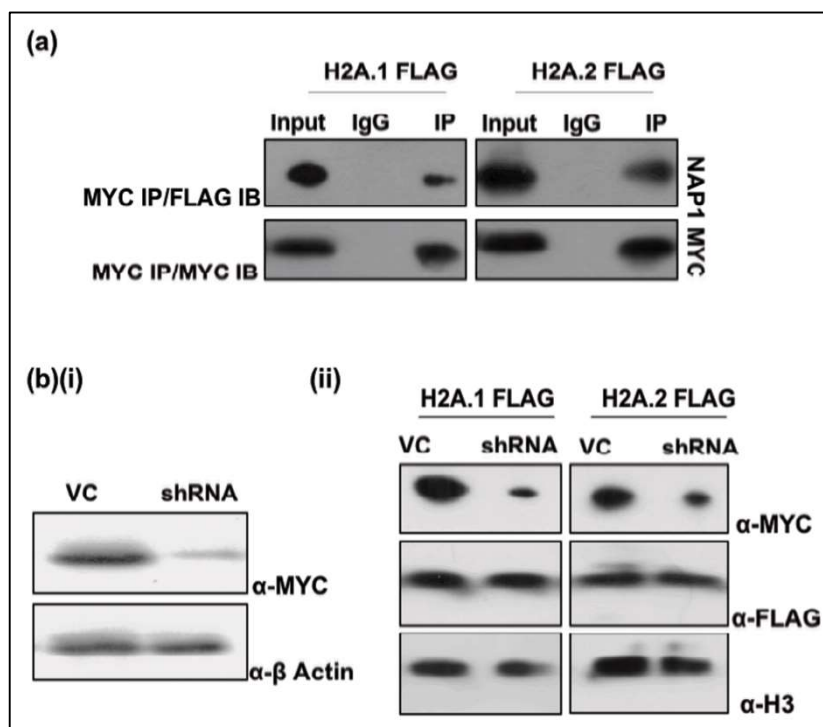
**Figure 3.4. Association of NAP1 with H2A.1 and H2A.2** (a) Western blotting depicting interaction of MYC NAP1 with both H2A.1 FLAG and H2A.2 FLAG. Immunoprecipitation was done with MYC antibody in CL38 cell line, after verifying the IP by performing western against MYC. The probing for FLAG-tagged histones was done. (b)(i) shRNA mediated knock down of NAP1. The shRNA used for NAP1 was able bring a significant downregulation, at least by 80%.(ii) Effect of depletion of NAP1 on H2A.1 and H2A.2 recruitment. From the cells depleted with NAP1, chromatin fraction was probed for the presence of FLAG-histones. H3 was used as a loading control.
IP: Immunoprecipitation; IgG: Isotype control; IB: Immunoblotting; VC: Vector Control.

However, to understand whether there exists any preferential dependence of either H2A.1 or H2A.2 towards NAP1 as their specific and exclusive histone chaperone we specifically knocked down NAP1 and monitored its effect on chromatin deposition/recruitment of H2A.1 and H2A.2. shRNA knock down of NAP1 was successful as seen by western blotting with MYC antibody **[Figure 3.4b(i)]**. Further, probing for FLAG signal in vector control and NAP1 knock down cell lines revealed no significant differences on chromatin enrichment of either H2A.1 or H2A.2 **[Figure 3.4b(ii)]**. This clearly suggests that NAP1 dependent H2A deposition is redundant and can be bought about by other H2A histone chaperones like FACT complex in its absence.

Interestingly, while analyzing the NAP1 protein we found out that none of the higher vertebrate NAP1 species is characterized. Apart from the well-defined crystal structure of yNAP1 details

regarding other species NAP1 are not known. To understand in-depth regarding NAP1 and its interaction with histones, we thought to first characterize rat NAP1 by use of biophysical and biochemical means.

### 3.3.3  Purification and structural validation of rNAP1

To purify rNAP1, we expressed 6X His tag NAP1 in BL21 (DE3) pLysS and found it to be highly soluble with the majority of the protein present in the soluble fraction **[Figure 3.5a, lane 3]**. For purification, the induced soluble fraction (ISF) was incubated with Ni-NTA beads. The proteins bound to the beads efficiently and were eluted with 70mM imidazole **[Figure 3.5a, lane 7]**.

The presence of higher oligomeric states of yNAP1 and xNAP1 have been reported[147,145]. To investigate the oligomeric states of rNAP1, we carried out size exclusion chromatography of purified NAP1 using calibrated gel filtration column (GFC) at 500mM NaCl **[Figure 3.5b]**. Gel filtration yielded a discrete peak at around 65ml expected to be of NAP1 dimeric species. In addition, a broad peak was observed spanning 42-60ml elution volume of the GFC **[Figure 3.5b]** which could be either aggregates or unresolved higher species of NAP1. Peak corresponding to NAP1 monomeric peak was not observed irrespective of the concentration of rNAP1 suggesting that rNAP1 does not exist as a monomer in solution. This is in contrast to the results seen with yNAP1, where at a 500mM NaCl concentration the predominant species is a dimer [147]. The results seen with yNAP1, where at a 500mM NaCl concentration the predominant species is a dimer[147].

### 3.3.4 Different rNAP1 complexes exhibit similar secondary and tertiary structures

The fraction for the broader peak spanning 42-60ml and the discrete peak with elution volume

at 65ml **[Figure 3.5b]** were collected separately, and the secondary structure analysis was

carried out.
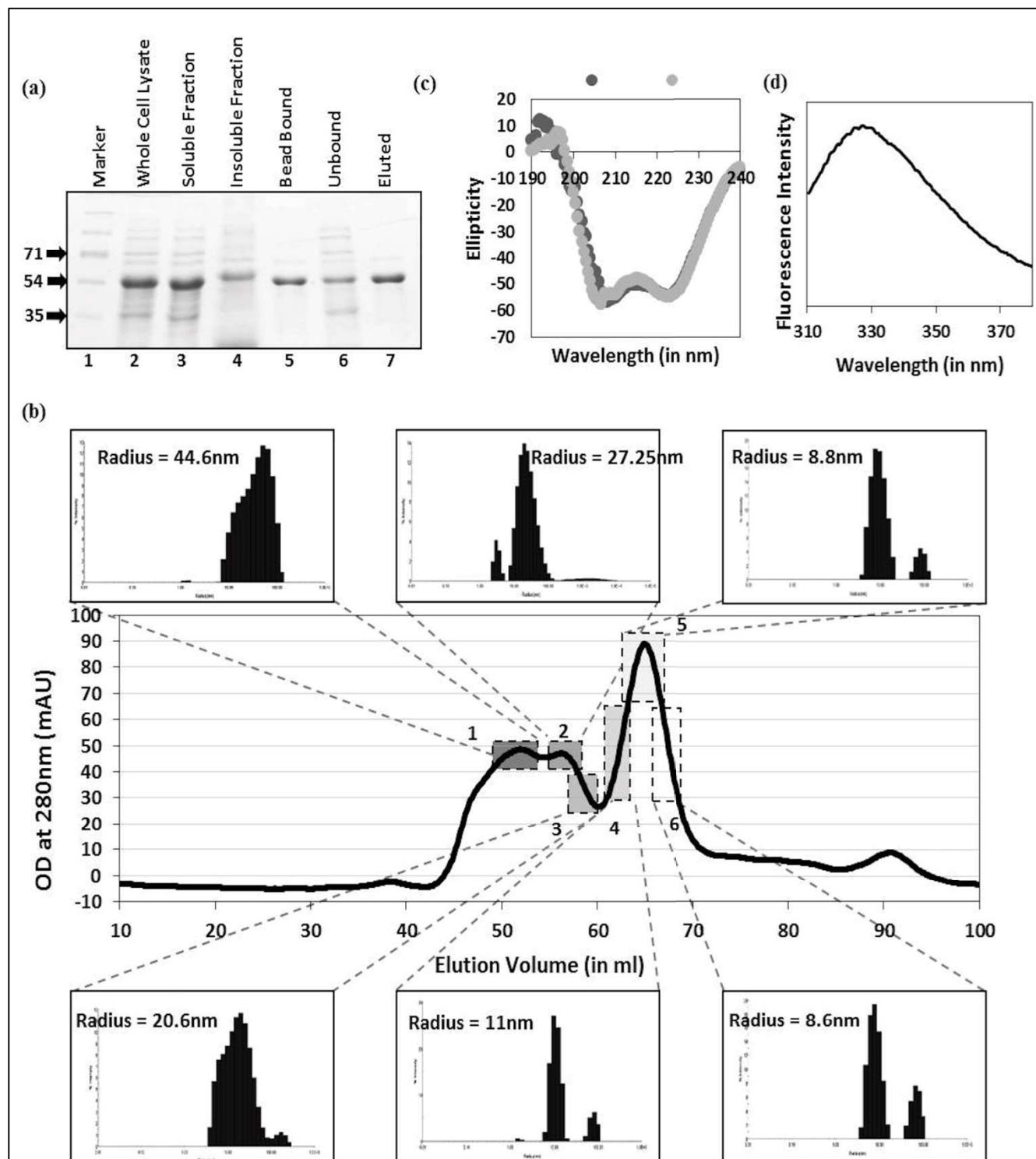


**Figure 3.5. Higher oligomer structures of rNAP1.** (a) Coomassie stained 10% SDS gel showing the purification profile of 6X His tagged rNAP1. (b) Gel elution profile of rNAP1 at 500mM NaCl concentration. Each region marked by a box was collected and subjected to Dynamic light scattering, the stokes radius of which is highlighted. 1, 2, 3 corresponds to DLS of protein eluted from 50-58ml and 4, 5, 6 corresponds that of 60-68ml. (c) Overlay of Far UV CD spectra of both oligomeric (50-58ml eluted protein) and Dimeric (60-68ml eluted protein) species. (d) Fluorescence spectra of rNAP1 with emission maxima at 320nM corresponding to a well a folded structure.

The data suggests that the secondary structures of the two fractions are identical **[Figure 3.5c]**. Dip at 222 and 208nm characteristic of α-helices confirmed that rNAP1 has a high proportion of helical structure and also contains β-sheets **[Figure 3.5c]**. This is consistent with the crystal structure of yNAP1, with which rNAP1 shares 37% sequence identity. rNAP1 has three tryptophan residues at positions 134, 171 and 262. Consistent with this, rNAP1 exhibited a fluorescence emission maximum at 320nm, **[Figure 3.5d]** suggesting that the tryptophan's are buried and the protein is properly folded.

### 3.3.5  rNAP1 dimers self-associate into hexameric and decameric complexes

Based on our CD and fluorescence data and the previous reports on yNAP1, the broad peak observed spanning 42-60ml elution volume of the GFC, we speculated it to consist of unresolvable higher order oligomeric structure of rNAP1. To better characterize the size distribution of oligomeric species in the different fractions obtained from GFC, the separately collected fractions **[Figure 3.5b]** were subjected to dynamic light scattering (DLS). Analysis of the rNAP1 dimer peak, fraction 5 shows that it has stokes radius of 8.8nm. Fraction 2, peak which is collected at 52ml, has stokes radius of ~27.25nm and is expected to be of hexameric species. Fraction 1 has stokes radius of around 44.6nm which is expected to be of decameric NAP1 complex. These observations are consistent with the data for xNAP1 which was reported to exhibit similar oligomeric complex by analytical ultracentrifugation[145]. The DLS results show a high polydispersity that might be due to the presence of a range of oligomers.

### 3.3.6  rNAP1 higher oligomers are more stable

Previous studies with yNAP1 and xNAP1 have shown that, although at the physiological ionic strength of 150mM NaCl, NAP1 exists in the form of higher oligomers, whereas at 500mM NaCl it primarily exists as a dimer [147][142]. Our results show that even at 500mM NaCl, a very high percentage population of rNAP1 exists in the form of higher oligomers **[Figure 3.5b]**. To

further characterize the *in-solution* behavior of rNAP1, we investigated the oligomeric status of rNAP1 in buffers with increasing ionic strength. In stark contrast to the reports for yNAP1 and xNAP1, the data suggests that even at 1M NaCl concentration there is no significant alteration in the rNAP1 elution profile during GFC, signifying the persistence of the higher oligomeric structures of rNAP1 **[Figure 3.6a]**.
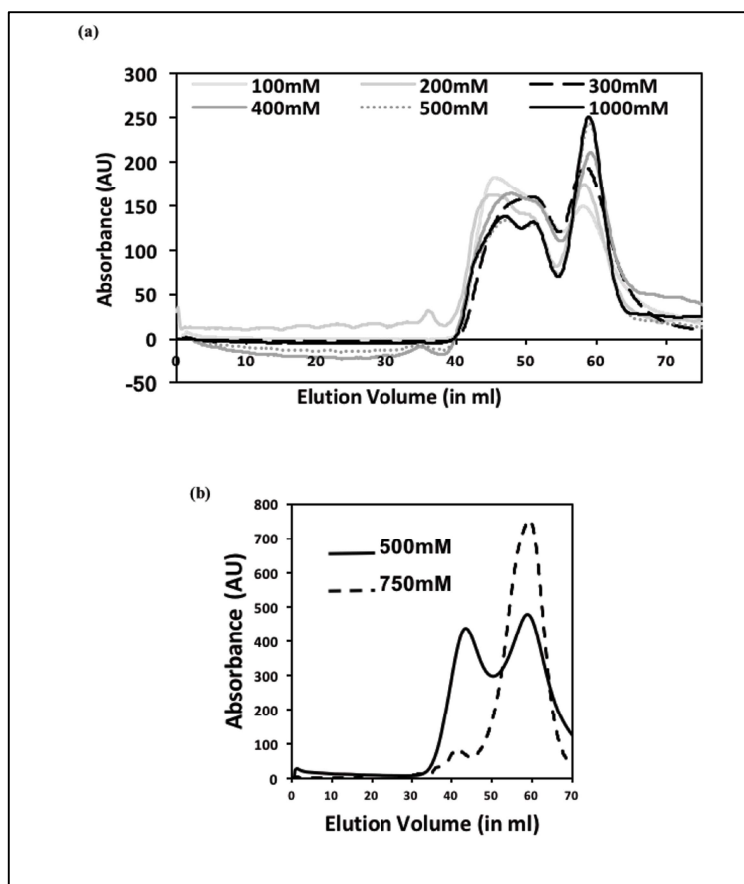


**Figure 3.6. Stability of rNAP1 Oligomers.** (a) Gel elution profile of 6X His tagged rNAP1 at various salt concentrations ranging from 100mM to 1000mM NaCl concentration. (b) Gel elution profile of rNAP1 purified by ion exchange, at 500 and 750mM NaCl concentrations.

Previously, the presence of 6X His tag has been shown to enhance the stability of proteins [162]. To address whether the enhanced stability observed for rNAP1 was due to 6X His tag, rNAP1 was expressed without tag using pET3a vector and purified using anion-exchange chromatography. The purified protein was subjected to size-exclusion chromatography. At 750mM NaCl concentration, unlike with 6X His tag, only the peak corresponding to dimeric rNAP1 was obtained. This suggests that indeed 6X His tag was in part responsible for altered

oligomerization property of NAP1. However, even at 500mM NaCl concentration a marked proportion of higher oligomeric peaks were observed for rNAP1, unlike yNAP1 and xNAP1 [**Figure 3.6b**]. This shows that rNAP1 irrespective of the presence of 6X His tag has a higher propensity to undergo oligomerization.

### 3.3.7 *rNAP1 dimers and oligomers follow a two-state unfolding model and have similar stability*
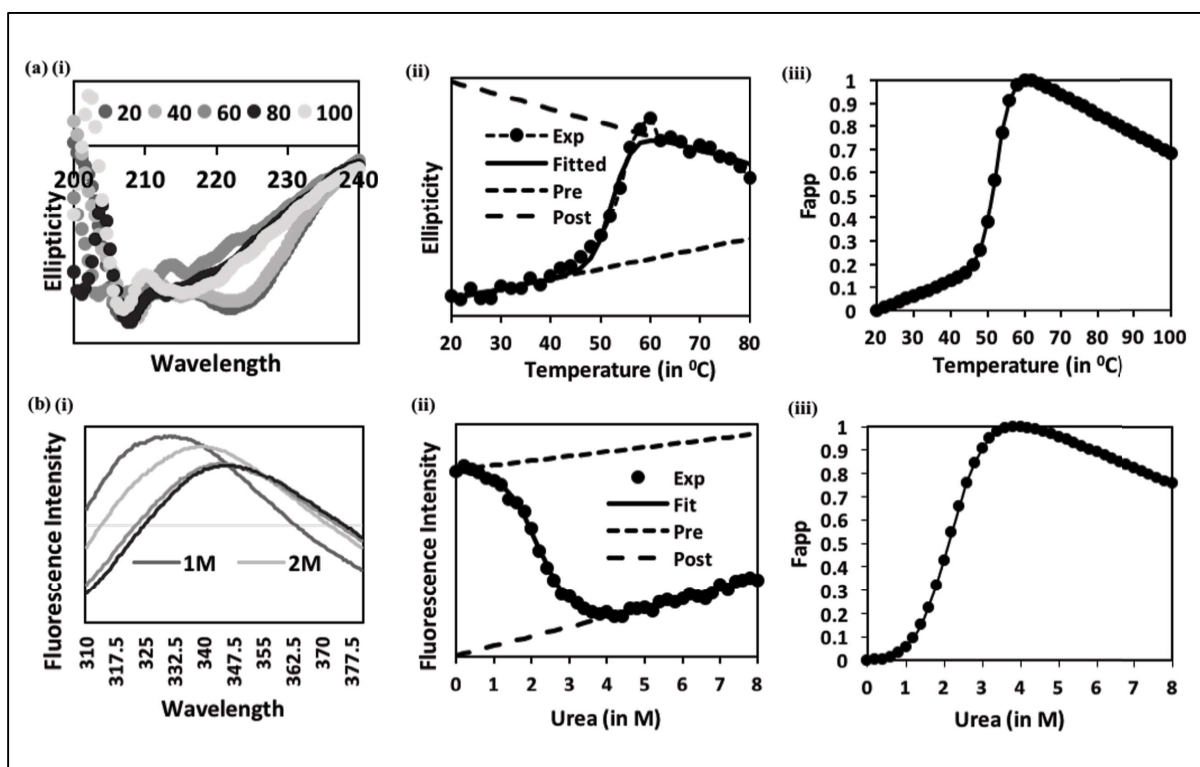


**Figure 3.7. Biophysical characterization of rNAP1.** (a) Secondary structure changes due to unfolding induced by temperature changes monitored by Far UV CD Spectra. (i) Far UV CD Spectra of rNAP1 at various temperatures, shown only 5 temperatures ranging from 20-100°C. (ii) The data obtained can be fitted into a two sate kinetics of unfolding. (iii) Graph showing the $F_{app}$ curves of transition. (b) Tertiary structure changes due to unfolding induced by urea monitored by Fluorescence Spectra. (i) Fluorescence spectra of rNAP1 at both 1M and 2M urea concentrations. (ii) The data obtained can be fitted into a two sate kinetics of unfolding. (iii) Graph showing the $F_{app}$ curves of transition.

We next wanted to study the unfolding characteristic of rNAP1 of both the dimeric complex and the higher order oligomers. The NAP1 dimeric and oligomeric fractions were subjected to equilibrium unfolding in response to thermal and chemical denaturants that was monitored by observing both secondary and tertiary structure changes. Analysis of the thermal unfolding

curves by far UV CD spectra suggest that dip at 222nm can serve as a good spectroscopic probe for monitoring secondary structure unfolding **[Figure 3.7a (i)]**. The data obtained could be fit into two-state unfolding model for dimeric proteins, i.e., the only populated states are native dimer and unfolded monomers **[Figure 3.7a (ii)]**. Similar to secondary structure unfolding data, the tertiary structure unfolding data could be fit into two-state model of unfolding **[Figure 3.7b (ii)]**. There was a drop in the fluorescence intensity along with red shift of fluorescence emission maxima with the unfolding of protein **[Figure 3.7b (i)]**. The Fapp curves of transitions monitored by both CD and FL probes were plotted **[Figure 3.7a (iii) and 3.7b (iii)]**. The $\Delta G°$ ($H_2O$) and m values of 14.6 (+/- 0.3 kcal $mol^{-1}$) and 7 (+/- 0.1 kcal $mol^{-1}$ $M^{-1}$, respectively were obtained for the dimeric species and the same was also seen for oligomeric species *(Figure S1 in Annexure I)*.

### *3.3.8 NAP1 in mammals is highly conserved and is structurally very similar to yNAP1*

In order to understand the possible changes in the structure which might be responsible for the altered oligomerization/stability/unfolding characteristics of rNAP1, the multiple alignment of NAP1 from rat, mouse, human and cow was carried out, which suggests that NAP1 protein is almost identical in mammals **[Figure 3.2]**.

We then matched sequences of rNAP1 with yNAP1. **Figure 3.8a** shows that there are substitutions by non-similar amino acids in key domains of NAP1 protein. In the dimerization domain, which reconstitutes α-helices 1 and 2, the identity is only 35%, and many amino acid substitutions are with glycine or proline. Further, they also differ in other regions of NAP1 like β-sheets. We carried out homology modelling to assess whether the differences in amino acid composition can possibly bring about any structural alterations in vertebrate NAP1 as

compared to yNAP1. The modelled structure of rNAP1 suggests that the overall structure of

NAP1 is highly conserved [Figure 3.8b].
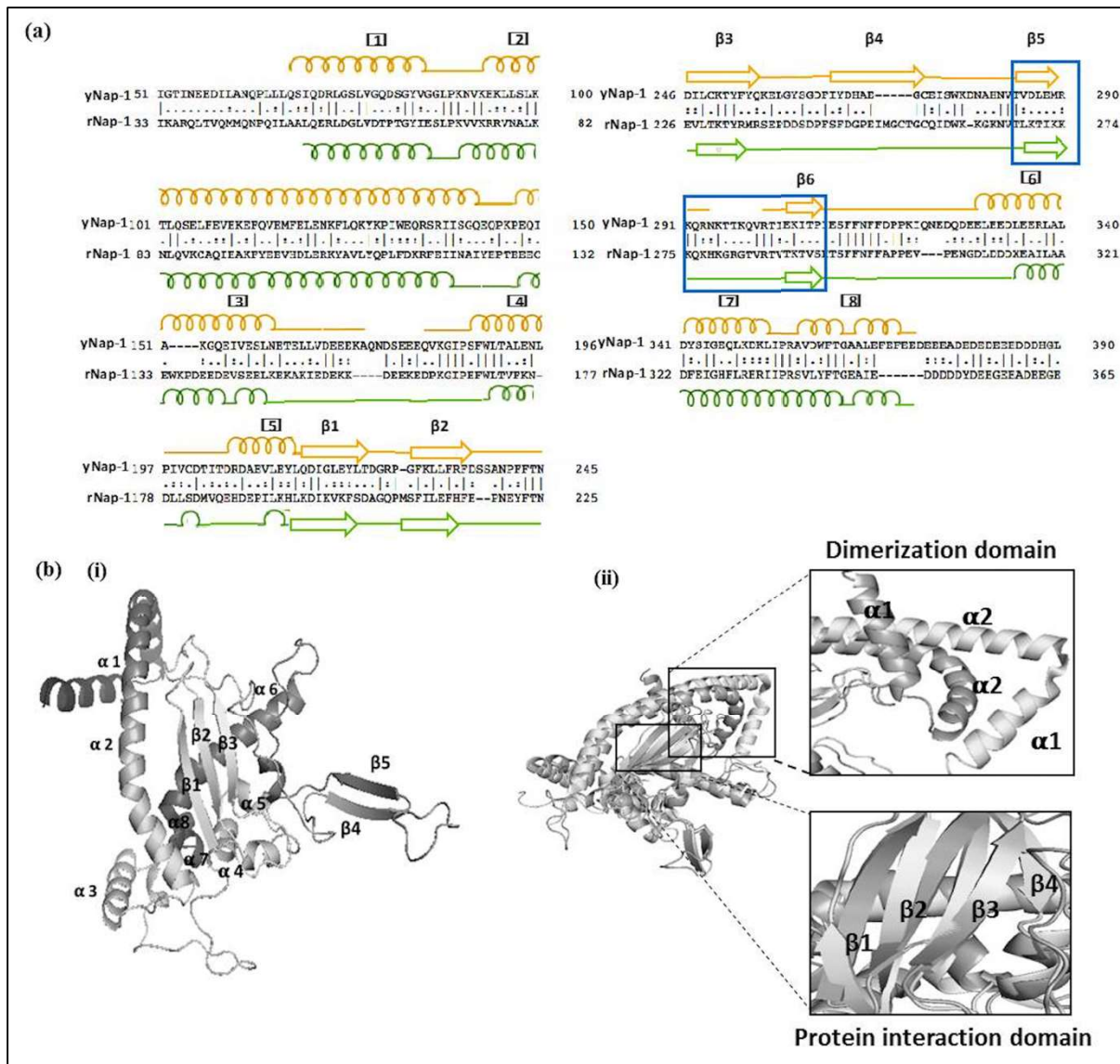


**Figure 3.8. Structural similarities of rNAP1 with yNAP1.** (a) Amino acid sequence alignment of yNAP1 and rNAP1 (http://www.ebi.ac.uk/Tools/msa/clustalw2). They are 37% identical with many amino acid substitutions. Blue box highlights the sequences reconstituting β-hairpin structure. (b)(i) Structure of rNAP1 generated by homology modelling (ii) Overlay of yNAP1 and rNAP1 structures, with zoom images highlighting their differences in Dimerization domain (reconstituting **α** helices 1 and 2) and protein interaction domain (comprising of three β-sheets in rNAP1 unlike that of four in yNAP1).

However, critical differences can be observed in the fold and loop of domain I (made up of α-helices 1 and 2), which shares identity of only 35% for this region, and the key differences are due to the substitutions of proline with serine and glutamine. Further, they differ in the number of β-sheets constituting the domain II. In case of rNAP1 domain II seems to contain only three

β-sheets unlike that of four in yNAP1 **[Figure 3.8b]**. Moreover, apart from these structural differences, there is a change in the amino acid composition of the β-hairpin structure, made up of β-sheets 5 and 6 in yNAP1 and 4 and 5 in rNAP1 (highlighted by box in Figure 3.7a). These differences appear very critical in determining the overall biophysical characteristics of the protein because the first difference lies in the dimerization domain and the second in the protein interaction domain[143].

### *3.3.9  rNAP1 dimer is more stable than yNAP1*

To gain in depth insights of the differential stability of rNAP1 and yNAP1, we performed molecular dynamic simulation (MDS) of both the dimeric structures for a span of 100nsec **[Figure 3.9]**. The convergence of the MD simulation in terms of structure was calculated by RMSD with respect to initial structure.

The RMSD analysis was in agreement with *in vitro* data with a lower RMSD of rNAP1 containing system, suggesting rNAP1 dimers are more stable than yNAP1 **[Figure 3.9a]**, in part owing to the extensive hydrogen bonding amongst rNAP1 monomers in comparison to yNAP1 **[Figure 3.9c]**. In addition, free energy binding analysis for both the structure also shows that rNAP1 with lower energy of binding is more stable than yNAP1 **[Figure 3.9d]**. RMSF of residues showed that, most of the regions for both proteins showed a similar fluctuation pattern except that amplitude of fluctuation in case of yeast is higher as compared to that of rat **[Figure 3.9b(i)]**. The residue ranges 1-292 depict the RMSF of one monomer and 293-584 for the second monomer in both rNAP1 and yNAP1. The residue ranges 90-105, are a part of single monomer and as can be seen fluctuate comparatively more than other residues in the rNAP1. These residues are part of the dimerization domain (Domain I) formed by α-helices 1 and 2. This same region corresponds to the residue range 383-398 in the second monomer of rNAP1, which also shows identical behavior. Also, the residue range 145-180 of

the monomer too shows more fluctuation in rNAP1 as compared to the corresponding region in yNAP1. The reason behind this can be attributed to the presence of four β-strands in yNAP1 in contrast to three in rNAP1.
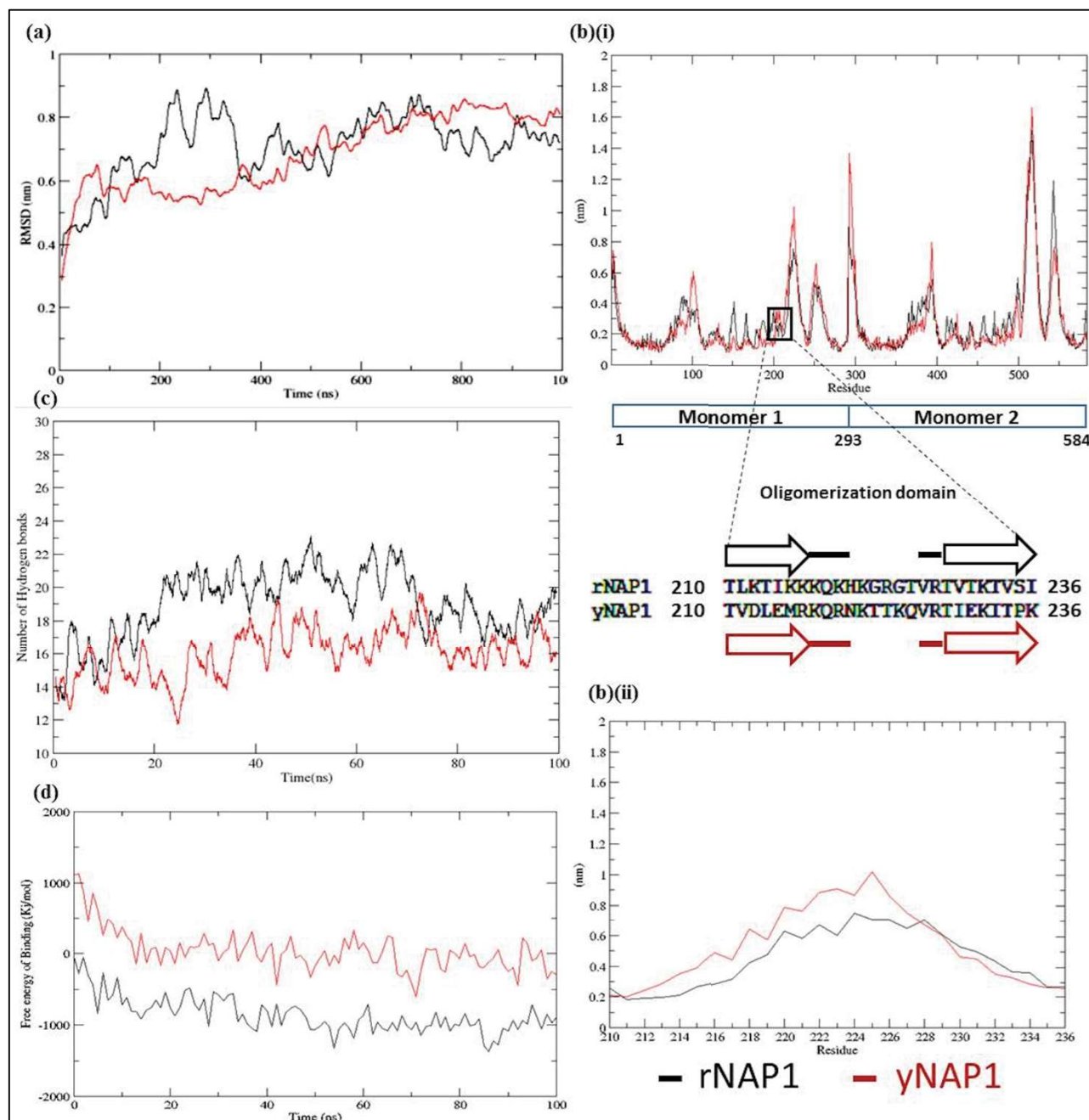


**Figure 3.9. Molecular dynamics simulation of yNAP1 and rNAP1.** (a) Graph showing the RMSD of yNAP1 and rNAP1 throughout the course of 100ns simulation. rNAP1 has lower RMSD, hence more stable. (b)(i) RMSF of residues showed that most of the region for both the proteins showed a similar fluctuation pattern except that amplitude of fluctuation in case of yeast is higher as compared to that of rat. Inset highlights the region 210-236 amino acids harbouring the oligomerization domain. (b)(ii) RMSF of rNAP1 and yNAP1 residues involved in the oligomerization domain, yNAP1 fluctuates more. (c) Graph showing the hydrogen bonds in the two systems through the course of the simulation. rNAP1 has more H-bonds. (d) Graph depicting the free energy of binding of the two systems. Based on free energy analysis rNAP1 is more stable as compared to yNAP1.

Our *in vitro* and *in silico* data suggests owing to high electrostatic interactions between monomers, rNAP1 is relatively more stable than yNAP1. Also, RMSF analysis of oligomerization domain ranging from 210-236 amino acids suggests that fluctuations are more in yNAP1 compared to rNAP1 **[Figure 3.9b(ii)]**, hence it might be possible that due to this difference in stability rNAP1 tends to more in oligomeric form than a dimer.

### 3.3.10 Phosphorylation favors oligomerization of rNAP1

Studies on *Drosophila* NAP1 (dNAP1) have revealed that NAP1 undergoes phosphorylation at key residue S284 located in the β-hairpin harboring the nuclear localization signal (NLS)[163]. It is noteworthy that the β- hairpin structure is known to harbor NLS[164]. It has also been suggested that possible PTMs occurring nearby this hairpin might lead to disruption of oligomers thus exposing NLS in case of yNAP1[142]. It has been postulated that phosphorylation happening in a cell cycle dependent manner controls the nuclear translocation of NAP1. In the oligomeric form of NAP1, the NLS is buried and hence the protein may not be translocated into the nucleus. Disruption of oligomers for the formation of dimers where NLS is exposed is required for translocation into nucleus. It has been suggested that the occurrence of PTMs may govern this process. In this regard, Casein Kinase 2 (CK2) binds to yNAP1 and phosphorylates at 11 sites, majority of which are located in regions of NAP1 which affects its nuclear localization[149].
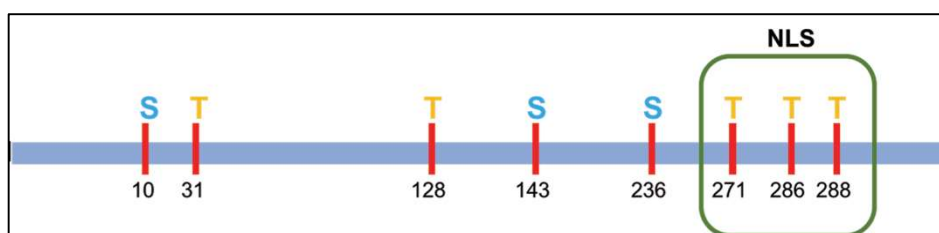


**Figure 3.10. Predicted CK2 sites on rNAP1.** Each red bar represents a putative site of phosphorylation with respective highlighted amino acid. Serine residues are in blue, threonine in yellow. Green box depicts the NLS signal. The sites were predicted using http://kinasephos2.mbc.nctu.edu.tw server.

We hypothesized that phosphorylation may play a role in governing oligomerization and thus may be regulating its nuclear transport via altering the structural organization of protein. We predicted the CK2 putative phosphorylation sites of rNAP1 and found out 8 sites, out of which 3 reside in NLS region **[Figure 3.10]**
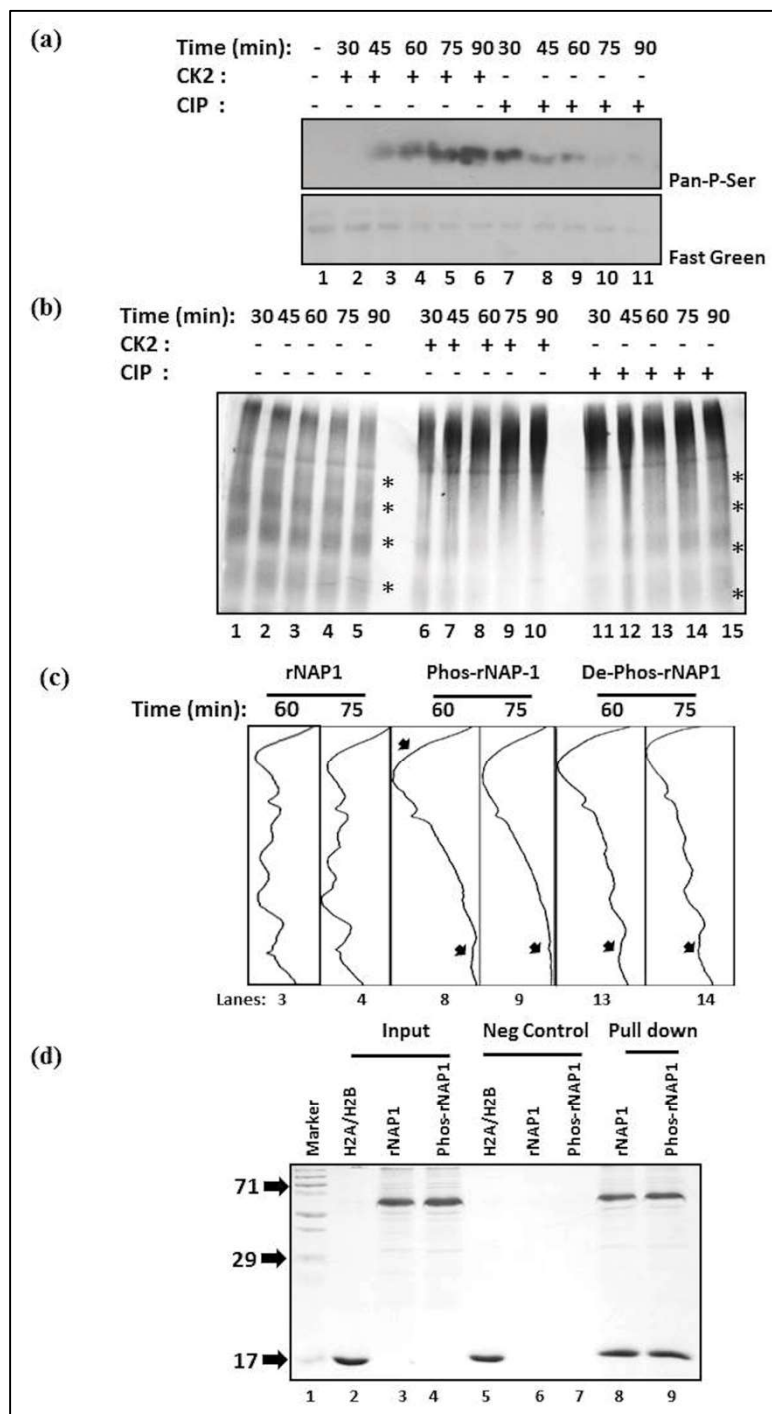


**Figure 3.11. Phosphorylation favors oligomerization of rNAP1.** (a) CK2 mediated *in vitro* phosphorylated (lanes 2-6) and CIP mediated dephosphorylation (lanes 7-11) of phosphorylated rNAP1 was loaded on 10% SDS gel and transferred to probe with pan-phosphoserine antibody. The assay was carried out at 30, 45, 60, 75 and 90 min time points. Unmodified rNAP1 is loaded as Lane 1 and used as a negative control. (b) Native gel stained with silver showing the oligomerization tendency of CK2 phosphorylated rNAP1 (lanes 6-10), Dephosphorylated rNAP1 (lanes 11-15). Lanes 1-5 are of unmodified NAP1 at different time points, as a negative control. Star (*) marks the various subspecies of rNAP1 on native gel. (c) Densitometry analysis of the native gel with arrows showing the critical differences at 75 and 90 time points of the assay. (d) Histone binding assay done using un-phosphorylated and phosphorylated rNAP1 with H2A/H2B dimers. Input protein was loaded on lanes 2-4, pull down samples on lanes 8 and 9. Negative control, lanes 5-7 involves incubation of Ni- NTA beads with individual proteins. CK2: Casein Kinase 2 and CIP: Calf intestinal phosphatase.

To this end, we performed *in vitro* kinase assay of rNAP1 using CK2 and bacterially purified

rNAP1 **[Figure 3.11a]** for various time points ranging from 30-90min and probed it with pan-phosphoserine antibody (Lane 2-6). After confirmation of phosphorylation, the rNAP1 **[Figure 3.11a; Lane 1-5]** and dephosphorylated rNAP1 **[Figure 3.11a; Lane 6-10]** were run on a native gel to understand any possible changes in oligomerization **[Figure 3.11b]**. The time dependent increase in appearance of higher molecular weight proteins and loss of lower molecular weight proteins upon phosphorylation compared to untreated **[Figure 3.11b; Lane 1-5]** clearly suggests that phosphorylation favors oligomerization **[Figure 3.11b; Lane 6-10]**.

To understand whether dephosphorylating the phosphorylated rNAP1 can affect the oligomeric propensity, we incubated the phosphorylated protein with CIP at various time points. Western blotting with pan-phosphoserine antibody confirmed the time-dependent dephosphorylation of phosphorylated rNAP1 **[Figure 3.11a; Lanes 7-11]**. The dephosphorylated rNAP1 proteins loaded on a native gel markedly showed a time-dependent increase in the low molecular weight proteins. **[Figure 3.11b, Lanes 11-15]**. Densitometry analysis of time points, 60 and 75min during the course of phosphorylation/dephosphorylation highlights the changes in oligomeric status of rNAP1 during *in vitro* kinase and phosphatase assay **[Figure 3.11c]**.

Along with CK2, a kinase whose sites have been mapped on NAP1 we also performed the assay using a pan kinase, protein kinase C (PKC) to further validate our earlier findings. After confirmation of phosphorylation by western blotting, phosphorylated rNAP1(Phos-rNAP1) and dephosphorylated (De-phos-rNAP1) was loaded on a native gel, data of which clearly suggest that irrespective of the kinase used oligomerization of rNAP1 is enhanced by phosphorylation *(Figure S2 in Annexure I)*. However, it was noteworthy that PKC phosphorylation mediated oligomerization was irreversible, even after CIP treatment, possibly due to phosphorylation of many other sites apart from NLS, which may have an inhibitory effect on de-oligomerization.

We next wanted to investigate whether phosphorylation mediated oligomerization of rNAP1 has any effect on its histone binding capability. Histone binding assays using rNAP1 and Phos-rNAP1 with reconstituted H2A/H2B (6X His tag) dimers **[Figure 3.11d]**, showed that, phosphorylation favored rNAP1-oligomers has no effect on its histone binding capacity, this is in accordance with the earlier report on yNAP1[149]. Indeed, the work on NAP2, a related protein of NAP1 also suggests that CK2 mediated phosphorylation aids in deciding the localization of the protein and has no effect on its histone binding capacity[165].

## 3.4. Discussion

Presence of differential histone chaperones for histone isoforms has not been studied in depth. Current study suggests for the possibility that may be isoforms share similar chaperones for their deposition on to DNA. This can be attributed to the way how chaperones interact with their cargo. Many chaperones like nucleoplasmin, yeast Asf1, yeast NAP1, Spt16 subunit of FACT and nucleolin contain long acidic amino acid stretches with which they interact with basic histones leading to charge neutralization[166,167,168]. However, charge neutralization does not justify for the specificity of the histone-chaperone interaction, and it cannot be the universal phenomenon for all the chaperones as, mammalian Asf1 and *Drosophila* NAP1 lack an acidic tail[168,146]. Therefore, it could be that these acidic regions may assist in strengthening histone-chaperone interaction.

Also, other chaperones like Asf-1, CAF-1 and HIRA are known to contain a conserved hydrophobic β -structure, which facilitates interaction with H3/H4[168,169,170,171]. Similar structure is also seen in H2A/H2B chaperones SET/TAF-1b and NAP1, mutational studies have implicated that this conserved β-sheet may be the primary histone recognition motif in these chaperones[167,146]. As histone isoforms differ in very few amino acids which may not reside exactly in the motif recognised by chaperones which might logically explain why H2A.1

and H2A.2 might have same set of chaperones. This explanation is further strengthened by the observation made by *Varadabasso et al.*, in context of isoforms of H2A.Z, H2AZ.1 and H2A.Z.2; their proteome/interactome analysis revealed the presence of similar set of histone chaperones.

rNAP1, though showed interaction with H2A.1 and H2A.2, its properties in context of oligomer formation, thermal unfolding and effect of PTMs on its histone binding capacity have not been studied in depth. Not only for rNAP1, not many studies have been done in context of understanding higher vertebrate species NAP1. Therefore, rNAP1 has been used as a model protein to characterise it biophysically and biochemically. Higher oligomeric structures seen for rNAP1 was more stable than yNAP1. Further, incubating it with increasing salt concentrations revealed hydrophobic interactions are the reason behind this stability. However, in order to understand that this profound increase in stability is due to 6x-His tag or is an inherent property of rNAP1 we performed similar experiments with untagged rNAP1 and showed that both forces are involved.

It is noteworthy that a tag has such a stabilizing effect on oligomeric states of a protein, especially considering that the N-terminal residues of NAP1 are not implicated in oligomerization. The side chains found in the protein-protein interface of higher order complexes are more likely polar in nature, and thus more easily disrupted by ionic strength. It is reasonable to conclude, therefore, that if the formation of higher order oligomers is due to electrostatic interactions, it would be readily abrogated by high salt. However, the stability of 6X His tag containing rNAP1 higher order complexes even at higher salt concentrations suggests the possibility of non-electrostatic forces at play. It is to be noted that apart from the stability differences between yNAP1 and a higher eukaryotic species - rNAP1, they also follow different models of unfolding. rNAP1 exhibits a two-state denaturation unlike yNAP1, where an apparent three state model of unfolding has been reported[147].

RMSF analysis of oligomerization domain ranging from 210-236 amino acids suggests that fluctuations are more in yNAP1 compared to rNAP1 suggesting that due to this difference in stability, rNAP1 tends to more in oligomeric form than a dimer. This 24 amino acid stretch is known to form a β5 and β6 hairpin loop and interacts with neighboring NAP1 through an extensive hydrogen bonding, thus leading to formation of higher oligomers. Notably, this region is 31% identical with yNAP1, with substitutions like threonine, lysine with glycine. Moreover, considering the fact that rNAP1 and hNAP1 have identical residues constituting the β-hairpin structure and also display similar oligomer stability, it is reasonable to speculate that the observed differences in the oligomerization propensity between rat and yeast NAP1 are indeed due to these sequence alterations. Possibly, the key differences in oligomerization property and substitutions in residues in the β-hairpin reflects the difference in the way the NAP1 complex and its interaction with histones is regulated in yeast versus higher vertebrates.

Our experiments with *in vitro* phosphorylated rNAP1 provides conclusive evidence that phosphorylation favors formation of oligomers, possibly by burying its NLS and thus affecting its nuclear translocation. Indeed, the dephosphorylation by CIP has in part, reversed this effect on oligomerization, thus, further proving that indeed phosphorylation of NAP1 effects its oligomerization capacity. Nonetheless phosphorylation does not seem to affect its histone binding capacity. However, what remains to be studied is whether, phosphorylation effects stoichiometric ratio of histone binding and also does it influence its nuclear import and export.

## 3.5. Conclusion

In summary, we show that rNAP1 interacts with both H2A.1 and H2A.2 and its knockdown has no effect on chromatin deposition of these histone isoforms. We also describe the biophysical and biochemical characterization of recombinant rNAP1 that is 98% identical to hNAP1. We found that rNAP1 forms stable oligomers in solution compared to yNAP1 and

exhibits two-state model of unfolding, with Tm of $51.2^0$C and $[Urea]_{1/2}$ of 2.1M where as yNAP1 displays three state model of unfolding. Molecular dynamic simulations revealed dimer of rNAP1 is more stable in comparison to yNAP1 owing to the higher number of hydrogen bonds. The homology based modelled structure of rNAP1 show key differences in the β-sheets of protein interaction domain and in α-helix of dimerization domain; these key differences might explain the differential stabilities of rNAP1 and yNAP1. Further, we also show that *in vitro* phosphorylation of rNAP1 increases its oligomerization potential indicating the importance of post-translational modifications in governing NAP1 functions.

*Chapter 4*

# IV. Chromatin Binding Partners of Histones H2A.1 and H2A.2

# 4.1. Introduction

DNA and the highly basic histone proteins assemble together to form chromatin. Cells exploit changes in DNA-histone and histone−histone interactions to regulate gene expression. The change in the conformation of chromatin states is either achieved by posttranslational modification (PTM) of histones or by changing the biochemical composition of nucleosomes by the replacement of major histone types with specific histone variants or isoforms[172]. Especially, histone variants upon deposition onto the chromatin by specific histone chaperones give rise to specialized nucleosomes which contribute to epigenetic regulation in various physiological states.

Histone variants endow chromatin with unique properties and show a specific genomic distribution that is regulated by specific deposition and removal machineries. These variants have important roles in early embryonic development, regulate the lineage commitment of stem cells, as well as the converse process of somatic cell reprogramming to pluripotency. Recent progress has also shed light on how mutations, transcriptional deregulation and changes in the deposition machineries of histone variants affect the process of tumorigenesis. These alterations promote or even drive cancer development through mechanisms that involve changes in epigenetic plasticity, genomic stability and senescence, and by activating and sustaining cancer-promoting gene expression programs. Not only individually, in combination also, various histone variants form 'double variant nucleosomes' or 'heterotypic nucleosomes', which differ in their stability thus influencing the gene expression pattern. One of the well-studied such nucleosome is formed by H3.3 and H2A.Z. These nucleosomes are known to be relatively unstable (labile) and susceptible to disruption even at low salt concentrations **[Figure 4.1]**[173].
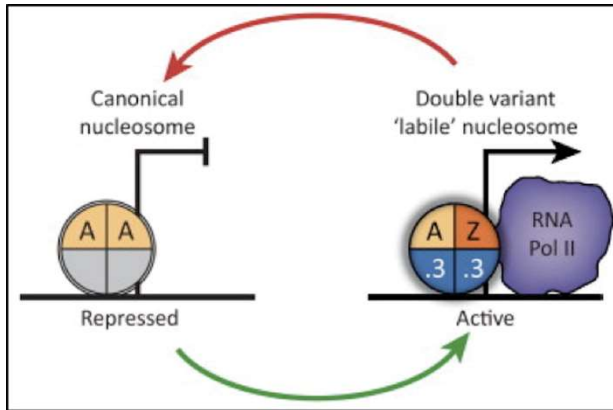
**Figure 4.1. A new model for transcriptional activation involving histone variant incorporation at the TSS using H3.3 and H2A.Z.** In this model, the nucleosome located at the TSS continuously cycles between the repressed canonical form (red arrow) and an unstable histone variant-containing state (green arrow) during every round of transcription, adding another regulatory step to the transcription process.
*Adapted from:*
*Tatiana A. Soboleva, et al., (2014). Histone variants at the transcription start-site. Trends in Genetics, 30(5):199-209.*
*DOI: http://dx.doi.org/10.1016/j.tig.2014.03.002*

These unstable Nucleosome Core Particles (NCPs) could serve as 'place holders' to prevent the region from being covered by adjacent quite stable (canonical) NCPs and/or nonspecific factors, as might occur if the region were completely free of nucleosomes[174]. At the same time, because of their relative instability the H3.3/H2A.Z NCPs could more easily be displaced by transcription factors [175]. Likewise, genome wide distribution analysis of these 'double variant' nucleosomes revealed their presence predominantly near the transcriptional start site suggesting that such labile nucleosomes when present on a promotor or enhancers, the energy required for cellular machinery to make the region nucleosome free is very less[173]. Further, many studies on the histone variant distribution pattern revealed that each variant or combination of variants has a highly specific pattern of distribution *in vivo*, signifying that these differences in stability are elaborately exploited in the regulation of gene expression[176].

Further, addition of differential PTMs the variants undergo, will lead to a repertoire of various NCPs. These NCPs together form an effective language guiding various cellular process as explained in 'Histone code hypothesis'. For example, Phosphorylation of the histone variant H2A.X at its unique serine at position 139 (the product of which is referred to as γH2A.X) is an early event in the detection of DNA double-strand breaks (DSBs)[177]. γH2A.X spreads around the DNA damage site to amplify the signal to the repair machinery[178]. Thus, ultimately acting as binding sites for recruitment of repair proteins. At low levels of genotoxic stress,

γH2A.X helps to activate the G2–M checkpoint and cell cycle arrest[179], and H2A.X-deficient mice are hypersensitive to radiation and develop T cell lymphomas on a p53-null background[180]. Therefore, not only various histone variants/isoforms in combination, their potential to undergo differential PTMs may influence the underlying gene expression pattern and thus have the prospective to govern tumor development.

Even though, histone isoforms H2A.1 and H2A.2 might have a similar set of chaperones, the possibility still exists for their differential chromatin or nucleosomal binding partners. If such a possibility exists either these NCPs may differ in their biochemical composition in terms of their PTMs and/or they might have differential stability. This part of the thesis discusses the work done in this regard.

## 4.2. Methods

### 4.2.1 Animal handling

All the experiments were performed on male Sprague- Dawley rats (spp. *Rattus norvegicus*) after approval of the Institute Animal Ethics Committee (IAEC# 29/2011 and 04/2014), Advanced Centre for Treatment Research and Education in Cancer and the Committee for the Purpose of Control and Supervision on Animals, India standards. The detailed protocol to induce liver carcinogenesis is as previously described[96]. Tissue samples were fixed in formalin and prepared as paraffin-embedded blocks according to standard protocols. The H&E-stained sections were microscopically reviewed for histopathological alterations to confirm normal and HCC.

### 4.2.2 Isolation of histones

a)    *From tissue:* Nuclei were isolated from liver tissues by sucrose density gradient centrifugation[181] and then, histones were extracted from isolated nuclei by low concentration acid extraction method. Liver tissues (~3g) excised from euthanized rats were rinsed in excess

of ice-cold 'nuclear buffer A' (15mM Tris-Cl pH7.5, 60mM KCl, 15mM NaCl, 2mM EDTA, 0.5mM EGTA, 0.34M sucrose, 0.15mM β-ME, 0.15mM spermine and 0.5mM spermidine). Liver tissues were minced and homogenized in motor driven glass-Teflon homogenizer in 30ml fresh nuclear buffer A. Homogenate was filtered through 8 layers of cheesecloth to remove large solid particles left over. The filtrate was centrifuged for 15min at 1500g (5000rpm in Rota 6R-V/Fm, Plasto Crafts) and $4^0$C. The crude nuclear pellet obtained was resuspended in fresh 30ml of nuclear buffer A. The suspension was layered on 10ml of 'nuclear buffer B' (15mM Tris-Cl pH7.5, 60mM KCl, 15mM NaCl, 0.1mM EDTA, 0.1mM EGTA, 1.8M sucrose, 0.15mM β-ME, 0.15mM spermine and 0.5mM spermidine) and centrifuged for 90min at 100000g (26000rpm in AH629 swinging bucket rotor), $4^0$C. The nuclear pellet was resuspended in 3ml nuclear buffer A. The nuclei were used for histone extraction as earlier described[182].

Nuclei were resuspended in 0.2M $H_2SO_4$ at a concentration of ~2mg DNA/ml and incubated overnight on a rocking platform at $4^0$C. For determining concentration, the nuclei were ruptured in 2M Urea- 5M NaCl and the absorbance was measured at 260nm. The suspension was centrifuged for 10min at ~12000g (15000rpm in Rota4R V/Fm, Plasto Crafts), $4^0$C. The supernatant comprising of acid soluble nuclear proteins was transferred to fresh clean microcentrifuge tube. Nuclear proteins (predominantly histones) in the supernatant were precipitated by adding 4 volumes of acetone and stored overnight at -$20^0$C. The mixture was centrifuged for 10min at ~12000g and $4^0$C as mentioned before to pellet the proteins. The pellet was washed once in chilled acidified acetone (0.05M HCl in 100% acetone) and once in chilled 100% acetone. Protein pellet was dried in vacuum centrifuge for 15min. The pellet was resuspended in 0.1% β-ME in water at a concentration of ~5μg/μl and stored at -$20^0$C. Histones resolved on 18% SDS-polyacrylamide gel were transferred to PVDF membrane, probed with

site-specific modified histones antibodies and signals were detected by using ECL plus detection kit (Millipore; Catalogue no. WBKLS0500).

b)      *From cell line:* Cell pellet was resuspended in 0.1ml PBS in a microcentrifuge tube. To this suspension 0.9ml lysis solution (250mM sucrose, 50mM Tris-Cl pH7.5, 25mM KCl, 5mM $MgCl_2$, 0.2mM PMSF, 50mM $NaHSO_3$, 45mM sodium butyrate, 10mM β-ME and 0.2% v/v Triton X-100) was added. Tube was inverted several times and centrifuged for 15min at 800g (4000rpm in Rota4R), $4^0C$. The nuclear pellet obtained was subjected to histone extraction by low concentration acid extraction method by adding 0.3ml of 0.2M $H_2SO_4$ as described previously.

### 4.2.3  Analysis of histones

Extracted histones were estimated and subjected to SDS-PAGE for western blot analysis or processed further for AUT-PAGE.

a)      *Protein estimation*: Histone concentrations in various samples were determined by Bradford method[183]. Protein standards were prepared containing a range of 0 to 100µg of Bovine Serum Albumin in 5ml of 1X Bradford reagent. Histone samples were also prepared similarly. Samples were vortexed and incubated at room temperature for 5min. Absorbance was measured at 595nm and the blank was adjusted. Histone samples were estimated for protein concentration by plotting standard curve.

b)      *SDS-PAGE of extracted histones*: Same as described in chapter III (page number 77). After the run was complete, the power supply was then disconnected and gel was subjected to Coomassie staining for protein visualization or subjected to western blot analysis.

### 4.2.4 Western Blot Analysis

Levels of particular proteins or their post-translational modifications were assessed by western blot analysis using the appropriate antibody. See *Annexure II* in *Appendix* for the details of the antibodies used in the study.

c)      *Electroblotting from SDS-PAGE:* Histones (5-10μg) were electroblotted from SDS-PAGE gels to PVDF membranes for western blot analysis. The transfer tank of electroblotting apparatus (Trans-Blot Cell, Bio-Rad) was filled with 1X transfer buffer (see *Annexure V* for composition). PVDF membrane was activated in 100% methanol for 5sec. The activated membrane and SDS-PAGE gel were equilibrated in 1X transfer buffer. The gel membrane transfer sandwich was prepared and inserted into the transfer tank with gel on cathode side and membrane on anode side. Transfer was conducted at a constant current of 300mA for 200min. Proteins transferred onto the membrane were detected by staining with Ponceau S (0.5% w/v Ponceau S in 1% v/v acetic acid) and destaining with several changes of water.

d)      *Immunoblot detection:* Proteins transferred onto PVDF membrane were probed with antibodies. In general, membrane with transferred proteins was incubated in 'blocking buffer' i.e. 5% BSA in Tween20/Tris-buffered saline (TTBS, 100mM Tris-Cl pH7.5, 0.9% w/v NaCl and 0.1% v/v Tween20) for 1h at room temperature on orbital shaker. Blocking buffer was then replaced by recommended dilutions of primary antibodies in TTBS and incubated for 1h at room temperature in orbital shaker. The membrane was vigorously washed four times with TTBS for 15min each at room temperature. Further the membrane was incubated in recommended concentrations of HRPO labelled secondary antibodies in TTBS for 1h at room temperature on orbital shaker. The membrane was again washed vigorously four times with TTBS at room temperature and developed using Immobilon Western (Millipore #P90719). The membrane was exposed to X-ray film in dark room and developed using Optimax X-ray film processor (Protec). Band intensities were analysed using ImageJ and GraphPad prism software.

The list of antibodies used throughout the work has been tabulated and presented as *Annexure II in Appendix* section.

### 4.2.5  Acetic acid, Urea, Triton (AUT) -PAGE Analysis

AUT-PAGE analysis of histones was done as described earlier [184]. For preparation of AUT-PAGE (15cm long) gel, glass-plate sandwich was assembled using 0.15cm thick spacers. Separating gel solution was prepared and poured into glass plate sandwich and was allowed to polymerize in light. Stacking gel solution was then prepared, poured and polymerized into the glass plate sandwich (*Annexure V* in *Appendix* for details of chemicals). The sandwich was attached to electrophoresis chamber and filled with electrophoresis buffer (1M acetic acid and 0.1M glycine). The gel was pre-electrophoresed for 2h at constant voltage of 200V. The buffer was then replaced and histone samples (see *Annexure V in Appendix* for sample preparation) were loaded in the wells. AUT gel was washed twice in ten gel volumes of buffer A (0.05M acetic acid, 0.5% w/v SDS), 30min each and once with modified buffer of O'Farrell (0.0625M Tris-Cl pH 6.8, 2.3% w/v SDS, 1% β-ME). The gel was treated with three washes of 50% methanol of 1h each for rapid fixation of proteins and proceeded for silver staining.

### 4.2.6  MALDI-TOF/TOF mass spectrometry

Core histones spots were subjected to in-gel digestion for identification by MALDI-MS fingerprint mapping as described earlier [185,186]. Core histones separated on AUT two-dimensional gel were visualized by SDS-silver staining method. Spots that appeared on the gel were numbered and subjected to MALDI-TOF/TOF mass spectrometry in a two-step process. First the proteins were digested using trypsin protease. Then, the tryptic peptides were subjected to MALDI-MS and the MALDI-MS spectrum was compared to database for identification of histone protein (*Annexure V* in *Appendix* for details of chemicals).

a)      *In gel digestion:* Core histones spots on gel were subjected to in-gel digestion for identification by MALDI-MS fingerprint mapping as described. Core histone spot of interest was excised and cut into small pieces (~1mm$^3$) using a scalpel and placed into microcentrifuge tube. Freshly prepared reducing solution was added ten volumes of the gel pieces and vortexed until brownish stain disappeared. They were rinsed few times with water to stop the reaction. Next, they were washed with 25mM ammonium bicarbonate for 15min. They were then dehydrated with 25mM ammonium bicarbonate in 50% v/v acetonitrile. Washing/rehydration step was repeated and gel pieces were vacuum dried.

Gel pieces were then covered with 10mM DTT solution and reduced for 1h at 56$^0$C. They were cooled to room temperature and DTT solution was replaced with 55mM iodoacetamide solution. They were incubated at room temperature for 45min in dark with occasional vortexing. They were washed, dehydrated and dried as mentioned in the previous paragraph. They were rehydrated in 1 volume of 20μg/ml Trypsin in 25mM ammonium bicarbonate by vortexing for 5min. They were covered in minimum volume of 25mM ammonium bicarbonate and incubated overnight at 37$^0$C.

Peptides were recovered as follows. Two volumes of water were added to the gel pieces, vortexed for 5 min. and sonicated for 5min. The peptide solution was removed and transferred to a fresh microcentrifuge tube. Two additional extractions were performed with 5% v/v TFA in 50% v/v acetonitrile. Recovered peptides were dried completely in vacuum centrifuge and reconstituted in 10μl of 5% v/v TFA in 50% v/v acetonitrile. Recovered peptides were stored at -20°C until required for sample preparation for MALDI-MS analysis.

b)      *Sample preparation and analysis:* One microliter of recovered peptides and 1μl of peptide matrix solution (20mg/ml HCCA in 0.1% v/v TFA in 50% v/v acetonitrile) were pipetted onto the sample target (plate), mixed and allowed to dry. External calibration was

prepared by mixing peptide standard mixture and peptide matrix solution similarly. Sample target (plate) was inserted into the MALDI-TOF/TOF mass spectrometer (Bruker Daltonics, Ultraflex II) and analysed as recommended by manufacturer.

In brief, mass spectra were acquired on reflector ion positive mode. Database searching for protein masses was carried out using MASCOT search engine (version 2.2.03) by comparing peptide masses with those in NCBInr protein database *(database version: NCBInr_20080812.fasta)* in *Rattus* spp. The searches were carried out with trypsin digestion, one missed cleavage, fixed carbamidomethylation of cysteine residues and optional oxidation of methionine with 100ppm mass tolerance for monoisotopic peptide masses.

### 4.2.7  Reverse Phase High Performance Liquid Chromatography (RP-HPLC)

Separation of mammalian core histones by RP-HPLC was done as described earlier[182]. Briefly, acid-extracted histones were separated by RP-HPLC on a C8 column a C18 column (1.0x250mm, 5mm, 300A°; Phenomenex).

Mobile phases A and B consisted of water and acetonitrile with 0.05% trifluoroacetic acid, respectively. The flow rate was 0.42ml/min, and total run length was for 180min with the following gradient, starting at 20% B, increased linearly to 30% B in 2min, to 35% B in 33min, 55% B in 120min and 95% B in 5min. After washing at 95% B for 10min, the column was equilibrated at 20% B for 30min, and a blank was run between each sample injection. Under these conditions histones H3 split into three distinct peaks. The H3-containing fractions were collected, dried under vacuum and stored at -80 °C. RP-HPLC fractions were subsequently resuspended in water, analyzed by SDS-PAGE and control-stained with Coomassie Brilliant Blue after which they were subjected to western blotting against desired antibodies.

### *4.2.8 RNA isolation*

All solutions were prepared in 0.1% diethylpyrocarbonate (DEPC) treated water for isolation of RNA. Glassware was baked at $300^0$C for 4h and compatible plasticware was rinsed with chloroform. Nitrile gloves were used to prevent RNase contamination.

RNA was isolated from liver tissue by guanidine method for total RNA preparation[151]. Frozen liver tissue (0.1g) was powdered in pre-chilled mortar and pestle. The powder was suspended in 1ml denaturing solution (4M guanidine thiocyanate, 25mM sodium citrate, 0.5% sarkosyl and 0.1M β-ME) in microcentrifuge tube. To this suspension, 0.1ml of 2M sodium acetate pH 4, 1ml of water saturated phenol and 0.2ml of chloroform/isoamyl alcohol (49:1) were added. The suspension was thoroughly mixed and incubated at 0-4$^0$C for 15min. The suspension was then centrifuged for 20min at 10000g (15000rpm in Rota 4R), 4$^0$C. The upper aqueous phase was transferred to fresh microcentrifuge tube. RNA was precipitated by adding equal volume of 100% isopropanol and incubating for 30min at -20$^0$C.

The precipitate was centrifuged for 10min at 10000g (15000rpm in Rota 4R), 4$^0$C. RNA pellet was dissolved in 0.3ml denaturing solution. RNA was precipitated with 0.3ml of 100% isopropanol for 30min at -20$^0$C and centrifuged for 10min at 10000g (15000rpm in Rota4R), 4$^0$C. RNA pellet was resuspended in 75% ethanol, vortexed, incubated for 10-15min at room temperature and again centrifuged for 5min at 10000g (15000rpm in Rota4R), 4$^0$C. RNA pellet was dried for 5min and dissolved in DEPC treated water. RNA was stored at -70$^0$C until required. RNA was quantitated by diluting 5μl in 1ml alkaline water (1mM $Na_2HPO_4$) and reading at A260. Quality of RNA was confirmed by A260/A280 (1.9-2.0), A260/A230 (2.0-2.2) and agarose formaldehyde gel electrophoresis.

### *4.2.9 Agarose formaldehyde gel electrophoresis*

The protocol for denaturing agarose gel electrophoresis is as described earlier[151]. Agarose was dissolved in water and cooled to ~60°C to prepare 1% agarose formaldehyde gel. After cooling, 5ml of 10X MOPS running buffer (0.2M MOPS pH7.0, 0.5M sodium acetate and 0.01M EDTA) and 9ml of 12.3M formaldehyde were added. The gel was poured into electrophoresis tray with comb and allowed to set. Comb was removed and gel was placed in gel tank. Gel tank was filled with 1X MOPS running buffer. For electrophoresis, 2μg RNA was loaded per lane. RNA volume was increase to 11μl by water and 5μl of 10X MOPS buffer, 9μl of 12.3M formaldehyde and 25μl of formamide were added and sample was incubated for 15min at 55°C. To this mixture 10μl formaldehyde loading buffer (1mM EDTA pH8.0, 0.25% w/v BPB, 0.25% w/v xylene cyanol, 50% v/v glycerol) was added and loaded onto the gel. The gel was run at 5V/cm until dye migrated one-third to two-third length of the gel. The gel was removed, transferred to RNase free glass dish with water and soaked twice for 20min each. After sufficient removal of formaldehyde, gel was soaked in 0.5μg/ml ethidium bromide and allowed to stain for 40min. The gel was destained in water for 1h and examined on a UV trans-illuminator at a wavelength of 365nm to visualize RNA.

### *4.2.10 cDNA synthesis and Real time PCR*

Extracted RNA was further treated with DNaseI (Fermentas) for 60min at 37°C to degrade any possible DNA contaminant. DNaseI was inactivated by incubating the samples at 72°C for 30min. RNA was visualized by ethidium bromide staining after electrophoresis on a 1% MOPS denaturing agarose gel. RNA (2μg) was subjected to reverse transcription using M-MLV Reverse Transcriptase and random hexamer primers according to the manufacturer's (Thermo-Scientific) instructions. cDNAs were then amplified with the corresponding gene-specific primer sets (*Annexure IV* in *Appendix* for primer sequences), designed to amplify the total coding sequence, by PCR for 30 cycles using the condition of 30s at 94°C, 1 min at 58°C, and

1 min at 72°C. The PCR products were analysed on a 1% agarose gels containing 0.5μg/ml ethidium bromide. The cDNA synthesized was further used for Real-time PCR experiments with Syber green dye (Applied Biosystems). The expression levels were plotted as relative fold change with respect to GAPDH.

### 4.2.11 Cell line maintenance

Experiments were performed with the neoplastic CL38 and pre-neoplastic CL44 cells of rat liver origin. The methodology for their maintenance is same as described in chapter III (page number 73).

For Azacytidine and Trichostatin A (TSA) treatment, the cells were cultured in the medium as described above along with 5μM Azacytidine or 10nM TSA for 16h and 72h respectively. Post incubation cells were harvested and proceeded for further assays.

### 4.2.12 Cell Fractionation

The harvested cells were washed twice with chilled PBS, lysed in MKK lysis buffer (10mM Tris-Cl, pH 7.4, 0.27M Sucrose, 1mM EDTA, 1mM EGTA, 1% Triton X-100) containing protease and phosphatase inhibitors (1mM sodium orthovanadate, 10mM sodium fluoride, 10mM β-glycerophosphate, 10μg/ml leupeptin, 10μg/ml aprotinin, 1mM PMSF) for 30min at 4$^0$C. Following hypotonic lysis, cells were centrifuged at 12,500rpm for 20min at 4$^0$C to separate chromatin fraction and total soluble protein fraction.

### 4.2.13 Salt dissociation experiment

CL38 cells were transfected with H2A.1 pcDNA FLAG/HA, H2A.2 pcDNA FLAG/HA, H3.2 pcDNAMYC and H3.3 pcDNA MYC in all the possible four combinations. The chromatin of these transfected cells were isolated as mentioned in the above section and then it was incubated with different NaCl concentrations (600-1000mM) at 4°C for 30min. Supernatants were collected and the proteins were precipitated with 20% TCA. The histone in the pellet remaining

after salt treatment was extracted with 0.2M $H_2SO_4$ as described in histone isolation protocol (page no. 111). The proteins were then resolved on 18% SDS-PAGE and probed with suitable antibodies.

### 4.2.14 Mononucleosomal Immunoprecipitation

Nuclei from cells were prepared as described earlier[187]. Cells were lysed for nuclei isolation with buffer containing 10mM Tris-HCl (pH 7.4), 10mM NaCl, 3mM MgCl2, and 0.4% NP-40. All buffers were supplemented with 10mM Na-butyrate, 0.5µg/ml aprotinin, 0.5µg/ml leupeptin, and 1µg/ml aprotinin. Nuclei were then pelleted was treated with 0.2% formaldehyde for 1min at room temperature to fix nuclei before MNase digestion and resuspended in the same buffer plus 1mM $CaCl_2$. The crosslinking was quenched by addition of 125mM glycine. 5µl nuclei suspension was mixed with 200µl of 5M urea-3M KCl solution. The A260 was adjusted to 1.25, and the resuspended nuclei were digested with MNase (USB# 70196Y), 100 units/mg DNA, for 30min at 37°C. The reaction was stopped by adding EDTA (pH 8.0) to a final concentration of 10mM, and the suspension was centrifuged at 2500rpm for 5min, retaining supernatant S1. The pellet was then resuspended in lysis buffer plus 0.25mM EDTA, incubated on ice for 30min, and recentrifuged at 10,000 rpm for 10min after passing four times through a 20-gauge needle followed by four passes through a 25-gauge needle. The supernatant S2 was combined with S1. Mononucleosomes were layered on glycerol-gradient (10 to 40%) containing 10mM or 80mM NaCl, 10mM Tris-HCl (pH 7.4), 0.2mM EDTA and centrifuged for 16h at 27,500rpm at 4°C in a Beckman SW28 rotor. The mononucleosomal ring obtained was collected and its quality was confirmed on 1.8% TAE-agarose gel. Mononucleosomes (0.7ml) in immunoprecipitation buffer (10mM Tris-HCl at pH 7.4, 50mM or 10mM NaCl, 0.2mMEDTA) were incubated with 5µg anti-FLAG or anti-MYC antibody overnight at 4°C, followed by incubation with protein G sepharose beads for 4h and then washed five times with immunoprecipitation buffer and proceeded for SDS-PAGE sample

preparation. Twenty microliters of immuno- precipitated proteins were fractionated by SDS-PAGE and electrotransferred to PVDF membranes. Blots were proceeded for western blot analysis (described on page no. 114).

## 4.2.15 Nucleosome system building

Sequence analysis of rat nucleosome identified human nucleosome PDB ID: 2CV5 as a closet matched based on histone variants. Histones H4 and H2B were 100% identical. In histone H2A.1 only one change was at 40th position from Ser40Ala. In order to convert H3.1 of human to H3.3 of rat, five point mutations Ala31Ser, Ser87Ala, Val89Ile, Met90Gly and Cys96Ser and for H3.2 four mutations, apart from Ala31Ser were introduced. Thus, rat nucleosome consisting of Histones {H2A.1, H2B, H4, H3.2} and {H2A.1, H2B, H4, H3.3} were built, labelled and as 'system 1' and 'system 3' respectively. From system 1 & 3, system 2 & 4 were generated where H2A.1 was converted to H2A.2 by introducing mutations at Thr16Ser, Leu51Met and Arg99Lys positions on both the copies of the histone variants. The rest of the histone variants (H2B, H4 and H3.3) were unchanged. In both the systems the DNA were identical as with PDB ID: 2CV5.

## 4.2.16 Molecular dynamic simulations

Molecular dynamics (MD) simulations experiments were performed based on principles described earlier[188] in collaboration with CDAC, Pune and BTIS, ACTREC. Simulation were performed in triplicates for both the systems in a truncated octahedron box by adding sufficient ions to balance the nucleosome charge. Nucleosomal complex were represented using amber ff03 force filed and the TIP3P model to describe the water molecules. System was energy minimized in two steps, initially using steepest-descent method putting restrain on nucleosomal complex and allowing water to relax. In next minimization step entire system was allowed to relax. Then system was equilibrated first by NVT followed by NPT ensemble. All the Molecular simulations were carried out using the Gromacs-4.6.5 software, with periodic

boundary conditions. The particle mesh Ewald method was used to treat the long-range electrostatics, together with a cut-off of 1.2 nm for the short-range repulsive and attractive dispersion interactions, which were modelled via a Lennard-Jones potential. The Settle algorithm was used to constrain bond lengths and angles of water molecules, and P-Lincs for all other bond lengths. The time step of 2fs was used for entire system. The temperature was kept constant at 300K by using the Nose-Hoover thermostat method. The simulation was carried out for 250ns. To control the pressure at 1 atmosphere, Parrinello-Rahman method was used. Gromacs tools were used for RMSD and H-bond calculation[189]. Principal component analysis (PCA) was done using prody software. VMD software was used for contacts analysis calculations using TCL script and for image generation.

### 4.2.17 Cell cycle synchronisation

Exponentially growing cells were trypsinized and counted as described earlier and plated ($2X10^5$ cells per 100mm X 15mm culture dish) in complete MEM. At 30-40% confluent density, complete MEM was replaced by serum free MEM and cells were incubated for 24, 48, 72 and 96h. After completion of incubation, CL38 cells were trypsinized, suspended in 1ml MEM and centrifuged for 10min at 200g (2000rpm in Rota4R). Cell pellet was either used for extraction of histones or processed for flow cytometry analysis.

### 4.2.18 Flow cytometry analysis

Cells were prepared for flow-cytometry analysis as described earlier[180]. Cells were centrifuged for 10min at ~200g (2000rpm in Rota4R) and resuspended in 0.1ml of PBS. Cells were transferred to 0.9ml of 70% ethanol v/v in PBS and stored at -20°C for ≥ 2h until required. Ethanol-suspended cells were centrifuged for 5min at 200g (2000rpm in Rota4R). Cell pellet was resuspended in 1ml PBS and re centrifuged at 200g (2000rpm in Rota4R). The cell pellet

was resuspended in 1ml PI (1μg/ml)/Triton X100 (0/1%) staining solution with RNase and incubated for 15min at $37^0$C.

Flow cytometer FACS Calibur (Becton Dickinson) was adjusted for excitation with blue light and detection of PI emission at red wavelength. Cell fluorescence was measured in flow cytometer using pulse width-pulse area signal to gate out the cell-doublets and analysed using DNA content frequency histogram deconvolution software (ModFit LT v2.0 for Mac OS 8.6).

### 4.2.19 MTT assay

Cell viability was quantified by its ability to reduce tetrazolium salt 3-(4,5-dimethylthiazole-2ϒ)-2,5-diphenyl tetrasodium bromide (MTT) to coloured formazan products as described earlier [190]. MTT reagent (5mg/ml in PBS) was added to the cells at 1/10th volume of the medium to stain only viable cells and incubated at $37^0$C for 4h. MTT solubilisation buffer (0.01M HCl, 10% SDS) of two-fold volume was added to cells, followed by incubation in the dark at $37^0$C for 24h. The absorbance was measured at 570nm with Spectrostar Nano-Biotek, Lab Tech plate reader. Cell viability was expressed as the percentage of absorbance obtained in control cultures.

### 4.2.20 Colony formation assay

Clonogenic assay was performed as described earlier [191]. The cells (n=1000) were plated in triplicate in 60mm tissue culture plates and they were allowed to grow in a monolayer for 14 days. Cells were incubated in complete culture medium, with media changes after every 2-3 days. After 14 days, the cells were fixed with 4% paraformaldehyde for 1h. The colonies were stained with 0.5% crystal violet (0.5% in 70% ethanol) for 1h at room temperature, rinsed and air-dried. Surviving colonies with more than 50 cells were counted and images were captured using a high-resolution Nikon D70 camera (Nikon, Tokyo, Japan). For quantification of the size of the colonies ImageJ was used.

### 4.2.21 Micrococcal nuclease digestion assays

The assay was performed as described earlier[181]. Nuclei containing 2mM $CaCl_2$ were incubated for 2, 4, 6, 8 and 10min with 5U MNase/mg of DNA at 37°C in MNase digestion buffer (15mM Tris-Cl pH 7.4, 15mM NaCl, 2mM $CaCl_2$, 60mM KCl, 15mM β-ME, 0.5mM spermidine, 0.15mM spermine, 0.2mM PMSF, protease and phosphatase inhibitors). The digestion was stopped by adding 2X lysis buffer (0.6M NaCl, 20mM EDTA, 20mM Tris-Cl pH 7.5, 1% SDS). MNase digested samples were treated with RNaseA (100μg/ml) for 30min at $37^0$C followed by proteinase K (80μg/ml) treatment for 2h at $50^0$C. The samples were extracted sequentially with phenol, phenol: chloroform and chloroform followed by ethanol precipitation at $-20^0$C. The precipitated DNA was recovered by centrifugation at 10000g for 20min. The DNA pellet was washed, air dried, dissolved in 50μl of TE buffer and concentration was determined by A260/A280 absorbance. MNase-digested samples were resolved on 1.8% 1XTAE agarose gel electrophoresis with 0.5μg/ml ethidium bromide. The image was scanned with ImageJ software version 1.43u; Java 1.6.0_10 (32-bit).

### 4.2.22 In vitro transcription assays

The transcription run-on analysis was performed as previously described[192], with some optimizing modifications for liver cells. Briefly, sucrose density purified nuclei obtained from either 1gm liver tissue or $4 \times 10^6$ were used for the assay. Nuclei obtained were resuspended in glycerol buffer (50mM Tris–HCl, pH 8.3, 40% glycerol, 5mM $MgCl_2$, 0.1M EDTA) and used for the assays directly or are stored at -80°C till use. For assay, nuclei (1mg/ml,100 μl) were incubated with 25μl 5X reaction buffer (10mM Tris–HCl, pH 8.0, 5mM $MgCl_2$, 300mM KCl, 5mM DTT) containing 0.5mM each of ATP, CTP, and GTP, 100μCi of [α- $^{32}$P] UTP, and 1 U/μl RNasin (Invitrogen). The reaction was performed at $30^0$C for 30min, with collection of nuclei after every 5min interval. The aliquots of the hot nuclei (α- $^{32}$P labelled) were spotted on GF/C filters (Whatman), washed with 5% trichloroacetic acid and rinsed with 70% ethanol.

The amounts of $\alpha$- $^{32}$P RNA on the GF/C filters were measured with a scintillation counter. The counts were directly plotted post normalisation using zero-minute time point.

### 4.2.23 Chromatin Immunoprecipitation assay

The protocol for Chromatin immunoprecipitation (ChIP) assay is similar to that of mononucleosomal immunoprecipitation (on page no. 126) till washing of beads post antibody incubation, and instead of protein G sepharose beads, Dyna beads (Invitrogen #10004D) were used. Further, the procedure described in the Acetyl-Histone H3 Immunoprecipitation Assay Kit by Millipore was employed. Elution buffer (150μl) containing 50mM Tris-HCl pH 8.0, 10mM EDTA, 1%SDS, 50mM NaHCO3 and 20μg proteinase K was added and incubated at $55^{0}$C for 3h. Tubes were applied to a magnetic rack and eluted DNA was collected. Purified DNA was then analyzed by real-time PCR. The reaction mixture (5μl) contained 0.5μl of the appropriately diluted DNA sample, 0.2 pmol/l primers, and 2.5μl of IQ SYBR Green Supermix (Applied Biosystems). The reaction was subjected to a hot start for 3min at $95^{0}$C and 50 cycles of $95^{0}$C, 10s; $55^{0}$C to $65^{0}$C, 30s; and $72^{0}$C, 30s. Melt curve analysis was done to verify a single product species. Percent enrichment in each pulldown was calculated relative to input DNA. The primers designed were +/- 100bp. nearby TSS for all the genes (*Annexure IV* for list).

### 4.2.24 Methyl DNA Immunoprecipitation assay

Genomic DNA was purified using sigma gDNA Miniprep kit (Sigma# G1N350), according to the manufacturer's instructions. Purified genomic DNA was diluted into a total of 300μl TE buffer and sonicated with a Bioruptor (10 cycles at low power, of 30sec 'on' and 30sec 'off') to an average size of 300–500bp. An aliquot of sonicated DNA was run on 1% agarose gel to confirm fragment size during each methylated DNA immunoprecipitation (MedIP) procedure. Sonicated DNA (4μg) was denatured by incubation at $95^{0}$C for 10min and was immediately transferred to ice for 10min. Immunoprecipitation buffer containing 10mM sodium phosphate,

140mM NaCl and 0.05% Triton X-100 was added to a final volume of 500μl. For each IP reaction, 2μg of antibody (Methyl cytosine: Diagenode# MAb-006-100 or Hydroxy methyl cytosine: Abcam# ab106918) was added and incubated overnight at $4^0$C with shaking. Five percent of DNA was kept as input. After incubation, 30μl of Dyna Protein G beads (Invitrogen# 10004D) were added and further incubated for 1h at $4^0$C. Beads were washed thrice with 500μl of IP buffer. Elution buffer (150μl) containing 50mM Tris-HCl pH 8.0, 10mM EDTA, 1%SDS, 50mM $NaHCO_3$ and 20μg proteinase K was added and incubated at $55^0$C for 3h. Tubes were applied to a magnetic rack and eluted DNA and input DNA were purified with the Qiaquick PCR purification kit (Qiagen) followed by SYBR Green real-time quantitative PCR to identify methylated regions. PCR measurements were performed in duplicate. The primers designed for H2A.1, H3.2 and H2A.2, H3.3 are part of the CpG sites and CpG island respectively (*Annexure IV* for list). The average cycle thresholds for the technical replicates were calculated to yield one value per primer set for each biological replicate and normalized to input using the formula $2^{(Ct(input)-\{Ct(immunoprecipitation))}$. Averages and standard deviations of the normalized biological replicate values were plotted in the figures and used in t-test calculations.

## 4.3. Results

### 4.3.1 Histone variant H3.2 is upregulated and H3.3 is downregulated in HCC

To apprehend whether there are any other global histone changes apart from H2A.1 and H2A.2 before understanding the histone-histone interactions at the nucleosome level, histones were isolated from control and NDEA induced HCC tumor tissues of Sprague-Dawley rats and resolved using AUT-PAGE which separates proteins on the basis of mass and hydrophobicity[192]. Along with the significant change in pattern of major H2A isoforms H2A.1 and H2A.2, which has been reported earlier[96], major alterations in H3 region was also seen **[Figure 4.2a]**. The upper band intensity was increased and lower band decreased. These two

spots were identified as H3.2 and H3.3 respectively by mass spectrometry (MS) **[Figure 4.2b(i)(ii)]**. Peptides obtained for both the proteins have been tabulated in *Supplementary Figure 3.* To understand the expression changes of H3 variants in a quantitative manner, RP-HPLC was standardized, which aids to resolve three H3 variants, H3.2, H3.3 and H3.1. As seen in the overlay of HPLC profile of control and tumor, the H3.2 was increased and H3.3 decreased **[Figure 4.2c(i)]**. The area under the peak obtained for H3.2 and H3.3 is plotted for control and tumor tissues **[Figure 4.2c(ii)]**. The complete HPLC profile with all core histones has been shown as *Supplementary figure 4 in Annexure I.*
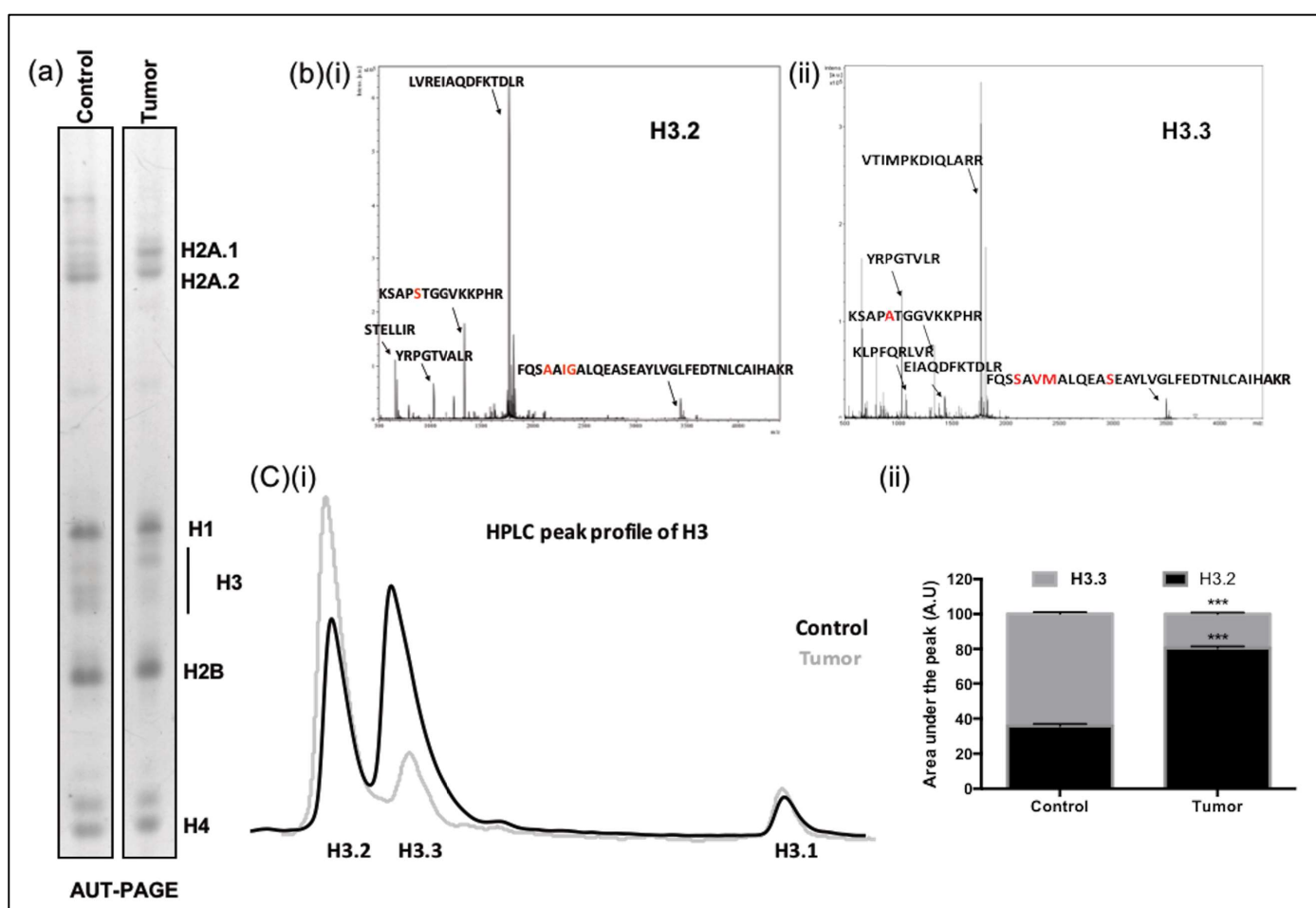


**Figure 4.2. Dysregulation of H3 variants correlates with tumor tissue at protein level.** (a) Silver stained AUT-PAGE analysis revealed changes in expression profile of H2A.1, H2A.2 and also in H3 region. Black line denotes the H3 region. Remaining histones are also marked. (b)(i)(ii) Mass spectrometry analysis of H3 region identified the upper band as H3.2 and lower protein band to be H3.3 respectively. The differential amino acids in the tryptic digested peptides are highlighted in red. (c)(i) Overlay of H3 variant RP-HPLC profile of control and tumor tissues showing upregulation of H3.2 and downregulation of H3.3 in tumor tissue. (ii) Quantitative graph plotted for showing the area under the peak for H3.2 and H3.3.

To understand whether the changes observed at the protein level is reflected at the RNA also. Measurement of these transcripts in tissues revealed a significant upregulation of H3.2 and downregulation of H3.3 **[Figure 4.3a(i)]**. Similar changes were observed in pre-neoplastic CL44 and neoplastic CL38 cells **[Figure 4.3a(ii)]**. These cell lines were derived from the liver of Sprague Dawley rats post administration of NDEA[193].

The transcription of replication-dependent histones like H3.2 markedly increases on entry of cells into S-phase[194,195]. The H3.3 variant, on the other hand, is a replication-independent histone variant and is expressed throughout the cell cycle[196]. Increased proliferation of cells is a hallmark of cancer, hence, to understand that whether the associated changes in the levels of the two H3 variants is due to changes in cell cycle phase between control and tumor samples.
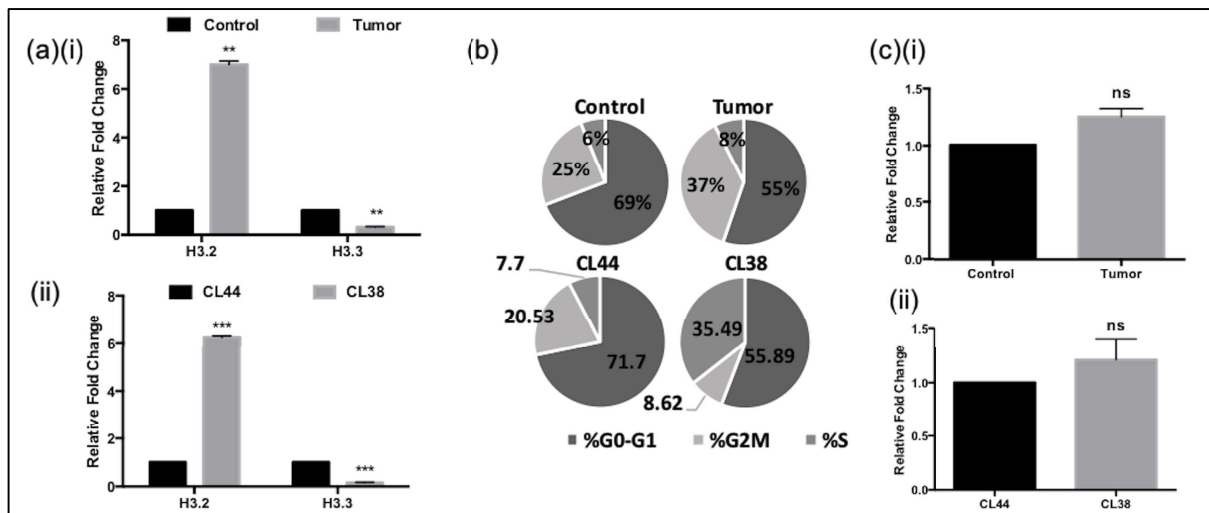


**Figure 4.3. Cell cycle dependent expression of H3 variants.** (a) Real time PCR, done to assess the changes in the transcript levels of H3.2 and H3.3 in (i) tissues and (ii) cell lines. (b) Flow cytometry analysis depicting the percentage of cells in various phases of cell cycle in form of a pie diagram for both tissues and cell lines. (c) Monitoring the changes in H3.1 expression in (i) tissues and (ii) cell lines at transcript level.

As expected, the tumor tissue and CL38 cells were more in S and G2/M phase compared to normal and CL44 cells respectively **[Figure 4.3b]**. Next, we asked whether other replication-dependent H3 variant, H3.1 is also upregulated in transformed cells like H3.2. Strikingly, the expression level of H3.1 was unaltered at transcript level in both the tissues and cell lines

**[Figure 4.3c(i)(ii)]**. Similar observation was also seen at protein level by RP-HPLC **[Figure 4.2c(i)]**, suggesting that H3.2 is specifically upregulated in HCC. Multiple alignment of the three H3 variants, highlighting the differential amino acids is shown in *Supplementary Figure 3.*

### 4.3.2  Mono-nucleosomal association of H2A isoforms and H3 variants

Our data suggests that in HCC histones, H2A.1 and H3.2 are upregulated and H2A.2 and H3.3 are downregulated. The similar expression profiles of H2A isoforms and H3 variants made us to hypothesize that either these histones may have specific interaction amongst each other, H2A.1 might interact predominantly with H3.2 and H2A.2 with H3.3 and/or they are transcriptionally regulated in a related manner. Firstly, to understand whether any specific protein-protein interaction exists amongst these four histones immunoprecipitation approach was taken. Due to lack of specific antibodies against all the histones in the study, it was imperative for us to tag these proteins, ectopically co-express, and perform co-immunoprecipitation analysis. To this end, both H2A isoforms were tagged with FLAG/HA and both H3 variants with MYC **[Figure 4.4a]**. H2A and H3 histone constructs were co-transfected in all possible four combinations and their specific interactions are assessed by
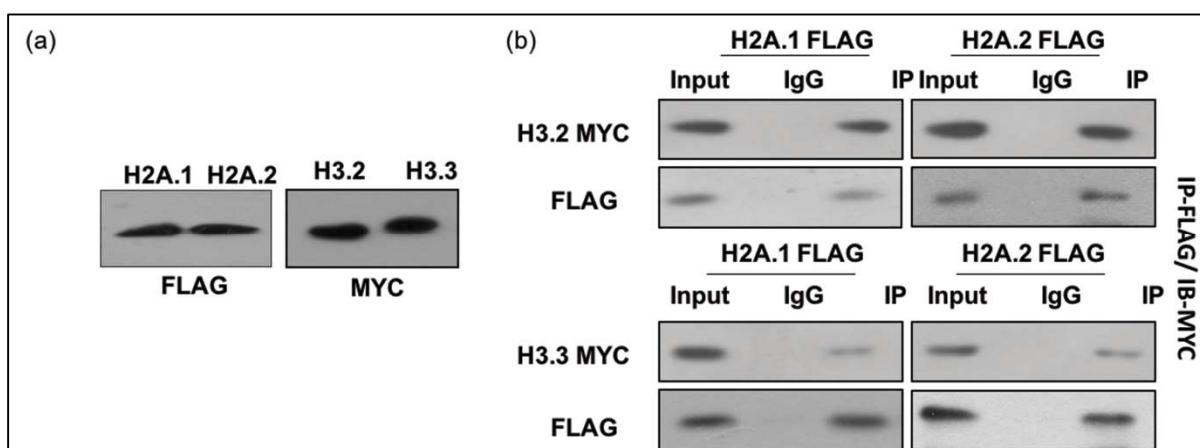


**Figure 4.4. Association between H2A isoforms and H3 variants.** (a) Western blot showing H2A isoforms tagged with FLAG and H3 variants with MYC. (b) Interaction between H2A isoforms and H3 variants are assessed by immunoprecipitation (IP) by FLAG and immunoblotting (IB) with MYC. Initially the IP was checked by performing western with FLAG then the blot was stripped to assess the H3 variant enrichment.

FLAG immunoprecipitation followed by MYC immunoblotting **[Figure 4.4b]**. The presence of FLAG signal in all the lanes indicated IP worked in all the reactions. Further, the MYC signal in all the immunoprecipitate indicates the interaction of MYC-histones with FLAG– histones. Conclusively, data suggest, for the possibility of occurrence of all interactions, thus, enabling us to conclude that histone isoforms H2A.1 and H2A.2 do not show any specific interaction with either of H3 variants, H3.2 and H3.3.

### 4.3.3  *Differential stabilities of the nucleosomes formed by H2A and H3 histones*

Though H2A isoforms and H3 variants interact with each other with no specificity, there still exists a possibility just like for H2A.Z and H3.3 that the NCPs formed by specific combination of histones might have differential stabilities[175]. To test this proposition salt dissociation experiment was performed by incubating the chromatin isolated from cell line co- transfected with H2A and H3 constructs in four combinations, by incubating the nuclei obtained with increasing salt concentrations. The data implies that of both the H2A isoforms, H2A.2 requires less salt concentration (600mM) than of H2A.1 (800mM) to get dissociated from the chromatin as seen by the FLAG western blot **[Figure 4.5a]**, re-establishing conclusion of earlier studies in the lab. Interestingly, just like H2A.1 and H2A.2, H3 variants also show differential salt
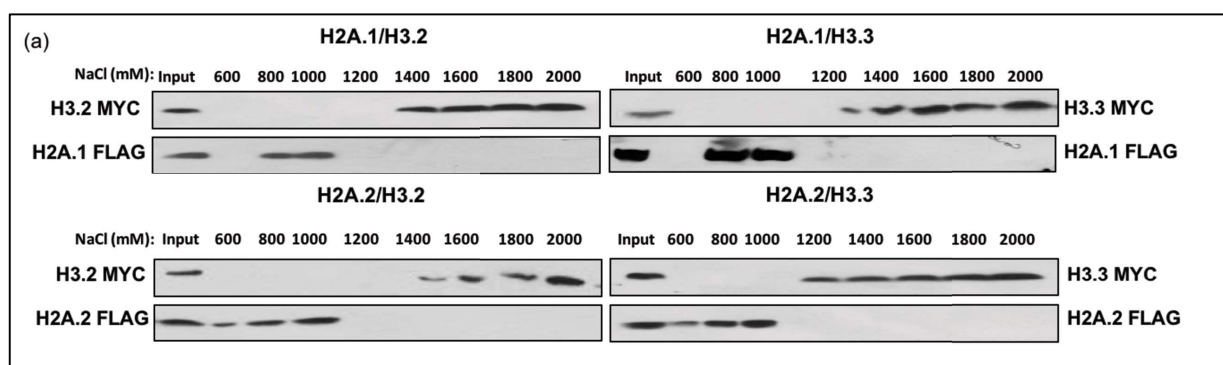


**Figure 4.5. effect of salt concentration on histone association.** (a) Incubation of chromatin with various concentrations of salt followed by western blotting of supernatant obtained by FLAG and MYC revealed the strength of association of H2A isoforms and H3 variants with chromatin. H2A.2 elution from chromatin starts at 600mM  onwards unlike H2A.1 and H3.3 at 1200mM unlike H3.2.

disruption, with H3.3 requiring low salt concentration (1200mM) than H3.2 (1400mM) **[Figure 4.5a]**.

However, as the experiment was carried out using whole chromatin and not on the individual mononucleosomal preparations it is difficult to conclude the relative stabilities of the NCPs which contain H2A isoforms and H3 variants together. Therefore, to directly answer the question of relative stabilities of four nucleosomes- H2A.1/H3.2, H2A.1/H3.3, H2A.2/H3.2 and H2A.2/H3.3 *in silico* approach, molecular dynamic simulations (MDS) was performed. As seen by the Root Mean Square Deviation (RMSD) of the four systems; H2A.1/H3.2 containing nucleosome has comparatively less RMSD and H2A.2/H3.3 has more RMSD indicating H2A.1/H3.2 system as most stable one and H2A.2/H3.3 as least stable one **[Figure 4.6a]**. Therefore, in conclusion these four nucleosomes differ amongst each other in their stabilities, and their sequential order of stabilities are shown in the **Figure 4.6b.**



**Figure 4.6. Differential stabilities of NCPs of H2A isoforms and H3 variants.** (a) Graph depicting the RMSD of the four systems. Blue – H2A.1/H3.2, Green - H2A.2/H3.2, red – H2A.1/H3.3 and Black is of H2A.2 /H3.3. (b) Diagrammatic representation of relative stabilities of the system.
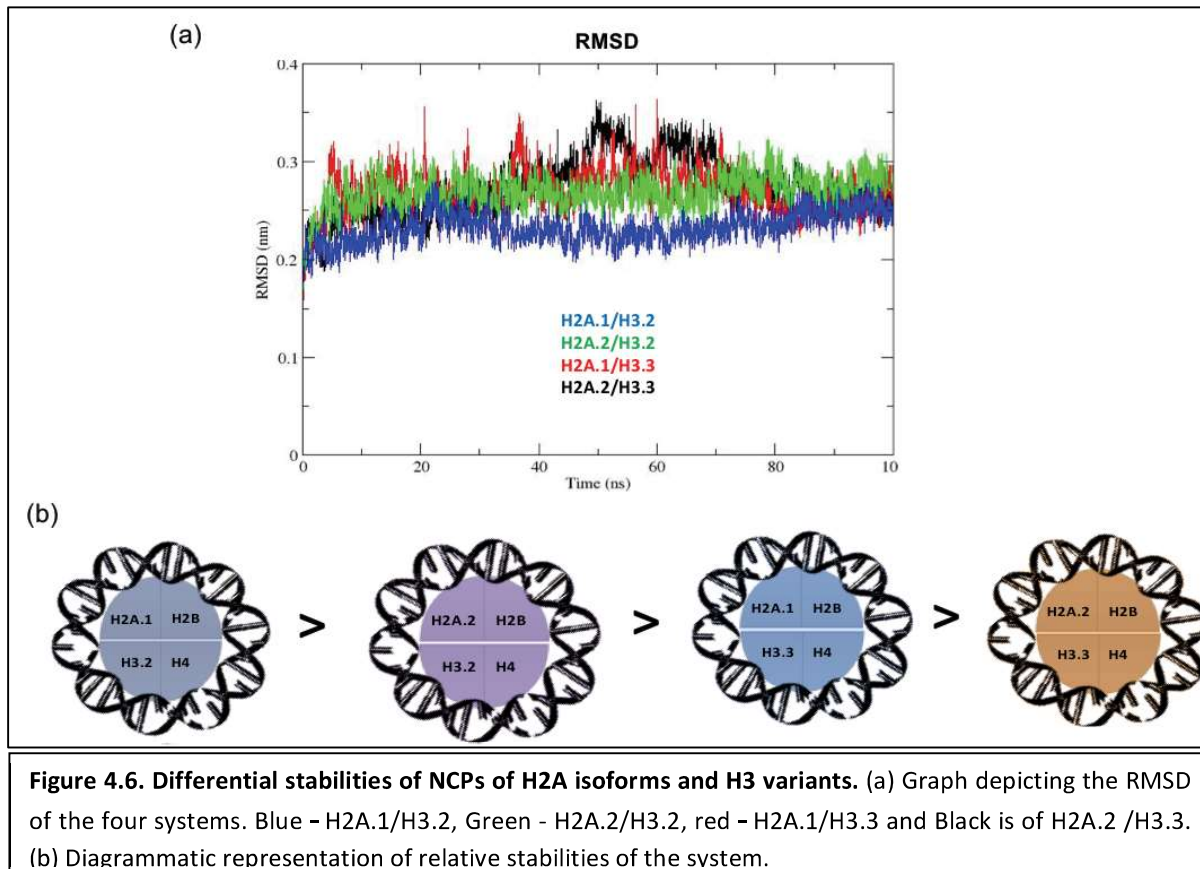
The striking observation which came out from investigation of binding partners of H2A isoforms is that not only H2A isoforms are changing in HCC but H3 variants levels also varies. Histone H3 variants are the most well studied histone variants and are attributed to have distinct locations in the genome and are known to undergo unique PTMs thus, are attributed to have specialized functions[23].

### 4.3.4 H3 variant level correlates with the H3 modification levels

Histone H3.3 is generally associated with transcriptionally active chromatin[197]. The downregulation of H3.3 in HCC prompted us to investigate the levels of histone PTMs that are associated with eu- or hetero-chromatin. There was a decrease in pan H3 acetyl mark in tumor and CL38 in comparison to control and CL44. Interestingly, all the histone acetylation marks that are associated with gene activation like H3K27Ac, H3K14Ac and H3K9Ac were found to be significantly downregulated along with H3K4Me3 **[Figure 4.7a]**. Further, there was
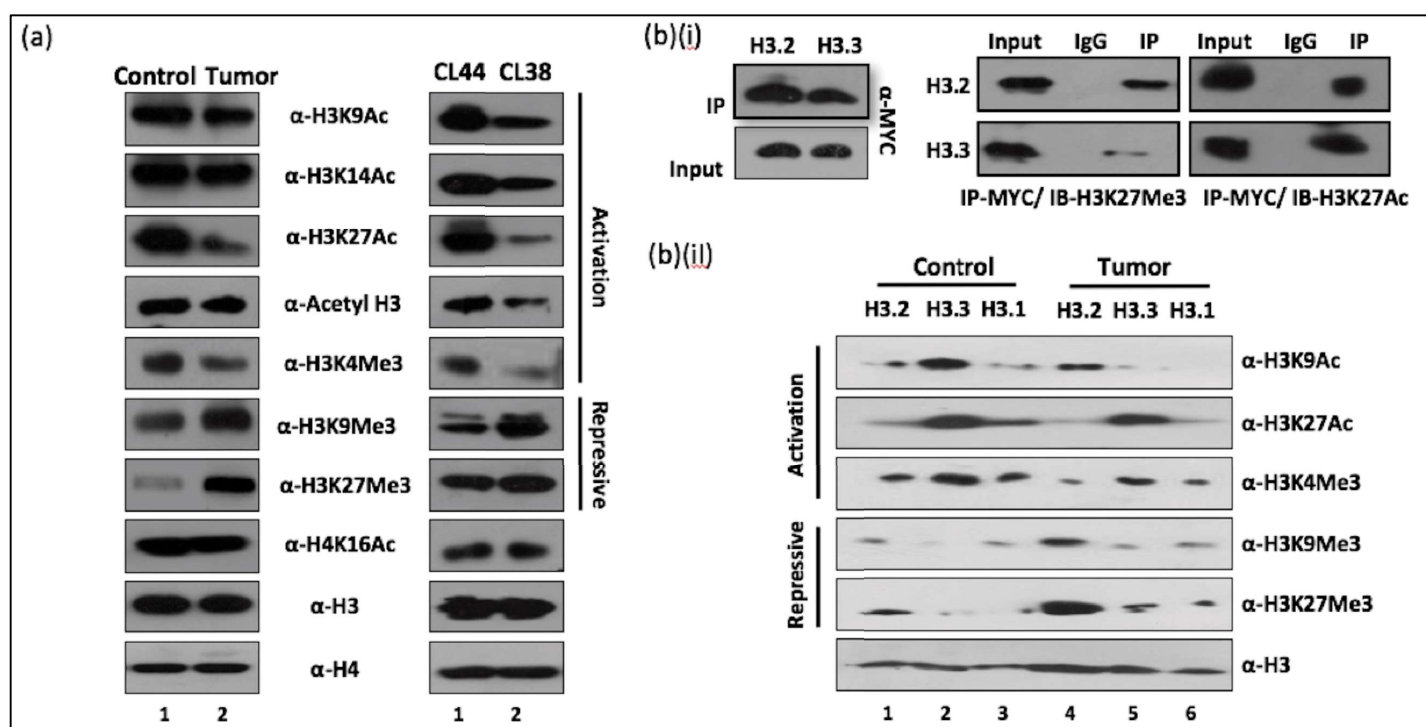


**Figure 4.7. Effect of H3 variant dyregulation on their associated PTMs.** (a) Western blotting of histones isolated from tumor and control tissues and cell lines with site specific histone modifications. H3 and H4 probing was used a loading control. Active and repressive marks are denoted.(b)(i) Mononucleosomal Immunoprecipitation of H3.2 and H3.3 with MYC followed by western blotting with H3K27Me3 (Repressive mark) and H3K27Ac (Active mark) (b)(ii) Monomeric histones of H3 variants separated by HPLC were probed for respective active and repressive histone PTMs for both control and tumor. Western for H3 was used as a loading control.

enrichment of repressive marks like H3K9Me3 and H3K27Me3 **[Figure 4.7a]**. A decrease in H4K16Ac, well-established histone PTM hallmark of cancer was also observed[119] **[Figure 4.7a]**.

To know whether the loss of activation marks and gain of repressive marks is due to changes in H3.3 and H3.2 respectively in tumor tissues and cell lines two approaches were employed. Firstly, ectopically MYC tagged H3 variants were immunoprecipitated with MYC and probed for H3K27Me3 (inactive mark) and H3K27Ac (active mark). The result suggests that indeed H3.3 is enriched with active marks and H3.2 with inactive marks **[Figure 4.7b(i)]**. However, as this approach does not account for the possibility of occurrence of heteronucleosomes (both H3.2 and H3.3 present in the single mononucleosome), which if present contribute to the PTM signal and thus leading to the mis-interpretation of results. Hence it was imperative to use another approach where with the help of RP-HPLC, separately collected monomeric H3 variants, H3.2, H3.3 and H3.1 fractions for both control and tumor tissues were probed with active and inactive PTM marks. As observed earlier, the loss of active marks is predominantly from H3.3 and gain is on H3.2 **[Figure 4.7b(ii)]**. However, H3.1 also showed a marginal decrease in active and increase in inactive marks **[Figure 4.7b(ii)]**. Nonetheless, the changes in PTM profile can be majorly attributed to changes in variant profile.

### 4.3.5 *Global chromatin condensation and repression of transcription is observed in HCC*

Histone variants are one of the epigenetic components known to influence chromatin architecture and thus bring about changes in transcription of the genes with which they are associated[198]. We hypothesized that global changes in the expression of H3 variants and their PTMs influence chromatin architecture. To this end, Micrococcal Nuclease (MNase) assay was performed. In brief, cell nuclei were isolated and a limiting concentration of MNase are added

to the nuclei, resulting in cleavage at nucleosome linker regions. The genomic DNA is then purified and the fragments are separated by agarose gel electrophoresis; as analyzed by slower disappearance of higher molecular weight DNA in tumor and a prominent appearance of mononucleosomes in lanes of normal liver, with increasing time points indicates tumor chromatin is more compact **[Figure 4.8a]**. The differences can be clearly also seen in the lanes corresponding to 8min time point of control and tumor, where a clear decrease in the band intensities of lower molecular weight DNA is seen in tumor in comparison to control, simultaneous increase in higher molecular weight is also observed.
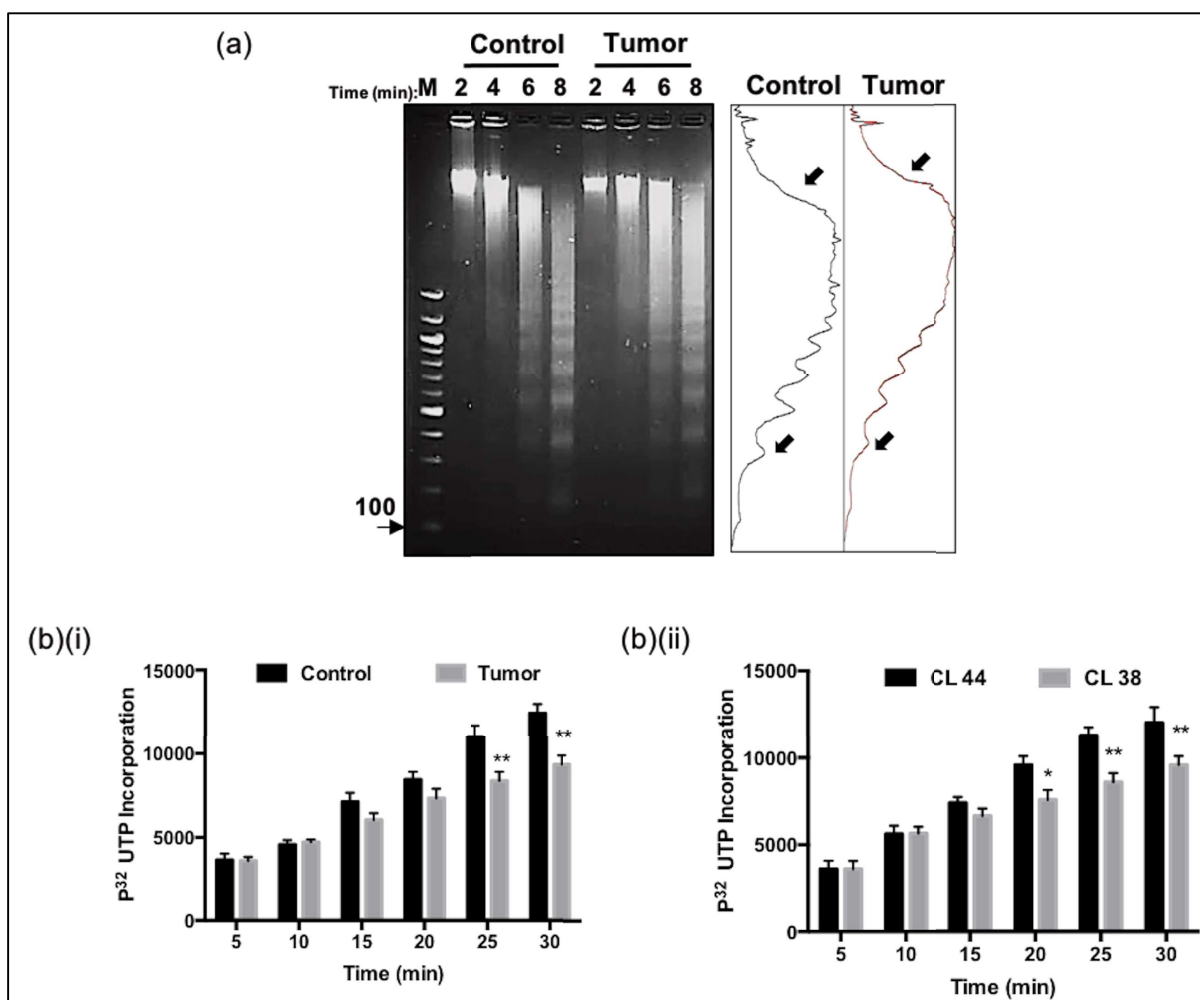


**Figure 4.8. Effect of H3 variants and their associated PTMs on chromatin organisation and global gene transcription.** (a) Agarose gel electrophoresis (1.8% gel) of Micrococcal nuclease digested chromatin of control and tumor tissues at various time points. Quantitative image of lanes corresponding to 8 minute time point is depicted. (b) Graph depicting the relative incorporation of $\alpha$-P$^{32}$UTP at various time intervals for (i) tissues and (ii) cell lines.

As transcriptional activation involves chromatin opening and repression is associated with the open state of chromatin[199]. Our observations, of increase in heterochromatin marks and chromatin condensation suggests a possibility of an overall decrease in transcription in tumor cells. To test this proposition, we carried out pulse chase *in vitro* transcription assay using purified nuclei isolated from tissues and cell lines, with $\alpha$-P$^{32}$UTP and chased for various time points. After counts were obtained, the data was plotted after normalization with zero minute. Data obtained suggests a significant drop in radioactive counts in tumor tissues and cell lines, a parameter which is directly proportional to the transcription rate **[Figure 4.8b(i)(ii)]**. Earlier time points did not show any significant changes, indicating that the initial pulse of $\alpha$-P$^{32}$UTP for both sets of reactions was equivalent and the differences at a later time points are indeed true changes attributed to the tumor cells.

### 4.3.6 *Global Dysregulation of H3 variant specific chaperones observed in HCC*

An intricate balance in expression of H3 variants, H3.2 and H3.3 seems to regulate chromatin architecture and thus effecting global gene transcription. We hypothesized any perturbation in this balance may lead to similar changes observed in cancer. To test this, MYC tagged H3.2 and H3.3 variants were overexpressed and checked for their effect on cell proliferation and histone PTM profile. Firstly, by immunofluorescence, it was confirmed that the ectopically expressed H3 variants localize in the nucleus **[Figure 4.9a]**. By cellular fractionation a further validation was done to see that the overexpressed H3 variants are incorporated into chromatin **[Figure 4.9b]**.

However, overexpression of the two variants did not lead to any effect on proliferation of cells, as judged by colony formation assay **[Figure 4.9d]**. Similarly, there was no change in the global histone PTM profile on overexpression of the two variants **[Figure 4.9c]**. This suggests
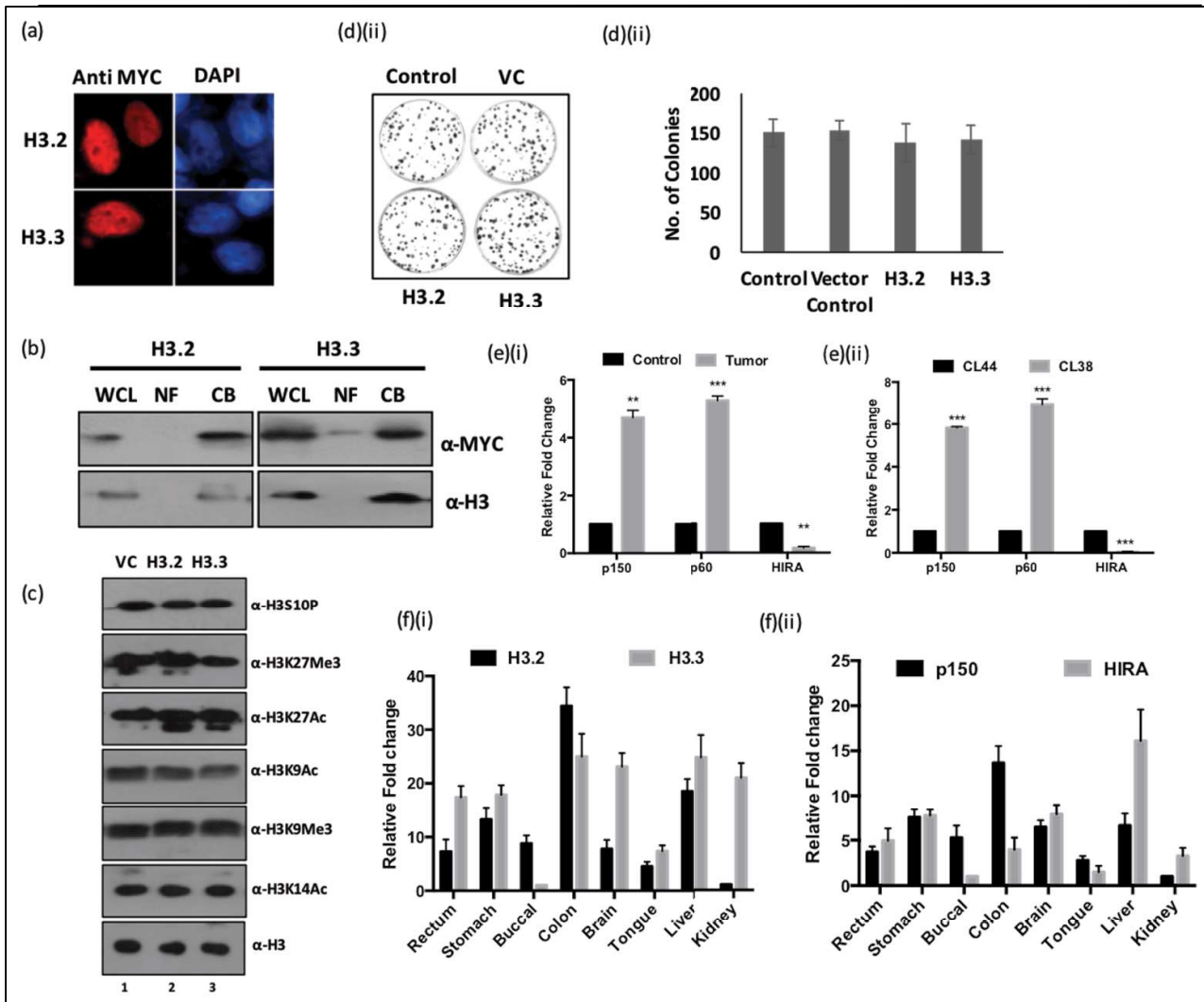
**Figure 4.9. Histone chaperones are dysregulated in HCC.** (a) Analysis of localisation of MYC tagged H3.2 and H3.3 by Immunofluorescence microscopy. Red depicts the Alexa 568 staining. DAPI in blue counter stains the nuclei. (b) Cellular fractionation followed by immunoblotting with the marked antibodies to determine sub cellular distribution of histones. H3 western was used as the control. WCL- Whole Cell Lysate, NF- Nucleosolic Fraction and CF- Chromatin Fraction. (c) Global profiling using site specific histone PTM antibodies on histones isolated from H3.2 and H3.3 overexpressing cell lines. VC- Vector Control. (d)(i)Picture depicting the colonies obtained after plating 1000 cells and allowing growth for 14 days. The colonies were fixed and stained with crystal violet stain. (ii) Quantitative analysis of the number of colonies of each set measured using ImageJ. (e) Quantitative real time PCR data showing the relative expression levels of histone chaperones CAF-1 (P150 and P60) and HIRA with respect to GAPDH in tissues (i) and cell lines (ii). (f) Graph depicting the relative levels of histone chaperones (i) and histone variants (ii) of various rat normal tissues.

that although the ectopically expressed H3 variants are incorporated into chromatin but it is only exchanged with the respective H3 variant with no overall enrichment. This is quite possible as H3.2 and H3.3 variants have their own dedicated chaperones CAF1 and HIRA respectively[200,201]. These chaperones are responsible for recruitment and incorporation of these two variants into the particular genomic loci. Next, the expression levels of the H3 chaperones

in control & tumor tissues and cell lines were investigated indeed, a significant upregulation of both the subunits of CAF1, p60 and p150 and downregulation of HIRA **[Figure 4.9e(i) and (ii)]**, just like the changes seen for their respective variants. In order to further understand the correlation between chaperones and variants, histone variants and their respective chaperones were profiled in various rat normal tissues. Indeed, as hypothesized in most of the tissues apart from tongue and stomach, the expression pattern of histone variants and their chaperones are correlated, meaning wherever, elevated levels of H3.3 was observed, its chaperone HIRA was also found to be increased **[Figure 4.9f(i) and (ii)]**.

### 4.3.7 Knockdown of P150 leads to increase in global transcription
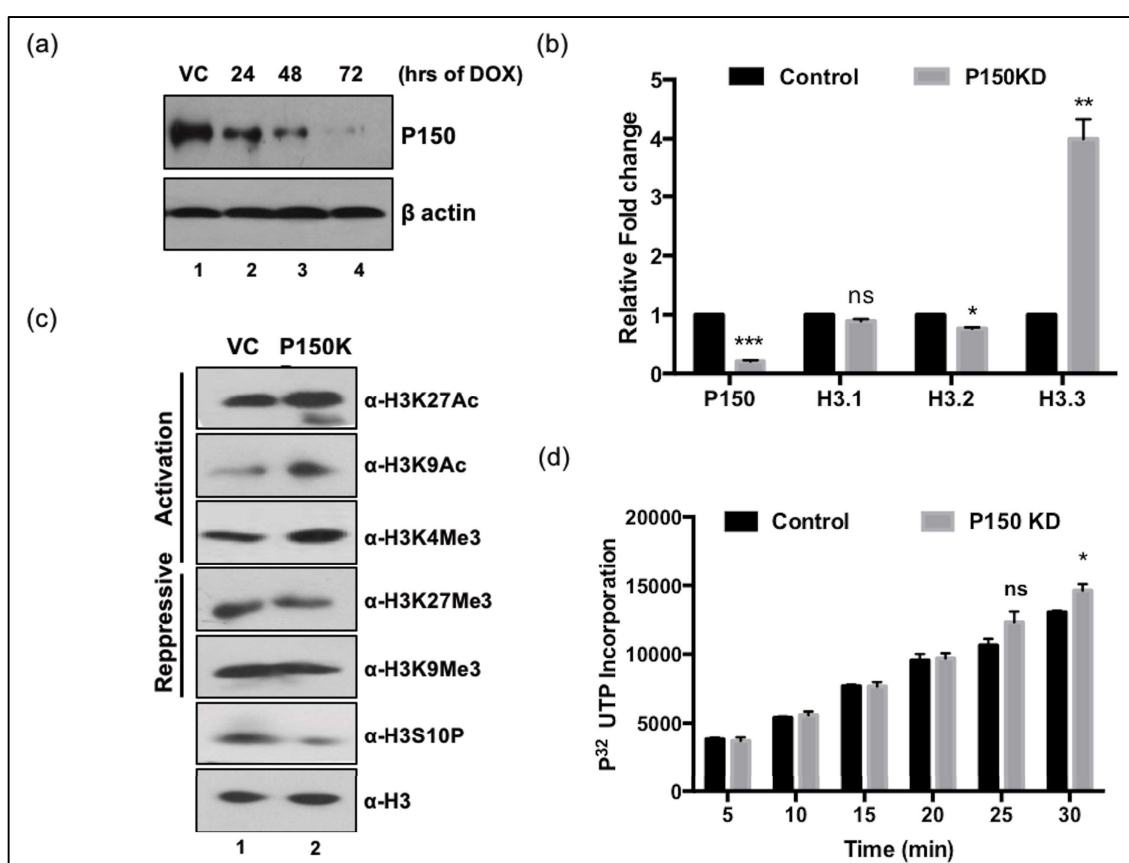


**Figure 4.10. Depletion of CAF-1 lead to increased euchromatin marks and elevated global transcription.** (a) Doxycycline mediated depletion of P150 subunit of CAF-1 at various time points. β-actin probing was used as a loading control. VC- Vehicle Control. (b) Relative transcript levels pf P150 and histone H3 variants – H3.1, H3.2 and H3.3 in knockdown and control cell lines. (c) Global histone PTM profiling for active and repressive marks by western blotting. (d) In vitro transcription assay

Encouraged by the finding that histone variants and their respective chaperones together determine the enrichment of respective histone variant and thus may influence HCC progression, experiments were conducted to understand the effect of knock down of P150, a subunit of CAF-1, histone chaperone of H3.2 and H3.1 in CL38, a neoplastic cell line. Due to the unsuccessful stable selection of clones during the constitutive knockdown of P150, an approach of inducible knockdown was used. The downregulation of P150 at various time points of doxycycline induction was confirmed by western blotting **[Figure 4.10a]**. At 24h time point approximately, 60%, 48h-80% and at 72h, no detectable amount of P150 were seen. Then, the levels of histone transcripts post 48h of doxycycline induction were measured, intriguingly, the expression of H3.3 was increased with slight decrease in H3.2 **[Figure 4.10b]**. A four fold increase in H3.3 was seen with a significant decrease in H3.2, suggesting for a sensory mechanism inside the cell to balance for the requirement of histones needed for DNA compaction.

Further, probing for various histone active and inactive marks in control and P150 knock down cell lines revealed an increase in activation and decrease in repressive marks suggesting a global increase in transcription **[Figure 4.10c]**. Further, an elevated incorporation of $\alpha$-P$^{32}$UTP was observed upon P150 knock down **[Figure 4.10d]** in pulse chase *in vitro* transcription assay. The observations seen here can be attributed to the elevated H3.3 levels and/or H3.2 loss in P150 cells.

### *4.3.8  P150 depletion led to cell cycle arrest*

The observation of decreased activation marks and global transcriptional repression in cancer suggest, that P150 could be the key molecule responsible to bring the changes in neoplastic cell lines, hence, its knock down led to the reversal of the changes. However, to confirm the role of P150 in cancer, phenotypic changes also are to be monitored. MTT and clonogenic

assay revealed a significant decrease in cell proliferation potential of the cells **[Figure 4.11 a and b]**, which also is reflected at the level of H3S10P, a mark correlated to proliferative status of cell **[Figure 4.10c]**. To understand its effect on cell proliferation, cell cycle status of knockdown cells was assessed at various time points of induction. A gradual increase in the number of cells in S-phase with the downregulation of P150, with 100% cells in S-phase just after 72 h of doxycycline treatment was seen **[Figure 4.11c]**. This could be the reason why stable knockdown of P150 was not successful. Conclusively, the changes observed upon P150 knockdown may be either due to arrest of cells in S-phase and/or to increase in H3.3 levels.
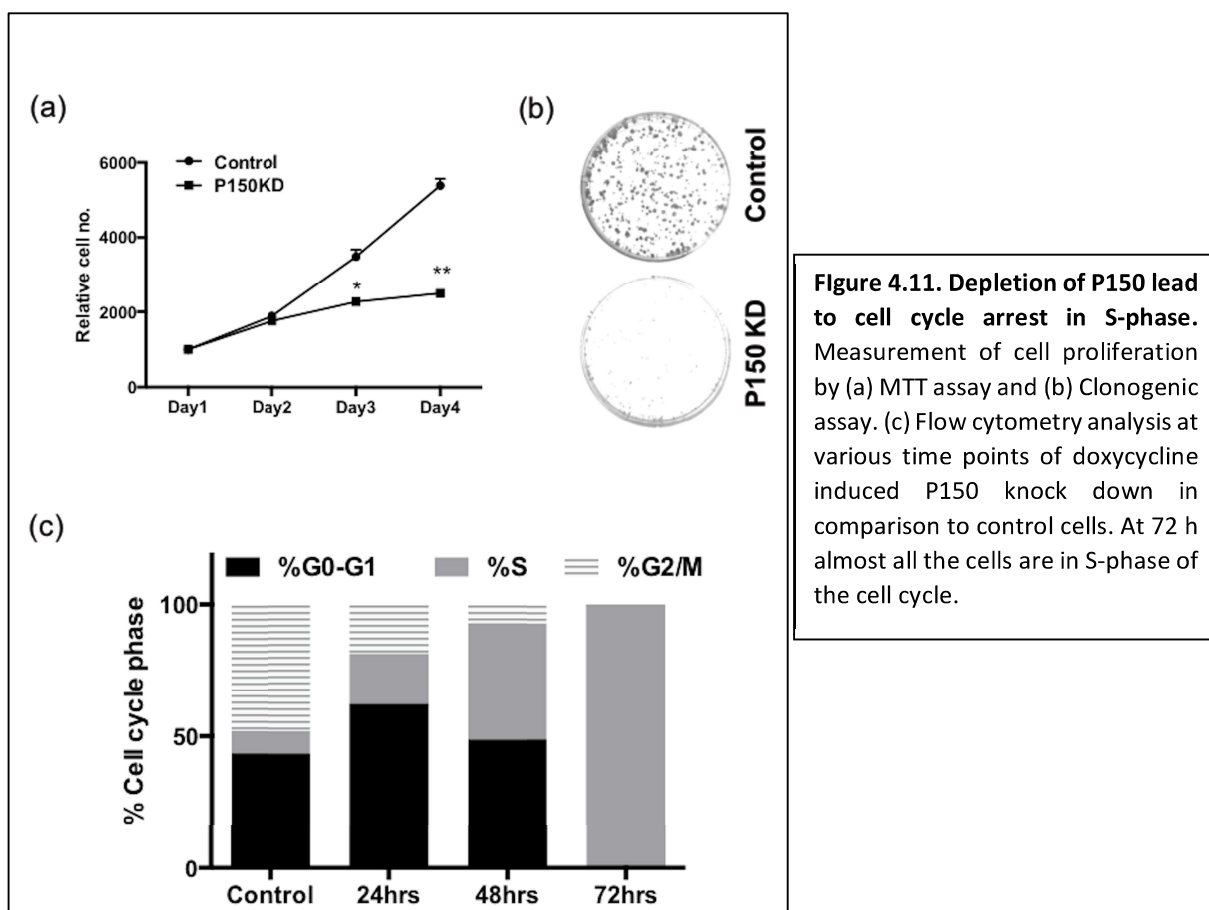


**FIgure 4.11. Depletion of P150 lead to cell cycle arrest in S-phase.** Measurement of cell proliferation by (a) MTT assay and (b) Clonogenic assay. (c) Flow cytometry analysis at various time points of doxycycline induced P150 knock down in comparison to control cells. At 72 h almost all the cells are in S-phase of the cell cycle.

## 4.3.9 Knockdown of H3.3 increase cell proliferation

Loss of H3.3 as seen in tumor cells correlates with changes in global chromatin organization and gene expression. To validate that the observed changes in cancer cells is indeed due to loss of H3.3, an shRNA approach was employed for H3.3 knock down in CL44 cells. The

knockdown of H3.3 was validated at both transcript **[Figure 4.12a]** and protein level **[Figure 4.12b]**. An approximate 80% decrease in H3.3 transcript and protein was seen. Interestingly, we observed an elevated expression of H3.2 and H3.1 upon decrease in H3.3 expression **[Figure 4.12a and b]**. An approximate 5-fold and 45% increase in H3.2; For H3.1, 4.2-fold and 550% was seen at transcript and protein level respectively. Further, a significant increase in cell proliferation was observed post H3.3 loss as seen in MTT assay **[Figure 4.12c]** and clonogenic assay **[Figure 4.12(d)]**.
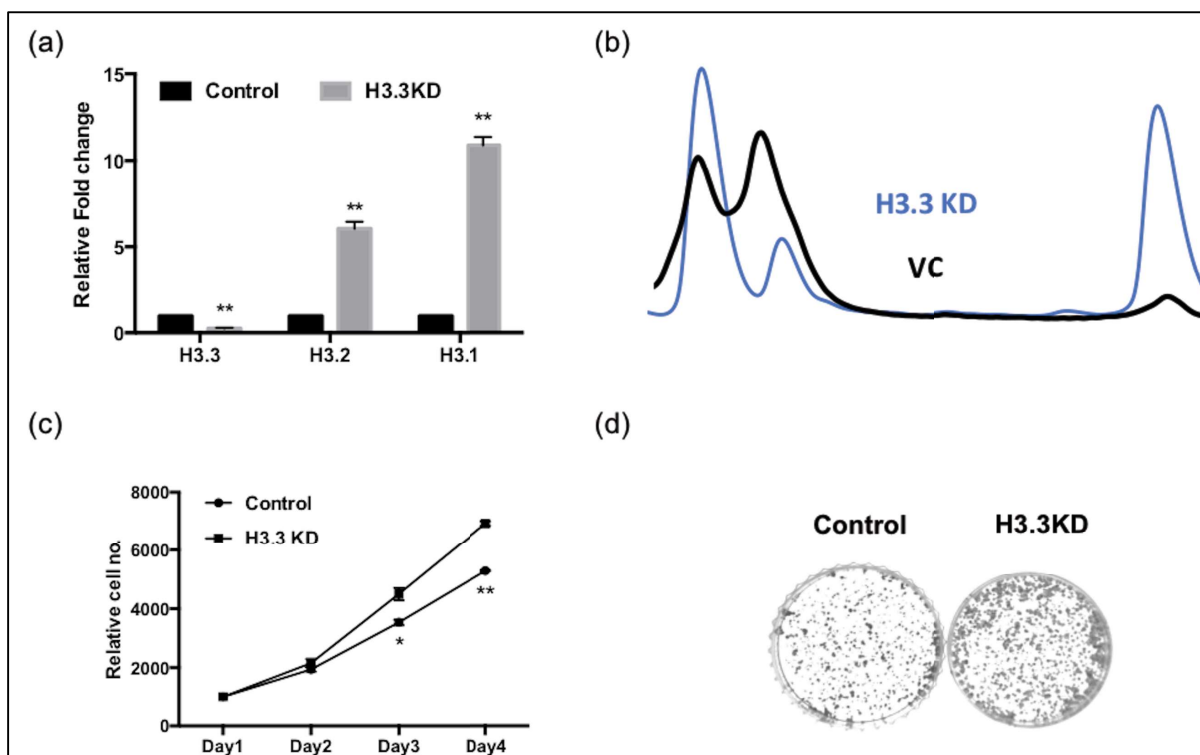


**Figure 4.12. Effect of H3.3 knockdown on cell phenotype.** (a) Quantitative real time PCR data showing the relative expression levels of histone variants H3.3, H3.2 and H3.1 upon knockdown of H3.3 with respect to GAPDH (b) RP-HPLC peak profile depicting the effect of H3.3 knock on H3 variant levels. Measurement of cell proliferation by (c) MTT assay and (d) Clonogenic assay.

### 4.3.10 Knockdown of H3.3 brings chromatin condensation and global transcriptional repression

Western blotting with a panel of activation and repressive histone PTM marks revealed an increase in repressive marks upon H3.3 loss **[Figure 4.13a]**. Intriguingly, an increased H3S10P and a drop in H4K16Ac- a hall mark of cancer accompanies H3.3 knockdown **[Figure 4.13a]**.

Marked increase in chromatin condensation **[Figure 4.13b]** was also seen in H3.3 knockdown cells as judged by MNase digestion pattern. Further, *in vitro* transcription assay performed for understanding scenario of transcription suggests a global gene suppression **[Figure 4.13c]**.
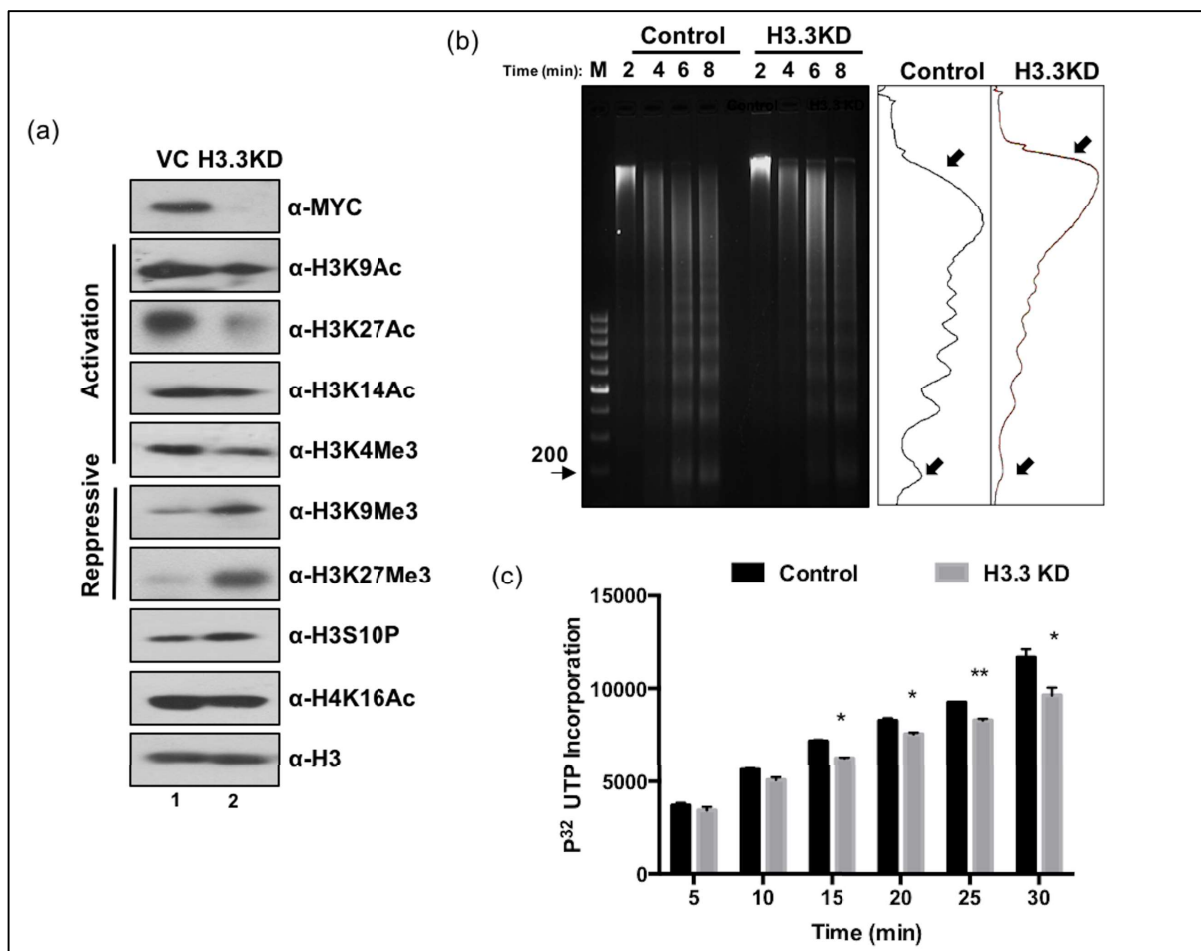


**Figure 4.13. Effect of H3.3 knockdown on chromatin structure and global gene expression.** (a) Global histone PTM profiling for active and repressive marks by western blotting. (b) MNase assay measures the effect of H3.3 knockdown on global chromatin compaction. (c) *In vitro* transcription assay measuring relative $\alpha$-P$^{32}$UTP incorporation.

These results suggest H3.3 might be the reason behind all the changes seen in tumor cells. Hence, its knockdown led to elevated cell proliferation, increase in repressive marks, loss of activation marks and global chromatin condensation and transcriptional repression. recapitulating the tumor specific changes and allowing us to conclude that H3.3 either mediates tumor development or contributes to carcinogenesis phenomenon. However, what remains to be understood is how H3.3 mediates increased cell proliferation? What are the molecular

mechanisms bringing out the changes in H3 variant profile? Finally, will the similar changes observed in human cancers and is this a universal phenomenon?

### 4.3.11 Knockdown H3.3 governs expression of tumor suppressor genes and play an important role in HCC.

In quest to understand how does H3.3 function for tumorigenesis phenomenon, chromatin immunoprecipitation of MYC tagged H3.3 and H3.2 was done to check their relative enrichment on various tumor suppressor genes. H3.3 seems to be associated with most of the tumor suppressors in study, unlike H3.2, suggesting the deposition of H3.3 on these genes may govern the expression of these genes. rDNA locus was used as a positive control for the experiment, as it is a housekeeping gene is mostly transcriptionally active **[Figure 4.14a]**. However, for CHD1 and ATM this scenario does not seem to apply. This observation led us to
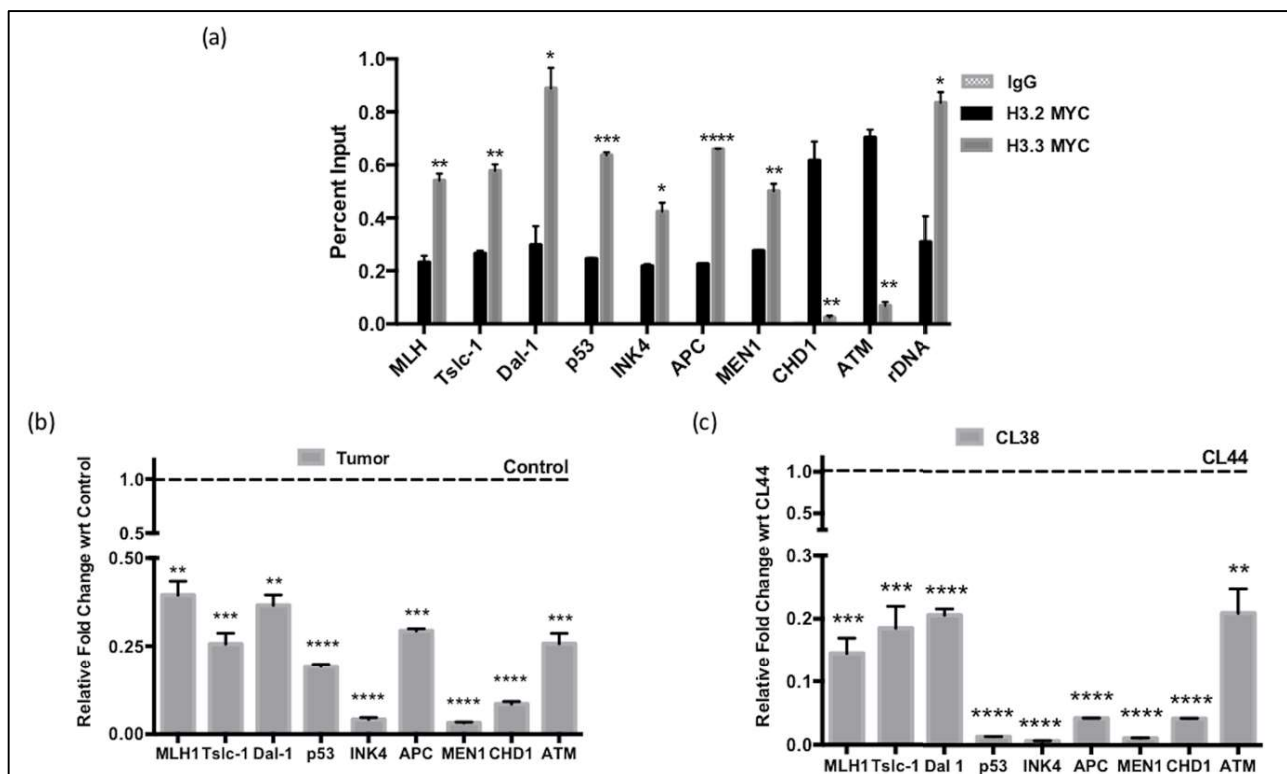


**Figure 4.14. H3.3 association with tumor suppressor gene expression.** (a) Measurement of relative enrichment of H3.2 and H3.3 on various tumor suppressor genes by ChIP-qPCR. rDNA locus was used as a control. IgG depicts Isotype control. Relative transcript levels of tumor suppressors in tumor tissue (b) and CL38 cell line (c). The dotted line on 1 of Y-axis is for control/CL44.

postulate that may be there could be two categories of tumor suppressor genes, one directly under the regulation of H3.3 and the other one do not.

To further validate that H3.3 indeed might be correlated to the expression status of these genes, their expression was monitored in tumor tissue and CL38 cell line. In comparison to control and CL44, tumor tissue and CL38 cells showed a global tumor suppressor gene repression **[Figure 4.14b and c].** H3.3 knockdown led to decrease in the gene expression of the tumor suppressor genes **[Figure 4.15a].** Further ChIP experiments revealed H3.3 loss from on tumor suppressor genes upon its knockdown and simultaneous gain of H3.2 **[Figure 4.15b]** thus, providing a proof of principle that H3.3 loss aids in tumor cell phenotype acquirement. However, we cannot undermine the fact that increase in H3.2 on these genes might also be responsible for their loss of expression. Interestingly, CHD1 was also affected upon loss of H3.3 even though the loss of H3.3 was not seen to that extent on its promotor.
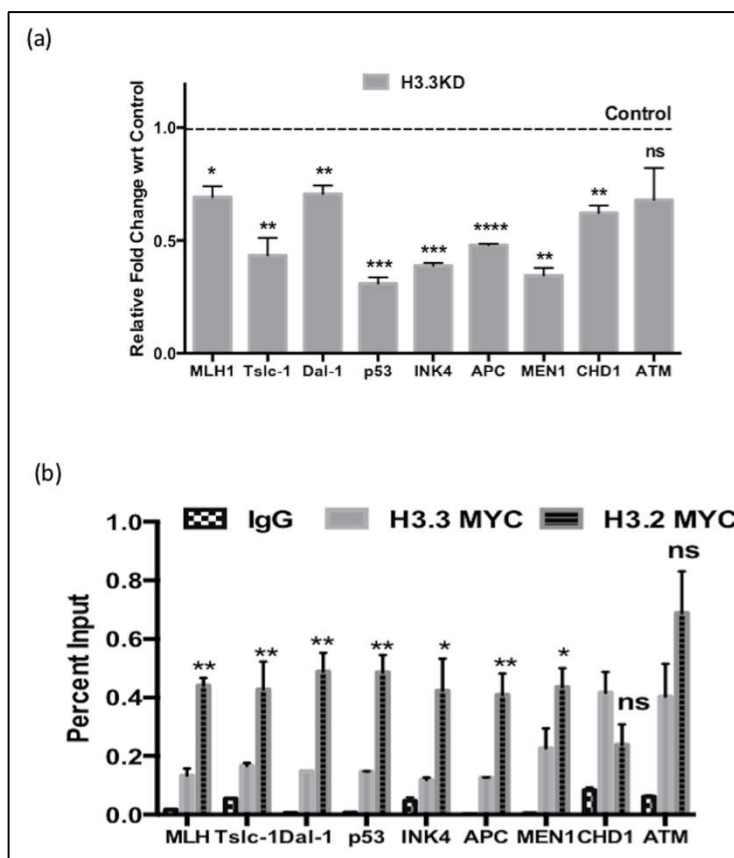


**Figure 4.15. Effect of H3.3 knockdown on tumor suppressor gene expression.** (a) Quantitative real time PCR data showing the relative expression levels of tumor suppressors upon knockdown of H3.3 with respect to GAPDH (b) ChIP-qPCR data showing relative levels of H3.3 and H3.2 on tumor suppressor genes upon H3.3 knock down.

## 4.3.12 DNA methylation governs the expression pattern changes of H3 variants

To understand the reason behind the differential expression of H2A isoforms and H3 variants their promoters were analyzed, intriguingly H3.3 and H2A.2 promoters contained CpG island, H3.2 and H2A.1 CpG sites at the predicted transcriptional start site of the genes **[Figure 4.16a]**. These DNA sequences were then cloned, to assess their activity by luciferase assay thus, confirming them to be as indeed promoters **[Figure 4.16b]**.
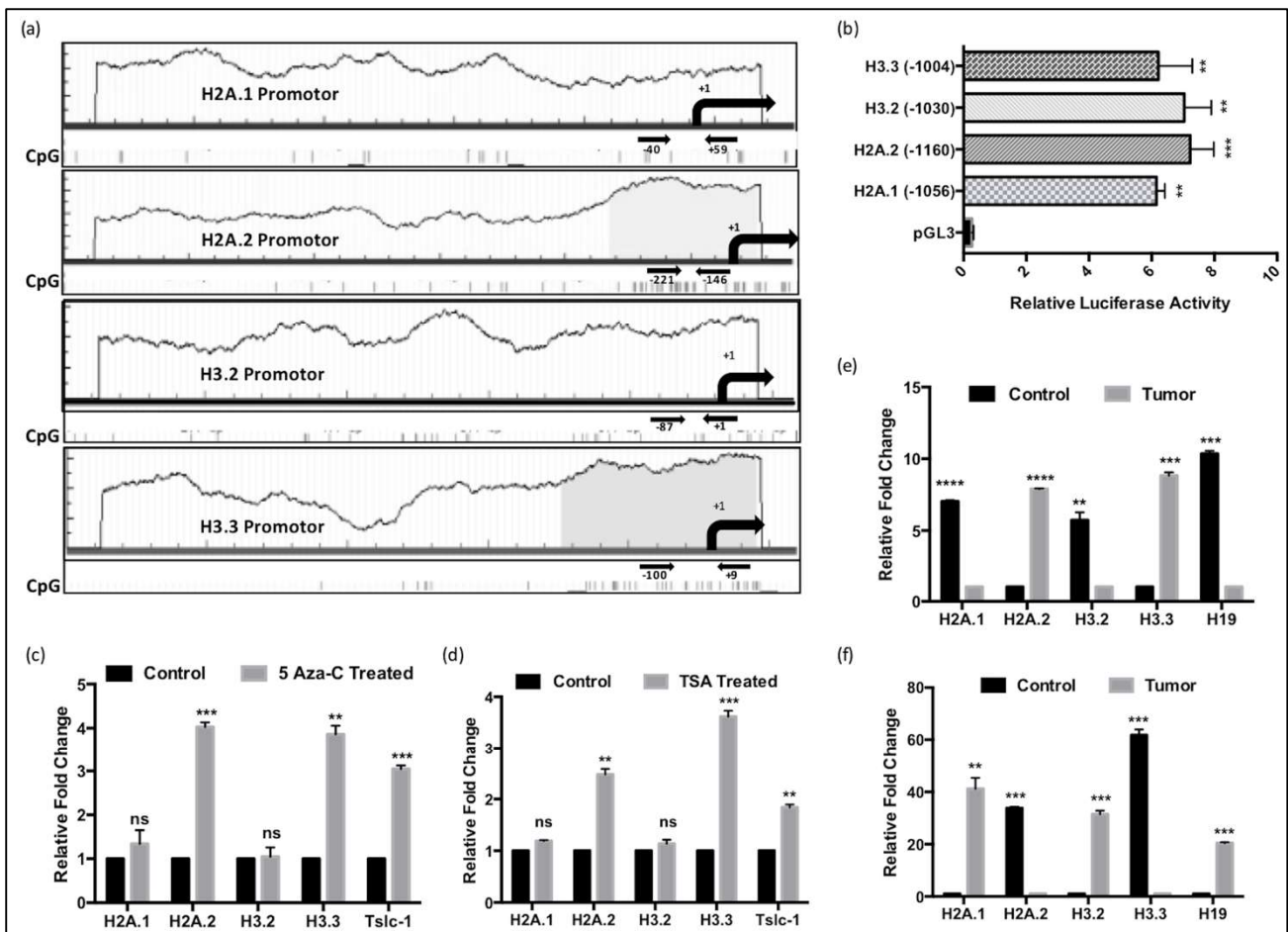


**Figure 4.16. DNA methylation governs expression changes of H2A isoforms and H3 variants.** (a) In silico analysis of putative promoter elements of all the four histones. +1 site has been depicted. Arrows indicate the primers used for Methyl Immunoprecipitation analysis. (b) Graph depicting the relative luciferase activity of DNA sequences cloned, proving them to be as promoters. Measurement of relative transcript levels of H2A.1, H2A.2 , H3.2 and H3.3 upon treatment with Azacytidine (5 Aza-C) (c) and TSA (d). Relative enrichment of 5-Methyl Cytosine (e) and 5- hydroxyl-methyl cytosine (f) on promoters of respective histones in control and tumor tissues.

To determine whether DNA methylation regulates their expression, expression status of these histones after treatment of CL38 cell line with small molecule inhibitors of DNMT and HDAC

like 5'-Azacytidine (Aza-C) and Trichostatin A (TSA) was examined. Indeed, treatment with both the inhibitors led to increase in H2A.2 and H3.3, no changes in H2A.1 and H3.2. This could be because the experiment was done on CL38 cell line, were already a high expression of H2A.1 and H3.2 is seen. Tslc-1 was used as a positive control for the inhibitor treatments[202] **[Figure 4.16c and d]**.

Further to establish that DNA methylation is an important factor in regulating expression of these isoforms and variants, Methyl DNA immunoprecipitation (MeDIP) with control and tumor tissues were performed. Interestingly, methyl cytosine levels, a transcriptional inactive mark was found to be higher on the promoters of H2A.2 and H3.3, and less on H2A.1 and H3.2 promoters in tumor tissue compared to control **[Figure 4.16e]**. MeDIP analysis of H19 promoter was used as a positive control, expression of which is known to be governed by DNA methylation[203]. Further, monitoring status of Hydroxyl- methyl cytosine, a transcriptional active mark also corroborated with the expression status of the variants, with elevated levels on genes actively expressed like H3.2 in tumor tissue **[Figure 4.16f]**. Thus, indeed DNA methylation is a dynamic player governing the expression pattern changes of histone H2A isoforms and H3 variants in HCC.

### *4.3.13 H3 variant profile changes in human cell lines*

To understand whether the changes in expression profile of H3 variants, a major contributor to tumor specific phenotypic changes in the rat HCC model system is true for human systems also, H3 variants at transcript level were measured in 4 different types of cancer cell lines alongside the immortalized or normal counterparts. Decreased expression of replication independent variant, H3.3 was seen in all the cancer cell lines, 25% for HepG2 (liver) **[Figure 4.17a]**, 34% for AGS (stomach) **[Figure 4.17b]**, 35% for MCF7 (breast) **[Figure 4.17c]**, and 300% for A431 (skin) **[Figure 4.17d]**, compared to HHL5 (liver), normal gastric cDNA, MCF10A (breast) and HACAT (skin). Further, for replication dependent H3 variants, H3.2

was found to be increased all the tumor cell lines with along with H3.1 only in gastric and skin cell lines.
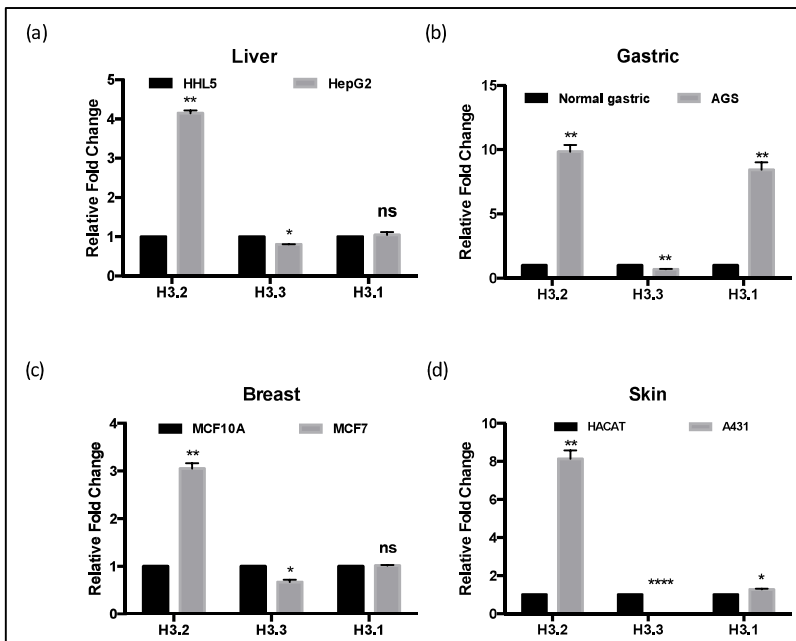


**Figure 4.17. H3 variant expression changes in human cell lines.** (a)(b)(c)(d) Quantitative real time PCR data showing the relative expression levels of H3.2, H3.3 and H3.1 in Liver, Gastric a, Breast and Skin cell lines.

## 4.4. Discussion

The epigenetic regulatory network has become a matter of intense investigation over the years from the perspective of disease pathology because unlike the genetic changes they are more amenable to reversal and are better targets for therapeutic intervention. In the present study, initially to understand the chromatin binding partners of H2A isoforms other chromatin changes specifically the histone H3 variants were screened in HCC rat model system. Interestingly, a decreased expression of H3.3 along with increase in H3.2 at transcript and protein level was seen.

Global changes in H3 variants profile in conjunction to H2A isoform changes prompted us to investigate whether these proteins interact specifically with each other and/or are they regulated by a similar transcriptional mechanism. Initially their specific interactions were tested, in this regard, co-immunoprecipitation analysis revealed that both H2A isoforms interact with H3 variants. However, the NCPs formed by the combination of these histones differ in their

stability with, H2A.1/H3.2 being the most stable and H2A.2/H3.3 being least stable. Of note, this is intriguing because owing to high levels of H2A.1 and H3.2 in tumor cells, the most abundant NCP formed will contain H2A.1/H3.2, suggesting its genome wide enrichment in the tumor landscape will affect global chromatin structure and gene expression patterns. In regard to understand the similar expression pattern of H2A and H3 histones, their promoters were analyzed, which led us to conclude that the control of H2A.1, H3.2 and H2A.2, H3.3 expression is bought by DNA methylation changes on their promoters, however we cannot rule out the role of transcription factors. Interestingly, the changes in methylation profile on histone promoter's correlates with the hallmark of cancer- CpG island hypermethylation and global hypomethylation[204].

Intriguingly, even though tumor cells are residing more in S-phase only H3.2 is elevated and not the other replication dependent histone H3.1, indicating that may be these cells are tuned in such a way to express specifically H3.2 so as to affect all the downstream pathways. One way histone variants can influence the pathways is by undergoing various PTMs, known to affect nucleosomal dynamics and thus chromatin organization[205]. Thus indeed, not only histone variants, histone PTM profiles also are altered in HCC directly effecting transcriptional status of genes. Though previous studies have investigated the histone modification profile or the histone variant changes, however, to the best of our knowledge, our study for the first time shows that the histone variant and modification profile might be intimately linked. Based on our results it would be interesting to investigate that in other cancers where histone PTM changes are often observed, this correlation exists or not.

Global gene repression is one of a hallmark which distinguishes between a cirrhotic tissue and HCC[206]. mRNA under-expression in the cancerous hepatocyte results in two major and final events, namely: (i) a limitation of cell type- specific metabolism and associated secretion of plasma proteins and (ii) a repression of apoptosis[206,207]. Though a very limited understanding

exists for a reason behind such a drastic change in transcriptome of liver cells, the current study puts forth the role of histone H3 variants in this process. Histone H3.3 is one of the very well-studied variant in context of development, differentiation and disease. H3.3 deficient mice embryos display reduced levels of open chromatin mark like H4K16Ac, leading to compaction of chromatin[208]. However, H3.3 knockout mice also have reduced viability, and surviving adults are infertile[209]. It also maintains the somatic epigenetic memory in nuclear transferred *Xenopus* nuclei and supports differentiation of cultured murine muscle precursor cell[210]. In zebrafish, reduced levels of H3.3 in the nuclei leads to defects in cranial neural crest cell differentiation[211]. Together, these findings indicate that H3.3 is involved in establishing a finely balanced equilibrium between open and condensed chromatin states during various cellular processes. Further, cancer specific mutations in H3 variants are known, which mainly function by bringing the changes in PTM profile, thus influencing the underlying gene expression[108,212]. Not only mutations, dysregulation of H3.3 expression in cancer is also now well appreciated. MLL5 mediated loss of H3.3 in adult glioma has been attributed to be a trade mark of cells undergoing differentiation[60]. Elevated H3.3 drives lung cancer progression by influencing metastasis related gene expression[61].

Previously, in case of human cancers, alteration in the level of histone variants have been reported[213,73,74]. However, the levels of specific chaperones for the variants, for instance, Chz1 for H2A.Z[214] and for macroH2A was not investigated. Our results suggest that simultaneous upregulation of the corresponding chaperone is important for proper incorporation of the variant. In fact, prior studies have shown that in absence of its specific chaperone, the centromere specific histone variant CENP-A is mis-incorporated into other genomic loci leading to chromosome instability[215]. Interestingly, the p150 unit of the CAF1 chaperone has been found to be upregulated in many cancers[216,217] and its elevated expression level was significantly correlated with poor clinicopathological features in patients with HCC and also

as an independent prognostic factor for predicting both the overall and disease-free 5-year survival[218]. It would therefore be interesting to investigate whether in these scenarios chromatin enrichment of H3.2 occurs. P150 knock down has been linked to decrease in the cell proliferation, however, our results indicate that this can be due to arrest of cells in S-phase owing to the decrease in deposition of H3 variants needed for DNA compaction post its synthesis. The CAF-1 complex is also known to be important to safeguard somatic cell identity, as CAF-1 suppression led to a more accessible chromatin structure at enhancer elements early during reprogramming. These changes were accompanied by a decrease in somatic heterochromatin domains, increased binding of Sox2 to pluripotency-specific targets and activation of associated genes suggesting again its role in maintaining the chromatin structures.

Association of H3.3 with transcriptional activation is a well-established fact, though, is it due to the PTMs it undergoes or is it because of the inherently unstable nucleosome is not yet known. H3.3 knock down in hepatocytes led to elevated expression of H3.2 and H3.1 probably to compensate for its loss. Thus, the changes in PTM marks could be because of both, the H3.3 decrease and H3.2 increase. Further, a slight increase in H3S10P level and high clonogenic potential of H3.3 knock down cells indicates these are highly proliferating. Interestingly, similar to the tumor cell chromatin architecture, H3.3 knockdown also leads to closed chromatin and brings a change in global transcription. ChIP-qPCR of H3.2 and H3.3 suggests the later variant to be relatively enriched on most of the tumor suppressor genes in the study. Further, owing to the association of H3.3 with these genes, knockdown resulted in decrease in their expression thus, cementing the fact that H3.3 governs the tumor cell state.

Interestingly, not all tumor suppressor genes are affected upon H3.3 knockdown, aiding us to believe that probably there might be only a specific subset of genes which are under the control of H3.3 either directly or indirectly. But the question remains to be addressed is what determines this specificity. However, elevated cell proliferation upon H3.3 loss, possibly may

be due to loss of expression of APC, a negative regulator of WNT signaling pathway among any other possibilities. Change in H3.3 levels in the rat model, prompted us to investigate whether this change is universal and can be seen in various other human cancer. To this end, we profiled for transcriptomic changes of these variants in human transformed and immortalized counterparts. The results enable us to conclude that the changes could be universal, however, studies on tumor tissue samples will establish this further.

Of note the observation in drop of H4K16Ac upon knock down of H3.3, incites that may be one of the mechanism, the hallmark of cancer- loss of H4K16Ac [119] is brought about might be due to H3.3 loss along with hMOF dysregulation. However, further mechanistic studies are essential for in depth analysis of this observation. Nonetheless, the low H3.3 levels we report in HCC, affects chromatin compaction, suggesting a potential cross-talk between chromatin architecture and transcription factor recruitment, thus effecting gene expression pattern.

## 4.5. Conclusion

To understand the precise role of H3.3 in cancer, we have used NDEA-induced hepatocellular carcinoma model system in Sprague-Dawley rat to induce liver cancer. On screening for histone pattern changes between the control and tumor tissues and have identified that there is a DNA methylation mediated downregulation in the histone H3 variant H3.3 in HCC and a concomitant increase in level of H3.2 variant both at the protein and transcript level. Strikingly, the alteration in the histone PTM profile shows a similar pattern with a decrease in gene activation marks and increase in repressive marks leading to global chromatin condensation and transcription repression in cancer cells. Impairing the deposition of H3.2 by P150 knockdown lead to increase in H3.3 expression, but also arrested the cells in S-phase. Further, we also show that H3.3 occupies promoters of tumor suppressor genes and influence their expression, thus its knockdown led to decrease in their expression and recapitulating the cancer

cell phenotype changes. Our report suggests that there is co-operative interplay between histone variants, chaperones and their transcriptional regulation which results in the stable maintenance of the highly dynamic histone marks required for maintaining the deregulated epigenetic landscape found in cancer cells **[Figure 4.18]**.
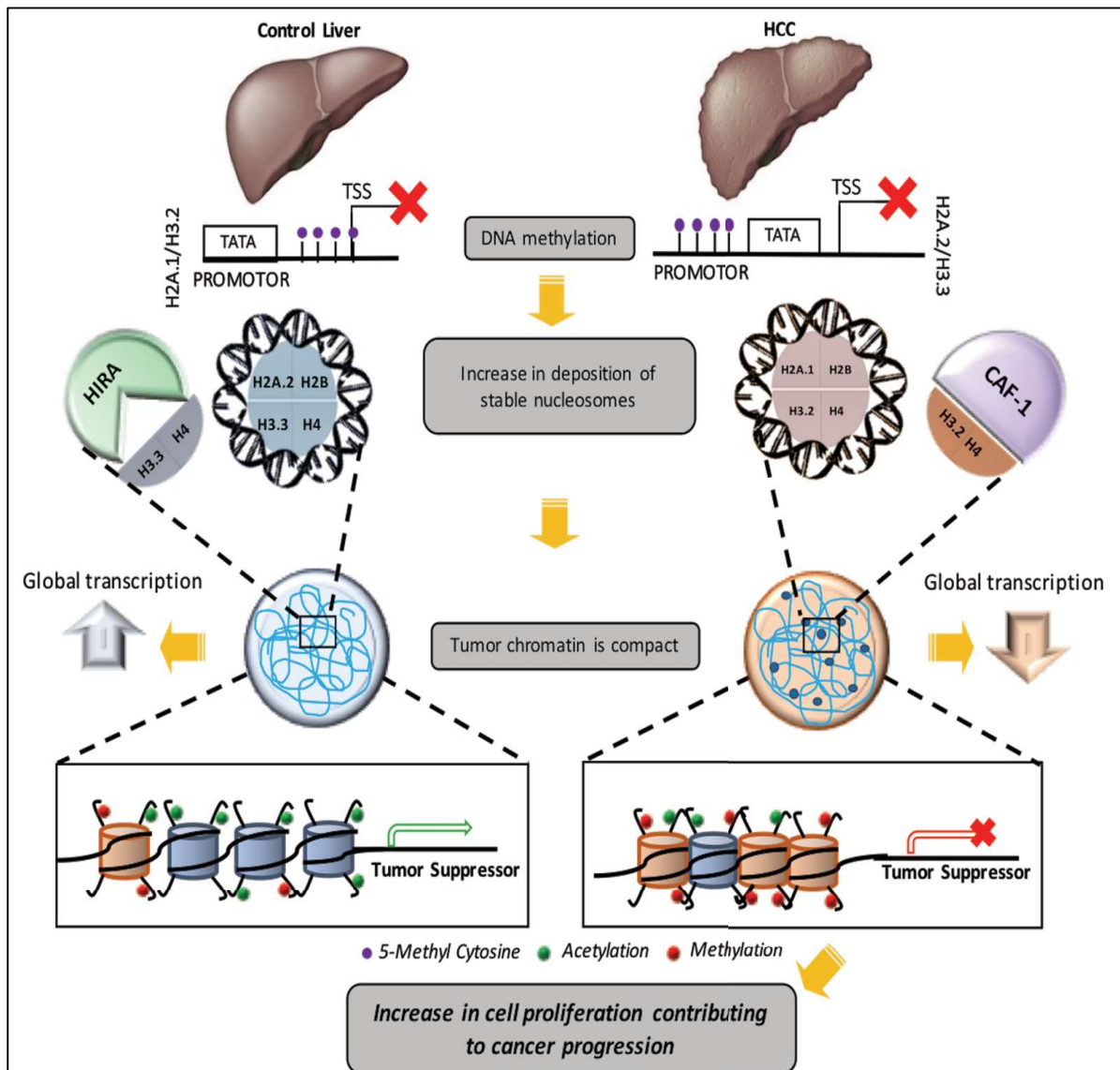


**Figure 4.18. Probable Scenario in HCC.** DNA methylation changes on promoters influences the expression changes in H3 variant profile leading to production of more of H3.2, which then will be incorporated on to DNA by virtue of changes in histone chaperone levels in tumor tissue. Pronounced incorporation of H3.2 containing histone and loss of H3.3 from chromatin effects global histone PTM pattern, chromatin compaction and global gene transcription with major influence on tumor suppressor gene expression.

These observations prompt us to stipulate that probably the reversal of such changes can be bought about by use of DNMT and HDAC inhibitors. Therefore, we conclude that the dysregulation of H3 variants act as the central node of this reversible epigenetic process seen in cancer and therefore can have a potential therapeutic implication.

*Chapter 5*

# V. Identification of Epigenetic Alterations in Serum and its Clinical Implications

## 5.1. Introduction

Histone PTMs dynamically maintain the chromatin states and thus any deregulation may lead to altered gene expression as observed in diseases like cancer[219]. Indeed, the loss of histone H4 lysine 16 acetylation (H4K16Ac) and lysine 20 trimethylation (H4K20Me3) are considered as hallmark of most human cancers[119]. Similarly, global H3 and H4 hypo-acetylation have been proven to correlate with tumor phenotype, prognostic factors and patient outcome in breast and prostate cancers[122,120]. Our work on identification of histone PTM alterations in HCC animal model also has resulted in identification of a panel of PTMs. However, in order to understand their clinical relevance there is need to first evaluate these changes in large cohort of samples. Similarly, decades of research have discovered a battery of histone PTMs that are altered in cancer and are now referred as 'histone onco-modifications', but none has reached clinics primarily due to technological limitations in the diagnosis of solid tumors.

Traditionally, cancer diagnosis and staging of solid tumors is done with an imaging technique followed by a surgical biopsy. But, biopsy being invasive, requires a complex setting, well-trained clinician and occasionally difficult and risky for some advanced stage patients. Therefore, diagnosis or monitoring of solid tumors utilizing circulating epigenetic biomarkers in blood samples, if possible, will prove to be a very powerful tool and will overcome all the earlier limitations. Indeed, research conducted over the last few years has identified and detected epigenetic biomarkers associated with cancer, including aberrant DNA methylation patterns, miRNAs profiles and histone signatures (in form of nucleosmes) in body fluids of the patients[220,221][**Figure 5.1**].

The levels of circulating nucleosomes (cNUCs) and histones are found to be elevated in a number of disease conditions like inflammation caused by bacterial infections, autoimmune diseases like SLE, stress and trauma. cNUCs are released into the blood by apoptotic cells during these processes[222,223]. Elevated levels of cNUCs nucleosomes have been reported in
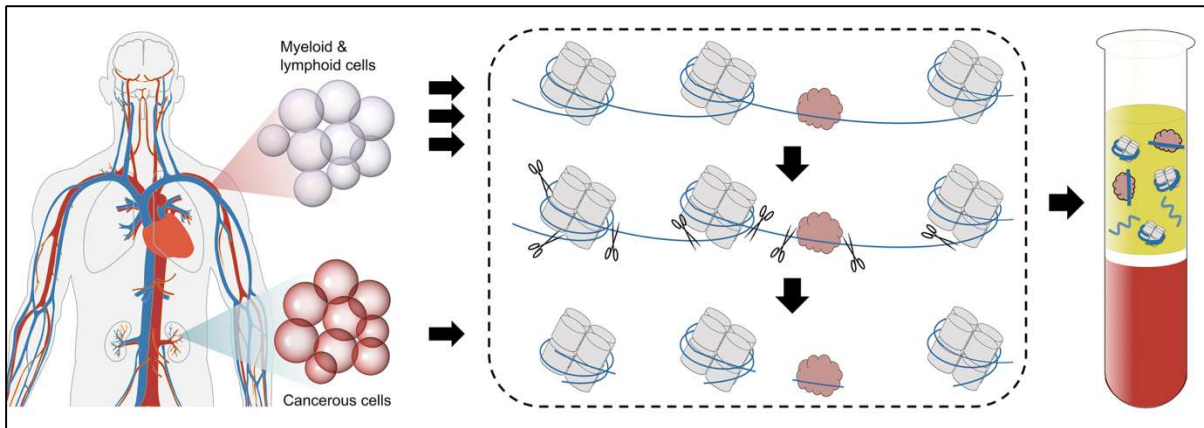
**Figure 5.1. Origins and Characteristics of circulating nucleosomes in plasma.** Apoptotic or necrotic cell death results in near-complete digestion of native chromatin. Protein-bound DNA fragments, typically associated with histones or TFs, preferentially survive digestion and are released into the circulation, while naked DNA is lost. DNA Fragments can be recovered from peripheral blood plasma following proteinase treatment. In healthy individuals, cNUCs are primarily derived from myeloid and lymphoid cell lineages, but contributions from one or more additional tissues may be present in certain medical or physiological conditions such as cancer. cNUCs – circulating nucleosomes, TF- transcription factors.
*Adapted from:*
*Matthew W. Snyder et al., (2016). Cell-free DNA Comprises an In Vivo Nucleosome Footprint that Informs Its Tissues-Of-Origin. Cell, 164, 57-66.. DOI: http://dx.doi.org/10.1016/j.cell.2015.11.050*

lung, breast, colorectal, renal and gastric cancer compared to patients with inflammation and healthy individuals[224]. In case of gastrointestinal tumors a positive correlation between cNUCs levels, tumor stage and metastasis has been established[225]. In case of advanced non-small cell lung carcinoma and cervical cancer a correlation between clinical outcome in response to chemotherapy and cNUCs has been observed[225]. On Circulating DNA, hypo-methylation pattern has been established in CRC patients[226]. Histone modifications like H3K9Me3 and H4K20Me3 have been detected on cNUCs[117]. In another study the ratio of H3K9Me3/nucleosome and H4K20Me3/nucleosome was found to be less in serum of breast and colorectal cancer patients compared to healthy individuals[227].

Though studies on histone PTMs on cNUCs have revealed interesting aspects, but how similar is circulating epigenetic signature to solid tumor signature in terms of their histone PTMs and their modifiers has not been established yet. This especially is important as because any changes in the tissue epigenetic signature, if possible can be read via the use of serum histones

can act a good prognosis and a diagnostic marker. In this regard our aim in this part of the work was initially to develop a protocol for isolation of histones from serum and then evaluate its closeness to tissue biopsy in terms of histone PTMs via use of the animal model system. Later on to validate these finding if possible on human samples.

## 5.2. Methods

### 5.2.1 Animal handling and experiments

All the experiments were performed on male Sprague- Dawley rats (spp. *Rattus norvegicus*) after approval of the Institute Animal Ethics Committee (IAEC# 04/2014), Advanced Centre for Treatment Research and Education in Cancer and the Committee for the Purpose of Control and Supervision on Animals, India standards. The detailed protocol to induce liver carcinogenesis is as previously described[96]. Tissue samples (liver, lung, kidney and brain) were fixed in formalin and prepared as paraffin-embedded blocks according to standard protocols. The H&E-stained sections were microscopically reviewed for histopathological alterations to confirm normal and HCC. Post-anaesthesia the blood was slowly collected by cardiac puncture (preferably from ventricle) from 120 days NDEA (late stage liver cancer) treated animals after which they were sacrificed. For early stage liver cancer, blood from tail vein was collected from 90 days NDEA treated animals.

### 5.2.2 Human blood sample collection and serum isolation

Blood samples of 24 cancer patients were collected retrospectively from Tumor Tissue Repository (TTR) of Advanced Centre of Treatment, Research and Education in Cancer (ACTREC), Tata Memorial Centre after Ethical Approval from Institute Ethics Committee III (Project number 164) along with six healthy adult human volunteers. As the samples were collected retrospectively, institute ethics committee III approved waiver of consent for working on patient samples. Whole blood from patients was collected prior to surgery, allowed to clot

at room temperature for 15-30min. The clot was then removed by centrifugation at 5000 rpm for 10min at $4^0$C. The resulting supernatant (serum) is transferred into multiple tubes to avoid freeze and thaw cycles and finally stored in liquid nitrogen containers in ACTREC, TMH-TTR. The samples collected were from 2013-2016 with confirmed histopathological tumor type as mentioned in Table 5.2.

### 5.2.3  Isolation of histones from serum

Total proteins were precipitated from the serum (5ml) by the slow addition of Trichloroacetic acid (TCA) to a final concentration of 20% with continuous and vigorous mixing. The precipitation was allowed to carry out on the ice for 30min, followed by centrifugation at 15,000 rpm for 15min. The obtained protein pellet was homogenized with glass teflon homogenizer in 3 volumes (w/v) of 0.2M sulphuric acid ($H_2SO_4$), till the pellet was completely dispersed and a milky white liquid is formed, which then was intermittently vortexed for >2h at 4°C. This mixture was then centrifuged at 16,000 rpm for 20min at 4°C. To the supernatant obtained post centrifugation, 4 volumes of acetone was added and histones were precipitated overnight at $-20^0$C. The pellet obtained post centrifugation at 16,000 rpm for 20min at 4°C was washed twice with 2 volumes each of acidified acetone and acetone twice. The histone pellet was air dried and eventually suspended in 50μl of 0.1% β-mercaptoethanol in $H_2O$ and stored at -20°C. Histone concentrations were determined by Bradford method of protein estimation. Protein standards were prepared containing a range of 0 to 5μg of Bovine Serum Albumin in 5ml of 1X Bradford reagent. Histone samples were also prepared similarly. Samples were vortexed and incubated at room temperature for 5min. Absorbance was measured at 595nm and the blank was adjusted. Histone samples were estimated for protein concentration by plotting a standard curve.

### *5.2.4 Isolation of histones from liver tissue*

The methodology is same as described in chapter IV (page number 111).

### *5.2.5 Resolution and analysis of histones*

The methodology is same as described in chapter IV (page number 113).

### *5.2.6 Analysis of histones by LC-MS*

The purified histones (15μg) were subjected to in-solution trypsin (20ng/μl) digestion in 50mM ammonium bicarbonate, pH 8.0 at 37°C for 2h (1:200 enzyme:substrate) as described previously[20]. Enzymatic digestion was stopped by adding 10% trifluoroacetic acid (TFA) to a final pH <3. Peptides were then desalted with ZipTip C18 columns (Millipore) and lyophilized prior to analysis by LTQ Orbi-trap-MS/MS (ABSCIEX). The MS instrument was operated in the data-dependent mode to automatically switch between full scan MS and MS/MS acquisition. Mascot generic format (mgfs) files were generated and were searched against protein database using Mascot version 2.3 (Matrix Science, London, UK) as described in chapter IV (page number 115)

### *5.2.7 HDAC and HAT activity assay*

Assays were performed using the colorimetric HDAC and HAT activity assay kits from BioVision (BioVision Research Products, USA) according to manufacturer's instructions. The kit uses HDAC/HATs in the biological sample in the study to convert a previously inactive enzyme to active enzyme, which then acts on a uncoloured substrate to generate a coloured product. The absorbance of which can be measured.

Briefly for HDAC activity assay, 50μl of serum was diluted in 85μl of $H_2O$; then, 10μl of 10XHDAC assay buffer were added followed by addition of 5μl of the colorimetric substrate; samples were then incubated at 37°C for 1h. Subsequently, the reaction was stopped by adding

10μl of lysine developer and left for additional 30min at 37°C. Samples were then read in an ELISA plate reader at 405 nm. Each sample was also treated with 2μl (12μM final concentration) of Trichostatin A (TSA) for 10min before performing HDAC activity assay, these readings are also plotted, labelled - with TSA, alongside the readings for serum samples not treated with TSA (W/O TSA). Experiments were performed in triplicates and average absorbance was plotted.

For HAT activity assay, 50μl of serum was diluted in 80μl $H_2O$ (final volume) and for background reading, 80μl $H_2O$ was added in the reaction instead of sample. Then, 50μl of 2× HAT assay buffer were added followed by addition of 5μl each of the colorimetric substrate 1 and 2, and 8μl NADH generating enzyme. The samples were incubated at 37°C for 1 to 4h depending on the colour development. Subsequently, samples were read in an ELISA plate reader at 440 nm. Experiments were done in triplicates and average absorbance was plotted.

### 5.2.8  Statistical analysis

All numerical data were expressed as average of values obtained ±standard deviation (SD). Statistical significance was determined by conducting paired Student's t test.

## 5.3.  Results

### 5.3.1  Isolation of Serum histones

We developed a minimally invasive and cost effective, robust protocol for isolation of histones from serum samples. This method comprises of precipitation of total serum proteins by acid followed by purification of basic proteins by the acid-extraction method. As the method involves precipitation and extraction by two acids, it is referred as Dual Acid Extraction (DAE) method. There are four key steps in the protocol: First step is the isolation of serum from the blood; Second step is the total protein precipitation by use of trichloroacetic acid (TCA). TCA, unlike other chemicals, precipitates all the proteins irrespective of their molecular weight and

is also independent of the physico-chemical properties of proteins; in third step histone extraction was carried out by use of the 0.2M $H_2SO_4$ to separate histones from other proteins, and in the final step, acetone and acidified (hydrochloric acid) acetone were used for removing he traces of TCA or $H_2SO_4$ by replacement of sulphate group ($SO_4^{2-}$) with chloride group ($Cl^-$) from isolated histones **[Figure 5.2]**. The quality of isolated histones was checked by loading on to a 18% SDS-PAGE followed by silver staining. The four core histones – H2A, H2B, H3 and H4 were visualised on the gel, but along with them other high molecular weight proteins were also noted **[Figure 5.3a]**.
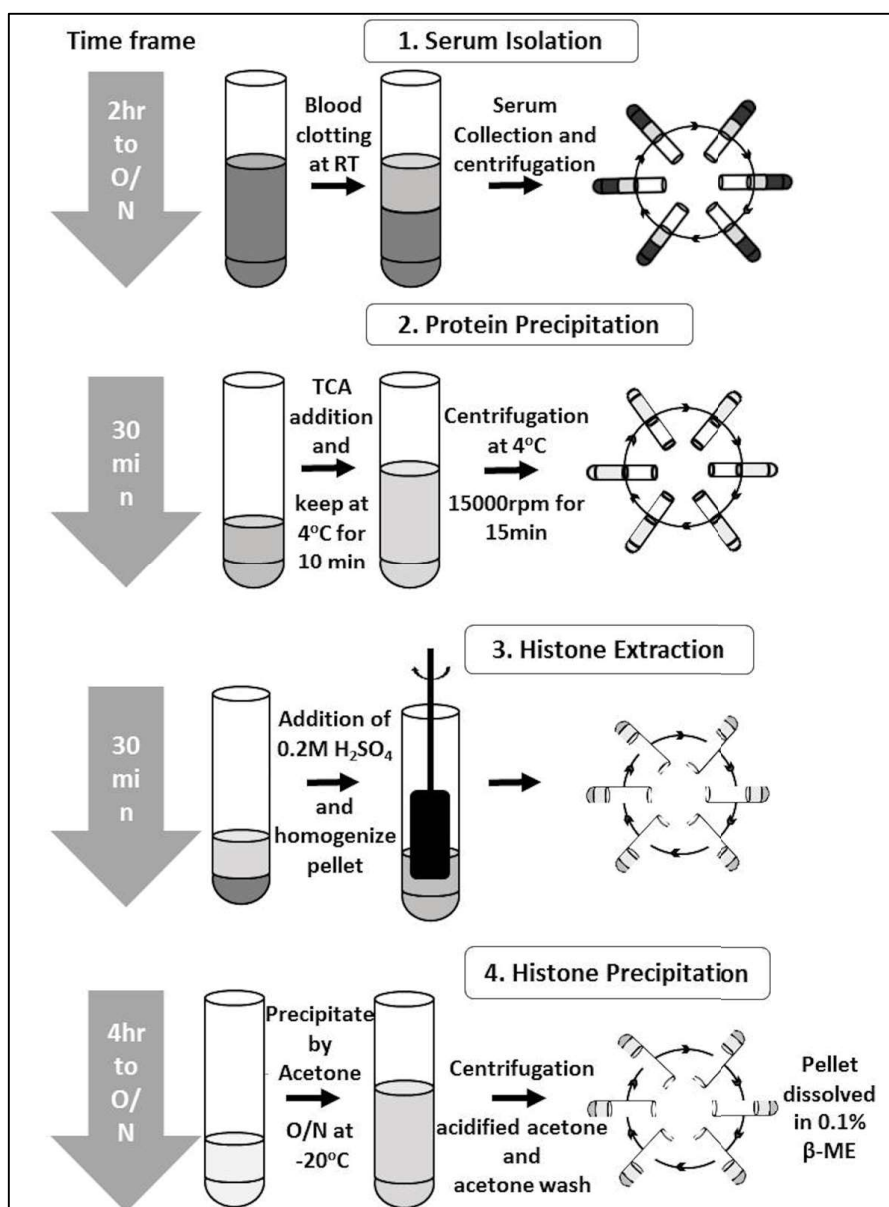


**Figure 5.2. Diagrammatic representation of protocol for isolation of histones from blood.**
The Dual Acid Extraction (DAE) protocol involves 4 crucial steps: 1. Serum isolation from blood; 2. Total Protein precipitation from serum by trichloroacetic acid; 3. Histone extraction from precipitate by sulphuric acid, and 4. Precipitation, washing and dissolution of extracted histone precipitate.

To understand whether histone PTM changes observed in the tissue samples can be seen in the histones purified from the serum, we used a rat animal model system. Hepatocellular carcinoma (HCC) was induced in Sprague-Dawley rats by administering N-nitrosodiethylamine (NDEA) in drinking water at a concentration of 1ppm/gm body weight. After 120 days of NDEA administration, HCC was confirmed by haematoxylin and eosin (H & E) staining **[Figure 5.3b]**.



| Sample | No. of proteins identified | No. of Histones identified | Identity of Histones | Sequence coverage |
|---|---|---|---|---|
| Tissue Normal | 13 | 8 | H2A,H3,H2B,H4 | > 90% |
| Tissue Tumor | 11 | 5 | H2A,H3,H2B,H4 | >98% |
| Serum  Normal | 13 | 6 | H2A,H3, H2B,H4 | >50% |
| Serum Tumor | 24 | 10 | H2A,H3,H2B,H4 | >30% |
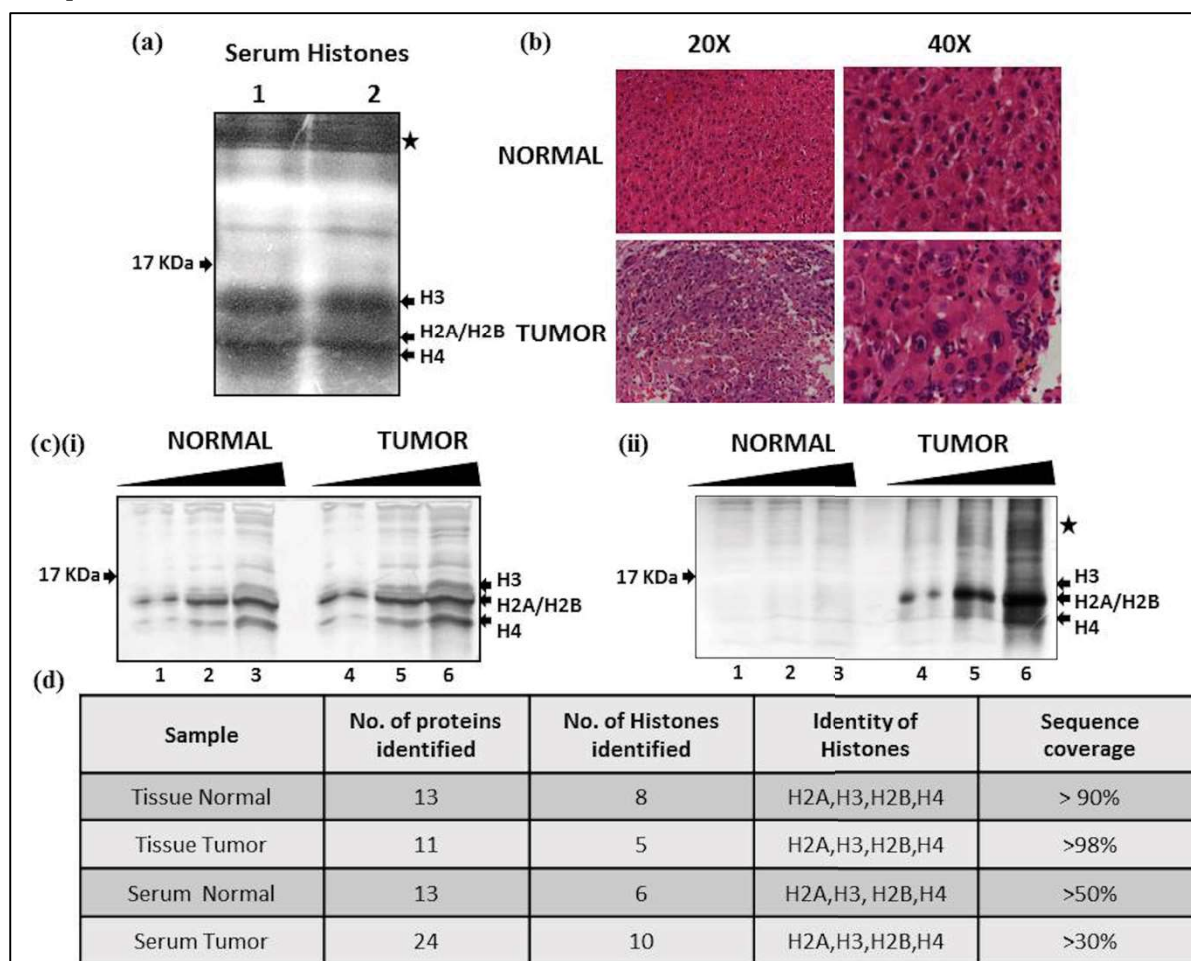
**Figure 5.3. Resolution and identification of purified histones from paired serum and liver tissue of normal and tumor.** (a) Silver stained 18% SDS-PAGE confirmed he integrity of the histones isolated from serum samples (1 and 2) of HCC harboring rats by DAE protocol. All the core histones, H3, H2A, H2B and H4 are marked with an arrow, whereas the '★' marks high molecular weight proteins; (b) H&E stained section of normal liver and HCC showing the altered histology in HCC at 20X and 40X magnification; (c) Silver stained 18% SDS-PAGE showing the integrity of the purified histones loaded in increasing volumes (5, 10 and 15µl) (i) samples of normal and tumor tissues, and (ii) serum of normal and tumor bearing rats by the DAE protocol. The core histones H2A, H2B, H3 and H4 are marked. (d) Histones isolated from tissues and serum of both normal and tumor harboring rats are subjected to LC-MS after trypsin digestion. The obtained data on number of peptides of histones identified along with sequence coverage are tabulated and confirmed the identity of purified proteins by DAE method.  H&E: Hematoxylin and Eosin; NDEA: N-nitrosodiethylamine.

| Proteins | Tissue Normal | Tissue Tumor | Serum Normal | Serum Tumor |
|---|---|---|---|---|
| Histones | H2A type 1 (91.5%) H2A type 2-A (915%) H2A type 1-C (91.5%) H2A type 1-F (86.1%) H2B type 1E (91.5%) H2B type 1C (91.5%) H3.1 (99.2%) H4 (59.2%) | H2A type 2-A (98.4%) H2A type 1-C (98.4%) H2B type 1E (98%) H3.1 (99.2%) H4 (98.4%) | H2A type 2-A (81.5%) H2A type 1 (74.62%) H2A type 1-C (50%) H3.1 (59.2%) H2B type 1E (57%) H4 (60%) | H2A type 2-A (46.9%) H2A type 1-C (33%) H2A type 1-F (38.4%) H2A type 1-E (30%) H2A type 1 (33%) H2A type 4 (33%) H2B type 1E (57%) H2B type 1C (35%) H3.1 (40.7%) H4 (47%) |
| Non-Histones | Prelamin A/C (26%) KDM5D (274%) ESF1 (30.6%) ESF1 homolog (23.9%) Acid-sensing ion channel 5 (12.9%) | Prelamin A/C (62.4%) KDM5D (30.32%) EIF2S3Y (29.8%) ESF1 homolog (41%) Acid-sensing ion channel (17.9%) Ribonuclease UK114 (40.1%) | Fibrinogen beta chain (65.75%) Fibrinogen alpha chain (56.91%) Isoform 2 of Fibrinogen alpha chain (69.45%) Isoform 2 of Fibrinogen beta chain (70.96%) Translation initiation factor eIF-2B (46.1%) Fetuin-B (47.6%) Putative pheromone receptor (18.7%) | Fibrinogen beta chain (65.3%) Fibrinogen alpha chain (43.3%) Isoform 2 of Fibrinogen beta chain (67.4%) Isoform 2 of Fibrinogen alpha chain (59.6%) Matrix extracellular phosphoglycoprotein (60%) Potassium voltage-gated channel subfamily C member 2 (30.8%) ESF1 homolog (57.9%) Alkaline phosphatase (57%) Indoleamine 2,3-dioxygenase 1 (37.8%) Aldehyde oxidase 2 (29.6%) Astrocytic phosphoprotein (69.9%) Transcription factor YY2 (32.9%) Cannabinoid receptor 1 (11.1%) Putative pheromone receptor (19.1%) |

**Table 5.1.** Total proteins detected in LC-MS of serum and tissue purified histones of normal and tumor samples.

The H &E stained slides showed classical features of HCC like well vascularized tumors with wide trabeculae, prominent acinar pattern, cytologic atypia and vascular invasion. Histones were isolated from both liver tissues and serum of normal and tumor bearing rats. The histones obtained from serum were quantified by Bradford method using BSA as standard. The histone quantity in the serum of the HCC bearing rat group was found to be significantly higher than the normal group **[Figure 5.3c(ii)]**. The concentration was 0.8μg/ml and 5.4μg/ml serum for normal and tumor respectively. The purified histones from tissues **[Figure 5.3c(i)]** as well as serum **[Figure 5.3c(ii)]** were resolved on a 18% SDS-PAGE and silver stained to check their integrity. To confirm their identity, the histones were subjected to liquid chromatography coupled mass spectrometry analysis (LC-MS). All the core histones were identified in both the

serum samples (normal and tumor) with query coverage of > 50% in case of normal and >30% for tumor **[Figure 5.3d]**. Also, of total 13 proteins identified in serum of normal rats, three correspond to histone H2A and one each to histone H3.1, H2B and H4. In case of the serum of of which are presented as a part of the **Table 5.1**. Histones isolated from the tissue were used as a positive control in LC-MS, where all the core histones were detected with >90% query coverage in both normal and HCC.

### 5.3.2 *Histone PTM pattern is comparable in liver tissues and respective serum samples*

The histone PTMs profiling of normal and HCC tissues was compared with respective serum samples by immunoblotting with site specific antibodies against H4K16Ac and H4K20Me3, as the loss of these marks are established as hallmark of human cancer [119]. As reported for human tumors, rat tumor tissue has also showed hypo-acetylation and hypo-methylation at H4K16 and H4K20 respectively **[Figure 5.4a]**. Interestingly, respective serum histones also showed the same pattern as of tissue histones **[Figure 5.4a]**. The other crucial histone PTM marks like γH2AX - a DNA damage mark[216], H3K27Me3 & H3K9Me3 – transcriptional repressive marks[228] and H3S10P - a mitotic mark[229], known to be deregulated in many of the human cancers were also probed. Intriguingly, we noted a significant increase in these marks in both the tumor samples - tissue as well as serum **[Figure 5.4a]**. This shows that the key histone modifications like acetylation, methylation and phosphorylation are retained during the course of histone extraction from serum samples by DAE method and also profiling between tissue samples and their respective serum samples mirrored each other.

In order to understand that the changes seen in serum histone is due to liver tumor and not due to changes in the entire PTM profile of all the other organs, we profiled for histone PTMs in
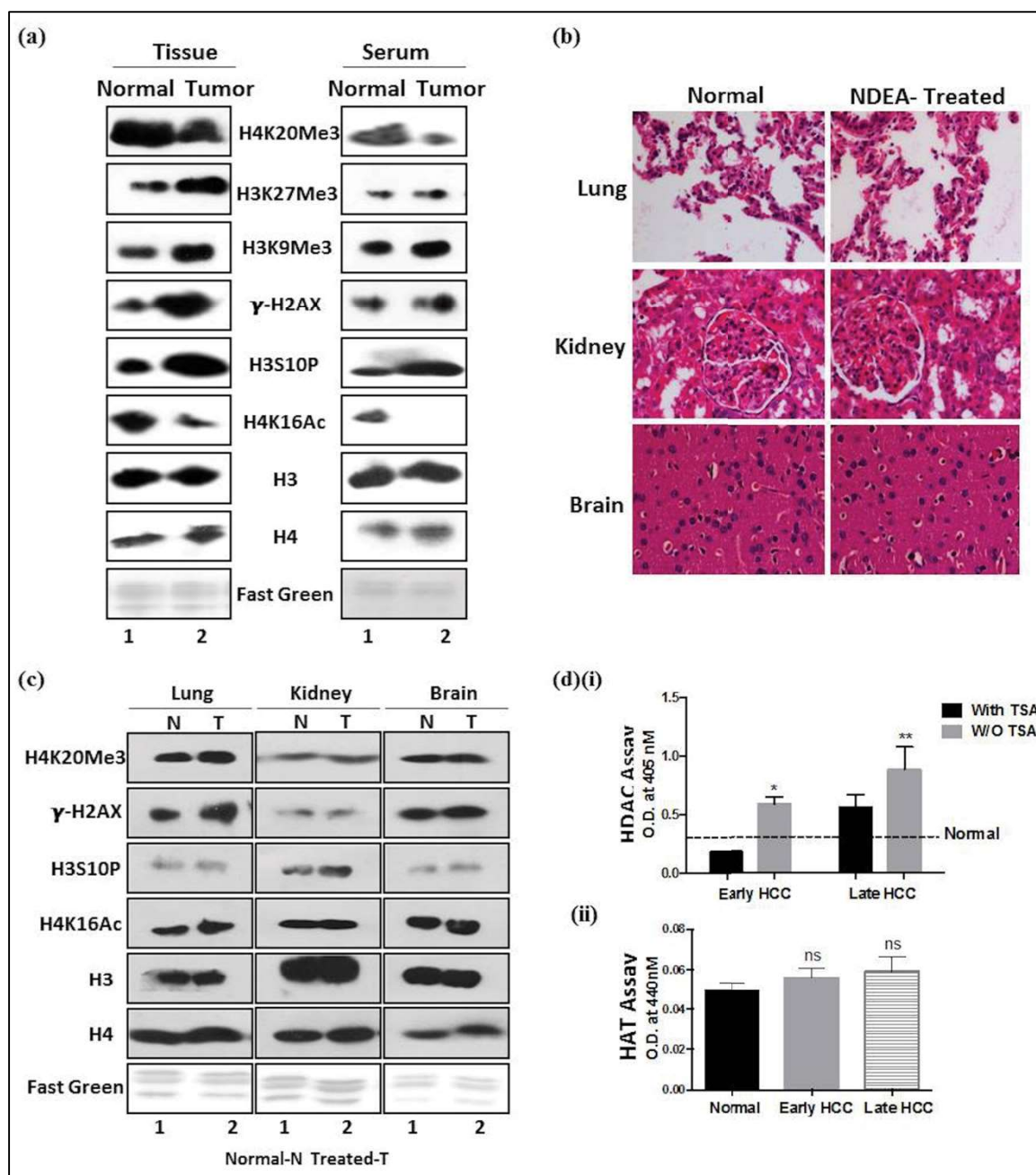
**Figure 5.4. Profiling of site-specific histone modifications and modifiers in paired serum and liver tissue of normal and tumor.** (a)(i) Western blots of histones isolated from tissues and serum with site specific histone PTM antibodies of, H4K20Me3, H3K27Me3, H3K9Me3, γ-H2AX, H3S10P and H4K16Ac in tumor tissue and serum compared to normal. Antibodies against H3 and H4, and fast green stained histone transferred PVDF membrane were used as equal loading control. (b) H&E stained section (40X) of tissues (Lung, Kidney and Brain) from NDEA-treated or untreated (normal) animals. (c) Western blotting of histones isolated from normal tissues (Lung, Kidney and Brain) and serum of NDEA-treated or untreated animals with site specific histone PTM antibodies against H4K20Me3, γ-H2AX, H3S10P and H4K16Ac. Antibodies against H3 and H4, and fast green stained histone transferred PVDF membrane were used as equal loading control. (d) Colorimetry based assay done using serum isolated from normal, early and late stage tumor bearing rats (i) HDAC activity assay was performed on both the TSA treated and untreated samples (ii) HAT activity. Statistical tests are done by using students t-test. * p<0.05, ** p<0.01.

lung, kidney and brain isolated from both the normal and NDEA-treated (tumor bearing)

animals. The tissues isolated from the animals treated with NDEA were first histologically examined for any aberrations by H and E staining **[Figure 5.4b]**. Grossly, no differences were seen with respect to control tissues in untreated animals. Histones were then isolated and probed for site specific PTM antibodies **[Figure 5.4c]**. The data demonstrates that the alterations of modifications are specific to tumor liver tissue and not to other histologically normal organs, thus strengthening that the liquid biopsy (serum histone) is very similar to its parent tissue (tumor tissue-liver) and hence can be used for clinical purpose.

### 5.3.3 *Increased HDAC activity in HCC tissues correlates with corresponding serum samples*

So far we have seen a positive correlation for histone PTMs in HCC, tissue and serum histones. We next contemplated whether the reported increased HDAC activity in tumor tissue[230] can also be seen in serum to understand how similar the liquid biopsy (serum) is to tissue biopsy in context of histone PTM modifiers. This is particularly interesting due to the observation of H4 hypo-acetylation seen in serum and HCC purified histones. HDAC activity assay conducted using serum isolated from normal, early (90 days NDEA treatment) and late stage (120 days NDEA treatment) HCC bearing rats demonstrated the presence of significantly higher HDAC activity in both the tumor serum samples compared to normal serum **[Figure 5.4d(i)]**. Interestingly, the serum of early stage liver cancer animals also showed an elevated HDAC in comparison to normal, indicating a HDAC activity gradually increases during the course of HCC development **[Figure 5.4d(i)]**. As a proof of principle that the calorimetric assay performed is indeed a true measure of HDAC activity, treatment of serum samples with TSA was done prior to HDAC assay. As seen in **[Figure 5.4d(i)]**, the activity in samples treated with TSA is less compared to the untreated samples validating the robustness of the assay. To understand the status of HAT's, levels of which are also reported to change in human tumors [231], we performed a HAT activity assay in normal, early and late stages of tumor serum, but no

significant differences were observed, suggesting the H4 hypo-acetylation seen might be due to enhanced HDAC activity in tumor samples compared to normal **[Figure 5.4d (ii)]**.
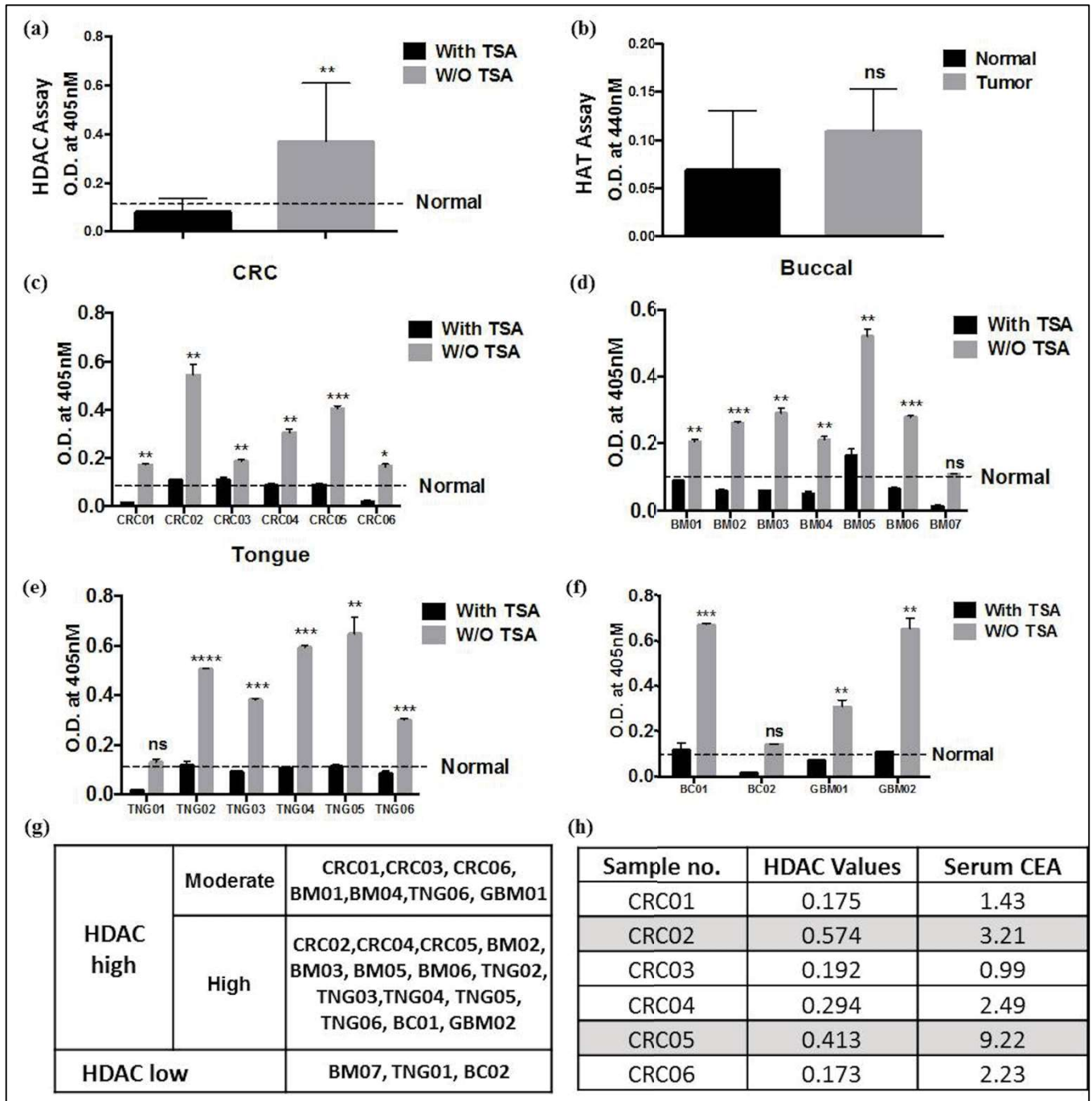


**Figure 5.5. Profiling of histone modifiers in human serum samples.** Cumulative analysis of (a) HDAC and (b) HAT activity assay done using the human serum of 6 healthy subjects and 24 cancer patients. With TSA- involves serum pre-treated with TSA for 10 minutes and W/O TSA- untreated samples. (c) Graph showing the relative activity of HDACs in CRC, (d) Buccal, (e) Tongue, (f) Breast and Glioblastoma samples. Statistical tests are done by using students t-test. * p<0.05, ** p<0.01. (g) Table representing the subgrouping of all 24 human samples as per their HDAC activities. (h) Correlation between serum CEA levels and HDAC activity in six CRC samples. Highlighted samples show high CEA and HDAC levels.

Intrigued by the observation of elevated HDAC activity in tumor serum samples of rat model, we asked whether the HDAC activity can also be detected in human serum samples. To this end, we performed HDAC activity assay in serum isolated from six healthy subjects (normal) and 24 different types of cancer patients, including colorectal (CRC#6), buccal (BM#7), tongue (TNG#6), breast (BC#2) and glioblastoma (GBM#2). The histopathological details of patient samples included in the study are tabulated in **Table 5.2**. The cumulative analysis of all the 24 samples revealed a higher HDAC activity in serum of cancer patients compared to normal **[Figure 5.5a]** with no significant change in HAT activity **[Figure 5.5b]**. Also, grouping of serum samples based on the cancer type show an elevated activity in most of the samples of CRC **[Figure 5.5c]**, buccal **[Figure 5.5d]**, tongue **[Figure 5.5e]**, and breast & glioblastoma **[Figure 5.5f]**.

Interestingly, we found that even with a sample size of 24, the HDAC activity is different amongst each patient sample, therefore highlighting the importance of subgrouping the patients on the basis of inherent epigenetic background for success of epi-drug therapy. Thus, monitoring the HDAC activity in the serum sample has helped us to categorise the patients into two subgroups: (1) High HDAC and (2) low HDAC. Group 1 can further be subdivided into two, high and moderate HDAC activity groups **[Figure 5.5g]**. This subgrouping of patients on the basis of HDAC activity will assist in selection of patients, determining the dose of epi-drug, thus increasing the success of therapy.

During the diagnosis of a disease like cancer, measurement of many serum based biomarkers is usually performed. One such marker is the quantification of serum CEA levels in CRC patients. We observed differential levels of CEA amongst the six CRC samples used in the study. Interestingly, high CEA levels seen for CRC02 and CRC05 samples correlated with high HDAC activity in comparison to other samples with low CEA values **[Figure 5.5h]**. Thus,

serum based measurement of HDAC activity compares positively to CEA, a cancer biomarker for CRC.

| Sample | Origin | Histopathological Analysis |
|--------|--------|----------------------------|
| BM01 | Buccal | Moderately differentiated squamous carcinoma |
| BM02 | Buccal | Moderately differentiated squamous carcinoma |
| BM03 | Buccal | Moderately differentiated squamous carcinoma |
| BM04 | Buccal | Moderately differentiated squamous carcinoma |
| BM05 | Buccal | Moderately differentiated keratinizing squamous carcinoma |
| BM06 | Buccal | Moderately differentiated keratinizing squamous carcinoma |
| BM07 | Buccal | Poorly differentiated squamous carcinoma |
| TNG01 | Tongue | Moderately differentiated squamous carcinoma |
| TNG02 | Tongue | Moderately differentiated squamous carcinoma |
| TNG03 | Tongue | Moderately differentiated squamous carcinoma |
| TNG04 | Tongue | Squamous carcinoma |
| TNG05 | Tongue | Moderately differentiated squamous carcinoma |
| TNG06 | Tongue | Moderately differentiated squamous carcinoma |
| CRC01 | Colon | Moderately adenocarcinoma |
| CRC02 | Colon | Poorly differentiated adenocarcinoma |
| CRC03 | Colon | Moderately differentiated adenocarcinoma |
| CRC04 | Colon | Moderately differentiated adenocarcinoma |
| CRC05 | Rectum | Moderately differentiated adenocarcinoma |
| CRC06 | Rectum | Adenocarcinoma |
| BC01 | Breast | Infiltrating duct carcinoma, Grade II |
| BC02 | Breast | Infiltrating lobular carcinoma, Grade II |
| GBM01 | Glioblastoma | Glioblastoma (WHO grade IV) |
| GBM02 | Glioblastoma | Glioblastoma (WHO grade IV) |

**Table 5.2.** Histopathological analysis of human patient samples used in the study.

## 5.4. Discussion

The DAE protocol developed for the isolation of histones from serum samples is simple, robust, time-efficient and cost-effective. Further, the comparison of key site-specific histone PTMs in tissue verses serum, for both normal and tumor samples have revealed a similar pattern among

the respective biological samples. Also, we illustrate for the first time a higher HDAC activity in serum samples tumor compared to normal.

Earlier protocols for isolation of cNUCs are based on chromatin immunoprecipitation (ChIP) by specific histone antibodies. ChIP depends critically on the quality of the antibody and is not cost-effective. Though numerous histone antibodies as ChIP-grade are available, but they need stringent validation by western blotting and MS, because of their cross-reactivity with unmodified histones, similar histone modifications and some with non-histone proteins. The developed protocol overcomes all the limitations of the existing ChIP method as it is based on dual acid extraction. The good quality and quantity of purified histones by this novel technique has opened a new avenue for studying the pattern of histone PTMs as well as histone variants in serum samples by western blotting or mass spectrometry in different pathophysiological states.

To gain insights into global serum histone PTM pattern and understand whether the observed alteration matches with that of cancer tissue, NDEA induced HCC rat model system has been used. The quantity of histones isolated from the normal serum was very less compared to the serum samples of NDEA induced HCC rats. This could be directly attributed to the increased cell death seen in diseased conditions as opposed to the healthy subjects, due to which the abundance of cNUCs and hence histones will be more in a serum sample of diseased state. This is in conformity with the earlier reports where elevated cNUCs are observed in various human cancers [220224232233].

Studies on global histone modifications across various human cancers have identified alterations in a panel of histone PTMs[234]. The loss of H4K16Ac and H4K20Me3 are now regarded as the hallmark of most human cancers. Interestingly, we noted that these hallmarks are even true for the animal model system. Furthermore, similar changes are observed in serum

histones also proving that indeed, they are true hallmarks which change during cancer, irrespective of the cancer type in the study, species used and source of biological samples (liquid or solid biopsy). Profiling for other histone PTMs – H3K27Me3, H3K9Me3, γH2AX and H3S10P in both tissue and serum showed a same pattern of increase in tumor tissue and serum samples. Further, we also reveal that the changes in the histone PTM pattern observed in serum mirrors only liver tissue and no other organs, thus proving that the histones in serum are from tumor tissue.

Earlier studies had shown the presence of acetylated histones in blood cells, but its levels were not correlated with tumor tissue[235]. Such studies on global histone modifications are of importance because of their prognostic utility and predictive markers for recurrence. Now with the serum histones showing a similar pattern of histone PTMs as of tumor tissue, liquid biopsy (non-invasive) will be a good alternative to tissue biopsy (invasive) for monitoring the disease regression/progression in cancer patients. Further the antitumor effects of histone deacetylase, or histone methyltransferase inhibitors could be evaluated by monitoring changes in the quantities of the corresponding modification on the circulating histones thus overcoming the limitation of earlier studies wherein histones of blood cells were used.

Altered histone acetylation levels in cancer are the result of the imbalance of the activities of HAT and HDAC. Many reports have emphasised the altered levels of these enzymes, especially HDACs in various cancers [236]. Our data of an increased HDAC activity in serum and tumor tissue samples compared to normal is in accordance with the earlier reports. Thus, the present observation of HDAC activity in serum allows us to monitor the level of HDAC and possible tumor status in response to histone modifying enzyme inhibitors in real-time by liquid biopsy. Interestingly, some studies on global proteomic profiling of serum proteins has earlier reported the presence of HDACs in serum thus, it is not surprising that HDAC activity is detected in serum[237,238]. Intriguingly, measurement of HDAC activity in early (90 days

NDEA treatment) and late (120 days NDEA treatment) stages of liver cancer in an animal model system revealed that a gradual increase in HDAC activity as the animal develops a tumor. This observation proves that early monitoring of HDAC activity may assist in better diagnosis of cancer. Further, the assay can be employed to monitor the naive cancer, recurring and drug resistant tumors, where in periodic monitoring of HDAC activity in patients diagnosed with cancer will aid in their improved clinical management. However, large studies including more cancer patients at various stages, undergoing diverse chemotherapeutic treatments in combination with epi-drugs will provide conclusive evidences and help in employing the proposed hypothesis for better disease management.

Owing to the increased HDACs, use of HDAC inhibitors for treatment of cancer is considered to be a good treatment regime. But so far the use of HDAC inhibitors had limited success in solid tumors because of severe toxicities and other fatal effects[239]. One of the reasons behind the failure or limited success of HDAC inhibitors has been attributed to the inherent epigenetic background of the patients, where some may have high expression of HDACs others low levels[132,240]. This can further be seen in our data, where all the patients showed different extent of HDAC levels. Therefore, administering HDAC inhibitors to patients with inherent low levels of HDACs may be fatal. For example, based on our data we have segregated the samples into two groups, HDAC high and HDAC low. Treating the first group patients with HDAC inhibitors will be beneficial, as this group show elevated levels of these enzymes. Furthermore, this group can be sub divided in to two, which can help in deciding the dose and time span of epi-drug therapy, where a high HDAC activity patients can be given high doses of drugs for a longer span than the others. As for the second group epi-drug treatment might not be of much benefit. Thus, serum based detection of histone modifiers like HDAC/HAT will help with sub-grouping of patients and personalize the treatment, monitor patient's health status during

treatment with histone modifier inhibitors and response of the individual's tumor to treatment

**[Figure 5.5]**.
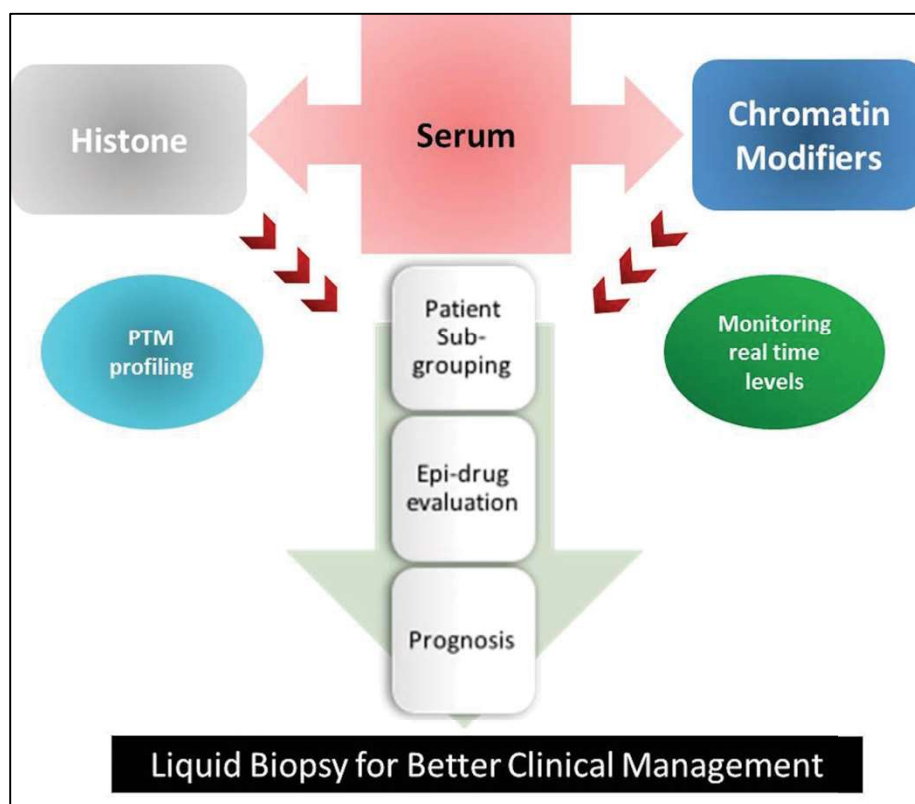


**Figure 5.6. Schematic representation of Liquid biopsy as tool for better clinical management of cancer patients.** The DAE protocol provides 'real-time' purification of serum histones and monitoring of levels of chromatin modifiers like HDACs and HATs that will help in sub-grouping patients eligible for epi-drug treatment and their response, aid in better prognosis and disease management.

## 5.5. Conclusion

In summary, the developed DAE technique for isolating serum histones will provide real time information of epigenome which will be helpful in understanding the overlap between paired serum and cancer tissue histone proteome by high end proteomics. Importantly, our data gave a novel rationale for using serum histone proteomics as a predictive tool for disease progression. This information will allow the development of efficient strategies for the treatment and better management of the underlying disease. The combination of different histone marks rather than a single histone mark is believed to further enhance sensitivity and specificity of detection of these marks and hence improve cancer management.

*Chapter 6*

# VI. Consolidated Discussion and Conclusion

## 6.1. Discussion

Genetic and epigenetic events both can control the initiation and progression of cancer. Genetic alterations are impossible to reverse however, epigenetic alterations are reversible through the inhibition of either the writer or the erasers of the modification of interest. In this context, a wealth of information has emerged over the past two decades demonstrating the functionally important role of histones apart from their fundamental role in packaging of the genome. Not only do histone PTMs and variants regulate gene expression patterns for proper development of an organism but also in cancer, which is often imagined as "development gone wrong", a variety of histone PTM and variant mediated mechanisms are perturbed leading to silencing of tumor suppressor genes and activation of oncogenes. The work described in this thesis not only re-emphasizes the functionally important role of histones, but also, demonstrates that not only individually, but as a co-ordinated events, DNA methylation and histone chaperone machinery together have marked consequences on the chromatin dynamics that may contribute to attainment of specific patho-physiological states.

The existence of specific chaperones for histone isoforms are not known yet. However, in our previous studies[7], the observed enrichment of both H2A.1 and H2A.2 upon their overexpression indicates that owing to a similar set of chaperones, ectopically overexpressed isoform is able to replace either of the endogenous histone. This is in accordance with the work carried out by *Vardabasso et al.,* where, they found out H2A.Z isoforms, H2AZ.1 and H2A.Z.2 differing in three amino acids, share similar genomic occupancy patterns and interact with similar histone chaperone complexes in their overexpression studies[241]. Therefore, we propose that even though histone isoforms are recruited by same machinery like NAP1 at a similar locus, their inherent differences in the nucleosomal stability as seen in our earlier work[7], will determine the gene expression output.

Further, the work done in regards to understanding the biology of NAP1 in higher vertebrates revealed few critical differences in the way the complexes function in various species. Current work suggests for a dynamic equilibrium between oligomeric and dimeric states of NAP1, where phosphorylation is a key player. The oligomeric states (Phosphorylated) possibly act as storage form of NAP1 *in vivo* in cytoplasm to prevent unintended interactions and the dimeric NAP1 (Dephosphorylated) probably engages the H2A-H2B dimer for its translocation into nucleus. Similar observations were also seen for NAP1 in *S. cerevisiae,* mutation of phosphorylating residues to either alanine or aspartic acid (phospho-mutants) resulted in cell cycle changes, including a prolonged S phase, suggesting that reversible phosphorylation of NAP1 by CK2 is important for cell cycle regulation[149]. Further, CK2 and NAP1 deletion led to a slight decrease in the number of cells with abnormal buds compared to the nap1Δ strain, suggesting a synthetic genetic interaction[149]. Taken together, these results suggest that these proteins function in overlapping but nonidentical pathways in the regulation of bud formation highlighting the critical role of CK2 in governing the functioning of NAP1, however, the authors propose, for an opposing theory that phosphorylation triggers its entry in to nucleus. Interestngly, *Rodriguez et al.,* reported similar series of events as our studies have shown for rNAP1, but for NAP2 protein (same function as that of NAP1) in HeLa cells, their work showed the distinct localization of NAP2 depends on its phosphorylation status. Phosphorylated NAP2 remains in the cytoplasm during the G0/G1 transition, whereas its dephosphorylation triggers its transport into the nucleus, at the G1/S-boundary[165]. These species-specific differences can be attributed to their structural and stability differences as our results have shown, which may also be implying functional divergences in higher eukaryotes for these proteins, promoting diverse histone exchange and chromatin organization.

In context to understanding other nucleosomal alterations apart from H2A isoform changes, a global increase in H3.2 and decrease in H3.3 in tumor cells similar to H2A.1 and H2A.2

respectively has been detected. However, at mononucleosome level, histone isoforms- H2A.1 and H2A.2 interact with both the H3 variants H3.2 and H3.3. Yet, the nucleosome formed by these four histones in combinations differ in their stabilities with H3.3/H2A.2 to be least stable, and H3.2/H2A.1 to be highly stable. This is in accordance with our previous study, where we have shown that amongst the two H2A isoforms, H2A.1 containing nucleosome is more stable[7]. Gaining access to a site occupied by a nucleosome for DNA binding, transcription or repair requires nucleosome eviction, sliding or DNA unwrapping.

Presence of unstable, heterotypic nucleosomes at these positions could be part of these dynamic processes. Observation of double variant H2A.Z/H3.3, highly unstable nucleosome at these sites indeed this is the case. Further their position corresponds to sites of tissue-specific DNase I hypersensitivity, which measures DNA accessibility caused by nucleosome mobility[173]. A similar conclusion was reached for *Drosophila* nucleosomes that were extracted from intact nuclei under low-to-moderate salt conditions; these are enriched in H3.3 at promoters and regulatory elements, suggesting that disrupted H3.3 nucleosomes have distinctive properties that make them relatively soluble[242]. In trypanosomes, nucleosomes containing H2A.Z and a special H2B variant are found exclusively at promoters and are salt unstable[243], which suggests that instability of promoter nucleosomes mediated in part by H2A.Z is an ancient, conserved mechanism for maintaining sites transiently free of nucleosomes. Similar to these finding, it could be possible that H2A.2/H3.3 nucleosomes could be mapped on those sites of genome where there is a need of continuous nucleosome displacement. An interesting thing which emerges from ours as well as other studies is - inherently H3.3 containing NCP's are relatively unstable, what destabilizes these nucleosomes is a fascinating aspect to work on. H3.3 differs from H3 at only four amino acid residues, none of which seem to interact directly with H2A.Z or H2A. Although it is possible that H3.3 is modified to make nucleosomes unstable, acetylation does not appear to be involved[47], and removal of the entire N-terminal tail has at

most a minor effect on its incorporation into active *Drosophila* chromatin[47]. Therefore, it is attractive to presume that the process that incorporates H3.3 into nucleosomes, involving histone chaperones and nucleosome remodellers, also facilitates H2A isoform incorporation and makes nucleosomes labile. There might be a possibility of extensive cross talk among the various histone deposition machinery to achieve this goal. However, to understand in depth the reason behind such changes in stability, further biophysical and/or biochemical assays need to be carried out.

Intriguingly, other replication dependent histone H3 variant, H3.1 remains relatively unaltered in tumor cells. In addition, a decrease in active H3 PTM marks and a simultaneous increase in H3 repressive marks were also observed. These changes correlate well with the changes in the H3 variants at mononucleosomal level and also on monomeric histones. For histone PTMs, especially, an important question arises that whether the alteration in histone modifications observed actively contribute to the gene regulation for attainment of the transformed state or whether they are merely biomarkers. This should be emphasized especially because most histone modifications are very dynamic in nature and undergo alteration with the cell cycle. Hence, the change in the histone PTM profile might simply be an indicative of the altered cell cycle stage, which is commonly observed in cancers as the cells tend to have higher proportion of S and G2/M population being more proliferative. On the other hand, if these modifications actively contribute to gene regulation for the attainment of such states, then it is intriguing that how such dynamic histone modifications are persistently maintained at an observed level. This can be achieved by regulating the levels of the histone modifiers or incorporation of histone variants. Our results show that the latter mechanism contribute to the attainment of such states. Overexpression of H3 variants did not bring any changes in phenotype and in global PTM profile though the ectopically tagged proteins were recruited onto DNA. This could be attributed to differential histone deposition machinery- histone chaperones for both the H3

variants. Thus, probably overexpression though led to recruitment of respective histone, it did not enrich the H3 variants on chromatin owing to restraint in the levels of chaperone. This hypothesis has been strengthened when just like the changes in H3 variant profile, changes in chaperones were also observed with an increase of CAF-1 (P150 and P60 subunits) and decrease of HIRA in HCC. Further, a matched expression pattern was observed for H3 variants and their chaperones across various normal tissues indicating that for the chromatin enrichment of a particular H3 variant respective chaperone also needs to be in appropriate levels.

Histone chaperone P150 is known to be upregulated in many cancers, and its depletion brings a decrease in cell proliferation[218,244,245]. Though deposition of H3.1 and H3.2 is effected in cells lacking P150, an increase in H3.3 was seen, which probably can explain the changes in context of PTM profile and gene expression. However, it also led to arrest of cells in S-phase, this could either be due to its prerequisite for replication of pericentric heterochromatin structures via its interaction with HP1[246] or a decrease in the supply of total H3 pool required for DNA compaction. Nonetheless CAF-1 complex is also known to be important to safeguard somatic cell identity, as CAF-1 suppression led to a more accessible chromatin structure at enhancer elements early during reprogramming[247]. These changes were accompanied by a decrease in somatic heterochromatin domains, increased binding of Sox2 to pluripotency-specific targets and activation of associated genes suggesting again for its role in maintaining the chromatin structures[248,249].

Association of H3.3 with transcriptional activation is a well-established fact, though, is it due to the PTMs it undergoes or is it because of the inherently unstable nucleosome is not yet known as discussed earlier. In this regard work done by Lin *et al.,* in mouse embryos revealed, H3.3 depletion leads to over-condensation and mis-segregation of chromosomes, with corresponding high levels of aneuploidy, but does not affect zygotic gene activation. These embryos have significantly reduced levels of markers of open chromatin, such as H3K36Me2

and H4K16Ac. In addition, the embryos have increased incorporation of linker H1. Knockdown of Mof (Kat8), an acetyltransferase specific for H4K16, similarly leads to excessive H1 incorporation[208]. These results reveal that H3.3 mediates a balance between open and condensed chromatin that is crucial for the fidelity of chromosome segregation during early mouse development. Likewise, H3.3 knock down in pre-neoplastic cells, CL44 led to gain of changes similar to neoplasia, which can be primarily attributed to alterations in the tumor suppressor gene expression. Further, elevated cell proliferation upon H3.3 loss, possibly may be due to loss of expression of APC, a negative regulator of WNT signaling pathway among many other probabilities. This could indeed be indeed the case because APC mutations are very less in case of HCC[250,251], unlike that of CRC cases[252,253], however, its low expression owing to DNA methylation has been reported in HCC[254,255]. It could therefore be possible that DNA methylation as well as H3.3 occupancy together may be determinant of this pathway. Interestingly, not all tumor suppressor genes are affected upon H3.3 knockdown, aiding us to believe that probably there might be only a specific subset of genes which are under the control of H3.3 either directly or indirectly. But the question remains to be addressed is what determines this specificity?

Our analysis to understand the reason behind similar expression pattern between H2A isoforms and H3 variants, revealed for the presence of CpG islands and sites on their promoters. Interestingly, CpG islands have been observed on histones being downregulated – H2A.2 and H3.3; CpG sites on genes being overexpressed in HCC – H2A.1 and H3.2. This correlate well with the one of the observed phenomenon in cancer- promoter specific hypermethylation and global hypomethylation[256]. Aberrant methylation of promoter CpG islands effects lot of tumor suppressor gene expression, linked to many cancer types[257]. Moreover, global genomic hypomethylation contribute to genomic instability, by activation of repetitive elements, transposons again a characteristic of human cancers[258]. DNA methylation mediated loss of

H3.3 leads to decrease in occupancy of H3.3 NCP's from tumor suppressor genes thus aiding in tumorigenesis. Further, use of small molecule inhibitors, 5-Aza-C (DNMTi) and TSA (HDACi) led to a reversal of these changes, elevating the expression of H2A.2 and H3.3. What remains to be seen though is whether epi-drug treatment during the cancer development will prevent such large scale epigenomic changes and delays its progression.

Previous reports have highlighted the importance of use of epi-drugs and their potential use as anti-cancer agents in many cell lines[122,259]. However, apart from certain case specific success, especially in leukemic patients[123], HDACi have failed in clinical trials. The reason has been attributed mostly to lack of selectivity of most of the HDAC inhibitors tested clinically and inherent epigenetic differences between patients. In this regard, it is therefore essential to develop class specific inhibitors and also stratify patients for therapy success. Monitoring HDAC activity in serum is one such way suggested by our study here for patient sub-grouping. Further, our novel, cost-effective serum histone isolation DAE protocol will enable us to monitor in real time histone PTM changes also. Similar epigenetic alterations observed in paired serum samples as that of tissues, puts forth a hypothesis for liquid biopsy in monitoring disease progression and also in determining the therapy regime.

## 6.2. Conclusion

Administration of chemical carcinogen led to development of HCC **[Figure 6]** with changes in DNA methylation pattern- promoter specific hypermethylation and global hypomethylation **(1)**. Owing to the presence of CpG rich promoters histone genes H2A.1, H3.2 are upregulated and H2A.2, H3.3 are upregulated in cancer cells. Therefore, DNA methylation is the dynamic player regulating the similar transcriptional output of H2A isoforms and H3 variants **(2)**. Further, immunoprecipitation analysis revealed the possibility of existence of the combination of nucleosomes and there is no variant/isoform specific interaction. However, these nucleosomes differ in their stability, H2A.1/H3.2 containing NCP more stable and H2A.2/H3.3
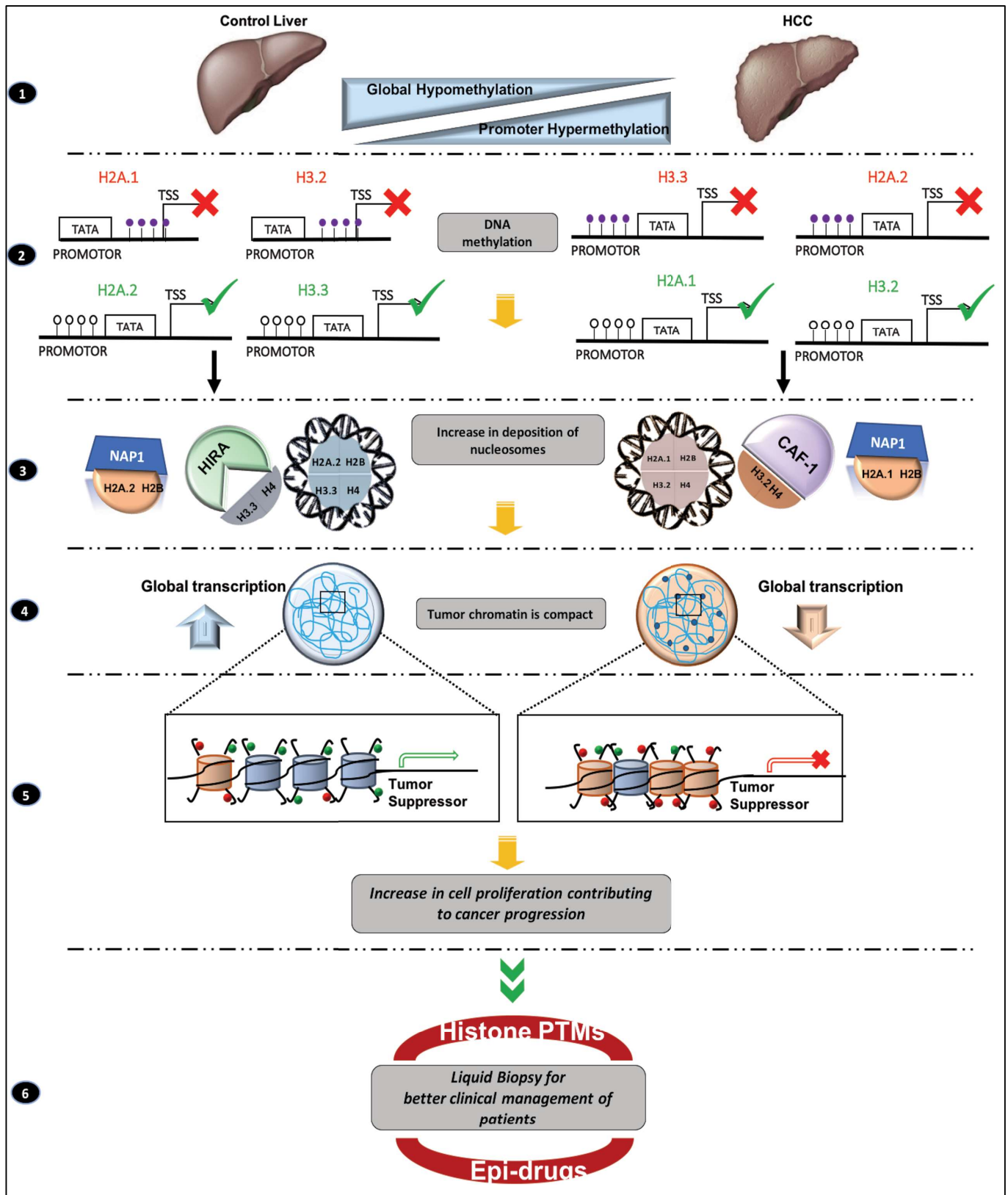
**Figure 6. Schematic representation of the conclusions of the work done.**

least stable. NAP1, a H2A/H2B chaperone do not show any specific interaction with either of the H2A isoforms. However, histone chaperones responsible for specific H3 variant deposition also seems to alter with CAF-1 complex of H3.2, being upregulated and HIRA of H3.3 downregulated. Therefore, owing to dysregulation of both histone variants and their chaperones, these NCPs are enriched on the chromatin **(3)**. Strikingly, the alteration in the histone PTM profile shows a similar pattern with a decrease in gene activation mark and an increase in repressive marks owing to which there is a global chromatin condensation and transcription repression in cancer cells **(4)**. Knockdown of H3.3 revealed its central role in chromatin organization and also its association with tumor suppressor gene expression **(5)**. Our report suggests that there is co-operative interplay between histone variants, chaperones and their transcriptional regulation which results in the stable maintenance of the highly dynamic histone marks required for maintaining the deregulated epigenetic landscape found in cancer cells. Further, the histone PTMs changes observed in tumor tissue can be seen in serum samples, which enable us to use serum as a liquid biopsy for both detecting and treating thus, aiding in better clinical management of the disease **(6)**.

*Chapter 7*

# VII. Salient Findings and Future Directions

# 7.1. Salient Findings

Histone isoforms and variants have been reported to be differentially expressed in various patho-physiological states including cancer[261,213]. However, is there any correlation between them and do they work together for the attainment of such a state inside the cell have not been investigated yet. Moreover, previous reports have emphasized only on individual changes in the variant and or isoform profiles and have not looked in depth into dysregulation of respective PTMs, chaperones and their interactors inside the nucleosome. The work done in the thesis provides insights into these aspects of cancer epigenetics and also provides a novel strategy to circumvent the challenges faced during epi-drug based chemotherapeutic treatment in cancer patients.

❖ Histone chaperone, NAP1 interacts with both the H2A isoforms, H2A.1 and H2A.2 and its knockdown did not affect the deposition of either of these isoforms onto DNA. Further, by use of GFC and DLS our results depict that rNAP1 exists as a higher oligomeric structure owing to both electrostatic and hydrophobic interactions and both the dimeric and oligomeric rNAP1 follow two-state model of unfolding with no detectable intermediates. Also, use of a N-terminal tag has a robust effect on the oligomerization capability of proteins. Hence, it is advisable to use native proteins to study protein oligomeric parameters.

❖ MDS analysis suggests that rNAP1 dimer is more stable than yNAP1, thus may influence the oligomeric property of this protein, hence probably rNAP1 has a higher tendency to remain as oligomer than of yNAP1. Further, a conclusive evidence has been provided to show that may be in higher eukaryotes like rat, PTMs like phosphorylation govern the oligomeric property of NAP1. However, phosphorylation does not have any effect on its histone binding capacity.

❖ Histone variants, H3.3 and H3.2 are also dysregulated in HCC with H3.2 showing increased and H3.3 a decreased expression at both protein and transcript level. Intriguingly, no changes in the expression profile of other replication dependent histone- H3.1 was observed. H2A isoforms and H3 variants are able to interact with each other, however, the nucleosomes formed from these combinations differ in stability with H2A.1/H3.2 being most and H3.2/H2A.2 least stable. The altered nucleosome stabilities may lead to the modulation of transcription or other chromatin mediated processes. DNA methylation acts as the transcriptional controlling machinery regulating co-expression of H2A isoforms and H3 variants.

❖ Similar to the changes observed in H3 variant profile, with decrease in H3.3 expression, there is a loss of histone activation PTM marks and with increase in H3.2 expression, a gain in repressive PTM marks was observed. This correlation was seen even on the mononucleosomes, where H3 variants are part of and also on monomeric histones. Indeed, tumor cells have pronounced heterochromatin and show a global gene repression. Overexpression of either of the H3 variants did not lead to any phenotypic changes even though their ectopic expression lead to their chromatin recruitment. This might be because of the histone chaperone machinery differences between the histones. Indeed an elevated expression in H3.2 chaperone levels CAF-1 (P150, P60) and decrease in H3.3 chaperone HIRA was observed in tumor cells. Further, the expression pattern of H3 variants matched with the pattern of their respective chaperones across various rat normal tissues.

❖ Altering the deposition of H3.2/H3.1 by knockdown of their chaperone subunit, P150 lead to increase in H3.3 levels, corroborated with elevated active PTM marks, global chromatin relaxation, loss of cell proliferation and clonogenic potential of cells indicating that reversing the H3 variant profile alters the cancer cell state towards

becoming normal. However, these changes could not be specifically attributed to elevated H3.3 levels as because P150 knock lead to S-phase arrest of cells, owing to the limited supply of H3 histone required for DNA compaction.

❖ Histone H3.3 knock down led to increase in H3.2 and H3.1 levels probably to maintain the total histone H3 pool required for DNA compaction. These changes led to compaction of chromatin, global transcriptional repression and elevated cell proliferation and clonogenic potential of cells similar to like a state of cancer cell. The balance of H3.3 and H3.2 acts as the master regulator governing the expression of various tumor suppressor genes either directly or indirectly, therefore, altering the expression status of these variants by H3.3 knockdown lead to attainment of cancer state by modulating the global epigenome profile of the cell.

❖ A novel protocol developed for histone isolation from serum demonstrates the similarities between liquid and solid biopsies in terms of histone PTM changes. Our study also shows monitoring HDAC activity in serum can act as a novel method to strategize patients for therapy, thus, may be helpful in elevating success of epi-drug based treatment modality.

## 7.2. Future Directions

The work described in this thesis emphasises the importance of co-ordinated epigenetic events in the acquirement and maintenance of cancer epigenetic state. However, much remains to be understood regarding the genome wide repercussions of these changes. Based on our own results we speculate that deposition of differentially stable nucleosomes alters the gene transcription. It would be therefore be interesting to know what are the subset of genes regulated by these combinatorial nucleosomes. Here are certain aspects which needs to be studied further.

❖ Genome wide distribution studies for H2A isoforms- H2A.1, H2A.2 and H3 variants- H3.2,H3.3 along with the global transcriptomic analysis will definitely be beneficial, will aid us to understand the extent of their contribution in governing expression pattern of genes and finally their role in governing various pathophysiological states like cancer.

❖ The interaction of histones with NAP1 though, seems to be redundant, its nuclear localisation might determine the extent of deposition of histones onto DNA. Phosphorylation at NLS of NAP1 lead to its oligomerization, by burial of NLS, this gives rise to the possibility of controlling the nucleosome formation and eviction at the level of chaperone availability in the nucleus. It can be hypothesized that the phosphorylated form of NAP1 may act as a storage form for histones in the cytoplasm and its entry into the nucleus is blocked due to the burial of NLS. May be phosphatase activity will then lead to exposure of NLS and thus gaining the entry of NAP1/histone complex into the nucleus. Exploiting the balance between kinase and phosphatase, NAP1 localisation can be altered and a tight control on levels of histone deposition can be achieved. Determining the localisation of phosphorylated and unphosphorylated NAP1 along with identification of other kinases and a phosphatase might enable to understand this dynamics better.

❖ A subset of human cell lines, though showed similar observation in respect to H2A and H3 histone alterations, it is however, essential to investigate in depth in human tissues whether these changes are true in other cancers also. Further, functional and biochemical studies in human cell lines will aid in better understanding in terms of epigenetic regulatory networks contribution in cancer development and progression.

❖ Also, how H3.3 is able to directly influence higher order chromatin structure is one aspect which needs immediate attention. Probably, H4K16Ac and H1 has a cross talk

with H3.3, knockdown of either hMOF or H1 may help in elucidating this mechanism. Association of H3.3 with certain tumor suppressor genes is intriguing and also raises the question that whether how many such genes and their pathways are under the control of H3.3. Genome wide analysis for relative enrichment of H3.3 and H3.2, transcriptomic analysis after their knockdown will shed light on this matter.

❖ DNA methylation is a dynamic player governing the expression of H3.3 and H3.2, and use of DNMT and HDAC inhibitor led to changes in H3 variant profile. This thus raises the possibility that, if indeed H3 variants are the central nodes regulating tumor suppressor gene expression, epi-drug based treatment modality is likely be beneficial in the treatment of such cancer patients.

❖ Liquid biopsy, though, has shown similar epigenetic alterations to tissue biopsy, in context of histone PTMs and HDAC/HAT activity, it is essential to understand how deep does these similarities run. Whether HMT activity can also be detected? Therefore, for bridging the gap between bench and bedside, to bring serum epigenetics to reality, for clinical use, study on more number of samples spanning various tumor types is essential.

187

# *Bibliography*

1. Luger K, Mäder a W, Richmond RK, Sargent DF, Richmond TJ. Crystal structure of the nucleosome core particle at 2.8 A resolution. Nature. 1997;389(6648):251–260.

2. Singh R, Mortazavi A, Telu KH, Nagarajan P, Lucas DM, Thomas-Ahner JM, Clinton SK, Byrd JC, Freitas MA, Parthun MR. Increasing the complexity of chromatin: functionally distinct roles for replication-dependent histone H2A isoforms in cell proliferation and carcinogenesis. Nucleic acids research. 2013;41(20):9284–95.

3. Brown DT, Wellman SE, Sittman DB. Changes in the levels of three different classes of histone mRNA during murine erythroleukemia cell differentiation. Molecular and Cellular Biology. 1985;5(11):2879–2886.

4. Khare SP, Sharma A, Deodhar KK, Gupta S. Overexpression of histone variant H2A.1 and cellular transformation are related in N-nitrosodiethylamine-induced sequential hepatocarcinogenesis. Experimental biology and medicine (Maywood, N.J.). 2011;236(1):30–5.

5. Su CH, Tzeng TY, Cheng C, Hsu MT. An H2A histone isotype regulates estrogen receptor target genes by mediating enhancer-promoter-3'-UTR interactions in breast cancer cells. Nucleic Acids Research. 2014;42(5):3073–3088.

6. Tyagi M, Khade B, Khan SA, Ingle A, Gupta S. Expression of histone variant, H2A.1 is associated with the undifferentiated state of hepatocyte. Experimental biology and medicine (Maywood, N.J.). 2014:1535370214531869.

7. Saikat Bhattacharya. Chromatin Organisation: Molecular Role of H2A Variants. A thesis submitted to the Board of Studies in Life Sciences. Homi Bhabha National Institute. 2016; LIFE09201004024.

8. Waddington CH. The Epigenotype. International Journal of Epidemiology. 2012;41(1):10–13.

9. Knezetic JA, Luse DS. The presence of nucleosomes on a DNA template prevents initiation by RNA polymerase II in vitro. Cell. 1986;45(1):95–104.

10. Baylin SB. DNA methylation and gene silencing in cancer. Nat Clin Prac Oncol.

11. Kulis M, Esteller M. 2 - DNA Methylation and Cancer. In: Genetics ZH and TUBT-A in, editor. Epigenetics and Cancer, Part A. Vol. Volume 70. Academic Press; 2010. p. 27–56.

12. Feinberg a P, Vogelstein B. Hypomethylation distinguishes genes of some human cancers from their normal counterparts. Nature. 1983;301(5895):89–92.

13. Kornberg RD. Chromatin Structure: A Repeating Unit of Histones and DNA. Science. 1974;184(4139):868 LP-871.

14. Olins AL, Olins DE. Spheroid Chromatin Units (ν Bodies). Science. 1974;183(4122):330 LP-332.

15. Huynh VAT, Robinson PJJ, Rhodes D. A Method for the In Vitro Reconstitution of a Defined "30 nm" Chromatin Fibre Containing Stoichiometric Amounts of the Linker Histone. Journal of Molecular Biology. 2005;345(5):957–968.

16. Robinson PJJ, Rhodes D. Structure of the "30 nm" chromatin fibre: A key role for the linker histone. Current Opinion in Structural Biology. 2006;16(3):336–343.

17. ConsortiumInternational HGS. Finishing the euchromatic sequence of the human genome. Nature. 2004;431(7011):931–945.

18. Elgin SCR. Heterochromatin and gene regulation in Drosophila. Current Opinion in Genetics & Development. 1996;6(2):193–202.

19. Burgess RJ, Zhang Z. Histone chaperones in nucleosome assembly and human disease. Nat Struct Mol Biol. 2013;20(1):14–22.

20. Radman-Livaja M, Rando OJ. Nucleosome positioning: how is it established, and why does it

matter? Developmental biology. 2010;339(2):258–266.

21. Yun M, Wu J, Workman JL, Li B. Readers of histone modifications. Cell Research. 2011;21(4):564–578.

22. Jenuwein T, Allis CD. Translating the Histone Code. Science. 2001;293(5532):1074 LP-1080.

23. Hake SB, Allis CD. Histone H3 variants and their potential role in indexing mammalian genomes : The "' H3 barcode hypothesis .'" 2006;103(17).

24. Legube G, Trouche D. Regulating histone acetyltransferases and deacetylases. EMBO Reports. 2003;4(10):944–947.

25. Wood A, Shilatifard A. Posttranslational Modifications of Histones by Methylation. In: Chemistry BT-A in P, editor. Proteins in Eukaryotic Transcription. Vol. Volume 67. Academic Press; 2004. p. 201–222.

26. Feng Q, Wang H, Ng HH, Erdjument-Bromage H, Tempst P, Struhl K, Zhang Y. Methylation of H3-Lysine 79 Is Mediated by a New Family of HMTases without a SET Domain. Current Biology. 2002;12(12):1052–1058.

27. Ng HH, Feng Q, Wang H, Erdjument-Bromage H, Tempst P, Zhang Y, Struhl K. Lysine methylation within the globular domain of histone H3 by Dot1 is important for telomeric silencing and Sir protein association. Genes & Development . 2002;16(12):1518–1527.

28. Bannister AJ, Kouzarides T. Reversing histone methylation. Nature. 2005;436(7054):1103–1106.

29. Martin C, Zhang Y. The diverse functions of histone lysine methylation. Nat Rev Mol Cell Biol. 2005;6(11):838–849.

30. Banerjee T, Chakravarti D. A Peek into the Complex Realm of Histone Phosphorylation . Molecular and Cellular Biology. 2011;31(24):4858–4873.

31. Rossetto D, Avvakumov N, C??t?? J. Histone phosphorylation: A chromatin modification involved in diverse nuclear events. Epigenetics. 2012;7(10):1098–1108.

32. Paull TT, Rogakou EP, Yamazaki V, Kirchgessner CU, Gellert M, Bonner WM. A critical role for histone H2AX in recruitment of repair factors to nuclear foci after DNA damage. Current biology : CB. 2000;10(15):886–895.

33. Abraham RT. Cell cycle checkpoint signaling through the ATM and ATR kinases. Genes & Development . 2001;15(17):2177–2196.

34. Mah L-J, El-Osta A, Karagiannis TC. [gamma]H2AX: a sensitive molecular marker of DNA damage and repair. Leukemia. 2010;24(4):679–686.

35. LEE HTAE, KIM SEKYE, CHOI MIRAN, PARK JIH, JUNG KHWA, CHAI YGYU. Effects of the activated mitogen-activated protein kinase pathway via the c-ros receptor tyrosine kinase on the T47D breast cancer cell line following alcohol exposure. Oncology Reports. 2013;29(3):868–874.

36. Lau ATY, Lee S-Y, Xu Y-M, Zheng D, Cho Y-Y, Zhu F, Kim H-G, Li S-Q, Zhang Z, Bode AM, et al. Phosphorylation of Histone H2B Serine 32 Is Linked to Cell Transformation. The Journal of Biological Chemistry. 2011;286(30):26628–26637.

37. Choi HS, Choi BY, Cho Y-Y, Mizuno H, Kang BS, Bode AM, Dong Z. Phosphorylation of Histone H3 at Serine 10 is Indispensable for Neoplastic Cell Transformation. Cancer research. 2005;65(13):5818–5827.

38. Sun J-M, Chen HY, Espino PS, Davie JR. Phosphorylated serine 28 of histone H3 is associated with destabilized nucleosomes in transcribed chromatin. Nucleic Acids Research. 2007;35(19):6640–6647.

39. Yang W, Xia Y, Hawke D, Li X, Liang J, Xing D, Aldape K, Hunter T, Yung WKA, Lu Z. PKM2 Phosphorylates Histone H3 and Promotes Gene Transcription and Tumorigenesis. Cell. 2012;150(4):685–696.

40. Ausió J. Histone variants—the structure behind the function. Briefings in Functional Genomics. 2006;5(3):228–243.

41. DE ROBERTIS EM, LONGTHORNE RF, GURDON JB. Intracellular migration of nuclear proteins in Xenopus oocytes. Nature. 1978;272(5650):254–256.

42. Richardson RT, Batova IN, Widgren EE, Zheng L-X, Whitfield M, Marzluff WF, O'Rand MG. Characterization of the Histone H1-binding Protein, NASP, as a Cell Cycle-regulated Somatic Protein. Journal of Biological Chemistry . 2000;275(39):30378–30386.

43. De Koning L, Corpet A, Haber JE, Almouzni G. Histone chaperones: an escort network regulating histone traffic. Nature structural & molecular biology. 2007;14(11):997–1007.

44. Mello JA, Silljé HHW, Roche DMJ, Kirschner DB, Nigg EA, Almouzni G. Human Asf1 and CAF-1 interact and synergize in a repair-coupled nucleosome assembly pathway. EMBO reports. 2002;3(4):329 LP-334.

45. Cho E-J, Kobor MS, Kim M, Greenblatt J, Buratowski S. Opposing effects of Ctk1 kinase and Fcp1 phosphatase at Ser 2 of the RNA polymerase II C-terminal domain. Genes & Development . 2001;15(24):3319–3329.

46. Hake SB, Allis CD. Histone H3 variants and their potential role in indexing mammalian genomes: The "H3 barcode hypothesis." Proceedings of the National Academy of Sciences of the United States of America. 2006;103(17):6428–6435.

47. Jin C, Felsenfeld G. Nucleosome stability mediated by histone variants H3.3 and H2A.Z. Genes and Development. 2007;21(12):1519–1529.

48. Hake SB, Garcia BA, Kauer M, Baker SP, Shabanowitz J, Hunt DF, Allis CD. Serine 31 phosphorylation of histone variant H3.3 is specific to regions bordering centromeres in metaphase chromosomes. Proceedings of the National Academy of Sciences of the United States of America . 2005;102(18):6344–6349.

49. Waterborg JH. Sequence analysis of acetylation and methylation in two histone H3 variants of alfalfa. Journal of Biological Chemistry . 1990;265(28):17157–17161.

50. McKittrick E, Gafken PR, Ahmad K, Henikoff S. Histone H3.3 is enriched in covalent modifications associated with active chromatin. Proceedings Of The National Academy Of Sciences (Of The United States Of America). 2004;101(6):1525–1530.

51. Loyola A, Bonaldi T, Roche D, Imhof A, Almouzni G. PTMs on H3 variants before chromatin assembly potentiate their final epigenetic state. Molecular cell. 2006;24(2):309–316.

52. Goldberg AD, Banaszynski LA, Noh K-M, Lewis PW, Elsaesser SJ, Stadler S, Dewell S, Law M, Guo X, Li X. Distinct factors control histone variant H3. 3 localization at specific genomic regions. Cell. 2010;140(5):678–691.

53. Chow C-M, Georgiou A, Szutorisz H, Maia e Silva A, Pombo A, Barahona I, Dargelos E, Canzonetta C, Dillon N. Variant histone H3.3 marks promoters of transcriptionally active genes during mammalian cell division. EMBO Reports. 2005;6(4):354–360.

54. Mito Y, Henikoff JG, Henikoff S. Genome-scale profiling of histone H3 . 3 replacement patterns. 2005;37(10).

55. Tagami H, Ray-Gallet D, Almouzni G, Nakatani Y. Histone H3. 1 and H3. 3 complexes mediate nucleosome assembly pathways dependent or independent of DNA synthesis. Cell. 2004;116(1):51–61.

56. Lacoste N, Puri A, Ray-gallet D, Woolfe A, Vassias I, Schultz DC, Pchelintsev NA, Adams PD, Jansen LET. Article Dynamics of Histone H3 Deposition In Vivo Reveal a Nucleosome Gap-Filling Mechanism for H3 . 3 to Maintain Chromatin Integrity. 2011:928–941.

57. Drané P, Ouararhni K, Depaux A, Shuaib M, Hamiche A. The death-associated protein DAXX is a novel histone chaperone involved in the replication-independent deposition of H3. 3. Genes & development. 2010;24(12):1253–1265.

58. Goldberg AD, Banaszynski LA, Noh K-M, Lewis PW, Elsaesser SJ, Stadler S, Dewell S, Law M, Guo X, Li X, et al. Distinct factors control histone variant H3.3 localization at specific genomic regions. Cell. 2010;140(5):678–691.

59. Schwartzentruber J, Korshunov A, Liu X-Y, Jones DTW, Pfaff E, Jacob K, Sturm D, Fontebasso AM, Quang D-AK, Tönjes M. Driver mutations in histone H3. 3 and chromatin remodelling genes in paediatric glioblastoma. Nature. 2012;482(7384):226–231.

60. Chromatin R, Gallo M, Coutinho FJ, Vanner RJ, Bazett-jones DP, Lupien M, Dirks PB, Gallo M, Coutinho FJ, Vanner RJ, et al. MLL5 Orchestrates a Cancer Self-Renewal State by Repressing the Histone Variant H3 . 3 and Globally Article MLL5 Orchestrates a Cancer Self-Renewal State by Repressing the Histone Variant H3 . 3 and Globally Reorganizing Chromatin. Cancer Cell. 2015;28(6):715–729.

61. Park S, Choi E, Bae M, Kim S, Park JB, Yoo H, Choi JK, Kim Y, Lee S, Kim I. migration through intronic regulation. Nature Communications. 2016;7:1–14.

62. Banaszynski LA, Wen D, Dewell S, Whitcomb SJ, Lin M, Diaz N, Elsässer SJ, Chapgier A, Goldberg AD, Canaani E, et al. Hira-dependent histone H3.3 deposition facilitates PRC2 recruitment at developmental loci in ES cells. Cell. 2013;155(1):10.1016/j.cell.2013.08.061.

63. Faast R, Thonglairoam V, Schulz TC, Beall J, Wells JRE, Taylor H, Matthaei K, Rathjen PD, Tremethick DJ, Lyons I. Histone variant H2A. Z is required for early mammalian development. Current Biology. 2001;11(15):1183–1187.

64. Thatcher TH, Gorovsky MA. Phylogenetic analysis of the core histones H2A, H2B, H3, and H4. Nucleic acids research. 1994;22(2):174–9.

65. Jackson JD, Gorovsky MA. Histone H2A. Z has a conserved function that is distinct from that of the major H2A sequence variants. Nucleic Acids Research. 2000;28(19):3811–3816.

66. Guillemette B, Bataille AR, Gévry N, Adam M, Blanchette M, Robert F, Gaudreau L. Variant histone H2A. Z is globally localized to the promoters of inactive yeast genes and regulates nucleosome positioning. PLoS Biol. 2005;3(12):e384.

67. Xu Y, Ayrapetov MK, Xu C, Gursoy-Yuzugullu O, Hu Y, Price BD. Histone H2A. Z controls a critical chromatin remodeling step required for DNA double-strand break repair. Molecular cell. 2012;48(5):723–733.

68. Swaminathan J, Baxter EM, Corces VG. The role of histone H2Av variant replacement and histone H4 acetylation in the establishment of Drosophila heterochromatin. Genes & development. 2005;19(1):65–76.

69. Rangasamy D, Greaves I, Tremethick DJ. RNA interference demonstrates a novel role for H2A. Z in chromosome segregation. Nature structural & molecular biology. 2004;11(7):650–655.

70. Barski A, Cuddapah S, Cui K, Roh T-Y, Schones DE, Wang Z, Wei G, Chepelev I, Zhao K. High-resolution profiling of histone methylations in the human genome. Cell. 2007;129(4):823–837.

71. Kelly TK, Miranda TB, Liang G, Berman BP, Lin JC, Tanay A, Jones PA. H2A. Z maintenance during mitosis reveals nucleosome shifting on mitotically silenced genes. Molecular cell. 2010;39(6):901–911.

72. Jin C, Zang C, Wei G, Cui K, Peng W, Zhao K, Felsenfeld G. H3. 3/H2A. Z double variant–containing nucleosomes mark'nucleosome-free regions' of active promoters and other regulatory regions. Nature genetics. 2009;41(8):941–945.

73. Yang X, Noushmehr H, Han H, Andreu-Vieyra C, Liang G, Jones PA. Gene reactivation by 5-aza-2′-deoxycytidine–induced demethylation requires SRCAP–mediated H2A. Z insertion to establish nucleosome depleted regions. PLoS Genet. 2012;8(3):e1002604.

74. Zhang H, Roberts DN, Cairns BR. Genome-wide dynamics of Htz1, a histone H2A variant that poises repressed/basal promoters for activation through histone loss. Cell. 2005;123(2):219–231.

75. Meneghini MD, Wu M, Madhani HD. Conserved histone variant H2A. Z protects euchromatin from the ectopic spread of silent heterochromatin. Cell. 2003;112(5):725–736.

76. Conerly ML, Teves SS, Diolaiti D, Ulrich M, Eisenman RN, Henikoff S. Changes in H2A. Z occupancy and DNA methylation during B-cell lymphomagenesis. Genome research. 2010;20(10):1383–1390.

77. Hua S, Kallen CB, Dhar R, Baquero MT, Mason CE, Russell BA, Shah PK, Liu J, Khramtsov A, Tretiakova MS. Genomic analysis of estrogen cascade reveals histone variant H2A. Z associated with breast cancer progression. Molecular systems biology. 2008;4(1):188.

78. Svotelis A, Gévry N, Grondin G, Gaudreau L. H2A.Z overexpression promotes cellular proliferation of breast cancer cells. Cell cycle (Georgetown, Tex.). 2010;9(2):364–70.

79. Kim K, Punj V, Choi J, Heo K, Kim J-M, Laird PW, An W. Gene dysregulation by histone variant H2A.Z in bladder cancer. Epigenetics & Chromatin. 2013;6(1):34.

80. Valdés-Mora F, Song JZ, Statham AL, Strbenac D, Robinson MD, Nair SS, Patterson KI, Tremethick DJ, Stirzaker C, Clark SJ. Acetylation of H2A. Z is a key epigenetic modification associated with gene deregulation and epigenetic remodeling in cancer. Genome research. 2012;22(2):307–321.

81. Dryhurst D, McMullen B, Fazli L, Rennie PS, Ausió J. Histone H2A.Z prepares the prostate specific antigen (PSA) gene for androgen receptor-mediated transcription and is upregulated in a model of prostate cancer progression. Cancer Letters. 2012;315(1):38–47.

82. Lacroix M. Significance, detection and markers of disseminated breast cancer cells. Endocrine-related cancer. 2006;13(4):1033–1067.

83. Lupien M, Eeckhoute J, Meyer CA, Wang Q, Zhang Y, Li W, Carroll JS, Liu XS, Brown M. FoxA1 translates epigenetic signatures into enhancer-driven lineage-specific transcription. Cell. 2008;132(6):958–970.

84. Gévry N, Hardy S, Jacques P-E, Laflamme L, Svotelis A, Robert F, Gaudreau L. Histone H2A . Z is essential for estrogen receptor signaling. Genes & Development. 2009;23(13):1522–1533.

85. Rangasamy D. Histone variant H2A.Z can serve as a new target for breast cancer therapy. Current medicinal chemistry. 2010;17:3155–3161.

86. Fried VA. MacroH2A, a core histone containing a large nonhistone region. Science. 1992;257(5075):1398–1400.

87. Costanzi C, Pehrson JR. MACROH2A2, a new member of the MACROH2A core histone family. Journal of Biological Chemistry. 2001;276(24):21776–21784.

88. Talbert PB, Ahmad K, Almouzni G, Ausió J, Berger F, Bhalla PL, Bonner WM, Cande WZ, Chadwick BP, Chan SWL. A unified phylogeny-based nomenclature for histone variants. Epigenetics & chromatin. 2012;5(1):1.

89. Chakravarthy S, Gundimella SKY, Caron C, Perche P-Y, Pehrson JR, Khochbin S, Luger K.

Structural characterization of the histone variant macroH2A. Molecular and cellular biology. 2005;25(17):7616–7624.

90. Buschbeck M, Di Croce L. Approaching the molecular and physiological function of macroH2A variants. Epigenetics. 2010;5(2):118–123.

91. Chadwick BP, Willard HF. Cell cycle–dependent localization of macroH2A in chromatin of the inactive X chromosome. The Journal of cell biology. 2002;157(7):1113–1123.

92. Angelov D, Molla A, Perche P-Y, Hans F, Côté J, Khochbin S, Bouvet P, Dimitrov S. The histone variant macroH2A interferes with transcription factor binding and SWI/SNF nucleosome remodeling. Molecular cell. 2003;11(4):1033–1041.

93. Sporn JC, Kustatscher G, Hothorn T, Collado M, Serrano M, Muley T, Schnabel P, Ladurner AG. Histone macroH2A isoforms predict the risk of lung cancer recurrence. Oncogene. 2009;28(38):3423–3428.

94. Kapoor A, Goldberg MS, Cumberland LK, Ratnakumar K, Segura MF, Emanuel PO, Menendez S, Vardabasso C, LeRoy G, Vidal CI, et al. The histone variant macroH2A suppresses melanoma progression through regulation of CDK8. Nature. 2010;468(7327):1105–1109.

95. Li X, Kuang J, Shen Y, Majer MM, Nelson CC, Parsawar K, Heichman KA, Kuwada SK. The atypical histone macroH2A1. 2 interacts with HER-2 protein in cancer cells. Journal of Biological Chemistry. 2012;287(27):23171–23183.

96. Khare SP, Sharma A, Deodhar KK, Gupta S. Brief Communication Overexpression of histone variant H2A . 1 and cellular transformation are related in N-nitrosodiethylamine-induced sequential hepatocarcinogenesis. 2011:30–35.

97. Su X, Lucas DM, Zhang L, Xu H, Zabrouskov V, Davis ME, Knapp AR, Young DC, Payne PRO, Parthun MR, et al. Validation of an LC-MS based approach for profiling histones in chronic lymphocytic leukemia. Proteomics. 2009;9(5):1197–206.

98. Gasparian A V, Burkhart CA, Purmal AA, Brodsky L, Pal M, Saranadasa M, Bosykh DA, Commane M, Guryanova OA, Pal S, et al. Curaxins: Anticancer Compounds That Simultaneously Suppress NF-κB and Activate p53 by Targeting FACT. Science Translational Medicine. 2011;3(95):95ra74 LP-95ra74.

99. Koman IE, Commane M, Paszkiewicz G, Hoonjan B, Pal S, Safina A, Toshkov I, Purmal AA, Wang D, Liu S, et al. Targeting FACT Complex Suppresses Mammary Tumorigenesis in &lt;em&gt;Her2&lt;/em&gt;/&lt;em&gt;neu&lt;/em&gt; Transgenic Mice. Cancer Prevention Research. 2012;5(8):1025 LP-1035.

100. Garcia H, Miecznikowski JC, Safina A, Commane M, Ruusulehto A, Kilpinen S, Leach RW, Attwood K, Li Y, Degan S, et al. Facilitates Chromatin Transcription Complex Is an "Accelerator" of Tumor Transformation and Potential Marker and Target of Aggressive Cancers. Cell Reports. 2013;4(1):159–173.

101. Lin L, Piao J, Ma Y, Jin T, Quan C, Kong J, Li Y, Lin Z. Mechanisms Underlying Cancer Growth and Apoptosis by DEK Overexpression in Colorectal Cancer. PLOS ONE. 2014;9(10):e111260.

102. Lin D, Dong X, Wang K, Wyatt AW, Crea F, Xue H, Wang Y, Wu R, Bell RH, Haegert A, et al. Identification of DEK as a potential therapeutic target for neuroendocrine prostate cancer. Oncotarget. 2015;6(3):1806–1820.

103. Wise-Draper TM, Allen H V, Jones EE, Habash KB, Matsuo H, Wells SI. Apoptosis Inhibition by the Human DEK Oncoprotein Involves Interference with p53 Functions . Molecular and Cellular Biology. 2006;26(20):7506–7519.

104. Wise-Draper TM, Morreale RJ, Morris TA, Mintz-Cole RA, Hoskins EE, Balsitis SJ, Husseinzadeh N, Witte DP, Wikenheiser-Brokamp KA, Lambert PF, et al. DEK Proto-Oncogene Expression Interferes with the Normal Epithelial Differentiation Program. The American Journal of Pathology. 2009;174(1):71–81.

105. Wise-Draper TM, Mintz-Cole RA, Morris TA, Simpson DS, Wikenheiser-Brokamp KA, Currier MA, Cripe TP, Grosveld GC, Wells SI. Overexpression of the Cellular DEK Protein Promotes Epithelial Transformation &lt;em&gt;In vitro&lt;/em&gt; and &lt;em&gt;In vivo&lt;/em&gt; Cancer Research. 2009;69(5):1792 LP-1799.

106. Riveiro-Falkenbach E, Soengas MS. Control of Tumorigenesis and Chemoresistance by the DEK Oncogene. Clinical Cancer Research. 2010;16(11):2932 LP-2938.

107. Jiao Y, Shi C, Edil BH, de Wilde RF, Klimstra DS, Maitra A, Schulick RD, Tang LH, Wolfgang CL, Choti MA, et al. &lt;em&gt;DAXX&lt;/em&gt;/&lt;em&gt;ATRX&lt;/em&gt;, &lt;em&gt;MEN1&lt;/em&gt;, and mTOR Pathway Genes Are Frequently Altered in Pancreatic Neuroendocrine Tumors. Science. 2011;331(6021):1199 LP-1203.

108. Schwartzentruber J, Korshunov A, Liu X-Y, Jones DTW, Pfaff E, Jacob K, Sturm D, Fontebasso AM, Quang D-AK, Tonjes M, et al. Driver mutations in histone H3.3 and chromatin remodelling genes in paediatric glioblastoma. Nature. 2012;482(7384):226–231.

109. Shogren-Knaak M, Ishii H, Sun J-M, Pazin MJ, Davie JR, Peterson CL. Histone H4-K16 Acetylation Controls Chromatin Structure and Protein Interactions. Science. 2006;311(5762):844 LP-847.

110. Shogren-Knaak M, Peterson CL. Switching on Chromatin: Mechanistic Role of Histone H4-K16 Acetylation. Cell Cycle. 2006;5(13):1361–1365.

111. Nguyen CT, Weisenberger DJ, Velicescu M, Gonzales FA, Lin JCY, Liang G, Jones PA. Histone H3-Lysine 9 Methylation Is Associated with Aberrant Gene Silencing in Cancer Cells and Is Rapidly Reversed by 5-Aza-2′-deoxycytidine. Cancer Research. 2002;62(22):6456 LP-6461.

112. Valk-Lingbeek ME, Bruggeman SWM, van Lohuizen M. Stem Cells and Cancer: The Polycomb Connection. Cell. 2004;118(4):409–418.

113. Chadee DN, Hendzel MJ, Tylipski CP, Allis CD, Bazett-Jones DP, Wright JA, Davie JR. Increased Ser-10 Phosphorylation of Histone H3 in Mitogen-stimulated and Oncogene-transformed Mouse Fibroblasts. Journal of Biological Chemistry . 1999;274(35):24914–24920.

114. Kim H-G, Lee KW, Cho Y-Y, Kang NJ, Oh S-M, Bode AM, Dong Z. Mitogen- and Stress-Activated Kinase 1 Histone H3 Phosphorylation is Crucial for Cell Transformation. Cancer research. 2008;68(7):2538–2547.

115. Leon SA, Shapiro B, Sklaroff DM, Yaros MJ. Free DNA in the Serum of Cancer Patients and the Effect of Therapy. Cancer Research. 1977;37(3):646 LP-650.

116. GEZER U, MERT U, ÖZGÜR E, YÖRÜKER EE, HOLDENRIEDER S, DALAY N. Correlation of histone methyl marks with circulating nucleosomes in blood plasma of cancer patients. Oncology Letters. 2012;3(5):1095–1098.

117. Deligezer U, Akisik EE, Erten N, Dalay N. Sequence-Specific Histone Methylation Is Detectable on Circulating Nucleosomes in Plasma. Clinical Chemistry . 2008;54(7):1125–1131.

118. Gezer U, Üstek D, Yörüker EE, Cakiris A, Abaci N, Leszinski G, Dalay N, Holdenrieder S. Characterization of H3K9me3- and H4K20me3-associated circulating nucleosomal DNA by high-throughput sequencing in colorectal cancer. Tumor Biology. 2013;34(1):329–336.

119. Fraga MF, Ballestar E, Villar-Garea A, Boix-Chornet M, Espada J, Schotta G, Bonaldi T, Haydon C, Ropero S, Petrie K, et al. Loss of acetylation at Lys16 and trimethylation at Lys20 of

histone H4 is a common hallmark of human cancer. Nat Genet. 2005;37(4):391–400.

120. Seligson DB, Horvath S, Shi T, Yu H, Tze S, Grunstein M, Kurdistani SK. Global histone modification patterns predict risk of prostate cancer recurrence. Nature. 2005;435(7046):1262–1266.

121. Seligson DB, Horvath S, McBrian MA, Mah V, Yu H, Tze S, Wang Q, Chia D, Goodglick L, Kurdistani SK. Global Levels of Histone Modifications Predict Prognosis in Different Cancers. The American Journal of Pathology. 2009;174(5):1619–1628.

122. Elsheikh SE, Green AR, Rakha EA, Powe DG, Ahmed RA, Collins HM, Soria D, Garibaldi JM, Paish CE, Ammar AA, et al. Global Histone Modifications in Breast Cancer Correlate with Tumor Phenotypes, Prognostic Factors, and Patient Outcome. Cancer Research. 2009;69(9):3802–3809.

123. Ellinger J, Kahl P, Mertens C, Rogenhofer S, Hauser S, Hartmann W, Bastian PJ, Büttner R, Müller SC, von Ruecker A. Prognostic relevance of global histone H3 lysine 4 (H3K4) methylation in renal cell carcinoma. International Journal of Cancer. 2010;127(10):2360–2366.

124. Manuyakorn A, Paulus R, Farrell J, Dawson NA, Tze S, Cheung-Lau G, Hines OJ, Reber H, Seligson DB, Horvath S, et al. Cellular Histone Modification Patterns Predict Prognosis and Treatment Response in Resectable Pancreatic Adenocarcinoma: Results From RTOG 9704. Journal of Clinical Oncology. 2010;28(8):1358–1365.

125. Barlési F, Giaccone G, Gallegos-Ruiz MI, Loundou A, Span SW, Lefesvre P, Kruyt FAE, Rodriguez JA. Global Histone Modifications Predict Prognosis of Resected Non–Small-Cell Lung Cancer. Journal of Clinical Oncology. 2007;25(28):4358–4364.

126. Bai X, Wu L, Liang T, Liu Z, Li J, Li D, Xie H, Yin S, Yu J, Lin Q, et al. Overexpression of myocyte enhancer factor 2 and histone hyperacetylation in hepatocellular carcinoma. Journal of Cancer Research and Clinical Oncology. 2008;134(1):83–91.

127. Park YS, Jin MY, Kim YJ, Yook JH, Kim BS, Jang SJ. The Global Histone Modification Pattern Correlates with Cancer Recurrence and Overall Survival in Gastric Adenocarcinoma. Annals of Surgical Oncology. 2008;15(7):1968.

128. Tzao C, Tung H-J, Jin J-S, Sun G-H, Hsu H-S, Chen B-H, Yu C-P, Lee S-C. Prognostic significance of global histone modifications in resected squamous cell carcinoma of the esophagus. Mod Pathol. 2008;22(2):252–260.

129. Wei Y, Xia W, Zhang Z, Liu J, Wang H, Adsay N V, Albarracin C, Yu D, Abbruzzese JL, Mills GB. Loss of trimethylation at lysine 27 of histone H3 is a predictor of poor outcome in breast, ovarian, and pancreatic cancers. Mol Carcinog. 2008;47.

130. Yu J, Yu J, Rhodes DR, Tomlins SA, Cao X, Chen G, Mehra R, Wang X, Ghosh D, Shah RB. A polycomb repression signature in metastatic prostate cancer predicts cancer outcome. Cancer Res. 2007;67.

131. Thurn KT, Thomas S, Moore A, Munster PN. Rational therapeutic combinations with histone deacetylase inhibitors for the treatment of cancer. Future oncology (London, England). 2011;7(2):263–283.

132. Wagner JM, Hackanson B, Lübbert M, Jung M. Histone deacetylase (HDAC) inhibitors in recent clinical trials for cancer therapy. Clinical Epigenetics. 2010;1(3–4):117–136.

133. Reddy D, Bhattacharya S, Gupta S. Histone Chaperones : Functions beyond Nucleosome Deposition. 2014;(May):546–556.

134. Ishimi Y, Kikuchi a. Identification and molecular cloning of yeast homolog of nucleosome assembly protein I which facilitates nucleosome assembly in vitro. Journal of Biological Chemistry. 1991;266(11):7025–7029.

135. McQuibban GA, Commisso-Cappelli CN, Lewis PN. Assembly, Remodeling, and Histone

Binding Capabilities of Yeast Nucleosome Assembly Protein 1. Journal of Biological Chemistry . 1998;273(11):6582–6590.

136. Noda M, Uchiyama S, McKay AR, Morimoto A, Misawa S, Yoshida A, Shimahara H, Takinowaki H, Nakamura S, Kobayashi Y, et al. Assembly states of the nucleosome assembly protein 1 (NAP-1) revealed by sedimentation velocity and non-denaturing MS. The Biochemical journal. 2011;436(1):101–12.

137. Ito T, Bulger M, Kobayashi R, Kadonaga JT. Drosophila NAP-1 is a core histone chaperone that functions in ATP-facilitated assembly of regularly spaced nucleosomal arrays. Molecular and Cellular Biology. 1996;16(6):3112–3124.

138. Mosammaparast N, Ewart CS, Pemberton LF. A role for nucleosome assembly protein 1 in the nuclear transport of histones H2A and H2B. EMBO Journal. 2002;21(23):6527–6538.

139. Zhang Q, Giebler HA, Isaacson MK, Nyborg JK. Eviction of linker histone H1 by NAP-family histone chaperones enhances activated transcription. Epigenetics & Chromatin. 2015;8(1):30.

140. Okuwaki M, Kato K, Shimahara H, Tate S, Nagata K. Assembly and disassembly of nucleosome core particles containing histone variants by human nucleosome assembly protein I. Molecular and cellular biology. 2005;25(23):10639–10651.

141. McBryant SJ, Park YJ, Abernathy SM, Laybourn PJ, Nyborg JK, Luger K. Preferential Binding of the Histone (H3-H4)2 Tetramer by NAP1 Is Mediated by the Amino-terminal Histone Tails. Journal of Biological Chemistry. 2003;278(45):44574–44583.

142. Tóth KF, Mazurkiewicz J, Rippe K. Association states of nucleosome assembly protein 1 and its complexes with histones. The Journal of biological chemistry. 2005;280(16):15690–9.

143. Zlatanova J, Seebart C, Tomschik M. Nap1: taking a closer look at a juggler protein of extraordinary skills. The FASEB journal : official publication of the Federation of American Societies for Experimental Biology. 2007;21(7):1294–1310.

144. Andrews AJ, Downing G, Brown K, Park Y-J, Luger K. A Thermodynamic Model for Nap1-Histone Interactions. The Journal of Biological Chemistry. 2008;283(47):32412–32418.

145. Newman ER, Kneale GG, Ravelli RBG, Karuppasamy M, Nejadasl FK, Taylor IA, McGeehan JE. Large multimeric assemblies of nucleosome assembly protein and histones revealed by small-angle x-ray scattering and electron microscopy. Journal of Biological Chemistry. 2012;287(32):26657–26665.

146. Park Y-J, Luger K. The structure of nucleosome assembly protein 1. Proceedings of the National Academy of Sciences of the United States of America. 2006;103(5):1248–1253.

147. McBryant SJ, Peersen OB. Self-association of the yeast nucleosome assembly protein 1. Biochemistry. 2004;43(32):10592–10599.

148. Aguilar-gurrieri C. Structural studies of nucleosome assembly. 2013:1–153.

149. Calvert MEK, Keck KM, Ptak C, Shabanowitz J, Hunt DF, Pemberton LF, Iol MOLCELLB. Phosphorylation by Casein Kinase 2 Regulates Nap1 Localization and Function □. 2008;28(4):1313–1325.

150. Engebrecht J. Minipreps of Plasmid DNA. Current Protocols in Molecular Biology. 1990;1(1991):1.6.1-1.6.10.

151. Sambrook J, Fritsch EF, Maniatis T. Molecular cloning. Cold spring harbor laboratory press New York; 1989.

152. Carey MF, Peterson CL, Smale ST. Dignam and Roeder Nuclear Extract Preparation. Cold Spring Harbor Protocols . 2009;2009(12):pdb.prot5330.

153. Pramod KS, Bharat K, Sanjay G. Mass spectrometry-compatible silver staining of histones resolved on acetic acid-urea-Triton PAGE. Proteomics. 2009;9(9):2589–2592.

154. Bhattacharya S, Gupta S. A Simple Method to Produce Sub-Nucleosome Complexes of High Purity In Vitro. 2016;(March):133–141.

155. Mann CJ, Matthews CR. Structure and Stability of an Early Folding Intermediate of Escherichia coli trp Aporepressor Measured by Far-UV Stopped-Flow Circular Dichroism and 8-Anilino- 1 -naphthalene Sulfonate Binding ? 1993:5282–5290.

156. Pace CN, Scholtz JM. Measuring the conformational stability of a protein. Protein structure: A practical approach. 1997;2:299–321.

157. Canonical sampling through velocity rescaling. The Journal of Chemical Physics. 2007;126(1):14101.

158. Molecular dynamics with coupling to an external bath. The Journal of Chemical Physics. 1984;81(8):3684–3690.

159. Hess B, Bekker H, Berendsen HJC, Fraaije JGEM. LINCS: A linear constraint solver for molecular simulations. Journal of Computational Chemistry. 1997;18(12):1463–1472.

160. Polymorphic transitions in single crystals: A new molecular dynamics method. Journal of Applied Physics. 1981;52(12):7182–7190.

161. Paissoni C, Spiliotopoulos D, Musco G, Spitaleri A. GMXPBSA 2.1: A GROMACS tool to perform MM/PBSA and computational alanine scanning. Computer Physics Communications. 2015;186:105–107.

162. Cheung KLY, Huen J, Kakihara Y, Houry WA, Ortega J. Alternative oligomeric states of the yeast Rvb1/Rvb2 complex induced by histidine tags. Journal of molecular biology. 2010;404(3):478–492.

163. Li M, Strand D, Krehan A, Pyerin W, Heid H, Neumann B, Mechler BM. Casein kinase 2 binds and phosphorylates the nucleosome assembly protein-1 (NAP1) in Drosophila melanogaster1. Journal of Molecular Biology. 1999;293(5):1067–1084.

164. Park YJ, McBryant SJ, Luger K. A ??-Hairpin Comprising the Nuclear Localization Sequence Sustains the Self-associated States of Nucleosome Assembly Protein 1. Journal of Molecular Biology. 2008;375(4):1076–1085.

165. Rodriguez P, Pelletier J, Price GB. NAP-2 : Histone Chaperone Function and Phosphorylation State Through the Cell Cycle. 2000.

166. Dutta S, Akey I V, Dingwall C, Hartman KL, Laue T, Nolte RT, Head JF, Akey CW. The Crystal Structure of Nucleoplasmin-Core: Implications for Histone Binding and Nucleosome Assembly. Molecular Cell. 2001;8(4):841–853.

167. Muto S, Senda M, Akai Y, Sato L, Suzuki T, Nagai R, Senda T, Horikoshi M. Relationship between the structure of SET/TAF-Iβ/INHAT and its histone chaperone activity. Proceedings of the National Academy of Sciences . 2007;104(11):4285–4290.

168. Daganzo SM, Erzberger JP, Lam WM, Skordalakes E, Zhang R, Franco AA, Brill SJ, Adams PD, Berger JM, Kaufman PD. Structure and Function of the Conserved Core of Histone Deposition Protein Asf1. Current Biology. 2003;13(24):2148–2158.

169. Mousson F, Lautrette A, Thuret J-Y, Agez M, Courbeyrette R, Amigues B, Becker E, Neumann J-M, Guerois R, Mann C, et al. Structural basis for the interaction of Asf1 with histone H3 and its functional implications. Proceedings of the National Academy of Sciences of the United States of America. 2005;102(17):5975–5980.

170. Kaufman PD, Kobayashi R, Kessler N, Stillman B. The p150 and p60 subunits of chromatin assemblyfactor I: A molecular link between newly synthesized histories and DNA replication. Cell. 1995;81(7):1105–1114.

171. DeSilva H, Lee K, Osley MA. Functional dissection of yeast Hir1p, a WD repeat-containing transcriptional corepressor. Genetics. 1998;148(2):657–667.

172. Kamakaka RT, Biggins S. Histone variants: deviants? Genes & Development . 2005;19(3):295–316.

173. Jin C, Zang C, Wei G, Cui K, Peng W, Zhao K, Felsenfeld G. H3.3/H2A.Z double variant-containing nucleosomes mark "nucleosome-free regions" of active promoters and other regulatory regions in the human genome. Nature genetics. 2009;41(8):941–945.

174. Studies B, Thakar A, Gupta P, Ishibashi T, Finn R, Silva-moreno B, Uchiyama S, Fukui K, Tomschik M, Ausio J, et al. H2A . Z and H3 . 3 Histone Variants Affect Nucleosome Structure : Biochemical and. 2009:10852–10857.

175. Jin C, Felsenfeld G. Nucleosome stability mediated by histone variants H3.3 and H2A.Z. Genes & Development. 2007;21(12):1519–1529.

176. Henikoff S. Labile H3.3+H2A.Z nucleosomes mark "nucleosome-free regions." Nat Genet. 2009;41(8):865–866.

177. Rogakou EP, Pilch DR, Orr AH, Ivanova VS, Bonner WM. DNA Double-stranded Breaks Induce Histone H2AX Phosphorylation on Serine 139. Journal of Biological Chemistry . 1998;273(10):5858–5868.

178. Bao Y. Chromatin response to DNA double-strand break damage. Epigenomics. 2011;3(3):307–321.

179. Fernandez-Capetillo O, Chen H-T, Celeste A, Ward I, Romanienko PJ, Morales JC, Naka K, Xia Z, Camerini-Otero RD, Motoyama N, et al. DNA damage-induced G2-M checkpoint activation by histone H2AX and 53BP1. Nat Cell Biol. 2002;4(12):993–997.

180. Hiom K. Coping with DNA double strand breaks. DNA Repair. 2010;9(12):1256–1263.

181. Zaret K. Micrococcal nuclease analysis of chromatin structure. Current protocols in molecular biology. 2005.

182. Shechter D, Dormann HL, Allis CD, Hake SB. Extraction, purification and analysis of histones. Nat. Protocols. 2007;2(6):1445–1457.

183. Kruger NJ. The Bradford method for protein quantitation. Basic protein and peptide protocols. 1994:9–15.

184. Ryan CA, Annunziato AT. Separation of histone variants and post-translationally modified isoforms by triton/acetic acid/urea polyacrylamide gel electrophoresis. Current Protocols in Molecular Biology. 2001:21–22.

185. Imai BS, Mische SM. Mass spectrometric identification of proteins from silver-stained polyacrylamide gel: a method for the removal of silver ions to enhance sensitivity. Electrophoresis. 1999;20:601–605.

186. Jiménez CR, Huang L, Qiu Y, Burlingame AL. In-Gel Digestion of Proteins for MALDI-MS Fingerprint Mapping. Current protocols in protein science. 2001:14–16.

187. Prioleau MN, Nony P, Simpson M, Felsenfeld G. An insulator element and condensed chromatin region separate the chicken beta-globin locus from an independently regulated erythroid-specific folate receptor gene. The EMBO Journal. 1999;18(14):4035–4048.

188. Haile JM. Molecular dynamics simulation. Wiley, New York; 1992.

189. Hess B, Kutzner C, Van Der Spoel D, Lindahl E. GROMACS 4: algorithms for highly efficient, load-balanced, and scalable molecular simulation. Journal of chemical theory and computation. 2008;4(3):435–447.

190. van Meerloo J, Kaspers GJL, Cloos J. Cell sensitivity assays: the MTT assay. Cancer cell culture: methods and protocols. 2011:237–245.

191. Franken NAP, Rodermond HM, Stap J, Haveman J, Van Bree C. Clonogenic assay of cells in vitro. Nature protocols. 2006;1(5):2315–2319.

192. Osakabe A, Tachiwana H, Takaku M, Hori T, Obuse C, Kimura H, Fukagawa T, Kurumizaka H. Vertebrate Spt2 is a novel nucleolar histone chaperone that assists in ribosomal DNA transcription. Journal of Cell Science. 2013;126(6):1323 LP-1332.

193. Holecek BU, Kerler R, Rabes HM, Rat N, Cell L. Chromosomal Analysis of a Diethylnitrosamine-induced Tumorigenic and a Nontumorigenic Rat Liver Cell Line Chromosomal Analysis of a Diethylnitrosamine-induced Tumorigenic and a. 1989:3024–3028.

194. Heintz N. The regulation of histone gene expression during the cell cycle. 1991;1088:327–339.

195. Rattray AMJ. The control of histone gene expression. 2012;40:880–885.

196. Sarma K, Reinberg D. Histone variants meet their match. Nat Rev Mol Cell Biol. 2005;6(2):139–149.

197. Ahmad K, Henikoff S. The histone variant H3.3 marks active chromatin by replication-independent nucleosome assembly. Molecular Cell. 2002;9(6):1191–1200.

198. Weber CM, Henikoff S. Histone variants : dynamic punctuation in transcription. 2014:672–682.

199. Li Y-J, Fu X-H, Liu D-P, Liang C-C. Opening the chromatin for transcription. The International Journal of Biochemistry & Cell Biology. 2004;36(8):1411–1423.

200. Szenker E, Ray-Gallet D, Almouzni G. The double face of the histone variant H3.3. Cell Research. 2011;21(3):421–434.

201. Latreille D, Bluy L, Benkirane M, Kiernan RE. Identification of histone 3 variant 2 interacting factors. Nucleic Acids Research. 2014;42:3542–3550.

202. Tsujiuchi T, Sugata E, Masaoka T, Onishi M, Fujii H, Shimizu K, Honoki K. Expression and DNA methylation patterns of Tslc1 and Dal-1 genes in hepatocellular carcinomas induced by N-nitrosodiethylamine in rats. Cancer science. 2007;98(7):943–8.

203. Manoharan H, Babcock K, Pitot HC. Changes in the DNA methylation profile of the rat H19 gene upstream region during development and transgenic hepatocarcinogenesis and its role in the imprinted transcriptional regulation of the H19 gene. Molecular Carcinogenesis. 2004;41(1):1–16.

204. Baylin SB, Jones PA. Epigenetic Determinants of Cancer. 2016.

205. Henikoff S. Nucleosome destabilization in the epigenetic regulation of gene expression. 2008;9(january).

206. Daveau R, Hiron M, Scotte M, Franc A, Daveau M, Salier J. Global gene repression in hepatocellular carcinoma and fetal liver , and suppression of dudulin-2 mRNA as a possible marker for the cirrhosis-to-tumor transition. 2005;42:860–869.

207. Chen X, Cheung ST, So S, Fan T, Barry C, Higgins J, Lai K, Ji J, Dudoit S, Ng IOL, et al. Gene Expression Patterns in Human Liver Cancers. 2002;13(June):1929–1939.

208. Lin C-J, Conti M, Ramalho-Santos M. Histone variant H3.3 maintains a decondensed chromatin

state essential for mouse preimplantation development. Development (Cambridge, England). 2013;140(17):3624–3634.

209. Yuen BTK, Bush KM, Barrilleaux BL, Cotterman R. Histone H3 . 3 regulates dynamic chromatin states during spermatogenesis. 2014:3483–3494.

210. Wen D, Banaszynski LA, Rosenwaks Z, Allis CD. nuclear transfer embryos. 2014;1034(October 2016).

211. Loppin B, Bonnefoy E, Anselme C, Laurencon A, Karr TL, Couble P. The histone H3.3 chaperone HIRA is essential for chromatin assembly in the male pronucleus. Nature. 2005;437(7063):1386–1390.

212. Lu C, Jain SU, Hoelper D, Bechet D, Molden RC, Ran L, Murphy D, Venneti S, Hameed M, Pawel BR, et al. Histone H3K36 mutations promote sarcomagenesis through altered histone methylation landscape. 2016;(April).

213. Kapoor A, Goldberg MS, Cumberland LK, Ratnakumar K, Segura MF, Emanuel PO, Menendez S, Vardabasso C, Leroy G, Vidal CI, et al. melanoma progression through regulation of CDK8. Nature. 2010;468(7327):1105–1109.

214. Luk E, Vu N, Patteson K, Mizuguchi G, Wu W, Ranjan A, Backus J, Sen S, Lewis M, Bai Y, et al. Article Chz1 , a Nuclear Chaperone for Histone H2AZ. 2007:357–368.

215. Hildebrand EM, Biggins S. Regulation of Budding Yeast CENP-A levels Prevents Misincorporation at Promoter Nucleosomes and Transcriptional Defects. PLOS Genetics. 2016;12(3):e1005930.

216. Staibano S, Mignogna C, Lo Muzio L, Mascolo M, Salvatore G, Di Benedetto M, Califano L, Rubini C, De Rosa G. Chromatin assembly factor-1 (CAF-1)-mediated regulation of cell proliferation and DNA repair: a link with the biological behaviour of squamous cell carcinoma of the tongue? Histopathology. 2007;50(7):911–919.

217. Staibano S, Mascolo M, Mancini FP, Kisslinger A, Salvatore G, Di Benedetto M, Chieffi P, Altieri V, Prezioso D, Ilardi G, et al. Overexpression of chromatin assembly factor-1 (CAF-1) p60 is predictive of adverse behaviour of prostatic cancer. Histopathology. 2009;54(5):580–589.

218. Wang Y. Chromatin assembly factor 1 , subunit A ( P150 ) facilitates cell proliferation in human hepatocellular carcinoma. 2016:4023–4035.

219. Fullgrabe J, Kavanagh E, Joseph B. Histone onco-modifications. Oncogene. 2011;30(31):3391–3403.

220. Holdenrieder S, Nagel D, Schalhorn A, Heinemann V, Wilkowski R, Von Pawel J, Raith H, Feldmann K, Kremer AE, Müller S, et al. Clinical Relevance of Circulating Nucleosomes in Cancer. Annals of the New York Academy of Sciences. 2008;1137(1):180–189.

221. Karachaliou N, Mayo-de-las-Casas C, Molina-Vila MA, Rosell R. Real-time liquid biopsies become a reality in cancer treatment. Annals of Translational Medicine. 2015;3(3):36.

222. Chen R, Kang R, Fan X-G, Tang D. Release and activity of histone in diseases. Cell Death Dis. 2014;5:e1370.

223. STROUN M, MAURICE P, VASIOUKHIN V, LYAUTEY J, LEDERREY C, LEFORT F, ROSSIER A, CHEN XUQI, ANKER P. The Origin and Mechanism of Circulating DNA. Annals of the New York Academy of Sciences. 2000;906(1):161–168.

224. Holdenrieder S, Stieber P, Bodenmüller H, Busch M, Fertig G, Fürst H, Schalhorn A, Schmeller N, Untch M, Seidel D. Nucleosomes in serum of patients with benign and malignant diseases. International Journal of Cancer. 2001;95(2):114–120.

225. Shapiro B, Chakrabarty M, Cohn EM, Leon SA. Determination of circulating DNA levels in patients with benign or malignant gastrointestinal disease. Cancer. 1983;51(11):2116–2120.

226. HOLDENRIEDER S, DHARUMAN Y, STANDOP J, TRIMPOP N, HERZOG M, HETTWER K, SIMON K, UHLIG S, MICALLEF J. Novel Serum Nucleosomics Biomarkers for the Detection of Colorectal Cancer. Anticancer Research . 2014;34(5):2357–2362.

227. LESZINSKI G, GEZER U, SIEGELE B, STOETZER O, HOLDENRIEDER S. Relevance of Histone Marks H3K9me3 and H4K20me3 in Cancer. Anticancer Research . 2012;32(5):2199–2205.

228. Healey MA, Hu R, Beck AH, Collins LC, Schnitt SJ, Tamimi RM, Hazra A. Association of H3K9me3 and H3K27me3 repressive histone marks with breast cancer subtypes in the Nurses' Health Study. Breast Cancer Research and Treatment. 2014;147(3):639–651.

229. Khan SA, Amnekar R, Khade B, Barreto SG, Ramadwar M, Shrikhande S V, Gupta S. of histone H3 serine 10 phosphorylation defines distance-dependent prognostic value of negative resection margin in gastric cancer. Clinical Epigenetics. 2016:1–16.

230. Wang L, Zou X, Berger AD, Twiss C, Peng Y, Li Y, Chiu J, Guo H, Satagopan J, Wilton A, et al. Increased expression of histone deacetylaces ( HDACs ) and inhibition of prostate cancer growth and invasion by HDAC inhibitor SAHA. 2009:62–71.

231. Cohen I, Schneider R. Histone Modifiers in Cancer : Friends or Foes ? 2011:631–647.

232. Holdenrieder S, Stieber P, von Pawel J, Raith H, Nagel D, Feldmann K, Seidel D. Circulating Nucleosomes Predict the Response to Chemotherapy in Patients with Advanced Non–Small Cell Lung Cancer. American Association for Cancer Research. 2004;10(18):5981–5987.

233. HOLDENRIEDER S, STIEBER P, BODENMÜLLER H, BUSCH M, VON PAWEL J, SCHALHORN A, NAGEL D, SEIDEL D. Circulating Nucleosomes in Serum. Annals of the New York Academy of Sciences. 2001;945(1):93–102.

234. Khan SA, Reddy D, Gupta S. Global histone post-translational modifications and cancer: Biomarkers for diagnosis, prognosis and treatment? World Journal of Biological Chemistry. 2015;6(4):333–345.

235. Rigby L, Muscat A, Ashley D, Algar E. Methods for the analysis of histone H3 and H4 acetylation in blood. Epigenetics. 2012;7(8):875–882.

236. Glozak MA, Seto E. Histone deacetylases and cancer. Oncogene. 26(37):5420–5432.

237. Xiaoyun, Liu; Valentine, Stephen J.; Plasencia MD. Mapping the Human Plasma Proteome by SCX-LC-IMS-MS. J Am Soc Mass Spectrom. 2007;18(7):1249–1264.

238. Sennels L, Salek M, Lomas L, Boschetti E, Righetti PG, Rappsilber J. Proteomic analysis of human blood serum using peptide library beads. Journal of Proteome Research. 2007;6(10):4055–4062.

239. Qiu T, Zhou L, Zhu W, Wang T, Wang J, Shu Y, Liu P. Effects of treatment with histone deacetylase inhibitors in solid tumors: a review based on 30 clinical trials. Future Oncology. 2013;9(2):255–269.

240. Gryder BE, Sodji QH, Oyelere AK. Targeted cancer therapy: giving histone deacetylase inhibitors all they need to succeed. Future Medicinal Chemistry. 2012;4(4):505–524.

241. Vardabasso C, Gaspar-maia A, Hasson D, Hernando E, Hake SB, Bernstein E, Vardabasso C, Gaspar-maia A, Hasson D, Pu S. Histone Variant H2A . Z . 2 Mediates Proliferation. 2015:75–88.

242. Henikoff S, Henikoff JG, Sakai A, Loeb GB, Ahmad K. Genome-wide profiling of salt fractions maps physical properties of chromatin. Genome Research. 2009;19(3):460–469.

243. Siegel TN, Hekstra DR, Kemp LE, Figueiredo LM, Lowell JE, Fenyo D, Wang X, Dewell S, Cross GAM. Four histone variants mark the boundaries of polycistronic transcription units in Trypanosoma brucei. Genes & Development. 2009;23(9):1063–1076.

244. Wu Z, Cui F, Yu F, Peng X, Jiang T, Chen D, Lu S, Tang H, Peng Z. Up-regulation of CHAF1A, a poor prognostic factor, facilitates cell proliferation of colon cancer. Biochemical and biophysical research communications. 2014;449(2):208–15.

245. Barbieri E, De Preter K, Capasso M, Chen Z, Hsu DM, Tonini GP, Lefever S, Hicks J, Versteeg R, Pession A, et al. Histone Chaperone CHAF1A Inhibits Differentiation and Promotes Aggressive Neuroblastoma. Cancer Research. 2014;74(3):765–774.

246. Cook AJL, Quivy J, Ge A. The HP1 − p150 / CAF-1 interaction is required for pericentric heterochromatin replication and S-phase progression in mouse cells. 2008;15(9):972–979.

247. Ge M. CAF-1 Is Essential for Heterochromatin Organization in Pluripotent Embryonic Cells. 2006;2(11).

248. Cheloufi S, Elling U, Hopfgartner B, Jung YL, Murn J, Ninova M, Hubmann M, Badeaux AI, Ang CE, Tenen D, et al. The histone chaperone CAF-1 safeguards somatic cell identity. Nature. 2015;528(7581):218–224.

249. Hatanaka Y, Inoue K, Oikawa M, Kamimura S, Ogonuki N, Kodama EN. Histone chaperone CAF-1 mediates repressive histone modifications to protect preimplantation mouse embryos from endogenous retrotransposons. 2015;112(47):14641–14646.

250. Chen T-C, Hsieh L-L, Ng K-F, Jeng L-B, Chen M-F. Absence of APC gene mutation in the mutation cluster region in hepatocellular carcinoma. Cancer Letters. 1998;134(1):23–28.

251. Boige V, Laurent-Puig P, Fouchet P, Fléjou JF, Monges G, Bedossa P, Bioulac-Sage P, Capron F, Schmitz A, Olschwang S, et al. Concerted Nonsyntenic Allelic Losses in Hyperploid Hepatocellular Carcinoma as Determined by a High-Resolution Allelotype. Cancer Research. 1997;57(10):1986 LP-1990.

252. Schell MJ, Yang M, Teer JK, Lo FY, Madan A, Coppola D, Monteiro ANA, Nebozhyn M V, Yue B, Loboda A, et al. A multigene mutation classification of 468 colorectal cancers reveals a prognostic role for APC. Nature Communications. 2016;7:11743.

253. Chen J, Röcken C, Lofton-Day C, Schulz H-U, Müller O, Kutzner N, Malfertheiner P, Ebert MPA. Molecular analysis of APC promoter methylation and protein expression in colorectal cancer metastasis . Carcinogenesis. 2005;26(1):37–43.

254. Yang B, Guo M, Herman JG, Clark DP. Aberrant Promoter Methylation Profiles of Tumor Suppressor Genes in Hepatocellular Carcinoma. The American Journal of Pathology. 2003;163(3):1101–1107.

255. Csepregi A, Röcken C, Hoffmann J, Gu P, Saliger S, Müller O, Schneider-Stock R, Kutzner N, Roessner A, Malfertheiner P, et al. APC promoter methylation and protein expression in hepatocellular carcinoma. Journal of Cancer Research and Clinical Oncology. 2008;134(5):579–589.

256. Roman-Gomez J, Jimenez-Velasco A, Agirre X, Castillejo JA, Navarro G, Garate L, Jose-Eneriz ES, Cordeu L, Barrios M, Prosper F, et al. Promoter hypermethylation and global hypomethylation are independent epigenetic events in lymphoid leukemogenesis with opposing effects on clinical outcome. Leukemia. 2006;20(8):1445–1447.

257. CHO YHEE, YAZICI H, WU H-C, TERRY MB, GONZALEZ K, QU M, DALAY N, SANTELLA RM. Aberrant Promoter Hypermethylation and Genomic Hypomethylation in Tumor, Adjacent Normal Tissues and Blood from Breast Cancer Patients. Anticancer research. 2010;30(7):2489–2496.

258. Daskalos A, Nikolaidis G, Xinarianos G, Savvari P, Cassidy A, Zakopoulou R, Kotsinas A, Gorgoulis V, Field JK, Liloglou T. Hypomethylation of retrotransposable elements correlates with genomic instability in non-small cell lung cancer. International Journal of Cancer. 2009;124(1):81–87.

259. Zhang P, Guo Z, Wu Y, Hu R, Du J, He X, Jiao X, Zhu X. Histone Deacetylase Inhibitors Inhibit the Proliferation of Gallbladder Carcinoma Cells by Suppressing AKT/mTOR Signaling. PLOS ONE. 2015;10(8):e0136193.

260. Sakajiri S, Kumagai T, Kawamata N, Saitoh T, Said JW, Koeffler HP. Histone deacetylase inhibitors profoundly decrease proliferation of human lymphoid cancer cell lines. Experimental Hematology. 2005;33(1):53–61.

261. Su C, Tzeng T, Cheng C, Hsu M. An H2A histone isotype regulates estrogen receptor target genes by mediating enhancer-promoter- 3 0 -UTR interactions in breast cancer cells. 2013;(155):1–16.

# *Appendix*

# *Annexure I – Supplementary Figures*

## *Figure S1*
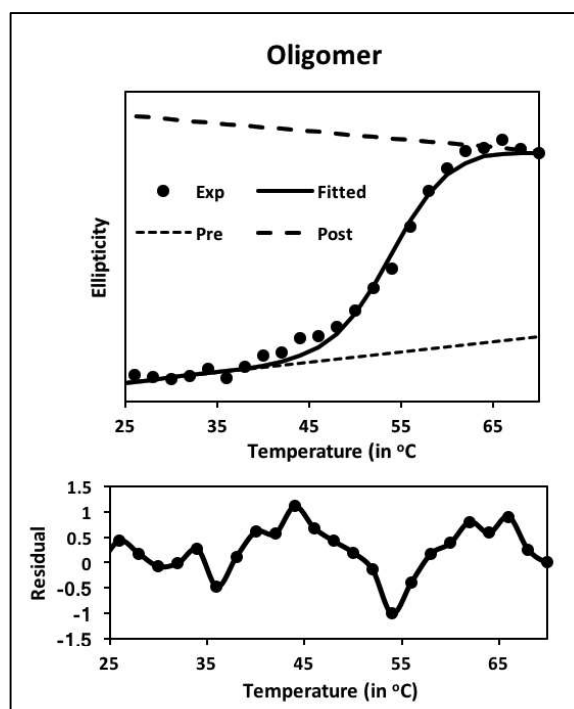


**Figure Supplementary 1: Biophysical characterisation of rNAP1 Oligomer.** Far UV CD Spectra of Oligomeric rNAP1. The data obtained can be fitted into a two sate kinetics of unfolding.

## *Figure S2*
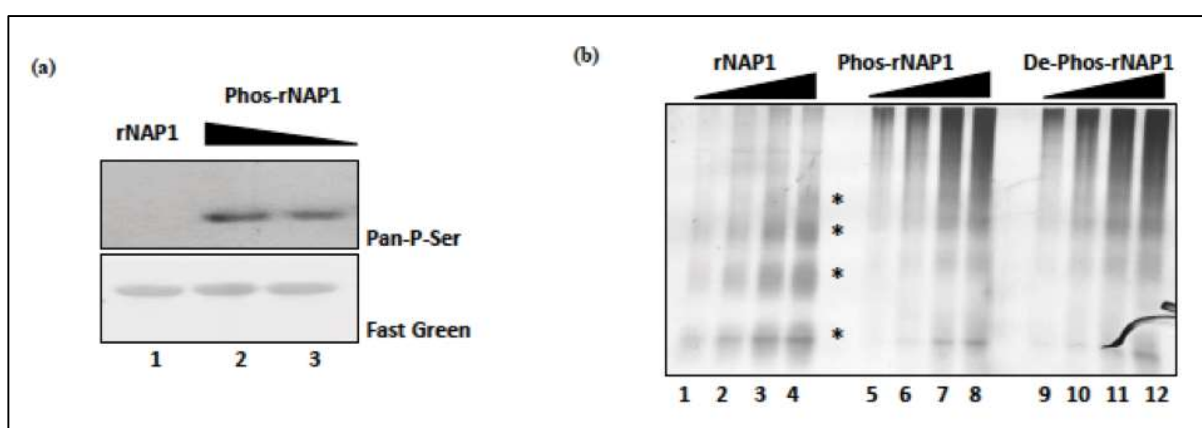


**Figure Supplementary 2: In vitro phosphorylation of rNAP1 with PKC (Protein kinase C).** (a) Western blotting with pan-phospho serine with 2 and 4mM ATP. (b) Native gel showing the loading of increasing concentration of rNAP1 (lanes 1-4), phos-rNAP1 (lanes 5-8) and de-phos-rNAP1 (lanes 9-12).

*Figure S3*

(a)

| Amino acid (Start-End) | Observed | Mol.Wt. (Expt) | Mol.Wt. (Calc) | ppm | Peptide |
|---|---|---|---|---|---|
| 28-41 | 1449.8177 | 1488.8105 | 1448.8212 | -7.20 | KSAPSTGGVKKPHR |
| 42-54 | 1600.9406 | 1599.9333 | 1599.9321 | -6.93 | YRPGTVALREIRR |
| 58-64 | 831.4884 | 830.4811 | 830.4861 | -6.05 | STELLIR |
| 65-73 | 1156.7266 | 1155.7193 | 1155.7240 | -4.11 | KLPFQRLVR |
| 71-84 | 1703.9254 | 1702.9181 | 1702.9366 | -10.8 | LVREIAQDFKTDLR |
| 85-117 | 3493.9232 | 3492.9154 | 3492.7984 | 32.7 | FQSAAIGALQEASEAYLVG LFEDTNLCAIHAKR |
| 118-130 | 1540.8909 | 1539.8836 | 1539.89.19 | -5.40 | VTIMPKDIQLARR |

(b)

| Amino acid (Start-End) | Observed | Mol.Wt. (Expt) | Mol.Wt. (Calc) | ppm | Peptide |
|---|---|---|---|---|---|
| 28-41 | 1433.8263 | 1432.8190 | 1432.8263 | -5.08 | KSAPATGGVKKPHR |
| 42-50 | 1032.5952 | 1031.5879 | 1031.5876 | -4.05 | YRPGTVALR |
| 58-64 | 831.4884 | 830.4811 | 830.4861 | -6.05 | STELLIR |
| 65-73 | 1156.7186 | 1155.7113 | 1155.7240 | -11 | KLPFQRLVR |
| 74-84 | 1335.6888 | 1334.6816 | 1334.6830 | -1.08 | EIAQDFKTDLR |
| 85-117 | 3513.7474 | 3512.7454 | 3512.7484 | 32.7 | FQSSAVMALQEASEAYLVGL FEDTNLCAIHAKR |
| 118-130 | 1540.8884 | 1539.8811 | 1539.8919 | -7.02 | VTIMPKDIQLARR |

(c)



**Figure Supplementary 3. H3 variants differences and similarities.** (a)(b) Tabulated peptides identified for H3.2 and H3.3 respectively by mass spectrometric analysis. (c) Multiple alignment of H3 variants, H3.1, H3.2 and H3.3 highlighting the differential amino acids along with their position.

*Figure S4*
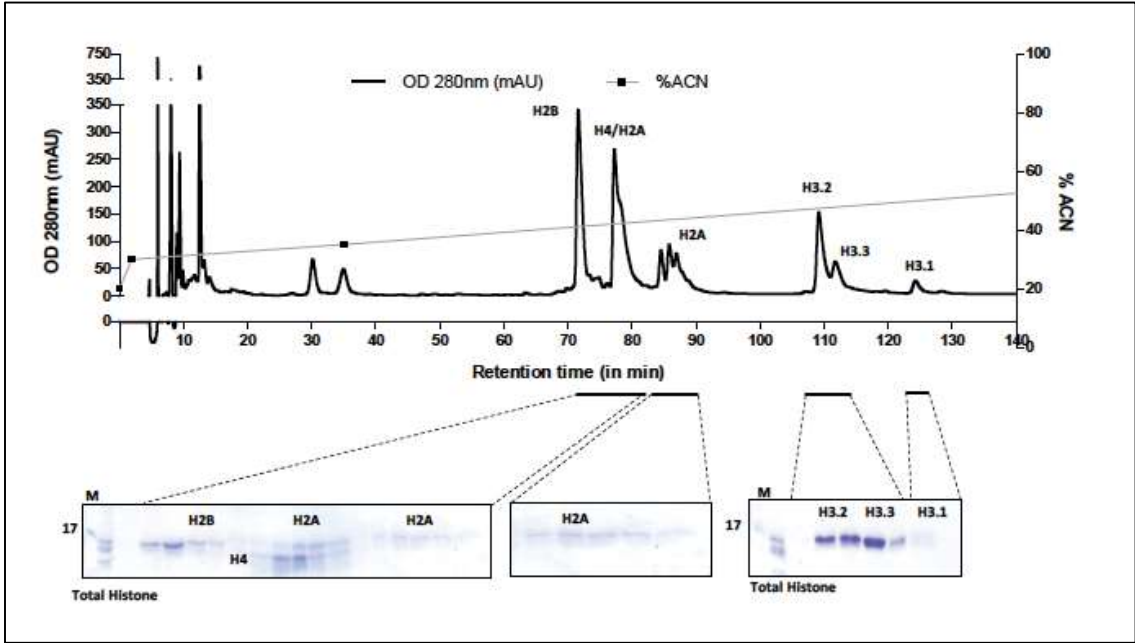


**Figure Supplementary 4. RP-HPLC chromatogram of histones isolated from rat.** The different fractions were resolved on an 18% SDS-PAGE and stained with coomassie.

## Annexure II – Chemicals and Antibodies

### List of Chemicals

| Serial Number | Chemical Name | Company |
|:---:|:---:|:---:|
| 1 | Acrylamide | Sigma |
| 2 | Agarose | USB |
| 3 | Ammonium persulfate | USB |
| 4 | Acetic Acid | Qualigens |
| 5 | Aprotinin | Sigma |
| 6 | Amido Black | Sigma |
| 7 | Ammoniacal Silver nitrate | Qualigens, SD fine |
| 8 | Ammonium hydroxide | Qualigens |
| 9 | Bovine Serum Albumin fraction V | Roche-Sigma |
| 10 | Bradford reagent | Biorad |
| 11 | BME | Sigma |
| 12 | Coomassie brilliant blue R-250 | USB |
| 13 | Calcium chloride | SD fine |
| 14 | Crystal Violet | Sigma |
| 15 | Disodium Hydrogen Phosphate | Qualigens |
| 16 | Dihydrogen Sodium phosphate | SD fine |
| 17 | Dimethyl Sulphoxide | Qualigens |
| 18 | EDTA | Sigma |
| 19 | EtBr | Sigma |
| 20 | ECL detection reagent | Millipore |
| 21 | Formaldehyde | Qualigenes |
| 22 | Femto | Pierce |
| 23 | Glycerol | Merck |

| 24 | Glycine | Sigma |
|----|---------|-------|
| 25 | Guanidine Chloride | Sigma |
| 26 | Hydrochloric Acid | Qualigens |
| 27 | IPTG | Sigma |
| 28 | Ketmin-50 | Themis Medicare |
| 29 | Leupeptin | Sigma |
| 30 | Magnesium Chloride | Qualigens |
| 31 | Methanol | Merck |
| 32 | MNase | USB |
| 33 | MTT | Sigma |
| 34 | N-N Methylene Bis-Acrylamide | Sigma, Amresco |
| 35 | Nonidet P-40 | Sigma |
| 36 | Potassium Acetate | SD fine |
| 37 | PMSF | Sigma |
| 38 | Potassium Chloride | Glaxo |
| 39 | Pepstatin A | Sigma |
| 40 | Protamine Sulfate | Sigma |
| 41 | Potassium Acetate | SD fine |
| 42 | PVDF membrane | Millipore |
| 43 | Paraformaldehyde | Sigma |
| 44 | Riboflavin 5 phosphate | Sigma |
| 45 | RNASE A | Amresco |
| 46 | Sodium Chloride | Qualigens |
| 47 | Sodium Orthovandate | Sigma |
| 48 | Sodium Citrate | Merck |
| 49 | Sodium Deoxycholate | BDH |
| 50 | Sodium Bicarbonate | SD fine |
| 51 | Sodium Hydroxide | SD fine |

| 52 | Sulphuric Acid | Qualigens |
|----|----------------|-----------|
| 53 | Spermine | USB |
| 54 | Spermidine | USB |
| 55 | SDS | Sigma |
| 56 | Sucrose | Sigma |
| 57 | Tween-20 | Sigma |
| 58 | Triton X-100 | Sigma |
| 59 | Tris | Sigma |
| 60 | Trypsin | Sigma |
| 61 | TEMED | Sigma |
| 62 | TMAO | Sigma |
| 63 | TSA | Sigma |
| 64 | Urea | Sigma |
| 65 | ATP,GTP, CTP and UTP | Sigma |

## *List of Antibodies*

| Serial Number | Antibody Name | Blocking | Condition |
|---------------|---------------|----------|-----------|
| 1 | H3<br><br>Upstate  06-755 | 5% BSA- TBST<br><br>60min RT | 1:2000 1%BSA -TBST<br><br>O/N   4°C |
| 2 | H3S10P<br><br>Millipore 06-570 | 5% BSA- TBST<br><br>60min RT | 1:5000 1%BSA-TBST<br><br>O/N 4°C |
| 3 | H3Ac<br><br>Upstate 06-599 | 5% Milk- TBST<br><br>60min RT | 1:3000 1%BSA-TBST<br><br>O/N 4°C |
| 4 | H3K9Ac<br><br>Millipore 07-352 | 1% BSA -TBST<br><br>60min RT | 1:5000 1%BSA-TBST<br><br>O/N 4°C |
| 5 | H3K9Me3<br><br>Millipore 07-442 | 5% BSA- TBST<br><br>60min RT | 1:4000 5%BSA-TBST<br><br>O/N 4°C |
| 6 | H3K14Ac<br><br>Abcam 52946 | 1% BSA -TBST<br><br>60min RT | 1:2000 1%BSA-TBST<br><br>O/N 4°C |

| | | | |
|---|---|---|---|
| 7 | H3K27Ac<br><br>Abcam 4729 | 1% BSA -TBST<br><br>60min RT | 1:3000 1%BSA-TBST<br><br>O/N 4°C |
| 8 | H3K27Me3<br><br>Millipore 07-449 | 5% BSA-TBST<br><br>60min RT | 1:4000 in 5%BSA-TBST<br><br>O/N 4°C |
| 9 | H3K4Me3<br><br>Abcam-1012 | 1% BSA -TBST<br><br>60min RT | 1:2500 1%BSA-TBST<br><br>O/N 4°C |
| 10 | H4<br><br>Millipore 07-108 | 5% BSA- TBST<br><br>60min RT | 1:4000 1%BSA-TBST<br><br>O/N 4°C |
| 11 | H4K16Ac<br><br>Millipore 07-329 | 5% BSA- TBST<br><br>60min RT | 1:8000 5%BSA-TBST<br><br>O/N 4°C |
| 12 | H4K20Me3<br><br>Ab 9053 | 5% BSA- TBST<br><br>60min RT | 1:4000 5%BSA-TBST<br><br>90min RT |
| 13 | Beta Actin<br><br>Sigma  A5316 | 5% Milk -TBST<br><br>60min RT | 1:10000 1%BSA-TBST<br><br>O/N 4°C |
| 14 | MYC<br><br>Sigma  C3956 | 5% BSA- TBST<br><br>60min RT | 1:5000 1%BSA-TBST<br><br>90min RT |
| 15 | FLAG<br><br>F3165 | 5% Milk -TBST<br><br>60min RT | 1:5000 TBST<br><br>90min RT |
| 16 | HA<br><br>Sigma H3665 | 5% Skim milk-TBST<br><br>60min RT | 1:5000 1%BSA-TBST<br><br>90min RT |
| 17 | Anti-Pan Serine Phospho<br><br>Abcam 9332 | 5% BSA- TBST<br><br>60min RT | 1:3000 1%BSA-TBST<br><br>O/N 4°C |
| 18 | Anti-rabbit HRP<br><br>Cell Signalling, 7074 | - | :8000 5%BSA-TBST<br><br>60min RT |
| 19 | Anti-mouse HRP<br><br>Sigma, A-4416 | - | 1:5000 5%BSA-TBST<br><br>60min RT |

## *Annexure III – Cell Lines/Strains*

| Serial Number | Cell Line/Strain | Origin | Medium |
|---|---|---|---|
| 1 | Rosetta (DE3) pLysS | Bacteria | LB/2xTY |
| 2 | CL38 | Rat Liver | MEM |
| 3 | CL44 | Rat Liver | MEM |
| 4 | HHL5 | Human Liver | DMEM |
| 5 | HEPG2 | Human Liver | RPMI |
| 6 | HACAT | Human Colon | DMEM |
| 7 | A431 | Human Colon | DMEM |
| 8 | MCF10A | Human Breast | DMEM |
| 9 | MCF7 | Human Breast | DMEM |
| 10 | AGS | Human Stomach | RPMI |

## *Annexure IV – Primers*

### *List of Cloning Primers*

| Gene | Vector | Primer | Sequence |
|---|---|---|---|
| H2A.1 | pCDNA FLAG HA | F | GTCGGATCCGAAATGTCTGGACGCGGCAAAC |
| | | R | GTCGAATTCTTTGCCCTTGGCCTTGTGGTGGCT |
| H2A.2 | pCDNA FLAG HA | F | GTCGGATCCGAAATGTCCGGCCGTGGCAA |
| | | R | GTCGAATTCCTTGCCCTTCGCCTTATGGTGGC |
| H3.2 | pCDNA MYC | F | GTCGATATCATGGCCCGTACTAAGCAGAC |
| | | R | GTCGCGGCCGCTTAGGCCCGCTCCCCGCGGAT |
| H3.3 | pCDNA MYC | F | GTCGATATCATGGCCCGAACCAAGC |
| | | R | GTCGCGGCCGCTTAAGCTCTCTCTCCCCGTATC |
| NAP1 | pCDNA MYC | F | GTCGCGGCCGCATGGCAGACATTGACAACA |

| | | | |
|---|---|---|---|
| | | R | GTCGATATCTCACTGCTGCTTGCACTCG |
| NAP1 | pET3A/pET28a | F | GTCCATATGGATATCATGGCAGACATTGACAACA |
| | | R | GTCGGATCCTCACTGCTGCTTGCACTCG |
| H3.3 Promoter | PGL3 | F | GTCGGTACCTTATGTAGCTATGGATGACCT |
| | | R | GTCCTCGAGGTAGCGATGAGGTTTCTTCAC |
| H3.2 Promoter | PGL3 | F | GTCGGTACCCCATTACTGTGCACCGCAGAA |
| | | R | GTCCTCGAGCTTCTTCACGCCGCCGGTGG |
| H3.3 shRNA | pLKO-GFP | F | CCGGGACTTGTTGGGTAGCTATTAACTGCAGTTAATAGCTACCCAACAAGTCTTTTTG |
| | | R | AATTCAAAAAGACTTGTTGGGTAGCTATTAACTGCAGTTAATAGCTACCCAACAAGTC |
| P150 shRNA | pLKO-puro | F | CCGGGGATGGTGTGCCTGAAAGGAACTGCAGTTCCTTTCAGGCACACCATCCTTTTTG |
| | | R | AATTCAAAAGGATGGTGTGCCTGAAAGGAACTGCAGTTCCTTTCAGGCACACCATCC |
| NAP1 shRNA | pLKO-GFP | F | CCGGGCCAAATTCTATGAGGAAGTTCTGCAGAACTTCCTCATAGAATTTGGCTTTTTG |
| | | R | AATTCAAAAGCCAAATTCTATGAGGAAGTTCTGCAGAACTTCCTCATAGAATTTGGC |

## *List of Primers used for transcript analysis*

| Gene | Application | Primer | Sequence |
|---|---|---|---|
| H2A.1 | RT/Real Time-PCR | F | CTGTGCTGGAGTACCTGACG |
| | | R | TGTGGTGGCTCTCAGTCTTC |
| H2A.2 | RT/Real Time-PCR | F | GAAGACGGAGAGCCACCATA |
| | | R | GGAAGAGTAGGGCACACGAC |
| H3.2 | RT/Real Time-PCR | F | ATGGCCCGTACAAAGCAG |
| | | R | AGGTTGGTGTCCTCGAACAG |

| Gene | Method | Primer | Sequence |
|---|---|---|---|
| H3.3 | RT/Real Time-PCR | F | TACCCTTCCAGAGGTTGGTG |
| | | R | GGGCATGATGGTGACTCTCT |
| H3.1 | RT/Real Time-PCR | F | GGCTTTTCATCTTTTTCTTCCTACCATG |
| | | R | ACCGGTGGCCGGGGCACTTTTA |
| Tslc-1 | RT/Real Time-PCR | F | TTATCCTCTGCAAGGCCTAAC |
| | | R | TGTTGAGGCATTTCGTCATC |
| GAPDH | RT/Real Time-PCR | F | GGATTTGGTCGTATTGGGCG |
| | | R | ATCGCCCCACTTGATTTTGG |
| P150 | RT/Real Time-PCR | F | CAGTGAACTAAGTCCTGACAC |
| | | R | CTTAGGACAGCTCTGTACTG |
| P60 | RT/Real Time-PCR | F | CTGAACAAGGAGAACTGGAC |
| | | R | GCACGTAACTTTTATGCTCG |
| HIRA | RT/Real Time-PCR | F | CTCAAGCTGATGATCGAAGT |
| | | R | TCATGGCATGAGCAGATACCA |
| MLL5 | Real Time-PCR | F | AGCCTCCTTCACAGCACCTA |
| | | R | CCTGAGGGTGTCTGGGTAAA |
| INK4 | Real Time-PCR | F | GGGAGGGCTTCCTAGACACT |
| | | R | CCCAGCGGAGGAGAGTAGAT |
| MEN1 | Real Time-PCR | F | TCTGGGCTTCGTAGAGCATT |
| | | R | TTTCTTCAGGGCAGCCGATT |
| TP53 | Real Time-PCR | F | AGATAGTACTCGGCCCCCTC |
| | | R | TAGGTGCCAGGTCCAACAAC |
| CHD1 | Real Time-PCR | F | TCGGCCTGAAGTGACTCGTA |
| | | R | AATCATAAGGCGGGGCTGTG |
| ATM | Real Time-PCR | F | CTAAGTCGCTGGCCATTGGT |
| | | R | TCTGGAGGAAGAAGCAACGC |
| H3.2 | Human Real Time-PCR | F | TCTGGTGCGAGAAATTGCT |
| | | R | TAGTGGATTCTTAAGCACGTTC |

| Gene | Application | Primer | Sequence |
|---|---|---|---|
| H3.3 | Human Real Time-PCR | F | GGTGGGGCTGTTCGAAG |
| | | R | CCGCCACTTCTTAAGCC |
| H3.1 | Human Real Time-PCR | F | TGCTCGGAAGTCTACTGGTG |
| | | R | GTGGACTTCTGATAACGGCG |

## *List of Primers used for MeDIP and ChIP qPCR*

| Gene | Application | Primer | Sequence |
|---|---|---|---|
| H2A.1 | MeDIP- Real Time-PCR | F | CGTCGTTCGCCTACAGCTT |
| | | R | TGCCGCGTCCAGACATAATT |
| H2A.2 | MeDIP- Real Time-PCR | F | CGCAACAACGGCCGCACGCA |
| | | R | CATAAGCCCGGCTCCCTGGC |
| H3.2 | MeDIP- Real Time-PCR | F | ATTCCGACGGAAGTCTGAGT |
| | | R | CGGCAGAGAAAAATTCCGGT |
| H3.3 | MeDIP- Real Time-PCR | F | CGGCGCAGCCTGAGTCATTA |
| | | R | TCACTTGGCTCCCGCTGCCA |
| H19 | MeDIP- Real Time-PCR | F | GAGCTAGGGTTGGAGAGGAAC |
| | | R | GGTCGAACCCTTCCCAGCA |
| MLL5 | MeDIP- Real Time-PCR | F | TCGCCGCCATTTTCCCAG |
| | | R | GCTGCTCAGAGTGTCTAT |
| INK4 | MeDIP- Real Time-PCR | F | CCTGGCCAGTCTGTCTGC |
| | | R | AAGGAAGGAGGGACCCACT |
| MEN1 | MeDIP- Real Time-PCR | F | GCGGTGCCTTGTGTGGGA |
| | | R | TCCCTGCAATCTCTACCTA |
| TP53 | MeDIP- Real Time-PCR | F | TCTGAAGCTCCAGTTCAT |
| | | R | GGAGCGTGACACCCTGCT |
| CHD1 | MeDIP- Real Time-PCR | F | CTGGTGTGGGAGCCGCGG |
| | | R | ACTGAGCTCGGGTGCGGT |

| ATM | MeDIP- Real Time-PCR | F | TCCTGTCACCTTAAGG |
| --- | --- | --- | --- |
| | | R | AAACCTGTAGCTTAAATA |
| rDNA | MeDIP- Real Time-PCR | F | CGGGAGCTGGACTTCTGA |
| | | R | GGTAGATAGCCTGAACAC |

# *Annexure V - Media and Buffer Composition*

### a. **Phosphate Buffered Saline**

1. Dissolve the following in 800ml distilled $H_2O$:
   - 8g of NaCl
   - 0.2g of KCl
   - 1.44g of $Na_2HPO_4$
   - 0.24g of $KH_2PO_4$
2. Adjust pH to 7.4 with HCl.
3. Adjust volume to 1L with additional distilled $H_2O$.
4. Sterilize by autoclaving.

The final concentration of the components are as follows:

   a. 137mM NaCl
   b. 2.7mM KCl
   c. 10mM $Na_2HPO_4$
   d. 2mM $KH_2PO_4$

### b. **2x BBS**

1. Add the following:
   - 266.56mg BES
   - 409.5mg NaCl
   - 6.65mg $Na_2HPO_4$
2. Adjust the pH to 6.95
3. Adjust volume to 25ml with distilled $H_2O$.
4. Sterile filter inside laminar hood

### c. **Electrophoresis Buffer**

1. Add the following:
   - 6.05g Tris
   - 28.5g Glycine
   - 1g SDS
2. Adjust volume to 1000ml with distilled $H_2O$.

### d. **Phosphate Buffer**

500ml of 1M potassium phosphate buffer pH 7.4 = 401ml of 1M $K_2HPO_4$ + 99ml of 1M $KH_2PO_4$

- 1M $K_2HPO_4$ = 87.09gm in 500ml
- 1M $KH_2PO_4$ = 13.6gm in 100ml

### e. Chemicals for In-gel Digestion

| Reagent | Stock | Working | For 1ml |
|---|---|---|---|
| $NH_4HCO_3$ | 1M (79g/mol) | 25mM | 79mg |
| DTT | 1M (154g/mol) | 10mM | 154mg |
| Iodoacetamide | 1M (185g/mol) | 55mM | 185mg |
| Trypsin | | 20ng/µl | |
| $K_3[Fe (CN)_6]$ | 1M (329g/mol) | 30mM | 329mg |
| Sodium thiosulphate | 1M(158g/mol) | 100mM | 158mg |

### f. Transfer Buffer

| Reagent | Stock | Working | For 1L |
|---|---|---|---|
| Glycine | | 0.19M | 14gm |
| Tris | | 25mM | 3.03gm |
| SDS | 10% | 0.01% | 1ml |
| Methanol | 100% | 20% | 200ml |
| $H_2O$ | | | Upto 1L |

### g. Chemicals for SDS-PAGE

**Acrylamide Main Stock:**

292g acrylamide and 8g bis-acrylamide are mixed and dissolved in 500ml of $H_2O$. Heating at $37^0C$ may be required to dissolve acrylamide. Volume is made up to 1000ml.

**Resolving Gel (18%):**

| Reagent | Stock | Working | For 10ml |
|---|---|---|---|
| Acrylamide – Bis-acrylamide (29:1) | 30% | 18% | 6ml |

| | | | |
|---|---|---|---|
| **Tris pH 8.8** | 1.5M | 375mM | 2.5ml |
| **SDS** | 10% | 0.1% | 100µl |
| **APS** | 10% | 0.05% | 50µl |
| **TEMED** | | 0.05% | 5µl |
| **H$_2$O** | | | 1.345ml |

**Resolving Gel (10%):**

| Reagent | Stock | Working | For 10ml |
|---|---|---|---|
| **Acrylamide – Bis-acrylamide (29:1)** | 30% | 10% | 4.076ml |
| **Tris pH 8.8** | 1.5M | 375mM | 2.5ml |
| **SDS** | 10% | 0.1% | 100µl |
| **APS** | 10% | 0.05% | 50µl |
| **TEMED** | | 0.05% | 5µl |
| **H$_2$O** | | | 3.269ml |

**Stacking Gel (4%):**

| Reagent | Stock | Working | For 10ml |
|---|---|---|---|
| **Acrylamide – Bisacrylamide (29:1)** | 30% | 4% | 1.3ml |
| **Tris pH 6.8** | 1M | 125mM | 1.25ml |
| **SDS** | 10% | 0.1% | 100µl |
| **APS** | 10% | 0.05% | 50µl |
| **TEMED** | | 0.1% | 10µl |
| **H$_2$O** | | | 7.29ml |

## h. 2x Sample Buffer for Histones

| Reagent | Stock | Working | For 10ml |
|---|---|---|---|
| **Tris pH 6.8** | 1M | 125mM | 1.25ml |
| **Glycerol** | 100% | 20% | 2ml |

| | | | |
|---|---|---|---|
| SDS | 10% | 4% | 4ml |
| β-Mercaptoethanol | 14.3M | 300mM | 200µl |
| Bromophenol blue | 0.5% | 0.05% | 5mg |
| H$_2$O | | | 2.55ml |

## i. Chemicals for AUT-PAGE

**Resolving Gel:**

| Reagent | Stock | Working | For 30ml |
|---|---|---|---|
| Acrylamide | 60% | 25mM | 7.5ml |
| Bis-acrylamide | 2.5% | 10mM | 1.2ml |
| Acetic acid | | | 1.8ml |
| Ammonium hydroxide | | | 98.4µl |
| Urea | | 8M | 14.4gm |
| H$_2$O | | | Upto 27.31ml |
| Vacuum to degas | | | |
| Triton-X | 25% | | 675µl |
| Riboflavin | | | 2ml |
| TEMED | | | 150µl |

**Stacking gel:**

| Reagent | Stock | Working | For 10ml |
|---|---|---|---|
| Acrylamide | 60% | 25mM | 670µl |
| Bis-acrylamide | 2.5% | 10mM | 640µl |
| Acetic acid | | | 570µl |
| Ammonium hydroxide | | | 35µl |
| Urea | | 8M | 4.8gm |
| H$_2$O | | | Upto 9.3ml |
| Vacuum to degas | | | |

| | | | |
|---|---|---|---|
| **Riboflavin** | | | 650μl |
| **TEMED** | | | 50μl |

**Sample Preparation for AUT-PAGE:**

2ml of Urea-DTT solution (0.864gm urea, 14mg of DTT) was prepared. AUT-sample buffer was prepared by taking 1.8ml of Urea-DTT solution and adding 100μl ammonia and 100μl of phenolphthalein. 50μl of the sample buffer was added on 20μg of vacuum dried histones. It was mixed and incubated for 30min at $37^0$C. Then 2.5μl acetic acid and 2.5μl concentrated dye (25μl acetic acid and a pinch of methylene blue in 500μl of Urea-DTT solution) was added.

## j. TELT Buffer

| Reagent | Stock | Working | For 40ml |
|---|---|---|---|
| **Tris-Cl pH 7.5** | 1M | 50mM | 2ml |
| **EDTA pH 8.0** | 0.5M | 62.5mM | 5ml |
| **Triton X-100** | 100% | 0.4% | 160μl |
| **LiCl** | | 2.5M | 4.239g |
| **$H_2O$** | | | Upto 40ml |

## k. SOB Media

| Reagent | Stock | Working | For 100ml |
|---|---|---|---|
| **Bactotryptone** | | 2% | 2gm |
| **Yeast Extract** | | 0.5% | 0.5g |
| **NaCl** | 5M | 10mM | 200μl |
| **KCl** | 3M | 2.5mM | 83.33μl |
| **$MgCl_2$** | 1M | 10mM | 1ml |
| **$MgSO_4$** | | 10mM | 0.246g |
| **$H_2O$** | | | Upto 100ml |

## l. Transforming Buffer

1. Add the following:
    - 1.0884g $MnCl_2.4H_2O$
    - 0.22053g $CaCl_2.2H_2O$
    - 1.8637g KCl
    - 0.30237g PIPES
2. Adjust pH to 6.7 with KOH
3. Adjust volume to 100ml with distilled $H_2O$.
4. Sterile filter

The final concentration of the components are as follows:

- 55mM $MnCl_2.4H_2O$
- 15mM $CaCl_2.2H_2O$
- 250mM KCl
- 10mM PIPES

## m. DMEM

1. Add the following:
    - DMEM
    - 81.4mg Non Essential Amino Acid
    - 0.293gm L-Glutamine (working 2mM)
    - 3.7gm Sodium Bicarbonate (working 44mM)
2. Adjust volume to 1000ml with distilled $H_2O$.
3. Sterile filter inside laminar hood

## n. MEM

1. Add the following:
    - 9.6gm MEM powder (Sigma, #M6043)
    - 81.4mg Non Essential Amino Acid
    - 0.293gm L-Glutamine (working 2mM)
    - 2.2gm Sodium Bicarbonate
    - 3.574gm HEPES
2. Adjust volume to 1000ml with distilled $H_2O$.
3. Sterile filter inside laminar hood

## o. RPMI

1. Add the following:
    - RPMI
    - 81.4mg Non Essential Amino Acid
    - 0.293gm L-Glutamine (working 2mM)
    - 2gm Sodium Bicarbonate
2. Adjust volume to 1000ml with distilled $H_2O$.
3. Sterile filter inside laminar hood

## p. Trypsin Composition

4. Add the following:
   - 2.5gm Trypsin (0.25%)
   - 0.2gm EDTA
   - 0.5gm Glucose
5. Adjust volume to 1000ml with distilled $H_2O$.
6. Sterile filter inside laminar hood

# *Publications*

Clinical Epigenetics

**METHODOLOGY**                                                          **Open Access**

CrossMark

# A novel method for isolation of histones from serum and its implications in therapeutics and prognosis of solid tumours

Divya Reddy[1,2], Bharat Khade[1], Riddhi Pandya[1] and Sanjay Gupta[1,2]*

## Abstract

**Background:** Dysregulation in post-translational modifications of histones and their modifiers are now well-recognized as a hallmark of cancer and can be used as biomarkers and potential therapeutic targets for disease progression and prognosis. In most solid tumours, a biopsy is challenging, costly, painful or potentially risky for the patient. Therefore, non-invasive methods like 'liquid biopsy' for analysis of histone modifications and their modifiers if possible will be helpful in the better clinical management of cancer patients.

**Methods:** Here, we have developed a cost-effective and time-efficient protocol for isolation of circulating histones from serum of solid tumor, HCC, called Dual Acid Extraction (DAE) protocol and have confirmed by mass spectrometry. Also, we measured the activity of HDACs and HATs in serum samples.

**Results:** The serum purified histones were profiled for changes in histone PTMs and have shown a comparable pattern of modifications like acetylation (H4K16Ac), methylation (H4K20Me3, H3K27Me3, H3K9Me3) and phosphorylation (γ-H2AX and H3S10P) to paired cancer tissues. Profiling for the histone PTM changes in various other organs of normal and tumor bearing animal suggests that the changes in the histone PTMs observed in the tumor serum is indeed due to changes in the tumor tissue only. Further, we demonstrate that the observed hypo-acetylation of histone H4 in tissue and serum samples of tumor bearing animals corroborated with the elevated HDAC activity in both samples compared to normal. Interestingly, human normal and tumor serum samples also showed elevated HDAC activity with no significant changes in HAT activity.

**Conclusions:** Our study provides the first evidence in the context of histone PTMs and modifiers that liquid biopsy is a valuable predictive tool for monitoring disease progression. Importantly, with the advent of drugs that target specific enzymes involved in the epigenetic regulation of gene expression, liquid biopsy-based 'real time' monitoring will be useful for subgrouping of the patients for epi-drug treatment, predicting response to therapy, early relapse and prognosis.

**Keywords:** cNUC, Histones, Serum, Cancer, HDACs, Diagnosis

## Background

Histones are well conserved basic proteins which associate to form an octameric core around which the DNA is wrapped to form a nucleosome [1]. The N-terminal tails of histones protrude out of the nucleosome and undergo a variety of post-translational modifications (PTMs) like acetylation, phosphorylation, methylation, sumoylation and ubiquitination. The occurrence and functioning of these PTMs are an orchestrated event of 'writers' (adds modifications), 'readers' (recognizes modification) and 'erasers' (remove the modifications). Histone PTMs dynamically maintain the chromatin states, and thus any deregulation may lead to altered gene expression as observed in diseases like cancer [2]. Indeed, the loss of histone H4 lysine 16 acetylation (H4K16Ac) and lysine 20

* Correspondence: sgupta@actrec.gov.in
[1]Epigenetics and Chromatin Biology Group, Gupta Lab, Cancer Research Institute, Advanced Centre for Treatment, Research and Education in Cancer (ACTREC), Tata Memorial Centre, Kharghar, Navi, Mumbai 410210, MH, India
[2]Homi Bhabha National Institute, Training School Complex, Anushakti Nagar, Mumbai, MH 400085, India

trimethylation (H4K20Me3) are considered as hallmark of most human cancers [3]. Similarly, global H3 and H4 hypo-acetylation have been proven to correlate with tumour phenotype, prognostic factors and patient outcome in breast and prostate cancers [4, 5]. Decades of research have discovered a battery of histone PTMs that are altered in cancer and are now referred as 'histone onco-modifications', but none has reached clinics primarily due to technological limitations in the diagnosis of solid tumours.

Traditionally, cancer diagnosis and staging of solid tumours are done with an imaging technique followed by a surgical biopsy. But biopsy, being invasive, requires a complex setting and well-trained clinician and is occasionally difficult and risky for some advanced stage patients. Therefore, diagnosis or monitoring of solid tumours utilizing circulating epigenetic biomarkers in blood samples, if possible, will prove to be a very powerful tool and will overcome all the earlier limitations. Indeed, research conducted over the last few years has identified and detected epigenetic biomarkers associated with cancer, including aberrant DNA methylation patterns, miRNA profiles and histone signatures in body fluids of the patients [6, 7].

The levels of circulating nucleosomes (cNUCs) and histones are found to be elevated in a number of disease conditions like inflammation caused by bacterial infections, autoimmune diseases like SLE, stress and trauma [8]. cNUCs are released into the blood by apoptotic cells during these processes [9]. Elevated levels of cNUCs have been reported in lung, breast, colorectal, renal and gastric cancer compared to patients with inflammation and healthy individuals [10]. In case of gastrointestinal tumours, a positive correlation between cNUC levels, tumour stage and metastasis has been established [11]. In case of advanced non-small cell lung carcinoma and cervical cancer, a correlation between clinical outcome in response to chemotherapy and cNUCs has been observed [12]. On circulating DNA, hypo-methylation pattern has been established in CRC patients [13]. Histone modifications like H3K9me3 and H4K20me3 have been detected on cNUCs [14]. In another study, the ratio of H3K9me3/nucleosome and H4K20me3/nucleosome was found to be less in serum of breast and colorectal cancer patients compared to healthy individuals [15]. Though studies on histone PTMs on cNUCs have revealed interesting aspects, but how similar is circulating epigenetic signature to solid tumour signatures in terms of their histone PTMs and their modifiers has not been established yet. This especially is important as because any changes in the tissue epigenetic signature, if possible, can be read via the use of serum histones that can act as a good prognosis and a diagnostic marker.

Here, we used a cost-effective method named as dual acid extraction (DAE) method, to isolate pure histones from serum with the aim to understand the correlation between circulating histone PTM with that of solid tumour (hepatocellular carcinoma, HCC) tissues in animal model. Furthermore, we for the first time measured the histone acetylase (HAT) and histone deacetylase (HDAC) activities in serum samples of normal and solid tumour-bearing animals and human patient samples.

## Methods
### Animal handling and experiments
All the experiments were performed on male Sprague-Dawley rats (spp. *Rattus norvegicus*) after approval of the Institute Animal Ethics Committee (IAEC# 04/2014), Advanced Centre for Treatment Research and Education in Cancer and the Committee for the Purpose of Control and Supervision on Animals, India standards. The detailed protocol to induce liver carcinogenesis is as previously described [16]. Tissue samples (liver, lung, kidney and brain) were fixed in formalin and prepared as paraffin-embedded blocks according to standard protocols. The H&E-stained sections were microscopically reviewed for histopathological alterations to confirm normal and HCC. Post-anaesthesia, the blood was slowly collected by cardiac puncture (preferably from ventricle) from 120 days NDEA (late stage liver cancer)-treated animals after which they were sacrificed [17]. For early stage liver cancer, blood from the tail vein was collected from 90 days NDEA-treated animals.

### Human blood sample collection and serum isolation
Blood samples of 24 cancer patients were collected retrospectively from the Tumor Tissue Repository (TTR) of Advanced Centre of Treatment, Research and Education in Cancer (ACTREC), Tata Memorial Centre after Ethical Approval from Institute Ethics Committee III (Project number 164) along with six healthy adult human volunteers. As the samples were collected retrospectively, institute ethics committee III approved waiver of consent for working on patient samples. Whole blood from patients was collected prior to surgery, allowed to clot at room temperature for 15–30 min. The clot was then removed by centrifugation at 5000 rpm for 10 min at 4 °C. The resulting supernatant (serum) is transferred into multiple tubes to avoid freeze and thaw cycles and finally stored in liquid nitrogen containers in ACTREC, TMH-TTR. The samples collected were from 2013 to 2016 with confirmed histopathological tumour type as mentioned in Table 2.

### Isolation of histones from serum
Total proteins were precipitated from the serum (5 ml) by the slow addition of Trichloroacetic acid (TCA) to a final concentration of 20% with continuous and vigorous

Reddy *et al. Clinical Epigenetics* (2017) 9:30

Page 3 of 11

mixing. The precipitation was allowed to carry out on the ice for 30 min, followed by centrifugation at 15,000 rpm for 15 min. The obtained protein pellet was homogenized with glass teflon homogenizer in three volumes (*w/v*) of 0.2 M sulphuric acid ($H_2SO_4$), till the pellet was completely dispersed and a milky white liquid is formed, which then was intermittently vortexed for >2 h at 4 °C. This mixture was then centrifuged at 16,000 rpm for 20 min at 4 °C. To the supernatant obtained post-centrifugation, four volumes of acetone was added and histones were precipitated overnight at −20 °C. The pellet obtained post-centrifugation at 16,000 rpm for 20 min at 4 °C was washed twice with two volumes of each of acidified acetone and acetone twice. The histone pellet was air dried and eventually suspended in 50 µl of 0.1% β-mercaptoethanol in $H_2O$ and stored at −20 °C. Histone concentrations were determined by Bradford method of protein estimation. Protein standards were prepared containing a range of 0 to 5 µg of bovine serum albumin in 5 ml of 1× Bradford reagent. Histone samples were also prepared similarly. Samples were vortexed and incubated at room temperature for 5 min. Absorbance was measured at 595 nm and the blank was adjusted. Histone samples were estimated for protein concentration by plotting a standard curve.

### Isolation of histones from liver tissue

Histones were extracted and purified as described earlier [18]. Briefly, liver tissues (1 g) were homogenized in 10 ml lysis buffer (15 mM Tris-Cl pH 7.5, 60 mM KCl, 15 mM NaCl, 2 mM EDTA, 0.5 mM EGTA, 0.34 M sucrose, 0.15 mM β-mercaptoethanol, 0.15 mM spermine and 0.5 mM spermidine) with 1× protease inhibitor cocktail and phosphatase inhibitor cocktail. Nuclei were then isolated by sucrose gradient centrifugation. The three volumes of homogenate was layered on top of one volume of 1.8 M sucrose. Nuclei pellet obtained by centrifugation at 26,000 rpm for 90 min at 4 °C was resuspended in 0.2 M $H_2SO_4$ and incubated for >2 h at 4 °C with intermittent vortexing. After centrifugation at 16,000 rpm for 20 min at 4 °C, the histones were precipitated at −20 °C for overnight with addition of four volumes of acetone to the supernatant. Post-centrifugations at 16,000 rpm for 20 mins at 4 °C, pelleted histones were air dried and suspended in 0.1% β-mercaptoethanol in $H_2O$ and stored at −20 °C.

### Resolution and analysis of histones

The purified histones from serum and tissue that were resolved on 18% sodium duodecyl sulphate-polyacrylamide gel electrophoresis (SDS-PAGE) was either stained by silver staining method [19] or transferred to PVDF membrane, probed with site-specific modified histone antibodies, against H4K16Ac (Millipore#07-329),

H4K20Me3 (Abcam#9053), γH2AX (Millipore#05-636), H3S10P (Millipore#06-570), H3K27Me3 (Millipore#07-449) and H3K9Me3 (Abcam#8898), and signals were detected by ECL plus detection kit (Millipore #WBKLS0500). Gel loading equivalence was done by silver staining method.

### Analysis of histones by LC-MS

The purified histones (15 µg) were subjected to in-solution trypsin (20 ng/µl) digestion in 50 mM ammonium bicarbonate, pH 8.0 at 37 °C for 2 h (1:200 enzyme:substrate) as described previously [20]. Enzymatic digestion was stopped by adding 10% trifluoroacetic acid (TFA) to a final pH <3. Peptides were then desalted with ZipTip C18 columns (Millipore) and lyophilized prior to analysis by LTQ Orbitrap-MS/MS (ABSCIEX). The MS instrument was operated in the data-dependent mode to automatically switch between full scan MS and MS/MS acquisition. Mascot generic format (mgfs) files were generated and were searched against protein database using Mascot version 2.3 (Matrix Science, London, UK).

### HDAC and HAT activity assays

Assays were performed using the colorimetric HDAC and HAT activity assay kits from BioVision (BioVision Research Products, USA) according to manufacturer's instructions. Briefly for HDAC activity assay, 50 µl of serum from normal, early and late tumours were diluted in 85 µl of $H_2O$; then, 10 µl of 10× HDAC assay buffer were added followed by addition of 5 µl of the colorimetric substrate; samples were then incubated at 37 °C for 1 h. Subsequently, the reaction was stopped by adding 10 µl of lysine developer and left for additional 30 min at 37 °C. Samples were then read in an ELISA plate reader at 405 nm. Each sample was also treated with 2 µl (12 µM final concentration) of Trichostatin A (TSA) for 10 min before performing HDAC activity assay, these readings are also plotted and labelled with TSA, alongside the readings for serum samples not treated with TSA (W/O TSA). Experiments were performed in triplicates and average absorbance was plotted.

For HAT activity assay, 50 µl of serum was diluted in 80 µl $H_2O$ (final volume), and for background reading, 80 µl $H_2O$ was added in the reaction instead of the sample. Then, 50 µl of 2× HAT assay buffer was added followed by addition of 5 µl of each of the colorimetric substrates 1 and 2 and 8 µl NADH-generating enzyme. The samples were incubated at 37 °C for 1 to 4 h depending on the colour development. Subsequently, samples were read in an ELISA plate reader at 440 nm. Experiments were done in triplicates and average absorbance was plotted.

## Statistical analysis

All numerical data were expressed as average of values obtained ±standard deviation (SD). Statistical significance was determined by conducting paired Student's $t$ test.

## Results

### Isolation of serum histones

We developed a minimally invasive and cost effective, robust protocol for isolation of histones from serum samples. This method comprises of precipitation of total serum proteins by acid followed by purification of basic proteins by the acid extraction method. As the method involves precipitation and extraction by two acids, it is referred as Dual Acid Extraction (DAE) method. There are four key steps in the protocol: First step is the isolation of serum from the blood; second step is the total protein precipitation by use of trichloroacetic acid (TCA). TCA, unlike other chemicals, precipitates all the proteins irrespective of their molecular weight and is also independent of the physico-chemical properties of proteins; in the third step, histone extraction was carried out by use of the 0.2 M $H_2SO_4$ to separate histones from other proteins; and in the final step, acetone and acidified (hydrochloric acid) acetone were used for removing the traces of TCA or $H_2SO_4$ by replacement of sulphate group ($SO_4^{2-}$) with chloride group ($Cl^{1-}$) from isolated histones (Fig. 1). The quality of isolated histones was checked by loading on to a 18% SDS-PAGE followed by silver staining. The four core histones—H2A, H2B, H3 and H4—were visualized on the gel, but along with



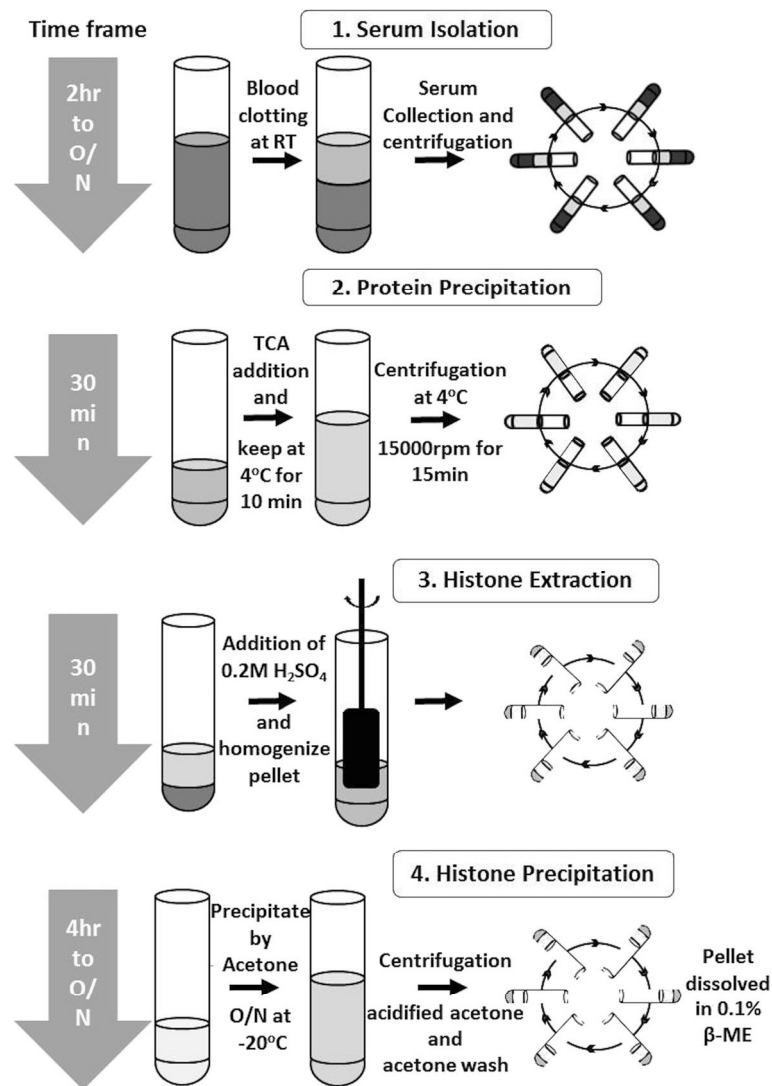**Fig. 1** Diagrammatic representation of protocol for isolation of histones from blood. The dual acid extraction (DAE) protocol involves four crucial steps: (1) serum isolation from blood; (2) total protein precipitation from serum by trichloroacetic acid; (3) histone extraction from precipitate by sulphuric acid and (4) precipitation, washing and dissolution of extracted histone precipitation

Reddy *et al. Clinical Epigenetics* (2017) 9:30

Page 5 of 11

them, other high molecular weight proteins were also noted (Fig. 2a).

To understand whether histone PTM changes observed in the tissue samples can be seen in the histones purified from the serum, we used a rat animal model system. Hepatocellular carcinoma (HCC) was induced in Sprague-Dawley rats by administering *N*-nitrosodiethylamine (NDEA) in drinking water at a concentration of 1 ppm/g body weight. After 120 days of NDEA administration, HCC was confirmed by haematoxylin and eosin (H&E) staining (Fig. 2b). The H &E-stained slides showed classical features of HCC like well-vascularized tumours with wide trabeculae, prominent acinar pattern, cytologic atypia and vascular invasion. Histones were isolated from both the liver tissues and serum of normal and tumour-bearing rats. The histones obtained from serum were quantified by Bradford method using BSA as a standard. The histone quantity in the serum of the HCC-bearing rat group was found to be significantly higher than the normal group (Fig. 2c (ii)). The concentration was 0.8 and 5.4 μg/mL serum for normal and tumour respectively. The purified histones from tissues (Fig. 2c (i)) as well as serum (Fig. 2c (ii)) were resolved on an 18% SDS-PAGE and silver stained to check their integrity. To confirm their identity, the histones were subjected to liquid chromatography-coupled mass spectrometry analysis (LC-MS). All the core histones were identified in both the serum samples (normal and tumour) with query coverage of >50% in case of normal and >30% for tumour (Fig. 2d). Also, of the total 13 proteins identified in serum of normal rats, three correspond to histone H2A and one each to histone H3.1, H2B and H4. In case of the serum of tumour-bearing rats, out of the 24 proteins identified, six were of histone H2A subtypes, two of histone H2B subtypes and one each of H3.1 and H4 histones (Fig. 2d and Table 1). Apart from histones, many other basic serum proteins were also identified in MS, the details of which are presented as a part of the Table 1. Histones isolated from the tissue were used as a positive control in LC-MS, where all the core histones were detected with >90% query coverage in both normal and HCC.



**Fig. 2** Resolution and identification of purified histones from paired serum and liver tissue of normal and tumour. **a** Silver stained 18% SDS-PAGE confirmed the integrity of the histones isolated from serum samples (1 and 2) of HCC-harboring rats by DAE protocol. All the core histones, H3, H2A, H2B and H4 are marked with an *arrow*, whereas the *star* marks high molecular weight proteins. **b** H&E-stained section of normal liver and HCC showing the altered histology in HCC at 20× and 40× magnification. **c** Silver-stained 18% SDS-PAGE showing the integrity of the purified histones loaded in increasing volumes (5, 10 and 15 μl) (*i*) samples of normal and tumour tissues and (*ii*) serum of normal and tumour bearing rats by the DAE protocol. The core histones H2A, H2B, H3 and H4 are marked. **d** Histones isolated from tissues and serum of both normal and tumour harboring rats are subjected to LC-MS after trypsin digestion. The obtained data on number of peptides of histones identified along with sequence coverage are tabulated and confirmed the identity of purified proteins by DAE method. *H&E* haematoxylin and eosin, *NDEA* N-nitrosodiethylamine

| Sample | No. of proteins identified | No. of Histones identified | Identity of Histones | Sequence coverage |
|---|---|---|---|---|
| Tissue Normal | 13 | 8 | H2A,H3,H2B,H4 | > 90% |
| Tissue Tumor | 11 | 5 | H2A,H3,H2B,H4 | >98% |
| Serum Normal | 13 | 6 | H2A,H3, H2B,H4 | >50% |
| Serum Tumor | 24 | 10 | H2A,H3,H2B,H4 | >30% |

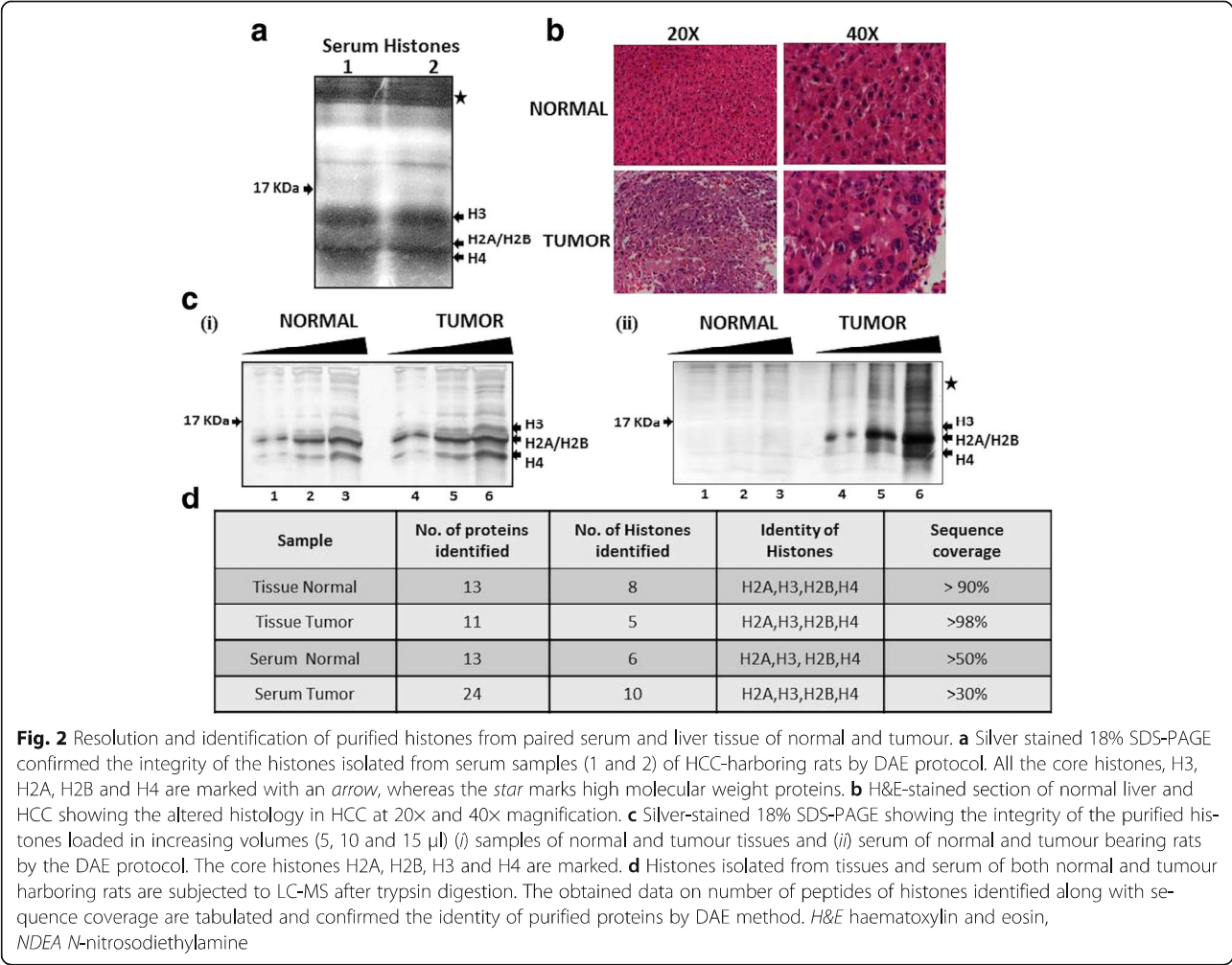Reddy *et al. Clinical Epigenetics* (2017) 9:30

Page 6 of 11

**Table 1** Total proteins detected in LC-MS of serum and tissue purified histories of normal and tumour samples

| Proteins | Tissue normal | Tissue tumour | Serum normal | Serum tumour |
|---|---|---|---|---|
| Histones | H2A type 1 (91.5%)<br>H2A type 2-A (91.5%)<br>H2A type 1-C (91.5%)<br>H2A type 1-F (86.1%)<br>H2B type 1E (91.5%)<br>H2B type 1C (91.5%)<br>H3.1 (99.2%)<br>H4 (59.2%) | H2A type 2-A (98.4%)<br>H2A type 1-C (98.4%)<br>H2B type 1E (98%)<br>H3.1 (99.2%)<br>H4 (98.4%) | H2A type 2-A (81.5%)<br>H2A type 1 (74.62%)<br>H2A type 1-C (50%)<br>H3.1 (59.2%)<br>H2B type 1E (57%)<br>H4 (60%) | H2A type 2-A (46.9%)<br>H2A type 1-C (33%)<br>H2A type 1-F (38.4%)<br>H2A type 1-E (30%)<br>H2A type 1 (33%)<br>H2A type 4 (33%)<br>H2B type 1E (57%)<br>H2B type 1C (35%)<br>H3.1 (40.7%)<br>H4 (47%) |
| Non-histones | Prelamin A/C (26%)<br>KDM5D (274%)<br>ESF1 (30.6%)<br>ESF1 homolog (23.9%)<br>Acid-sensing ion channel 5 (12.9%) | Prelamin A/C (62.4%)<br>KDM5D (30.32%)<br>EIF2S3Y (29.8%)<br>ESF1 homolog (41%)<br>Acid-sensing ion channel (17.9%)<br>Ribonuclease UK114 | Fibrinogen beta chain (65.75%)<br>Fibrinogen alpha chain (56.91%)<br>Isoform 2 of Fibrinogen alpha (69.45%)<br>Isoform 2 of Fibrinogen beta chain (70.96%)<br>Translation initiation factor elf-2B (46.1%)<br>Fertuin-B (47.6%)<br>Putative pheromone receptor (18.7%) | Fibrinogen beta chain (65.3%)<br>Fibrinogen alpha chain (43.3%)<br>Isoform 2 of Fibrinogen beta chain (67.4%)<br>Isoform 2 of Fibrinogen alpha chain (59.6%)<br>Matrix estracellular phosphoglycoprotein (60%)<br>Potassium voltage-gated channel subfamily C member 2 (30.8%)<br>ESF1 homolog (57.9%)<br>Alkaline phosphatase (57%)<br>Indoleamine 2.3-dioxygenase 1 (37.8%)<br>Aldehyde oxidase 2 (29.6%)<br>Astrocytic phosphoprotein (69.9%)<br>Transcription factor YY2 (32.9%)<br>Cannabinoid receptor 1 (11.1%)<br>Putative pheromone receptor (19.1%) |

## Histone PTM pattern is comparable in liver tissues and respective serum samples
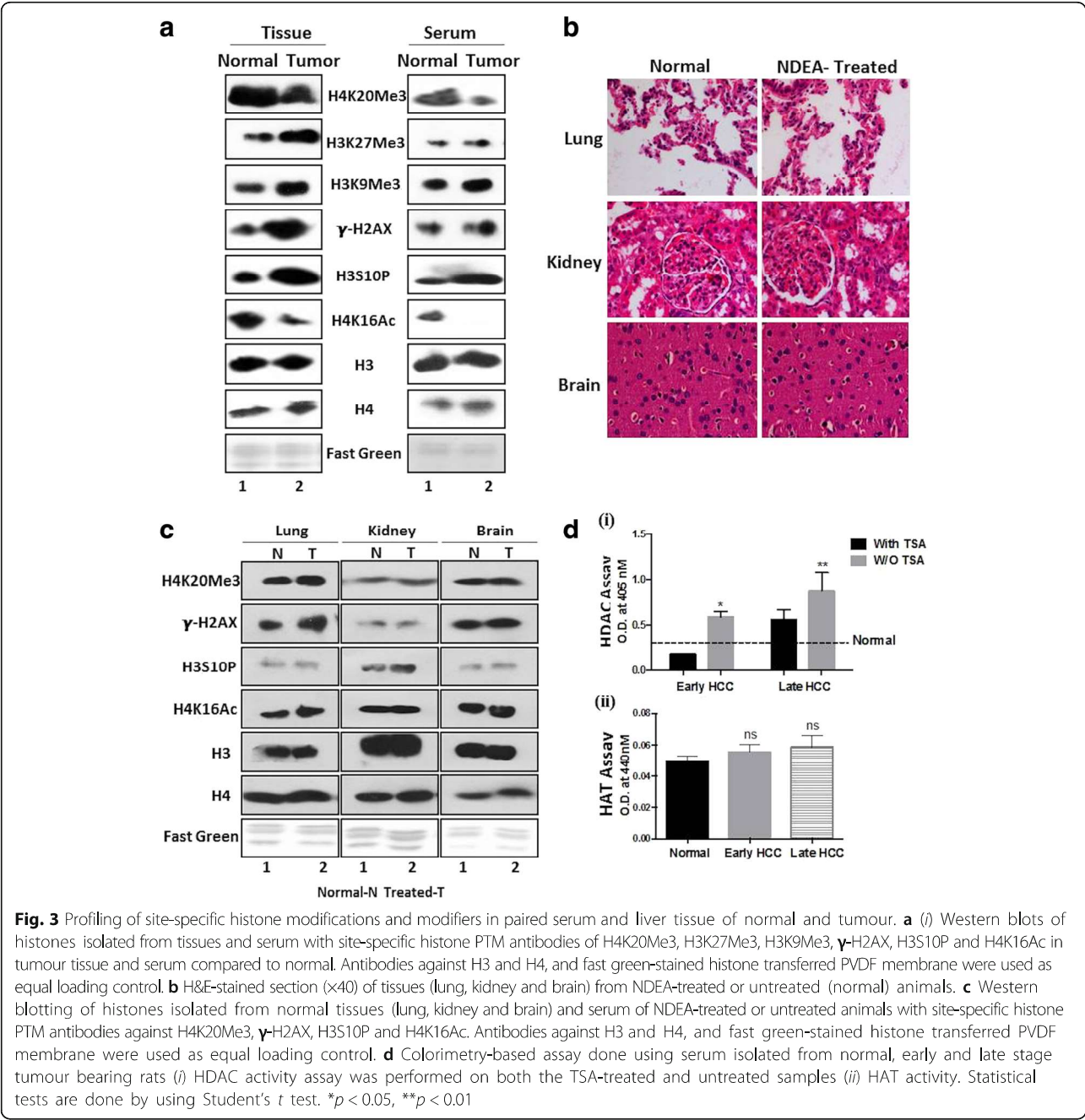
The histone PTM profiling of normal and HCC tissues was compared with respective serum samples by immuno-blotting with site-specific antibodies against H4K16Ac and H4K20Me3, as the loss of these marks are established as hallmark of human cancer [3]. As reported for human tumours, rat tumour tissue has also showed hypo-acetylation and hypo-methylation at H4K16 and H4K20 respectively (Fig. 3a). Interestingly, respective serum histones also showed the same pattern as of tissue histones (Fig. 3a). The other crucial histone PTM marks like γH2AX—a DNA damage mark, H3K27Me3 and H3K9Me3—transcriptional repressive marks and H3S1 0P—a mitotic mark, known to be deregulated in many of the human cancers [21, 22] were also probed. Intriguingly, we noted a significant increase in these marks in both the tumour sample tissue and serum (Fig. 3a). This shows that the key histone modifications like acetylation, methylation and phosphorylation are retained during the course of histone extraction from serum samples by DAE method and also profiling between tissue samples and their respective serum samples mirrored each other.

In order to understand that the changes seen in serum histone is due to liver tumour and not due to changes in the entire PTM profile of all the other organs, we profiled for histone PTMs in the lung, kidney and brain isolated from both the normal and NDEA-treated (tumour-bearing) animals. The tissues isolated from the animals treated with NDEA were first histologically examined for any aberrations by H&E staining (Fig. 3b).

Grossly, no differences were seen with respect to control tissues in untreated animals. Histones were then isolated and probed for site-specific PTM antibodies (Fig. 3c). The data demonstrates that the alterations of modifications are specific to tumour liver tissue and not to other histologically normal organs, thus strengthening that the liquid biopsy (serum histone) is very similar to its parent tissue (tumour tissue-liver) and hence can be used for clinical purpose.

## Increased HDAC activity in HCC tissues correlates with corresponding serum samples

So far, we have seen a positive correlation for histone PTMs in HCC, tissue and serum histones. We next contemplated whether the reported increased HDAC activity in tumour tissue [23] can also be seen in serum to understand how similar the liquid biopsy (serum) is to tissue biopsy in context of histone PTM modifiers. This is particularly interesting due to the observation of H4 hypo-acetylation seen in serum and HCC purified histones. HDAC activity assay conducted using serum isolated from normal, early (90 days NDEA treatment) and late stage (120 days NDEA treatment) HCC-bearing rats demonstrated the presence of significantly higher HDAC activity in both the tumour serum samples and normal serum (Fig. 3d (i)). Interestingly, the serum of early stage liver cancer animals also showed an elevated HDAC in comparison to normal, indicating that HDAC activity gradually increases during the course of HCC development (Fig. 3d (i)). As a proof of principle that the calorimetric assay performed is indeed a true measure of

Reddy *et al. Clinical Epigenetics* (2017) 9:30

Page 7 of 11



**Fig. 3** Profiling of site-specific histone modifications and modifiers in paired serum and liver tissue of normal and tumour. **a** (*i*) Western blots of histones isolated from tissues and serum with site-specific histone PTM antibodies of H4K20Me3, H3K27Me3, H3K9Me3, γ-H2AX, H3S10P and H4K16Ac in tumour tissue and serum compared to normal. Antibodies against H3 and H4, and fast green-stained histone transferred PVDF membrane were used as equal loading control. **b** H&E-stained section (×40) of tissues (lung, kidney and brain) from NDEA-treated or untreated (normal) animals. **c** Western blotting of histones isolated from normal tissues (lung, kidney and brain) and serum of NDEA-treated or untreated animals with site-specific histone PTM antibodies against H4K20Me3, γ-H2AX, H3S10P and H4K16Ac. Antibodies against H3 and H4, and fast green-stained histone transferred PVDF membrane were used as equal loading control. **d** Colorimetry-based assay done using serum isolated from normal, early and late stage tumour bearing rats (*i*) HDAC activity assay was performed on both the TSA-treated and untreated samples (*ii*) HAT activity. Statistical tests are done by using Student's *t* test. *$p < 0.05$, **$p < 0.01$

HDAC activity, treatment of serum samples with TSA was done prior to HDAC assay. As seen in (Fig. 3d (i)), the activity in samples treated with TSA is less compared to the untreated samples validating the robustness of the assay. To understand the status of HATs, levels of which are also reported to change in human tumours [24], we performed a HAT activity assay in normal, early and late stages of tumour serum, but no significant differences were observed, suggesting the H4 hypo-acetylation seen might be due to enhanced HDAC activity in tumour samples compared to normal (Fig. 3d (ii)).

Intrigued by the observation of elevated HDAC activity in tumour serum samples of rat model, we asked whether the HDAC activity can also be detected in human serum samples. To this end, we performed HDAC activity assay in serum isolated from six healthy subjects (normal) and 24 different types of cancer patients, including colorectal (CRC#6), buccal (BM#7), tongue (TNG#6), breast (BC#2) and glioblastoma (GBM#2). The histopathological details of patient samples included in the study are tabulated in Table 2. The cumulative analysis of all the 24 samples revealed a higher HDAC

Reddy *et al. Clinical Epigenetics* (2017) 9:30

Page 8 of 11

**Table 2** Histopathological analysis of human patient samples used in the study

| Sample | Origin | Histopathological analysis |
| --- | --- | --- |
| BM01 | Buccal | Moderately differentiated squamous carcinoma |
| BM02 | Buccal | Moderately differentiated squamous carcinoma |
| BM03 | Buccal | Moderately differentiated squamous carcinoma |
| BM04 | Buccal | Moderately differentiated squamous carcinoma |
| BM05 | Buccal | Moderately differentiated keratinizing squamous carcinoma |
| BM06 | Buccal | Moderately differentiated keratinizing squamous carcinoma |
| BM07 | Buccal | Poorly differentiated squamous carcinoma |
| TNG01 | Tongue | Moderately differentiated squamous carcinoma |
| TNG02 | Tongue | Moderately differentiated squamous carcinoma |
| TNG03 | Tongue | Moderately differentiated squamous carcinoma |
| TNG04 | Tongue | Squamous carcinoma |
| TNG05 | Tongue | Moderately differentiated squamous carcinoma |
| TNG06 | Tongue | Moderately differentiated squamous carcinoma |
| CRC01 | Colon | Moderately adenocarcinoma |
| CRC02 | Colon | Poorly differentiated adenocarcinoma |
| CRC03 | Colon | Moderately differentiated adenocarcinoma |
| CRC04 | Colon | Moderately differentiated adenocarcinoma |
| CRC05 | Rectum | Moderately differentiated adenocarcinoma |
| CRC06 | Rectum | Adenocarcinoma |
| BC01 | Breast | Infitrating duct carcinoma, Grade II |
| BC02 | Breast | Infitrating lobular carcinoma, Grade II |
| GBM01 | Glioblastoma | Glioblastoma (WHO grade IV) |
| GBM02 | Glioblastoma | Glioblastoma (WHO grade IV) |

activity in serum of cancer patients compared to normal (Fig. 4a) with no significant change in HAT activity (Fig. 4b). Also, grouping of serum samples based on the cancer type shows an elevated activity in most of the samples of CRC (Fig. 4c), buccal (Fig. 4d), tongue (Fig. 4e), and breast and glioblsatoma (Fig. 4f).

Interestingly, we found that even with a sample size of 24, the HDAC activity is different amongst each patient sample, therefore, highlighting the importance of subgrouping the patients on the basis of inherent epigenetic background for success of epigenetic drugs (epi-drug) therapy. Thus, monitoring the HDAC activity in the serum sample has helped us to categorize the patients into two subgroups: (1) high HDAC and (2) low HDAC (Fig. 4g). Group 1 can further be subdivided into two, high and moderate HDAC activity groups (Fig. 4g). This subgrouping of patients on the basis of HDAC activity will assist in selection of patients, determining the dose of epi-drug, thus increasing the success of therapy.

During the diagnosis of a disease like cancer, measurement of many serum based biomarkers is usually performed. One such marker is the quantification of serum CEA levels in CRC patients. We observed differential levels of CEA amongst the six CRC samples used in the study. Interestingly, high CEA levels seen for CRC02 and CRC05 samples correlated with high HDAC activity in comparison to other samples with low CEA values (Fig. 4h). Thus, serum based measurement of HDAC activity compares positively to CEA, a cancer biomarker for CRC.
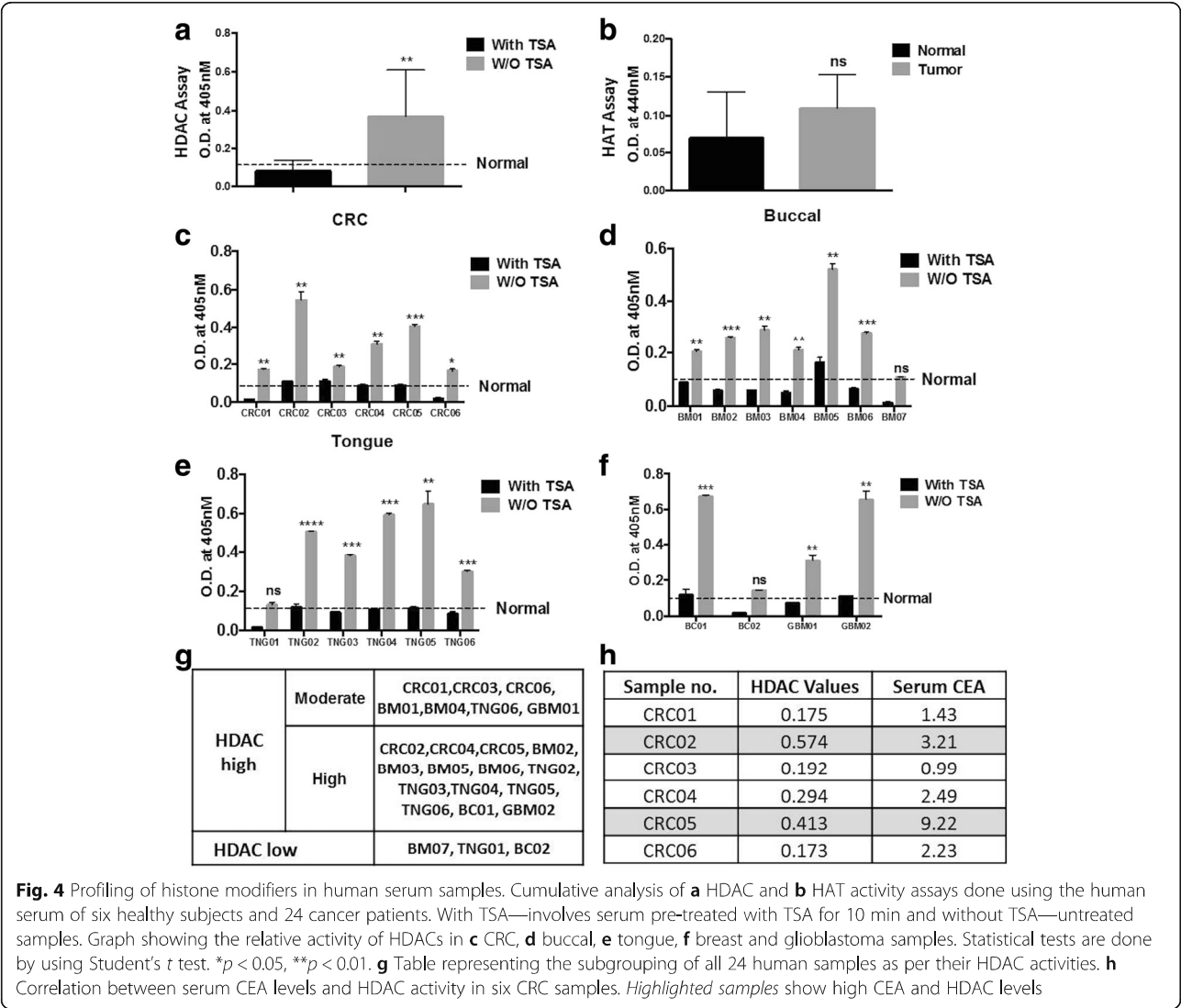
## Discussion

The DAE protocol developed for the isolation of histones from serum samples is simple, robust, time efficient and cost effective. Further, the comparison of key site-specific histone PTMs in tissue versus serum, for both normal and tumour samples, has revealed a similar pattern amongst the respective biological samples. Also, we illustrate for the first time a higher HDAC activity in serum tumour sample compared to normal.

Earlier protocols for isolation of cNUCs are based on chromatin immunoprecipitation (ChIP) by specific histone antibodies. ChIP depends critically on the quality of the antibody and is not cost-effective. Though numerous histone antibodies as ChIP-grade are available, they need stringent validation by western blotting and MS, because of their cross-reactivity with unmodified histones, similar histone modifications and some with non-histone proteins. The developed protocol overcomes all the limitations of the existing ChIP method as it is based on dual acid extraction. The good quality and quantity of purified histones by this novel technique has opened a new avenue for studying the pattern of histone PTMs as well as histone variants in serum samples by western blotting or mass spectrometry in different pathophysiological states.

To gain insights into global serum histone PTM pattern and understand whether the observed alteration matches with that of the cancer tissue, NDEA-induced HCC rat model system has been used. The quantity of histones isolated from the normal serum was very less compared to the serum samples of NDEA-induced HCC rats (Fig. 2c (ii)). This could be directly attributed to the increased cell death seen in diseased conditions as opposed to the healthy subjects, due to which the abundance of cNUCs and hence histones will be more in a serum sample of diseased state. This is in conformity with the earlier reports where elevated cNUCs are observed in various human cancers [6, 10, 12, 25].

Studies on global histone modifications across various human cancers have identified alterations in a panel of histone PTMs [26]. The loss of H4K16Ac and H4K20Me3 are now regarded as the hallmark of most human cancers [3]. Interestingly, we noted that these hallmarks are even true for the animal model system. Furthermore, similar changes are observed in serum histones also proving that indeed they are true hallmarks which change during

Reddy *et al. Clinical Epigenetics* (2017) 9:30

Page 9 of 11



**Fig. 4** Profiling of histone modifiers in human serum samples. Cumulative analysis of **a** HDAC and **b** HAT activity assays done using the human serum of six healthy subjects and 24 cancer patients. With TSA—involves serum pre-treated with TSA for 10 min and without TSA—untreated samples. Graph showing the relative activity of HDACs in **c** CRC, **d** buccal, **e** tongue, **f** breast and glioblastoma samples. Statistical tests are done by using Student's *t* test. *$p < 0.05$, **$p < 0.01$. **g** Table representing the subgrouping of all 24 human samples as per their HDAC activities. **h** Correlation between serum CEA levels and HDAC activity in six CRC samples. *Highlighted samples* show high CEA and HDAC levels

cancer, irrespective of the cancer type in the study, species used and source of biological samples (liquid or solid biopsy). Profiling for other histone PTMs—H3K27Me3, H3K9Me3, γH2AX and H3S10P, in both tissue and serum showed a same pattern of increase in tumour tissue and serum samples. Further, we also reveal that the changes in the histone PTM pattern observed in serum mirrors only liver tissue and no other organs, thus proving that the histones in serum are from tumour tissue.

Earlier studies had shown the presence of acetylated histones in blood cells, but its levels were not correlated with tumour tissue [27]. Such studies on global histone modifications are of importance because of their prognostic utility and predictive markers for recurrence. Now with the serum histones showing a similar pattern of histone PTMs as of tumour tissue, liquid biopsy (non-invasive) will be a good alternative to tissue biopsy (invasive) for monitoring the disease regression/progression in cancer patients.

Further, the antitumour effects of histone deacetylase or histone methyltransferase inhibitors could be evaluated by monitoring changes in the quantities of the corresponding modification on the circulating histones thus overcoming the limitation of earlier studies wherein histones of blood cells were used.
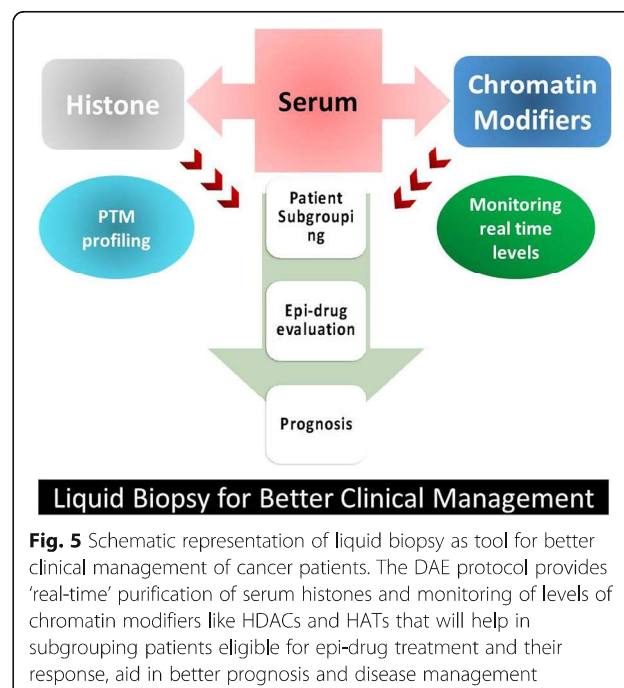
Altered histone acetylation levels in cancer are the result of the imbalance of the activities of HAT and HDAC. Many reports have emphasized the altered levels of these enzymes, especially HDACs in various cancers [28]. Our data of an increased HDAC activity in serum and tumour tissue samples compared to normal is in accordance with the earlier reports. Thus, the present observation of HDAC activity in serum allows us to monitor the level of HDAC and possible tumour status in response to histone-modifying enzyme inhibitors in real time by liquid biopsy. Interestingly, some studies on global proteomic profiling of serum proteins has earlier

Reddy *et al. Clinical Epigenetics* (2017) 9:30

Page 10 of 11

reported the presence of HDACs in serum, thus it is not surprising that HDAC activity is detected in serum [29, 30]. Intriguingly, measurement of HDAC activity in early (90 days NDEA treatment) and late (120 days NDEA treatment) stages of liver cancer in an animal model system revealed a gradual increase in HDAC activity as the animal develops a tumour. This observation proves that early monitoring of HDAC activity may assist in better diagnosis of cancer. Further, the assay can be employed to monitor the naive cancer, recurring and drug resistant tumours, where in periodic monitoring of HDAC activity in patients diagnosed with cancer will aid in their improved clinical management. However, large studies including more cancer patients at various stages, undergoing diverse chemotherapeutic treatments in combination with epidrugs will provide conclusive evidences and help in employing the proposed hypothesis for better disease management.

Owing to the increased HDACs, use of HDAC inhibitors for treatment of cancer is considered to be a good treatment regime. But so far, the use of HDAC inhibitors had limited success in solid tumours because of severe toxicities and other fatal effects [31]. One of the reasons behind the failure or limited success of HDAC inhibitors has been attributed to the inherent epigenetic background of the patients, where some may have high expression of HDACs others low levels [32, 33]. This can further be seen in our data, where all the patients showed different extent of HDAC levels (Fig. 4c, f). Therefore, administering HDAC inhibitors to patients with inherent low levels of HDACs may be fatal. For example, based on our data, we have segregated the samples into two groups, HDAC high and HDAC low (Fig. 4g). Treating the first group patients with HDAC inhibitors will be beneficial, as this group show elevated levels of these enzymes. Furthermore, this group can be subdivided into two, which can help in deciding the dose and time span of epi-drug therapy, where a high HDAC activity patient can be given high doses of drugs for a longer span than the others. As for the second group, epi-drug treatment might not be of much benefit. Thus, serum-based detection of histone modifiers like HDAC/HAT will help with subgrouping of patients and personalize the treatment, monitor patient's health status during treatment with histone modifier inhibitors and response of the individual's tumour to treatment (Fig. 5).

## Conclusions

In summary, the developed DAE technique for isolating serum histones will provide real time information of epigenome which will be helpful in understanding the overlap between paired serum and cancer tissue histone proteome by high-end proteomics. Importantly, our data gave a novel rationale for using serum histone proteomics



**Fig. 5** Schematic representation of liquid biopsy as tool for better clinical management of cancer patients. The DAE protocol provides 'real-time' purification of serum histones and monitoring of levels of chromatin modifiers like HDACs and HATs that will help in subgrouping patients eligible for epi-drug treatment and their response, aid in better prognosis and disease management

as a predictive tool for disease progression. This information will allow the development of efficient strategies for the treatment and better management of the underlying disease. The combination of different histone marks rather than a single histone mark is believed to further enhance sensitivity and specificity of detection of these marks and hence improve cancer management.

**Authors' contributions**
SG and DR contributed to the conception, design and major portion of the manuscript writing and editing. DR, BK and RP contributed in performing the experiments. The paper was critically read by all the authors and approved for publication.

**Availability of data and materials**
The protocols are detailed in the manuscript for scientists wishing to use them for their research work. Also, the supporting data will be made available to editors and peer-reviewers, if required for the purposes of evaluating the manuscript.

**Competing interests**
The authors declare that they have no competing interests.

Reddy *et al. Clinical Epigenetics* (2017) 9:30

Page 11 of 11

**Ethics approval**
The protocol was reviewed and approved by the Institutional Review Board and Ethics Committee of Tata Memorial Centre, ACTREC, Navi Mumbai (Project Number 164). And the waiver of consent was granted for the proposed study as the samples were collected retrospectively from TTR. Therefore, consent for publication is not applicable for our study. Also, the animal study is approved by the Institute Animal Ethics Committee of Advanced Centre for Treatment Research and Education in Cancer (ACTREC), Tata Memorial Centre, Navi Mumbai, India (IAEC# 04/2014).

**Publisher's Note**
Springer Nature remains neutral with regard to jurisdictional claims in published maps and institutional affiliations.

**References**
1. Luger K, Mader AW, Richmond RK, Sargent DF, Richmond TJ. Crystal structure of the nucleosome core particle at 2.8 A resolution. Nature. 1997; 389:251–60.
2. Bannister AJ, Kouzarides T. Regulation of chromatin by histone modifications. Cell Res. 2011;21:381–95.
3. Fraga MF, Ballestar E, Villar-Garea A, Boix-Chornet M, Espada J, Schotta G, et al. Loss of acetylation at Lys16 and trimethylation at Lys20 of histone H4 is a common hallmark of human cancer. Nat Genet. 2005;37:391–400.
4. Elsheikh SE, Green AR, Rakha EA, Powe DG, Ahmed RA, Collins HM, et al. Global histone modifications in breast cancer correlate with tumor phenotypes, prognostic factors, and patient outcome. Cancer Res. 2009;69: 3802–9.
5. Seligson DB, Horvath S, Shi T, Yu H, Tze S, Grunstein M, et al. Global histone modification patterns predict risk of prostate cancer recurrence. Nature. 2005;435:1262–6.
6. Holdenrieder S, Nagel D, Schalhorn A, Heinemann V, Wilkowski R, Von Pawel J, et al. Clinical relevance of circulating nucleosomes in cancer. Ann N Y Acad Sci. 2008;1137:180–9.
7. Karachaliou N, Mayo-De-Las-Casas C, Molina-Vila MA, Rosell R. Real-time liquid biopsies become a reality in cancer treatment. Ann Transl Med. 2015;3:36.
8. Chen R, Kang R, Fan X-G, Tang D. Release and activity of histone in diseases. Cell Death Dis. 2014;5:e1370.
9. Stroun M, Maurice P, Vasioukhin V, Lyautey J, Lederrey C, Lefort F, et al. The origin and mechanism of circulating DNA. Ann N Y Acad Sci. 2000;906:161–8.
10. Holdenrieder S, Stieber P, Bodenmüller H, Busch M, Fertig G, Fürst H, et al. Nucleosomes in serum of patients with benign and malignant diseases. Int J Cancer. 2001;95:114–20.
11. Shapiro B, Chakrabarty M, Cohn EM, Leon SA. Determination of circulating DNA levels in patients with benign or malignant gastrointestinal disease. Cancer. 1983;51:2116–20.
12. Holdenrieder S, Stieber P, von Pawel J, Raith H, Nagel D, Feldmann K, et al. Circulating nucleosomes predict the response to chemotherapy in patients with advanced non–small cell lung cancer. Am Assoc Cancer Res. 2004;10:5981–7.
13. Holdenrieder S, Dharuman Y, Standop J, Trimpop N, Herzog M, Hettwer K, et al. Novel serum nucleosomics biomarkers for the detection of colorectal cancer. Anticancer Res. 2014;34:2357–62.
14. Deligezer U, Akisik EE, Erten N, Dalay N. Sequence-specific histone methylation is detectable on circulating nucleosomes in plasma. Clin Chem. 2008;54:1125–31.
15. Leszinski G, Gezer U, Siegele B, Stoetzer O, Holdenrieder S. Relevance of histone marks H3K9me3 and H4K20me3 in cancer. Anticancer Res. 2012;32: 2199–205.
16. Khare SP, Sharma A, Deodhar KK, Gupta S. Overexpression of histone variant H2A.1 and cellular transformation are related in N-nitrosodiethylamine-induced sequential hepatocarcinogenesis. Exp Biol Med (Maywood). 2011; 236:30–5.
17. Parasuraman S, Raveendran R, Kesavan R. Blood sample collection in small laboratory animals. J Pharmacol Pharmacother. 2010;1:87–93.
18. Ryan CA, Annunziato AT. Separation of histone variants and post-translationally modified isoforms by triton/acetic acid/urea polyacrylamide gel electrophoresis. Curr Protoc Mol Biol. 2001. May; Chapter 21:Unit 21.2. doi:10.1002/0471142727.mb2102s45.
19. Chevallet M, Luche S, Rabilloud T. Silver staining of proteins in polyacrylamide gels. Nat Protoc. 2006;1:1852–8.
20. Yu Y-Q, Gilar M, Lee PJ, Bouvier ESP, Gebler JC. Enzyme-friendly, mass spectrometry-compatible surfactant for in-solution enzymatic digestion of proteins. Anal Chem. 2003;75:6023–8.
21. Bonner WM, Redon CE, Dickey JS, Nakamura AJ, Olga A, Solier S, et al. GammaH2AX and cancer. Nat Rev Cancer. 2011;8:957–67.
22. Khan SA, Amnekar R, Khade B, Barreto SG, Ramadwar M, Shrikhande S V, et al. of histone H3 serine 10 phosphorylation defines distance-dependent prognostic value of negative resection margin in gastric cancer. Clin Epigenetics. 2016;8(1):88.
23. Wang L, Zou X, Berger AD, Twiss C, Peng Y, Li Y, et al. Increased expression of histone deacetylaces (HDACs) and inhibition of prostate cancer growth and invasion by HDAC inhibitor SAHA. Am J Transl Res. 2009;1(1):62–71.
24. Cohen I, Schneider R. Histone modifiers in cancer: friends or foes? Genes Cancer. 2011;2(6):631–647.
25. Holdenrieder S, Stieber P, Bodenmuller H, Busch M, Von Pawel J, Schalhorn A, et al. Circulating nucleosomes in serum. Ann N Y Acad Sci. 2001;945:93–102.
26. Khan SA, Reddy D, Gupta S. Global histone post-translationl modifications and cancer: biomarkers for diagnosis, prognosis and treatment? World J of Biol Chem. 2015;6:333–46.
27. Rigby L, Muscat A, Ashley D, Algar E. Methods for the analysis of histone H3 and H4 acetylation in blood. Epigenetics. 2012;7(8):875–82.
28. Glozak MA, Seto E. Histone deacetylases and cancer. Oncogene. 2007; 26:5420–32.
29. Liu X, Valentine SJ, Plasencia MD. Mapping the human plasma proteome by SCX-LC-IMS-MS. J Am Soc Mass Spectrom. 2007;18:1249–64.
30. Sennels L, Salek M, Lomas L, Boschetti E, Righetti PG, Rappsilber J. Proteomic analysis of human blood serum using peptide library beads. J Proteome Res. 2007;6:4055–62.
31. Qiu T, Zhou L, Zhu W, Wang T, Wang J, Shu Y, et al. Effects of treatment with histone deacetylase inhibitors in solid tumors: a review based on 30 clinical trials. Futur Oncol. 2013;9:255–69.
32. Wagner JM, Hackanson B, Lübbert M, Jung M. Histone deacetylase (HDAC) inhibitors in recent clinical trials for cancer therapy. Clin Epigenetics. 2010;1:117–36.
33. Gryder BE, Sodji QH, Oyelere AK. Targeted cancer therapy: giving histone deacetylase inhibitors all they need to succeed. Future Med Chem. 2012;4:505–24.

# Genomic characterization and dynamic methylation of promoter facilitates transcriptional regulation of H2A variants, H2A.1 and H2A.2 in various pathophysiological states of hepatocyte

Monica Tyagi [a,b,1,2], Divya Reddy [a,b,2], Sanjay Gupta [a,b,*]

[a] Epigenetics and Chromatin Biology Group, Gupta Lab, Cancer Research Institute, Advanced Centre for Treatment, Research and Education in Cancer (ACTREC), Tata Memorial Centre, Kharghar, Navi Mumbai, 410210 MH, India
[b] Homi Bhabha National Institute, Training School Complex, Anushakti Nagar, Mumbai, MH 400085, India

## ARTICLE INFO

## ABSTRACT

Differential expression of homomorphous variants of H2A family of histone H2A.1 and H2A.2 have been associated with hepatocellular carcinoma and maintenance of undifferentiated state of hepatocyte. However, not much is known about the transcriptional regulation of these H2A variants. The current study revealed the presence of 43 bp 5′-regulatory region upstream of translation start site and a 26 bp 3′ stem loop conserved region for both the H2A.1 and H2A.2 variants. However, alignment of both H2A.1 and H2A.2 5′-untranslated region (UTR) sequences revealed no significant degree of homology between them despite the coding exon being very similar amongst the variants. Further, transient transfection coupled with dual luciferase assay of cloned 5′ upstream sequences of H2A.1 and H2A.2 of length 1.2 (−1056 to +144) and 1.379 kb (−1160 to +219) from experimentally identified 5′UTR in rat liver cell line (CL38) confirmed their promoter activity. Moreover, in silico analysis revealed a presence of multiple CpG sites interspersed in the cloned promoter of H2A.1 and a CpG island near TSS for H2A.2, suggesting that histone variants transcription might be regulated epigenetically. Indeed, treatment with DNMT and HDAC inhibitors increased the expression of H2A.2 with no significant change in H2A.1 levels. Further, methyl DNA immunoprecipitation coupled with quantitative analysis of DNA methylation using real-time PCR revealed hypo-methylation and hyper-methylation of H2A.1 and H2A.2 respectively in embryonic and HCC compared to control adult liver tissue. Collectively, the data suggests that differential DNA methylation on histone promoters is a dynamic player regulating their expression status in different pathophysiological stages of liver.

© 2017 Elsevier Ltd. All rights reserved.

## 1. Introduction

Genomic DNA is hierarchically packaged by histones into nucleosomes and array of these nucleosomes along with non-histone proteins further forms a compact chromatin structure inside the eukaryotic nucleus. The chromatin structure, acting as a barrier in all DNA-mediated cellular processes is regulated through ATP-dependent chromatin remodelling, post translational modification of histones and incorporation of histone variants into the nucleosomes (Becker and Ho, 2002). Histone variants are the non-allelic subtypes of canonical histones and multiple variants of H1, H2A, H2B and H3 histones have been identified. The variants are grouped as homomorphous and heteromorphous or replication-dependent and replication-independent on the basis of amino acid sequence similarity or expression during different stages of cell cycle, respectively (Marzluff et al., 2009).

Earlier studies from our lab have shown the differential expression of H2A variants, higher level of H2A.1 both in hepatocellular carcinoma and embryonic liver whereas H2A.2 expresses in normal adult liver in rats (Khare et al., 2011; Tyagi et al., 2014). H2A.1/H2A.2 proportion has been shown to decrease during development and differentiation of rat brain cortical neurons and during in vitro differentiation and aging of fibroblasts (Piña and Suau, 1987; Rogakou and Sekeripataryas, 1993; Urban and Zweidler, 1983). H2A.1 and

H2A.2 are 130 amino acids each and differ at three positions *viz.* 16 (Threonine to Serine), 51 (Leucine to Methionine) and 99 (Arginine to Lysine). Recently, a replication dependent histone coded by human HIST1H2AC gene locus, sequence similar to rat H2A.1 apart from the change in 15th position, has been associated with cell proliferation and tumorigenicity of bladder cancer cells (Singh et al., 2013). Collectively, these reports strongly suggest that imbalance in intricately maintained levels of the H2A variants may modulate the highly dynamic nature of the nucleosomes, reorganizing the chromatin landscape for differential gene expression profile and might be a critical event in carcinogenesis, embryogenesis, cellular differentiation and cell cycle control (Kouzarides, 2007).

The genes encoding for homomorphous histone variants, H2A.1 and H2A.2 in rat are mapped on chromosome 17p for H2A.1 and H2A.2 on 2q, thereby, suggesting their specific gene promoters and potentially different transcription regulatory mechanisms. Although regulation of H2A.1 and H2A.2 expression remains largely unknown, the observation that their mRNA levels vary significantly under different physiological states suggests that H2A.1 and H2A.2 are also regulated at the transcriptional level. Promoter activity affected by epigenetic modifications plays a critical role in regulating the expression of specific genes. *In silico* analysis of predicted promoter sequence for H2A.1 (NCBI Gene ID: 502125 and RGD Gene ID: 1594367) and H2A.2 (NCBI: 365877 and RGD: 1307165) suggests the presence of CpG sites and island respectively. Increased methylation of CpG islands at 5′ end of a gene is associated with gene repression. The possible mechanisms for repression include interference with transcription factor binding or through the recruitment of repressors proteins Lewis and Bird (2003). DNA methylation was initially considered a stable epigenetic mark; however, the discovery of 5-hydroxymethylcytosine (5-hmC) has revised this notion. Recent studies have shown that 5-hmC apart from being an intermediate product of an active demethylation process can also act as a stable epigenetic mark whose role in transcription regulation is now well appreciated. Indeed, enrichment of 5-hmC on genes has been associated with the activation of transcription (Kroeze et al., 2015). However, it is unknown whether DNA methylation of the H2A.1 and H2A.2 promoters are involved in regulating the divers/e expression profile of these two among different pathophysiological states.

In the present study we have structurally identified transcriptional start site, 5′UTR and conserved stem-loop with 62 bp and 88 bp long 3′UTR of H2A.1 and H2A.2 mRNA's. Further, the upstream 5′-flanking region of both the genes was identified, cloned and their transcriptional activity was confirmed. The cDNA sequences of H2A.1 and H2A.2 cDNA are 498 bp and 525 bp long containing a stem loop at their 3′UTR and also have been submitted to NCBI database with accession numbers JX-661508 and JX-661509 respectively. Moreover, we explored the methylation status of the CpG sites and CpG-island that spans the H2A.1 and H2A.2 promoters respectively, in hepatocellular carcinoma, embryonic liver and corresponding normal liver tissues and elucidate a potential molecular mechanism for the methylation-mediated alteration in histones H2A.1 and H2A.2 promoter activity.

## 2. Materials and methods

### 2.1. Animal experiments

All the experiments were carried out on male Sprauge–Dawley rats (*Rattus norvegicus*). The proposal to use the animals was duly approved by Institute Animal Ethics Committee, ACTREC, and the Committee, which is endorsed by the committee for the Purpose of Control and Supervision on Animals, Government of India.

The normal and N-nitrosodiethylamine (200 ppm/gm body weight) treated animals ($n = 5$, for each set of experiments) were euthanized after 4 months of treatment (Khare et al., 2011). The animals (22–24 weeks) for liver regeneration studies were subjected to two-third partial hepatectomy (PH). The surgeries were performed under sterile conditions as per protocol. A horizontal incision was made, approximately 2–3 cm long, below Xiphoid cartilage. Then left lateral and median lobes of liver (50–70% liver) were resected, and muscle and skin layers were closed. Animals were provided with an external source of heat for recovery. Animals were sacrificed, and regenerating liver tissues were collected after 36 h post PH in synchrony with DNA synthesis and were processed as mentioned earlier. Furthermore, for embryonic liver development studies, pregnant rats ($n = 6$, for each set of experiments) confirmed by the vaginal plug were obtained. The developing liver ($n = 6$, for each time point) was excised on e15 and processed as mentioned earlier (Tyagi et al., 2014).

### 2.2. 5′RLM-RACE to identify transcriptional start site

Intact total RNA isolated from rat liver tissue with A260/280 of ~2.0 with 2:1 ratio of 28S:18S rRNA was used to identify transcriptional start site using Ambion 5′RLM-RACE kit as per manufacturer's instructions. Briefly, decapped adaptor-linked mRNA was used as template to synthesize the first-strand cDNA by reverse transcriptase in presence of random primers (Fermentas RT-PCR Kit). The cap site region of these RNA was identified by reverse transcription-polymerase chain reaction (PCR). The PCR was performed using a sense DNA primer complementary to adaptor oligo-(5′-GCTGATGGCGATGAATGAACACTG-3′) paired with the gene-specific antisense primers either for H2A.1 or H2A.2. Samples were amplified for 35 cycles under the following conditions: denaturation for 30 s at 94 °C, annealing for 45 s at 56.4 °C, and extension for 1 min 30 s at 72 °C. The PCR products were excised from the 1.5% low melting temperature agarose gel, cloned into TA vector, and sequenced for identification of 5′UTR (Applied Bio systems Inc.). The primers used throughout the experiments are tabulated in Table 1.

### 2.3. mRNA circularization for mapping of 3′Untranslated region

Total RNA (10 μg) isolated from rat liver tissue was treated with calf intestine phosphatase (CIP) enzyme to remove 5′phosphate group followed by mRNA decapping by tobacco pyrophosphatase (TAP) enzyme treatment. Decapped mRNA was allowed to undergo circularization with 20 U of T4 RNA ligase in 400 μl reaction incubated at 16 °C for 16 h. Using gene specific primer cDNA synthesis was carried out by M-MLV reverse transcriptase enzyme (MBI-Fermentas). PCR was carried out by using forward reverse gene specific primer (Table 1) with cDNA as templates under reaction condition as follows: denaturation 94 °C for 45 s, denaturation for 30 s, annealing at 56.4 °C for 30 s, extension at 72 °C for 1 min 30 s. The amplified PCR product was extracted from 1.5% low melting agarose gel, further cloned in pTZRT vector. The clones were confirmed by sequencing for identification of 3′UTR and validation of 5′UTR.

### 2.4. Cloning of sequences encompassing upstream of 5′UTR

High MW DNA was used as template to amplify the 5′ upstream sequences of 1.2 (−1056 to +144) and 1.379 kb (−1160 to +219) using gene specific primers mentioned in Table 1 from experimentally identified 5′UTR and *in silico* predicated H2A.1 and H2A.2 gene promoters. PCR amplified DNA was cloned in pGL3 basic vector at KpnI-XhoI site yielding the promoter reporter plasmids. Further, the deletion constructs were prepared for both the genes. The software Motif finder (http://motifsearch.

**Table 1**
Primers sequences for cDNA synthesis, UTR's, promoter activity, quantitative PCR and methylation DNA immunoprecipitation.

| | Primer sequence |
|---|---|
| **A. cDNA synthesis** | |
| FH2A.1 | 5′-GTCGGATCCATGTCTGGACGCGGCAAACAA-3′ |
| RH2A.1 | 5′-GTCGAATTCCTATTATTTGCCCTTGGCCTTGTG-3′ |
| FH2A.2 | 5′-GTCGGATCCATGTCCGGCCGTGGCAAGCAA-3′ |
| RH2A.2 | 5′-GTCGAATTCTTATCACTTGCCCTTCGCCTTATG-3′ |
| **B. 5′UTR** | |
| H2A.1 | 5′-GTCGAATTCCTATTATTTGCCCTTGGCCTTGTG-3′ |
| Adaptor primer | 5′-GCTGATGGCGATGAATGAACACTG-'3 |
| H2A.2 | 5′-GTCGAATTCTTATCACTTGCCCTTCGCCTTATG-3′ |
| Adaptor primer | 5′-CGCGGATCCGAACACTGCGTTTGCTGGCTTTGATG-3′ |
| **C. 3′UTR** | |
| H2A. 1 | 5′ATGAGGAACTCAACAAGCTGCTGGGCCGTGTGA3′ |
| For cDNA | 5′CGTAGTTGCCTTTGCGAAGCAAACGGTGCACA 3′ |
| H2A.2 | 5′-CAAAGTGACGATCGCGCAGG-3′ |
| For cDNA | 5′-CGGTCACAACCAGGAAACTGT-3′ |
| **D. PROMOTER** | |
| −1056 FH2A. 1 | 5′GGTACCAGCAATGTGAATGTGTAAGCG3′ |
| +144 RH2A. 1 | 5′CTCGAGAAACGGTGCACACGGCCCACG3′ |
| −1160 FH2A.2 | 5′GGTACCCTGAACCCTTGATCCATCTCTC 3′ |
| +219 RH2A.2 | 5′CTCGAGATCTCGGCGGTCAGGTACT3′ |
| −131 FH2A. 1 | 5′-GGTACCAAGAGTACGCCTTATGCAAATGA-3′ |
| −135FH2A.2 | 5′-GGTACCGGTTCTTAACTCAGGCCTTCTTG- 3′ |
| **E. REAL TIME PCR** | |
| H2A.1 F | 5′-CTGTGCTGGAGTACCTGACG-3′ |
| H2A.1 R | 5′-TGTGGTGGCTCTCAGTCTTC-3′ |
| H2A.2 F | 5′-GAAGACGGAGAGCCACCATA-3′ |
| H2A.2 R | 5′-GGAAGAGTAGGGCACACGAC-3′ |
| 18S F | 5′-CGCGGTTCTATTTTGTTGGT-3′ |
| 18S R | 5′-AGTCGGCATCGTTTATGGTC-3′ |
| Tslc−1 F | 5′ TTATCCTCTGCAAGGCCTAAC 3′ |
| Tslc−1 R | 5′ TGTTGAGGCATTTCGTCATC 3′ |
| **F. METHYL-DNA IP** | |
| H2A. 1 MeIP F | 5′CGTCGTTCGCCTACAGCTT3′ |
| H2A. 1 MeIP R | 5′TGCCGCGTCCAGACATAATT3′ |
| H2A. 2 MeIP F | 5′CGCAACAACGGCCGCACGCA3′ |
| H2A. 2 MeIP R | 5′CATAAGCCCGGCTCCCTGGC3′ |
| H19 MeIP F | 5′GAGCTAGGGTTGGAGAGGAAC3′ |
| H19 MeIP R | 5′GGTCGAACCCTTCCCAGCA3′ |

com) and Bio-base-Transfac (http://www.biobase-international.com/product/transcription-factor-binding-sites) was used to analyze potential transcription factors binding sites.

### 2.5. Cell culture, transient transfection and luciferase assay

Rat CL38 hepatoma cells were maintained in DMEM medium supplemented with 10% heat inactivated fetal bovine serum, 1% antibiotic in humidified 5% $CO_2$, 95% air at 37 °C. Cell culture was passaged twice a week to maintain a cell density of $1 \times 10^6$ cells/ml. Cells were counted in haemocytometer chamber and viability assayed by 0.1% trypan blue. For the transfection experiments, the cells were grown on 12-well plate to ~40% confluence. Either 1.5 μg pGL3-Basic plasmid or an equivalent molar amount of test plasmid was co-transfected into CL38 cells along with 2.5 ng of pRL-TK plasmid using cation-based transfection reagent, Turbofect (MBI-Fermentas), according to the manufacturer's instructions. The pRL-TK vector containing the *Renilla* luciferase gene under control of the HSV-TK promoter (Promega) was used as an internal control for differences in transfection efficiency and cell number. The functional analysis of the basal promoter and full length promoter constructs of the histone H2A.1 and H2A.2 gene was carried out by transfecting the cells and maintaining for 72 h in serum-supplemented medium before harvesting. At the end of the culture period, the cells were lysed, and the luciferase activity in the lysate was measured by dual-luciferase reporter assay system (Promega). Transfections were carried out in triplicate, and each experiment was repeated at least twice.

For Azacytidine and Trichostatin A (TSA) treatment, the cells were cultured in the medium as described above along with 5 μM Azacytidine and 10 nM TSA for 16 h and 72 h respectively. Post incubation cells were harvested and RNA was isolated using Trizol reagent. cDNA was synthesized using a random hexamer and gene specific primers were used for real-time PCR.

### 2.6. Methylated DNA immunoprecipitation

Genomic DNA was purified using sigma gDNA Miniprep kit (G1N350), according to the manufacturer's instructions. Purified genomic DNA was diluted into a total of 300 ml TE buffer and sonicated with a Bioruptor (10 cycles at low power, of 30 s 'on' and 30 s 'off') to an average size of 300–500 bp. An aliquot of sonicated DNA was run on 1% agarose gel to confirm fragment size during each methylated DNA immunoprecipitation (MedIP) procedure. Sonicated DNA (4 μg) was denatured by incubation at 95 °C for 10 min and was immediately transferred to ice for 10 min. Immunoprecipitation buffer containing 10 mM sodium phosphate, 140 mM NaCl and 0.05% Triton X-100 was added to a final volume of 500 μl. For each IP reaction, 2 μg of antibody (Methyl cytosine: Diagenode MAb-006-100, Hydroxy methyl cytosine: Abcam ab106918) was added and incubated overnight at 4 °C with shaking. Five percent of DNA was kept as input. After incubation, 30 μl of Dynal Protein G beads (Invitrogen: 10004D) were added and further incubated for 1 h at 4 °C. Beads were washed thrice with 500 μl of IP buffer. Elution buffer (150 μl) containing 50 mM Tris–HCl pH 8.0, 10 mM EDTA, 1%SDS, 50 mM NaHCO₃ and 20 μg proteinase K was added and incubated at 55 °C for 3 h. Tubes were applied to a magnetic rack and eluted DNA and input DNA were purified with the Qiaquick PCR purification kit (Qiagen) followed by SYBR Green real-time quantitative PCR to identify methylated regions. PCR measurements were performed in duplicate. The primers designed for H2A.1 and H2A.2 are part of the CpG sites and CpG island respectively (Table 1). The average cycle thresholds for the technical replicates were calculated to yield one value per primer set for each biological replicate and normalized to input using the formula $2^{(Ct(input)-\{Ct(immunoprecipitation))}$. Averages and standard deviations of the normalized biological replicate values were plotted in the figures and used in *t*-test calculations.

### 2.7. Statistical analysis

All numerical data were expressed as average of values obtained ± standard deviation (SD). Statistical significance was determined by conducting a paired students' *t*-test.

## 3. Results

### 3.1. Identification of transcriptional start site (TSS), 3′UTR and promoter for H2A.1 and H2A.2 gene

Histone variants H2A.1 and H2A.2 fall under the category of homomorphous variants sharing 89% homology between their predicted cDNA sequences. Therefore, the cDNA for both the variants were cloned and sequenced (data not shown) for designing of gene specific primers for further experiments (Table 1). The NCBI database (Gene ID: H2A.1-XM-577573, H2A.2-XM-345255) suggested the predicted transcriptional start site (TSS) for H2A.1 is positioned 10 bp upstream the translational start site (ATG), and for H2A.2, 88 bp upstream of the first ATG site. However, the experimentally identified TSS for H2A.1 gene is positioned 31 bp upstream the predicted TSS in the NCBI data base and/or 43 bp upstream the Translational Start Site (Fig. 1A and B). Further, TSS of H2A.2 gene is 46 bp downstream of the predicted start site in the NCBI data base and/or 43 bp upstream the ATG site as identified using
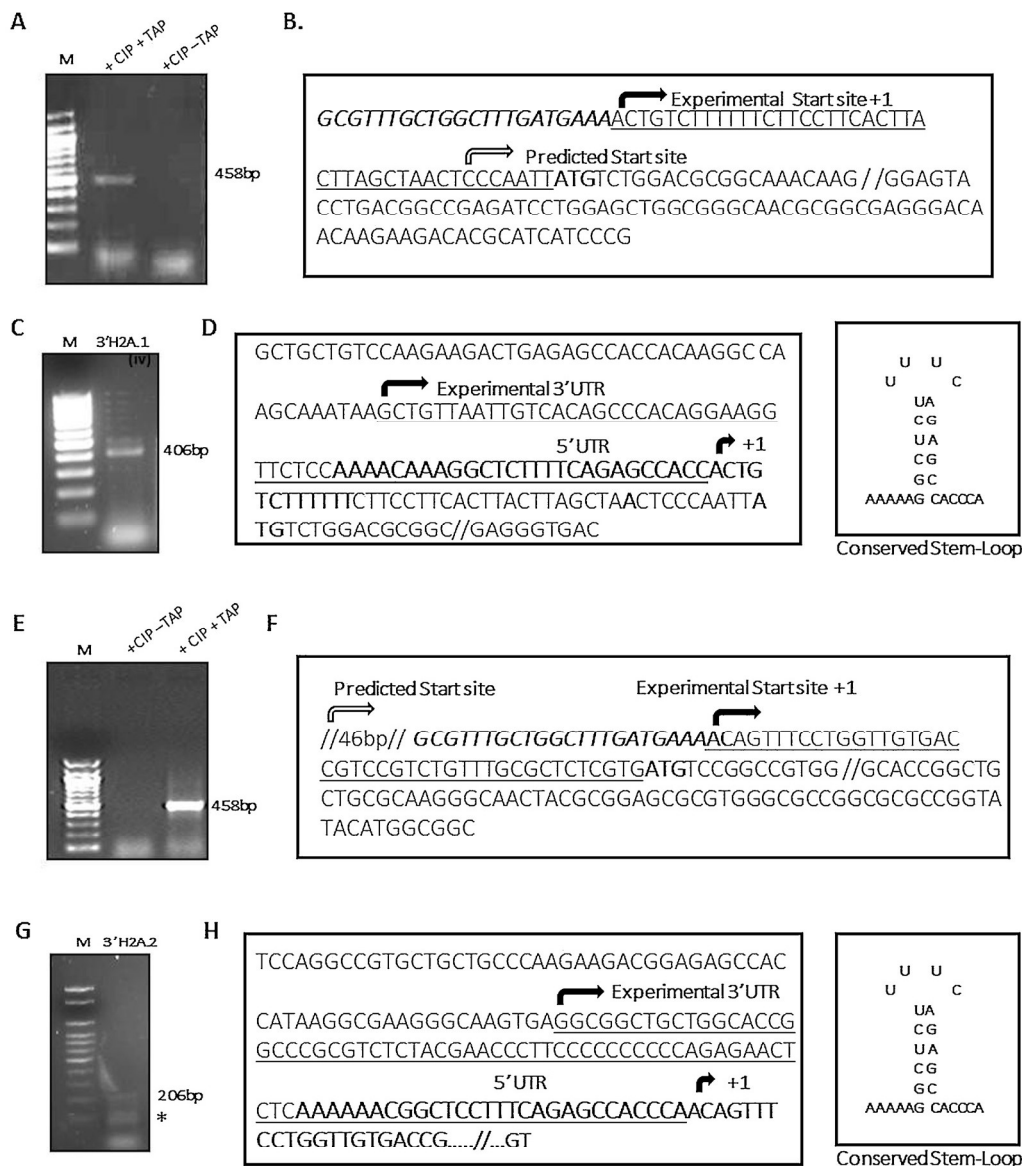
**A**

M   +CIP +TAP   +CIP −TAP

458bp

**B.**

*GCGTTTGCTGGCTTTGATGAAA*<u>ACTGTCTTTTTTCTTCCTTCACTTA</u>   Experimental Start site +1

<u>CTTAGCTAACTCCCAATT</u>**ATG**TCTGGACGCGGCAAACAAG//GGAGTA   Predicted Start site
CCTGACGGCCGAGATCCTGGAGCTGGCGGGCAACGCGGCGAGGGACA
ACAAGAAGACACGCATCATCCCG

**C**

M   3'H2A.1 (iv)

406bp

**D**

GCTGCTGTCCAAGAAGACTGAGAGCCACCACAAGGC CA
AGCAAATAAGCTGTTAATTGTCACAGCCCACAGGAAGG   Experimental 3'UTR
<u>TTCTCC**AAAACAAAGGCTCTTTTCAGAGCCACC**ACTG
TCTTTTTTCTTCCTTCACTTACTTAGCTAACTCCCAATTA
TG</u>TCTGGACGCGGC//GAGGGTGAC   5'UTR   +1

     U   U
U        C
   UA
   CG
   UA
   CG
   GC
AAAAAG CACCCA
Conserved Stem-Loop

**E**

M   +CIP −TAP   +CIP +TAP

458bp

**F**

Predicted Start site        Experimental Start site +1

//46bp// *GCGTTTGCTGGCTTTGATGAAA*<u>ACAGTTTCCTGGTTGTGAC
CGTCCGTCTGTTTGCGCTCTCGTGATG</u>TCCGGCCGTGG//GCACCGGCTG
CTGCGCAAGGGCAACTACGCGGAGCGCGTGGGCGCCGGCGCGCCGGTA
TACATGGCGGC

**G**

M   3'H2A.2

206bp
*

**H**

TCCAGGCCGTGCTGCTGCCCAAGAAGACGGAGAGCCAC
CATAAGGCGAAGGGCAAGTGA<u>GGCGGCTGCTGGCACCG</u>   Experimental 3'UTR
<u>GCCCGCGTCTCTACGAACCCTTCCCCCCCCCCCAGAGAACT
CTC**AAAAAACGGCTCCTTTCAGAGCCACCCA**ACAGTTT
CCTGGTTGTGACCG</u>.....//...GT   5'UTR   +1

     U   U
U        C
   UA
   CG
   UA
   CG
   GC
AAAAAG CACCCA
Conserved Stem-Loop

**Fig. 1.** Genomic characterization of H2A.1 and H2A.2 genes. 5′RLM-Rapid Amplification of cDNA was carried out using total RNA from rat liver tissue as template. Single band of PCR amplified product indicated single transcriptional start site for (A) H2A.1 and (E) H2A.2. The sequence analysis for (B) H2A.1 and (F) H2A.2 indicates ***GCGTT*. . .*GAAA*** (bold and italics) sequence as the ligated adaptor sequence to the 5′end of the mRNA, the black arrow (experimental start site) demarcates the first nucleotide just after the adaptor sequence corresponding to +1 and also the unfilled arrow is a predicted start site as per NCBI data base (H2A.1: XM-577573, H2A.2 XM-345255), the underlined sequence, <u>ACTGTCT</u>between the experimental transcription start site and translational start site 'ATG' (in bold) is the 5′untranslated region. EtBr stained 1.5% TAE agarose gel picture showing resolved PCR amplified product obtained from cDNA template of circularized RNA for H2A.1 (C) H2A.1 and (G) H2A.2. '*' denotes non-specific amplified product. The amplified product was cloned in pTZ57R/T vector and sequencing data confirmed the exact end of 3′untranslated region underlined for (D) H2A.1 and (H) H2A.2 lying just ahead of the 5′UTR (bold and underlined sequence) and downstream the predicted end of 3′UTR as reported in NCBI data base. The 3′UTR structure includes a 26 bp conserved stemloop present in the histone family.

5′RLM-RACE technique (Fig. 1E and F). The identified sequences of H2A.1 and H2A.2 cDNA are 498 bp and 525 bp long containing a stem loop at their 3′UTR and have been submitted to NCBI database with accession numbers JX-661508 and JX-661509 respectively.

The histone variants are categorized as replication-dependent or independent on the basis of their expression during the specific phases of cell cycle. Histones transcripts synthesized during the S phase majorly consists of the stem loop structure, whereas in other phases of cell cycle poly A+ tails are usually found at the 3′ end of mRNA. Therefore, mapping of the 3′UTR region of H2A.1 and H2A.2 gene will define whether these variants are synthesized in a replication-dependent or independent manner. The experimentally identified 3′UTR of H2A.1 and H2A.2 using mRNA circularization approach followed by cloning (Fig. 1C and G) and

sequencing confirmed the presence of 26 bp conserved stem loop in both the variants (Fig. 1D and H). However, the 3′UTR is 62 bp long in H2A.1 (Fig. 1D), whereas, 88 bp long in H2A.2 mRNA (Fig. 1H). The first base in the mRNA is labeled as +1 for both the genes. These results suggest that H2A.1 and H2A.2 variants might be transcribed in a replication-dependent manner.

### 3.2. In silico analysis of H2A.1 and H2A.2 transcription regulatory elements upstream of TSS

To identify the promoter regions of H2A.1 and H2A.2 genes and to locate the key regulatory regions involved in their gene expression, basing on the NCBI (Gene ID: H2A.1: 502125, H2A.2 365877) and RGD (Gene ID: H2A.1: 1594367, H2A.2: 1307165)

```
-1056                            NFAT_1                                                    Sox10
AGCAATGTGAATGTGTAAGCGGAAAAAACCCTTTCCTTTCCAACTTGATTTTAGGTCATGATGCTTTGTGCAGGA
-981
ATAGAAACCCTACGACGCAGGCCTTGGTTTTCTCCTTGAATATACATGTTTCATCTGTTTTCTCCAGTCACCATG
-906
ACATCAGTGCTTTTCAGTGCACAGACTTCAGGATCTCTCCGGGCTCATACATTGCAGGCTTTCCTGGGTCAGTCA
-831 p53
TGGGACATGCTCTCCTTCTCCTCAGGCTCTATTTTCCAGGCAGTTTAAGGATAATTCAGCCATAATAAAGAAGTA
-756                                                ELF1
TTTGCATGCTTTTACTTTGAGATTTGAGATTTGTAGAGCTATAAGGAAGCCTGGCGTAGAACCTCAAAATATGTA
-681                ING-4                                       ELF1
CTAAACCCGTTATGAGGAGCCCACCAAAGCAGTGTATAGCCAATTTAAATGATTTCTTCCTGGTGTTGAGAACC
-606            CTCF                                          BRCA-1
ACATCCTGGCATCGCTCTGCCGCTAGAGGGAGCATTTGTTGTTTGTGAGAGTAGTTCAACAGAAGCTTAGTTAGC
-531                               C/EBP alpha
TGGGCAATCCTGACCTCTGGCTCATAAAATAGAAATTTGGCAATATCCTATGAGATACTACATCAAGATCAAATT
-456                      ELF1
CTAATTAAACCTTAGCAGGACGACAAGGTGGAGGAAGCTCCGCACGGTCTTTGCTTGTCACAAAACCACGATTAT
-381 CDX-1
AAACCCGGTAATAAAGGCCTGTGCCTCAACAAGTCAGAACTCATAAACCAGATTTTAATACCAAGAACTTGATGG
-306                                             GATA-3          CDXA
AAAAAAAAATTCATTTACTTATGTGTATTCTAGTAAAAGCAGGAATAGAGTCAAAAAGATCTCAACTATTAATC
-231
                                                               GATA_1
ATGGGAACCAGAGTTTAAATCACAGAACCCGAACTTTTATTTTTTAAAGTAAAATTTCAAATAAAAAGCGACTCG
-156            NFAT_1                           OCT-1/2
ATAAGGGAAGGGGGGAAAAAAAAAAAAAGAGTACCCCTTATGCAAATGAGGGATTTCAAGTACTATTTTCTATTG
-81        NFY/CAAT BOX         Smad 3               GABA alpha/vMyb
GGTGCTACTATTAACCAATGAGAGAAGCACAGACAGAATACCTTCCGTTAGTATAAATATTCGTCGTTCGCCTAC
-6      +1             ELF1
AGCTTCACTGTCTTTTTTCTTCGTTCACTTACTTAGCTAACTCCCAATTATGTCTGGACGCGGCAAACAAGGCGG
+70     E2F1                                                              +144
TAAGGCTCGCGCCAAGGCCAAGACCCGCTCCTCCCGGGCCGGCCTGCAGTTCCCCGTGGGCCGTGTGCACCGTTT
```

**Fig. 2.** Nucleotide sequence of Rat H2A.1 gene promoter. +1 denotes the transcriptional start site obtained from 5′RLM RACE experiments. Position −1056 to ATG is the non-coding region and from ATG to +144 is the part of coding region. The region between +1 and ATG is experimentally identified 5′ untranslated region, TATA Box is position from −30 to −25. The complete gene sequence of H2A.1 has been assigned accession numbers JX661508 by GenBank-NCBI, USA. The highlighted sequences shows putative transcription factor binding sites identified using motif-finder and Biobase software.

sequence database, we defined the reported sequence upstream the experimentally identified TSS, designated as position +1. Computer assisted analysis of this region suggested presence of multiple putative transcription factor binding sites in region encompassing −1056 to +144 for H2A.1, and −1160 to +219 for H2A.2 gene. Further, the data suggested that both the genes were TATA driven with location of TATA box (TATAAA) at 25–30 bp upstream and CCAAT box at 63–67 bp upstream from the transcription initiation site. Moreover, H2A.1 gene promoter contains various putative *cis-acting* binding sites, like Sox10, NFAT1, p53, Oct-1, CTCF, cEBPα, cdxA, E2F (Fig. 2), whereas, H2A.2 contains putative binding sites for AP4, E2F, Oct-1, cEBPβ and family of Sox-binding sites for transcription factors (Fig. 3).

To identify the functional proximal promoter of H2A.1 and H2A.2 genes we mapped the reported sequence upstream the experimentally identified TSS, designated as position +1 (Fig. 4A). Full length and a single deletion construct harbouring the TATA box was cloned in to luciferase reporter plasmids for both H2A.1 and H2A.2. These constructs were transiently transfected into CL38 cell line and promoter activity was assessed by measuring the luciferase activity. The cloned H2A.1 (−1056 to +144) and H2A.2 (−1160 to +219) DNA sequence showed transcriptional activity and confirmed the presence of potentially active promoter in the predicted sequences. Further, luciferase assay using the deletion construct for H2A.1 (−131 to +144) and H2A.2 (−135 to +219) revealed its importance as a basal promoter for these genes (Fig. 4B and C).

### 3.3. DNA methylation on H2A.1 and H2A.2 genes govern their expression pattern changes

DNA methylation and histone modification are two key epigenetic mechanisms that are known to regulate cellular gene promoters (Fuks, 2005). Interestingly, differential mapping of the CpG islands or −CCGG-sequences were observed in the promoter regions of both the histone variants. The H2A.2 gene promoter (−1160 to +219) contains CpG Island, having greater than 90% G + C composition in the 5′ untranslated segment spanning from −290 to +219, while, H2A.1 (−1056 to +144) has no CpG islands but contains multiple −CCGG-sites within its promoter (Fig. 5A).

To understand whether methylation play a role in regulation of H2A.1 and H2A.2 gene expression we used 5′Azacytidine (5′AzaC), a well-known DNA methyl transferase inhibitor. CL38, a rat neoplastic cell line was treated with 5′AzaC for 72 h and assessed the transcript levels of H2A.1 and H2A.2. Tslc-1 was used as a positive control, expression of which has already been established to be governed by DNA methylation phenomenon (Tsujiuchi et al., 2007). A 4-fold upregulation of H2A.2 expression is seen with no significant change in the levels of H2A.1 upon 5′AzaC treatment (Fig. 5B). The changes in the expression levels was also studied in light of the status of DNA methylation levels on these promoters as assessed by 5′-methyl cytosine DNA immunoprecipitation (MedIP) and 5′-hydroxyl methyl cytosine immunoprecipitation (MeHdIP) analysis (Fig. 5C and D). The primers designed encompass the region

```
-1160
CTGAACCCTTGATCCATCTCTCAAATTTGTGATTCCACACATGAACATGAACATCAAACTATTAAATTTAATCAG
-1085    Nanog
AATGCTTGCCCTACCTTTGTCTTCTGACCTTAAATTGCTTCTCTGTGCTCCATTCTAATAACACTGCCTACCCAG
-101BRCA-1        ING-4
ATTCAACCCAAAATCCTGGTGGTTACACTCTTACCTATTCCTGCACAGACTTAGAATTCTATCTCCACAATATGT
-935       Sox9                            SoX5           Oct-4
TACAATGTAAAATACAAGAACAATGTGACCATGCTACTGTGTAACAATATACCTGTTTCTAGTGCTAAACTCCCA
-860                                    Sox10
CTCTGTCTAATCTGTGATTCTTAATGCCACACATTAGAATCGCTCACAAAGCCTATCACACATTTCAGAGATTAA
-785
AAAATGCTGGATGTATTTCTCCGGTTATGACTGATGAGATACTAAAATACTGCCAGTCTACACCCAAACACCGTG
-710
GAAGGCTCCTAAACAGAGCTTCTGAGTAGCTATCATAGGTCAAATCGACAAAAGCAGCAGCAGTTTAATTCTTAT
-635
TTCGATTACTGTATACAAATCTAAGTTAAAAAAAAAAAAAAAAAGCAATTTGAGTAAACTCCCCGCAAACTGTATCTG
-560    P300                         C/EBP beta/ BRCA-1
GTCTTTTCAAGCACTCCCAGGTGTGGATGGATTGAGAAATTTTGTTGCCGTTGTATGGAAATAACATTTAAATGT
-485
AACGAATTTAAGTGAGGCTCCTACGGGTAAACGTTTAAAATGTAACAAGTAGGTTTTACACTGTTTCAAGTAGAA
-410
NFAT-1                        ELF-1
GGAAAAAGAGGATATCGGAATTACTCTTTACTTCCTAGGTATCAAAAACGCAGTTTCCAGCATTCCTAAAAGGAA
-335                                                              C-ETS-2
AACCTTCTCATACACAAGGAGGTTCTTAACTCAGGCCTTCTTGGAGGCAAGGCACATTTCGCCAGCTTCCTGACC
-260
AGCAGAGAGCGCGAGCAGGCCGGGCGACCCGCTGAGTGTCGCAACAACGGCCGCACGCAAATGAGGCCGCCGAGC
-185        E2F-1                                      OCT-1
ACGCGCGTCGTGATTCGCGCGTTCCAAGGCGACGCTGGGGCCAGGGAGCCGGGCTTATGTAAATGAGAGGATTCT
-110                           NF-Y
GTCTCTGCGCTCCTATTGGCCGCGGCGCCAGGACGCGTGTGGGCCAATGAGAGCGTCGGGCGGACAATCGGGTGT
-35    TATA Box                    +1
CTGTCTATAAAAGGGTGAGGCGTCGGCGTTGGCGCACAGTTTCCTGGTTGTGACCGTCCGTCTGTTTGCGCTCTC
+41                              E2F                              E2F
GTGATGTCCGGCCGTGGCAAGCAAGGAGGCAAGGCCCGCGCCAAGGCCAAGTCGCGGTCGTCCCGCGCCGGGCTG
+116                          Cmyc    E2F
CAGTTCCCAGTGGGTCGCGTGCACCGGCTGCTGCGCAAGGGCAACTACGCGGAGCGCGTGGGCGCCGGCGCGCCG
+191
GTATACATGGCGGCGGTGCTGGAGTACCT+219
```

**Fig. 3.** Nucleotide sequence of Rat H2A.2 gene promoter. +1 denotes the experimentally identified transcriptional start site. The genomic sequence from position −1160 to ATG is the noncoding region and from ATG to +219 is the part of coding region. The sequence between +1 and translational start site 'ATG' is experimentally recognized 5′ untranslated region. TATA Box is positioned from −30 to −25. The other highlighted sequences show putative transcription factor binding sites as suggested using motif-finder and Biobase software. The complete gene sequence of H2A.2 is submitted to GenBank-NCBI, USA and accession number JX661509 has been assigned.

−40 to +59 for H2A.1 and −221 to −146 for H2A.2, both of which are the sequences predicted to undergo methylation. MedIP-qPCR confirmed hypomethylation of H2A.1, H2A.2 and positive control, Tslc-1 gene promoters with significant changes on H2A.2 promotor in comparison to untreated cells (Fig. 5C). Further, MeHdIP-qPCR analysis showed significant increase in hydroxymethylation of H2A.2 and Tslc-1 without any significant change in H2A.1 after 5′AzaC treatment compared to untreated cells (Fig. 5D).

We next examined whether global histone acetylation status affects the expression and DNA methylation status of H2A.1 and H2A.2 promoters. CL38 cells were treated with a well-known HDAC inhibitor (HDACi), Trichostatin A (TSA) overnight (O/N) and levels of H2A.1 and H2A.2 were quantitatively monitored. An increased expression of H2A.2 (2.4 fold) was seen upon HDAC inhibition with no changes in levels of H2A.1 (Fig. 5E). Further, MedIP and MeHdIP analysis also revealed changes in the methylation status on these promoters. Indeed the mRNA expression correlated with decrease in DNA methylation, as assessed by MeDIP-qPCR (Fig. 5E and F).

Moreover, significant increase in DNA hydroxymethylation was observed for H2A.2 gene promoter (Fig. 5G).

To understand that indeed DNA methylation plays a role in governing the expression pattern of H2A.1 and H2A.2 during differentiation and de-differentiation we performed MedIP and MeHdIP analysis on control, tumor and embryonic liver tissues. Firstly, we monitored the expression changes of H2A.1 and H2A.2 in these physiological states (Fig. 5H). Partial hepatotectomised (36 h) liver tissue was used as a negative control for the experiment as we have previously reported that during cell proliferation the expression profile of H2A.1 and H2A.2 remains unchanged (Tyagi et al., 2014). In accordance with our earlier report we observed a significant increase of H2A.1 and decrease of H2A.2 in tumor and embryonic liver compared to control (Fig. 5H). A 7-fold decrease of MedIP signal on H2A.1 promoter of tumor and embryonic tissue is seen in comparison to control (Fig. 5I). For H2A.2, a 8-fold and 7-fold increase in MedIP signal is seen in tumor and embryonic tissues respectively (Fig.re 5I). Interestingly the MeHdIP signal was
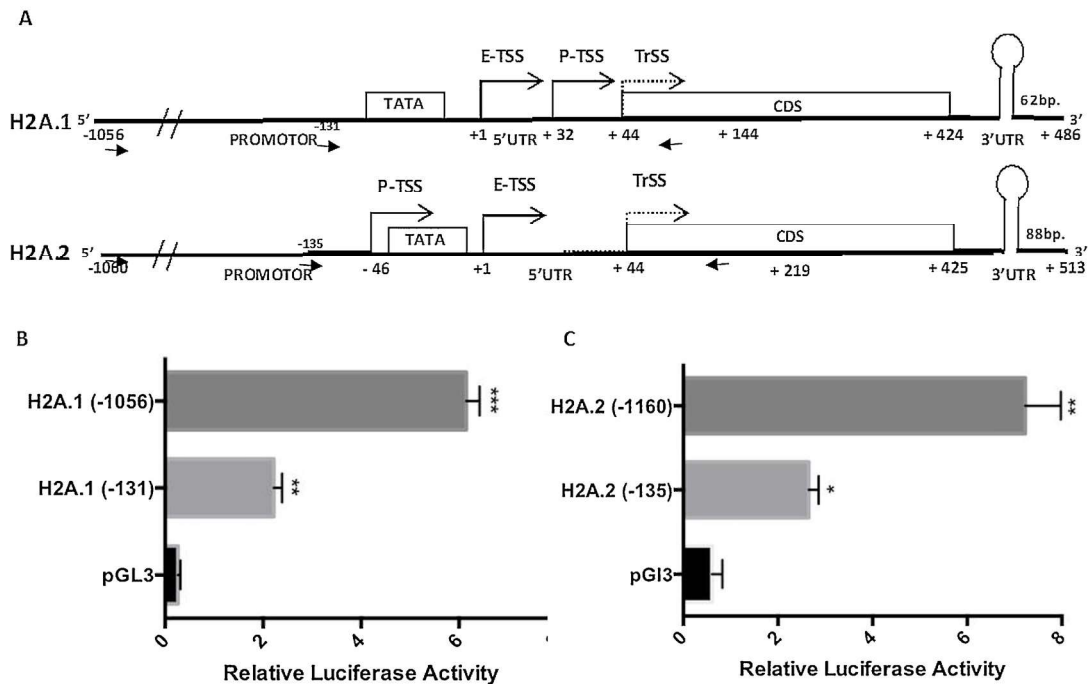
**Fig. 4.** Identification of functional promoter for H2A.1 and H2A.2 gene. (A) Line diagram depicting the characterized genomic regions of H2A.1 (−1056 to +486) and H2A.2 (1060 to +513) with key highlighted regions like promoter, 5′UTR, CDS, 3′UTR *etc.* Black head arrows indicate the region used for the primer designing for cloning of PCR amplified fragments in pGL3 vector for Dual luciferase assay. The primer sequences are mentioned in Table 1. E-TSS: Experimental transcription start site; P-TSS: Predicted transcription start site; TrSS: Translational start site. Analysis of (B) H2A.1 and (C) H2A.2 promoter activity using Dual Luciferase assay. pGL3-Basic plasmid, full length H2A.1 (−1056 to +144) and H2A.2 promoter (−1060 to +219) and minimal H2A.1 (−131 to +144) and H2A.2 (−135 to +219) promoter containing TATA and CAAT box were transfected into CL38 cells along with pRL-TK vector containing the *Renilla* luciferase gene as an internal control. Cells were lysed and firefly and *Renilla* luciferase activities were determined. The data shown represent the means of three experiments, with the bars showing standard deviation.

in contrast to the MedIP signal for both H2A.1 and H2A.2 across all the tissues (Fig. 5J). H19 was used a control for the experiment as DNA methylation levels on its promoter is known to regulate its expression in all the pathophysiological states used in the study (Manoharan et al., 2004). These data combined suggest that our systematic approach can provide important insights into understanding the mechanisms underlying epigenetic regulation, *via* DNA methylation, that in turn alters transcriptional programs of histone variant genes that lead to different pathophysiological states.

## 4. Discussion

In this study, for the first time, we identified and characterized the 5′, 3′ un-translated region (UTR), promoters of rat H2A.1 and H2A.2 genes and analyzed their transcriptional regulation during differentiation and de-differentiation of a hepatocyte. Both H2A genes are intron-less and are localized on Chromosome 17 (H2A.1) and Chromosome 2 (H2A.2). The transcription start site was mapped and the data showed that there is single transcriptional start site for both H2A.1 and H2A.2, which is positioned 43 bp upstream of the ATG (translational start site). However, alignment of both H2A.1 and H2A.2, 5′-UTR sequences revealed no significant degree of homology between them despite the single coding exon being very similar amongst the variants. By mRNA circularization experiments we have identified a presence of 62 bp and 88 bp long 3′UTR for H2A.1 and H2A.2 respectively. Interestingly, both the genes have 26 bp long conserved stem loop structure at their 3′UTR, a typical signature of the replication-dependent histone genes. A single protein, the stem–loop binding protein (SLBP), binds to 26 nucleotide sequence and participates in all aspects of histone mRNA metabolism (Dominski et al., 1995; Hanson et al., 1996;

Rattray, 2012). Hence the presence of conserved stem loop in both H2A.1 and H2A.2 suggests that the downstream mechanisms, like post transcriptional regulation involved in differential regulation of expression are similar and may not contribute to the observed expression changes during differentiation/de-differentiation of hepatocytes.

*In silico* studies followed by reporter based promoter assay confirmed the transcriptional activity for cloned 1.2 and 1.3 kb sequence as H2A.1 and H2A.2 gene promoters. The proximal promoter of the H2A.1 gene contains typical TATA and CCAAT boxes, including several consensus transcription factor binding sites, features that are also present in the promoter of H2A.2. These are well positioned as earlier reported for replication dependent gene promoters (Rattray, 2012). Excluding the TATA and CAAT regions, both promoters do not show a high degree in sequence homology (less than 20%). Replication-dependent histone gene transcription is known to be regulated by transcription factors like Oct-1, NFAT, E2F-1 and OCT-1 amongst others (Heintz, 1991; Wijnen et al., 1994; Zhang et al., 2012; Zhao et al., 2000). Indeed, our *in silico* analysis for identification of transcription factor sites revealed the presence of all these sites in both the promoters. Interestingly, E2F-binding motifs are highly conserved in both the H2A promoters, and it is known that E2F plays an important role in the coordinate regulation of S-phase-specific histone gene expression again indicating towards similar type of transcriptional regulatory mechanism exists for both the genes (Becker et al., 2007; Oswald et al., 1996). However, H2A.1 gene has CpG sites in 5′UTR and coding region whereas, H2A.2 gene promoter is having a CpG island from position −292 to +378. Thus, the sequence disparity in both the 5′-UTR and the promoter regions along with presence of CpG sites and islands indicate that differential H2A.1 and H2A.2 gene expression among different
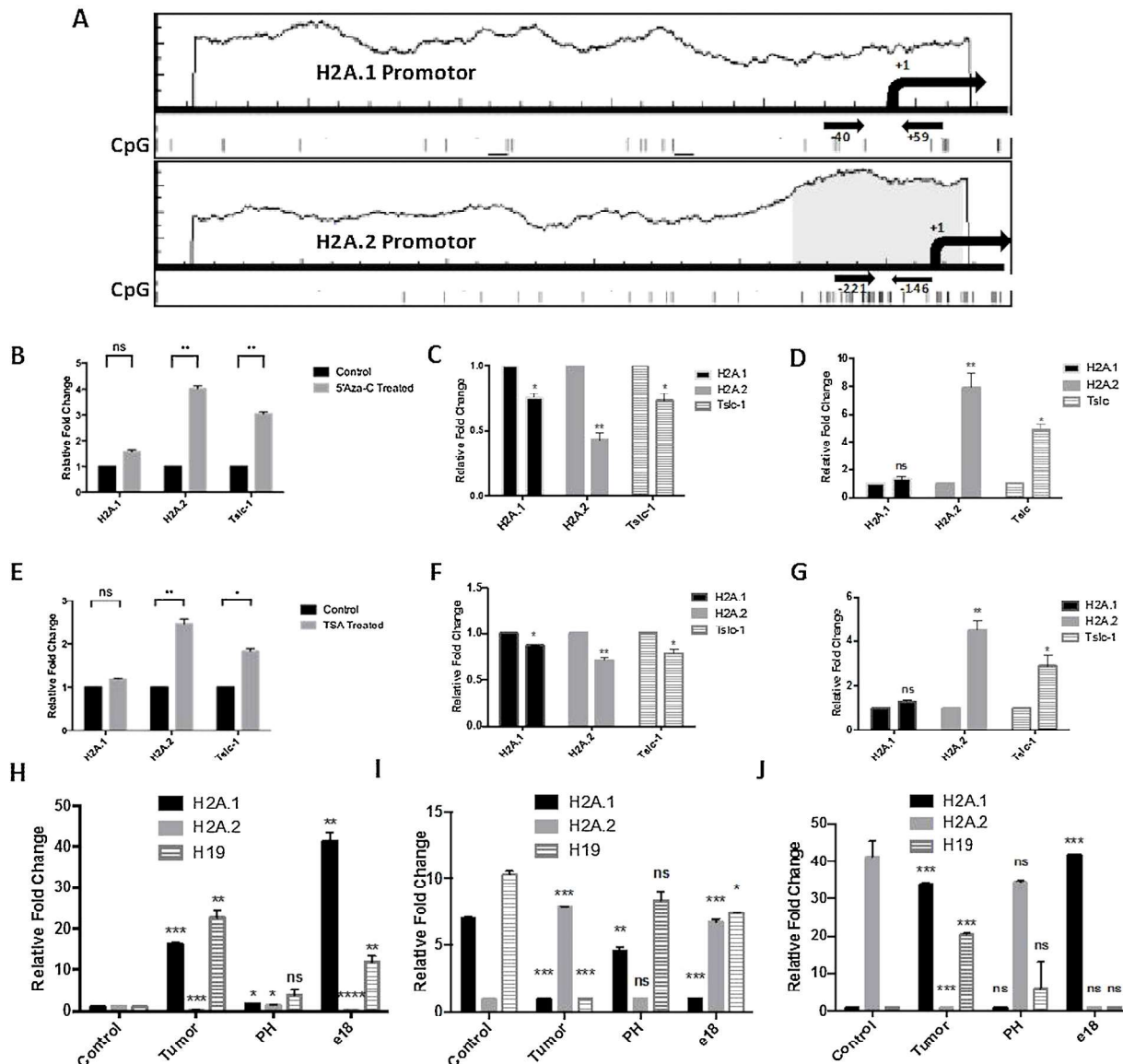
**Fig. 5.** Status of methylated CpG (5mC) and hydroxymethylated CpG (5hmC) on H2A.1 (−40 to +59) and H2A.2 (−221 to −146) in different patho–physiological states. (A) H2A.1 and H2A.2 promoter sequences were analyzed by the MethPrimer program for presence of putative CpG sequence or islands. CpG sites were found evenly distributed on the H2A.1 promoter, whereas a single CpG island was predicted in the H2A.2 promoter sequence starting from the nucleotide −290 and extending in to the CDS. The region also contains the cis–acting elements for basal transcription like TATA box, CAAT box. Real-time PCR (qPCR) was done to check the expression status of histone variants in CL38 cell line post treatment with (B) DNA methyltransferase inhibitor (5-AzadC) and (E) HDAC inhibitor, TSA. Tslc-1 was used as a positive control. Graphs (C) and (F) showing the status of 5′methyl cytosine, and (D) and (G) status of 5′hydroxy-methyl cytosine levels on promoters of H2A.1, H2A.2 and Tslc-1, post treatment with 5-Aza-C and TSA respectively. (H) Expression changes of H2A.1, H2A.2 and H19 in various pathophysiological states. (I) Graph showing the results of MedIP and (J) MeHdIP on liver tissue genomic DNA followed by qPCR for H2A.1 and H2A.2 genes in control, tumor, embryonic and partial hepatectomy. H19 was used a positive control for the study. For all the qPCR assays the data was normalized with control gene expression. For MedIP and MeHdIP analysis, the relative fold change was plotted post normalization with input. Error bars represent standard deviation.

physiological conditions might be governed by DNA methylation.

Transcriptional repression of tumor suppressor genes *via* DNA methylation has been found in certain types of cancer (Baylin et al., 2001). Accordingly, inhibition of epigenetic suppression *in vitro* using specific drugs can reactivate expression of genes silenced in cancer. Our findings indicate that H2A.2 gene expression can be induced in CL38 cell line upon treatment with the DNA methyltransferase-blocking agent 5-AzadC or with histone deacetylase inhibitor TSA. Transcriptional repression of a gene can be bought out by a coordinated series of events like DNA hypermethylation of CpG sites, histone deacetylation, and histone H3K9 methylation (Sawan et al., 2008). However, little is known about the precise hierarchical order of events for epigenetic silencing during development and differentiation. As H2A.2 gene expression is induced by inhibition of both DNMT and HDAC, it appears that the histone promoter is silenced by a combination of both epigenetic processes, however, it will be very interesting to know which event precedes the other.

Further, methyl DNA immunoprecipitation analysis on H2A.1 and H2A.2 promoters during various physiological states of liver revealed indeed, DNA methylation dynamically governs the expression pattern changes of the histone variants. H2A.1 level is known to be increased significantly in tumor and embryonic tissue and indeed MedIP signal is very less both in comparison to control (Fig. 5D). Intriguingly, the MeHdIP signal in contrast to that of MedIP, in accordance with its relation to be a positive effector of transcription. Though having similar genomic organization (Fig. 4A)
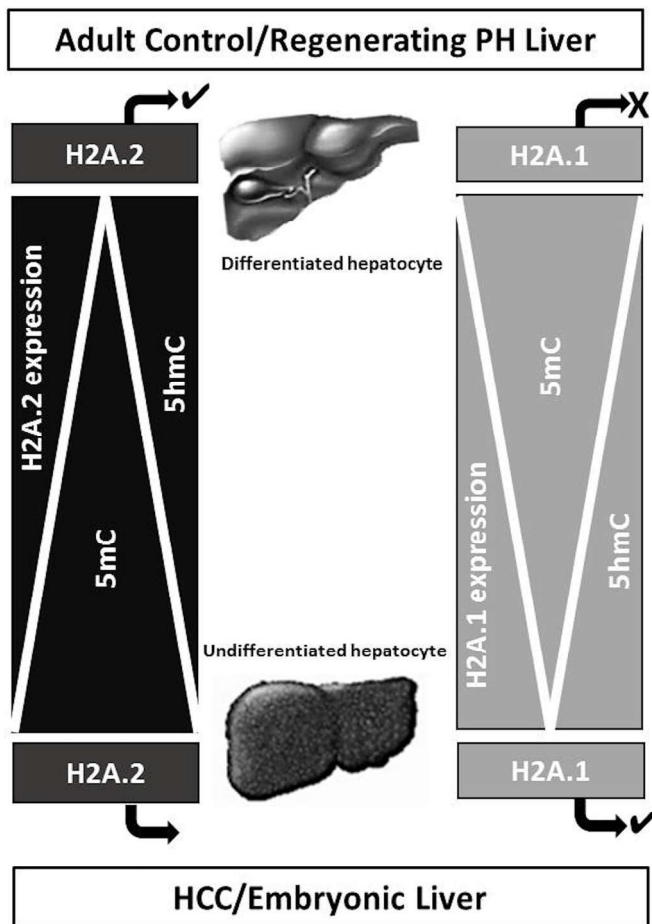
**Fig. 6.** DNA methylation, methylated CpG (5mC) and hydroxymethylated CpG (5hmC) governs expression changes of H2A.1 and H2A.2 in various pathophysiological states of hepatocyte. Model depicting the inverse correlation of 5mC and direct correlation of 5hmC with expression status of H2A.1 and H2A.2 genes in control, PH and tumor, embryo.

H2A.1 and H2A.2 differ in the context of promoter sequence which further contributes to their DNA methylation differences, thus regulating their differential expression pattern.

The role of DNA methylation in regulation of histone H2A gene transcription has not been previously studied. However, many genome wide methylation analysis has revealed the presence of methylation on certain set of replication-dependent histone genes (Daugaard et al., 2016; Decock et al., 2012; Kachakova et al., 2013; Rabinovich et al., 2012; Sandoval et al., 2013; Schostak et al., 2009). Moreover, till date, no functional relationship between DNA methylation status and histone gene expression level has been observed. One of the well-chronicled epigenetic change during cancer is DNA hypermethylation at the CpG islands of the promoters and global DNA hypomethylation. DNA hypermethylation has been linked to silencing of many tumor suppressor genes during carcinogenesis. Global DNA hypomethylation in cancer occurs at various genomic sequences including repetitive elements, retrotransposons, CpG poor promoters, introns and gene deserts (Jones et al., 2002). Interestingly, increased DNA hypermethylation is seen on H2A.2 promoter CpG island and hypomethylation on CpG sites of H2A.1 promoter which is in sync with the observed hallmark of cancer. Tumor-specific CpG island methylation can occur through a sequence- specific instructive mechanism by which DNMTs are targeted to specific genes by their association with oncogenic transcription factors. However, in case of histone variants, how the

differential DNA methylation status is maintained and what cell signalling events trigger the changes need to be investigated.

In summary, we have provided experimental results of characterizing the structural organization of the rat histone H2A.1 and H2A.2 gene, further, we show that the process of DNA methylation in the context of stage-type specific manner regulates the gene expression of H2A.1 and H2A.2 and, in turn, they regulate large numbers of gene expression variations. Here, we present a strong line of evidence that the balance of H2A.1 and H2A.2 is maintained through DNA methylation in various pathophysiological states of liver (Fig. 6). However, what are the factors contributing to the change in methylation pattern thus effecting the expression of these two variants needs further investigation.

## Competing interests

The authors declare that they have no competing interests.

## Author contribution

S.G. conceived the idea, planned the experiments and wrote the manuscript. Genomic characterization experiments were performed by M.T. and D.R performed methylation studies for both the genes. M.T. and D.R. wrote and edited the manuscript.

## Sequence submission

The complete gene sequence of H2A.1 and H2A.2 are submitted to GenBank-NCBI, USA and accession numbers JX661508 and JX661509 are assigned. The data are simultaneously made available to EMBL, Europe and the DNA Data Bank, Japan.

## Acknowledgments

## References

Baylin, S.B., Esteller, M., Rountree, M.R., Bachman, K.E., Schuebel, K., Herman, J.G., 2001. Aberrant patterns of DNA methylation, chromatin formation and gene expression in cancer. Hum. Mol. Genet. 10, 687–692, http://dx.doi.org/10.1093/hmg/10.7.687.

Becker, K.A., Stein, J.L., Lian, J.B., van Wijnen, A.J., Stein, G.S., 2007. Establishment of histone gene regulation and cell cycle checkpoint control in human embryonic stem cells. J. Cell. Physiol. 210, 517–526, http://dx.doi.org/10.1002/jcp.20903.

Becker, P.B., Ho, W., 2002. ATP dependent nucleosome remodelling. Annu. Rev. Biochem., http://dx.doi.org/10.1146/annurev.biochem.71.110601.135400.

Daugaard, I., Dominguez, D., Kjeldsen, T.E., Kristensen, L.S., Hager, H., Wojdacz, T.K., Hansen, L.L., 2016. Identification and validation of candidate epigenetic biomarkers in lung adenocarcinoma. Nat. Publ. Gr., 1–11, http://dx.doi.org/10.1038/srep35807.

Decock, A., Ongenaert, M., Hoebeeck, J., Preter, K.D., Peer, G.V., Criekinge, W.V., Ladenstein, R., Schulte, J.H., Noguera, R., Stallings, R.L., Damme, A.V., Laureys, G., Vermeulen, J., Maerken, T.V., Speleman, F., 2012. Genome-wide promoter methylation analysis in neuroblastoma identifies prognostic methylation biomarkers. Genome Biol. 13, R95, http://dx.doi.org/10.1186/gb-2012-13-10-r95.

Lewis, J., Bird, A., 2003. DNA methylation and chromatin structure. FEBS Lett., 158–163, http://dx.doi.org/10.1016/0014-5793(91)80795-5.

Dominski, Z., Sumerel, J., Hanson, R.J., Marzluff, W.F., 1995. The polyribosomal protein bound to the 3′ end of histone mRNA can function in histone pre-mRNA processing. RNA, 915–923.

Fuks, F., 2005. DNA methylation and histone modifications: teaming up to silence genes. Curr. Opin. Genet. Dev. 15, 490–495, http://dx.doi.org/10.1016/j.gde.2005.08.002.

Hanson, R.J., Sun, J., Willis, D.G., Marzluff, W.F., 1996. Efficient extraction and partial purification of the polyribosome–associated stem–loop binding protein

bound to the 3′ end of histone mRNA. Biochemistry 35, 2146–2156, http://dx.doi.org/10.1021/bi9521856.

Heintz, N., 1991. The regulation of histone gene expression during the cell cycle. BBA 1088, 327–339, http://dx.doi.org/10.1016/0167-4781(91)90122-3.

Jones, P.A., Baylin, S.B., Kimmel, S., 2002. The fundamental role of eigenetic events in cancer. Nat. Rev. Genet., http://dx.doi.org/10.1038/nrg816.

Kachakova, D., Mitkova, A., Popov, E., Beltcheva, O., Vlahova, A., Dikov, T., Hristova, S., 2013. Evaluation of the clinical value of the newly identified urine biomarker HIST1H4K for diagnosis and prognosis of prostate cancer in Bulgarian patients. J. BUON 18, 660–668.

Khare, S.P., Sharma, A., Deodhar, K.K., Gupta, S., 2011. Brief Communication Overexpression of histone variant H2A.1 and cellular transformation are related in N-nitrosodiethylamine-induced sequential hepatocarcinogenesis. Exp. Biol. Med. (Maywood), 30–35, http://dx.doi.org/10.1258/ebm.2010.010140.

Kouzarides, T., 2007. Chromatin modifications and their function. Cell 128, 693–705, http://dx.doi.org/10.1016/j.cell.2007.02.005.

Kroeze, L.I., Reijden, B.A., Van Der, Jansen, J.H., 2015. 5-Hydroxymethylcytosine: an epigenetic mark frequently deregulated in cancer. Biochim. Biophys. Acta BBA – Rev. Cancer 1855, 144–154, http://dx.doi.org/10.1016/j.bbcan.2015.01.001.

Manoharan, H., Babcock, K., Pitot, H.C., 2004. Changes in the DNA methylation profile of the rat H19 gene upstream region during development and transgenic hepatocarcinogenesis and its role in the imprinted transcriptional regulation of the H19 gene. Mol. Carcinog. 41, 1–16, http://dx.doi.org/10.1002/mc.20036.

Marzluff, W.F., Wagner, E.J., Duronio, R.J., 2009. Metabolism and regulation of canonical histone mRNAs: life without a poly(A) tail. Nat. Rev. Genet., 843–854, http://dx.doi.org/10.1038/nrg2438.

Oswald, F., Dobner, T., Lipp, M., Al, O.E.T., 1996. The E2F transcription factor activates a replication-dependent human H2A gene in early S phase of the cell cycle. Mol. Cell. Biol. 16, 1889–1895, http://dx.doi.org/10.1128/MCB.16.5.1889.

Piña, B., Suau, P., 1987. Changes in histones H2A and H3 variant composition in differentiating and mature rat brain cortical neurons. Dev. Biol. 123, 51–58, http://dx.doi.org/10.1016/0012-1606(87)90426-X.

Rabinovich, E.I., Kapetanaki, M.G., Steinfeld, I., Gibson, K.F., Pandit, K.V., Yu, G., Yakhini, Z., Kaminski, N., 2012. Global methylation patterns in idiopathic pulmonary fibrosis. PLoS ONE 7, 1–9, http://dx.doi.org/10.1371/journal.pone.0033770.

Rattray, A.M.J., 2012. The control of histone gene expression. Biochem. Soc. Trans. 40, 880–885, http://dx.doi.org/10.1042/BST20120065.

Rogakou, E.P., Sekeripataryas, K.E., 1993. A biochemical marker for differentiation is present in an in vitro aging cell system. Biochem. Biophys. Res. Commun. 196, 1274–1279, http://dx.doi.org/10.1006/bbrc.1993.2390.

Sandoval, J., Mendez-gonzalez, J., Nadal, E., Chen, G., Carmona, F.J., Sayols, S., Moran, S., Heyn, H., Vizoso, M., Gomez, A., Sanchez-cespedes, M., Assenov, Y., Bock, C., Taron, M., Mora, J., Muscarella, L.A., Liloglou, T., Davies, M., Pollan, M., Pajares, M.J., Torre, W., Montuenga, L.M., Brambilla, E., Field, J.K., Roz, L., Iacono, M.L., Scagliotti, G.V., Rosell, R., Beer, D.G., 2013. A prognostic DNA methylation signature for stage I non-small-cell lung cancer. J. Clin. Oncol. 31, 4140–4147, http://dx.doi.org/10.1200/JCO.2012.48.5516.

Sawan, C., Herceg, Z., Vaissie, T., 2008. Epigenetic interplay between histone modifications and DNA methylation in gene silencing. Mutat. Res./Rev. Mutat. Res. 659, 40–48, http://dx.doi.org/10.1016/j.mrrev.2008.02.004.

Schostak, M., Payne, S.R., Strauss, A., Thelen, P., Model, F., Day, J.K., Liebenberg, V., Morotti, A., Yamamura, S., Lograsso, J., Sledziewski, A., Semjonow, A., Franklin, C.B., 2009. DNA methylation biomarkers of prostate cancer: confirmation of candidates and evidence urine is the most sensitive body fluid for non-invasive detection. Prostate, 1269, http://dx.doi.org/10.1002/pros.20967.

Singh, R., Mortazavi, A., Telu, K.H., Nagarajan, P., Lucas, D.M., Thomas-Ahner, J.M., Clinton, S.K., Byrd, J.C., Freitas, M.A., Parthun, M.R., 2013. Increasing the complexity of chromatin: functionally distinct roles for replication-dependent histone H2A isoforms in cell proliferation and carcinogenesis. Nucleic Acids Res. 41, 9284–9295, http://dx.doi.org/10.1093/nar/gkt736.

Tsujiuchi, T., Sugata, E., Masaoka, T., Onishi, M., Fujii, H., Shimizu, K., Honoki, K., 2007. Expression and DNA methylation patterns of Tslc1 and Dal-1 genes in hepatocellular carcinomas induced by N-nitrosodiethylamine in rats. Cancer Sci. 98, 943–948, http://dx.doi.org/10.1111/j.1349-7006.2007.00480.x.

Tyagi, M., Khade, B., Khan, S.A., Ingle, A., Gupta, S., 2014. Expression of histone variant, H2A.1 is associated with the undifferentiated state of hepatocyte. Exp. Biol. Med. (Maywood), 1335–1339, http://dx.doi.org/10.1177/1535370214531869.

Urban, M.K., Zweidler, A., 1983. Changes in nucleosomal core histone variants during chicken development and maturation. Dev. Biol. 95, 421–428, http://dx.doi.org/10.1016/0012-1606(83)90043-X.

Wijnen, A.J.V.A.N., Aziz, F., Graniat, X., Lucat, A.D.E., Desai, R.K., Jaarsveld, K., Last, T.J., Soprano, K., Giordanot, A., Lian, J.B., Stein, J.L., Stein, G.S., 1994. Transcription of histone H4, H3, and Hi cell cycle genes: promoter factor HiNF-D contains CDC2, cyclin A, and an RB-related protein. Proc. Natl. Acad. Sci. U. S. A. 91, 12882–12886.

Zhang, X., Zhang, Z., Cheng, J., Li, M., Wang, W., Xu, W., Wang, H., Zhang, R., 2012. Transcription factor NFAT1 activates the mdm2 oncogene independent of p53. J. Biol. Chem. 287, 30468–30476, http://dx.doi.org/10.1074/jbc.M112.373738.

Zhao, J., Kennedy, B.K., Lawrence, B.D., Barbie, D.A., Matera, A.G., Fletcher, J.A., Harlow, E., 2000. NPAT links cyclin E-Cdk2 to the regulation of replication-dependent histone gene transcription. Genes Dev., 2283–2297, http://dx.doi.org/10.1101/gad.827700.

Scientific Research

# Histone Chaperones: Functions beyond Nucleosome Deposition

## Divya Reddy, Saikat Bhattacharya, Sanjay Gupta*

Epigenetics and Chromatin Biology Group, Gupta Lab., Cancer Research Institute, Advanced Centre for Treatment, Research and Education in Cancer, Tata Memorial Centre, Navi Mumbai, India
Email: dvelga@actrec.gov.in, sbhattacharya@actrec.gov.in, *sgupta@actrec.gov.in

## Abstract

**Histones, the structural unit of chromatin, must be assembled/dissembled to preserve or change chromatin organization in accordance to cellular needs. Initially, function of histone chaperones was thought to be only "histone carriers/vehicles", but now with accumulating evidences they are known to be the key actors of histone metabolism. With this outburst of knowledge, histone chaperones are now placed at the center of gene regulation, having roles to play in DNA replication, repair and transcription. This review will focus on the current knowledge we have about the role of histone chaperones in regulating cellular processes and their relation to disease. In addition, we discuss the potential of histone chaperones as a therapeutic target.**

## Keywords

**Histones, Chromatin, Cancer, Therapeutic Target**

## 1. Introduction

If the DNA of all the cells of a human body is joined end to end, it can cover the distance from the sun to the Pluto and back. It was always a matter of interest to understand how the DNA of a cell which is over a meter long is packaged inside the nucleus only about 10 microns in diameter. Later, it was found that basic proteins called "histones" play a major role in packaging of DNA, in a very orderly fashion so that it can be unwound quickly when required in specific foci, and then wound back without getting into a tangle. During compaction, at first ~147 bp of DNA is wrapped around histone octamer comprising 2 each of histones H2A, H2B, H3, H4, thus giving rise to nucleosome core particle (NCP)—a basic unit of chromatin [1]. This conformation achieved is also known as "beads on a string structure" or 10-nm chromatin fibre. The nucleosome assembly occurs in an

_____
*Corresponding author.

orderly fashion. First H3/H4 tetramers are deposited on DNA, thus marking the site for NCP formation (nucleosome positioning) followed by deposition of two H2A/H2B dimers [2]. Then linker histone H1 seals off the NCP by sitting at the entry and exit site of DNA in the octamer. This leads to further compaction giving rise to the 30-nm chromatin fibre [3]. This structure further folds on itself with the help of other non-histone proteins ultimately leading to the formation of the highly compact metaphase chromosome. The disassembly of nucleosome follows the same events in a reverse order.

What recruits the H3/H4 tetramer and the H2A/H2B dimer onto the DNA? How do the disassembly of NCP achieve? What prevents the histones? Which are highly basic in nature to form non-specific aggregates within themselves and with DNA? Which is negatively charged? All these functions are carried out by a class of proteins designated as histone chaperones.

Quite a few histone chaperones have been characterized and the last decade has seen the discovery of many novel histone chaperones. Besides the discovery of new chaperones in recent years, an outburst of knowledge about histone chaperones in relation to gene regulation and disease has been seen. The same can be said about the parcel of the chaperones, the histones and their variants. This review will focus on the current knowledge we have about the role of histone chaperones in DNA replication, repair and transcription followed by their role in regulating cellular processes and their relation to disease. Further, we discuss the potential of using histone chaperones as a therapeutic target.

## 2. Histone Chaperones: The Efficient Molecular Couriers

Histones being highly basic in nature are designed to bind to a variety of DNA sequences. However, it was discovered that octamer has got a propensity to bind preferentially to certain DNA sequences like that to a sequence contained within 5S RNA gene of sea urchin [4]. This preference is also apparent in *in vitro* nucleosomal array reconstitution experiments using the salt dialysis method in which equally spaced arrays are formed only when positioning sequences like Widom 601 are used [5]. This preference possibly has to do with the bendability of the DNA sequence. However, despite the presence of heterogeneous DNA sequence in living organisms equally spaced arrays are formed with the aid of histone chaperones and chromatin remodelling complexes. In *in vitro* systems also when a chaperone like NAP1 is added evenly spaced arrays are formed [6], demonstrating that the histone chaperones clearly have the ability to form nucleosomes irrespective of sequence preference.

Histone chaperones can be illustrated on the basis of their histone binding selectivity and thus deposition, using which they can be differentiated into those favorably interacting with H3-H4 from those that prefer H2A-H2B. Some of the very well-studied chaperones of H2A/H2B includes Nap-1 (nucleosome assembly protein-1), first identified in HeLa cell extracts as an activity that facilitates the *in vitro* reconstitution of nucleosomes using pure histones in combination with other factors. Another H2A/H2B chaperone is FACT (Facilitates Active Chromatin Transcription) complex composed of two subunits hSpt16 and SSRP1, identified initially as a factor indispensable for transcriptional elongation through chromatin [7]. Later it has been shown to form stable complexes with the histone H2A-H2B dimer and functions through restructuring of nucleosomes within the ORFs of actively transcribed genes [8]. Examples of H3/H4 chaperones are CAF-1 (Chromatin Assembly Factor) complex consisting of three subunits: p150, p60 and p48 [9], formerly identified by complementation as a factor participating in the assembly of chromatin during SV40 origin-dependent DNA replication in human cell extracts. N1/N2 is also an H3/H4 chaperone, isolated first from oocytes of *X. laevis.* Later on its homologs were discovered in budding and fission yeast [10]. Apart from the core histones, linker histone H1 also has a chaperone-NASP (Nuclear Autoantigenic Sperm Protein), aiding its deposition on to the DNA.

Apart from showing selectivity towards different core histones, some chaperones are also known to be specific towards certain H3 and H2A isoforms/variants. These chaperones specially bind either replicative variants, which form the bulk of the histone pool, are expressed and deposited in a replication-coupled manner during S phase of cell cycle, or replacement variants, which are expressed and incorporated in a replication-independent fashion. The best studied examples of such specificity are chaperones CAF-1 and HIRA (Histone Regulator A) preferentially depositing H3.1 (replication coupled) and H3.3 (replication independent) respectively [11]. Other histone variant specific chaperones include Chz1 (Chaperone of H2A.Z/H2B) of yeast [12], ANP32E a specific H2A.Z chaperone in humans [13], DAXX and DEK for chaperoning H3.3 histones [14]. Although examples of preferential chaperone-histone interaction exist, one should not undermine those chaperones which bind to multiple histones in a specific manner. For example, Nap1 despite being a H2A/H2B chaperone binds to linker histone in *X. laevis* eggs [15]. Similarly, nucleoplasmin, a H2A/H2B chaperone binds to linker histones and re-

moves them from sperm and somatic chromatin during fertilization and early development [16]. The same is also observed for Nucleophosmin (NPM-1) which interacts with histones H3/H4 and H1 [17].

This raises the question of how histone chaperones interact with histones. Many chaperones like nucleoplasmin, yeast Asf1, yeast Nap1, the Spt16 subunit of FACT and nucleolin contain long acidic amino acid stretches with which they interact with basic histones leading to charge neutralization [18]. However, charge neutralization does not justify for the specificity of the histone-chaperone interaction and it cannot be the universal phenomenon for all the chaperones as, mammalian Asf1 and Drosophila Nap-1 lacks an acidic tail [19]. Therefore, it could be that these acidic regions may assist in strengthening histone-chaperone interaction. May be due to this reason, Nap-1 undergoes extensive polyglutamylation [20], also Nap-1 is known to aid in nucleosome assembly by eliminating the non-nucleosomal histone DNA interactions. Other chaperones like Asf-1, CAF-1 and HIRA are known to contain a conserved hydrophobic $\beta$-structure, which facilitates interaction with H3/H4 [21]-[23]. Similar structure is also seen in H2A/H2B chaperones SET/TAF-1b and Nap-1, mutational studies have implicated that this conserved $\beta$ sheet may be the primary histone recognition motif in these chaperones [24]. For more extensive examples of how chaperones recognize their target readers may refer to some other well written review [25].

## 3. Only a Vehicle or More?

Formerly chaperones were thought to be as mere "histone carriers/vehicles" but now with accumulating evidence they are known to be key players at all phases of histone existence. Chaperones interact with histones upon their synthesis thus preventing their aggregation and interaction with other cellular moieties. Also guide them into the nucleus, and help in their specific association with DNA during different processes involving DNA-replication, repair and transcription (discussed in detail below). They bring about these varied functions by interacting with many cellular factors with the help of which they determine the site and position of nucleosome assembly/disassembly and thus affecting gene regulation. Therefore, from being just an observer to an active participant, chaperones have evolved as the crucial component in maintaining chromatin integrity and dynamics.

### 3.1. Histone Chaperones: Role in DNA Replication and Repair

Chromatin acts as a barrier for the DNA pol and RNA pol enzymes for replication and transcription respectively. Hence, for genome duplication the nucleosomes should be dissembled first and once the replication fork has progressed and daughter strands have been synthesized they should be assembled back. The same is consistent for transcription. During replication the hexameric MCM2-7 helicase unwinds double-stranded DNA to facilitate the progress of DNA polymerase. In doing so it disrupts existing nucleosomes, releasing histones. With the aid of its interaction with Mcm4, FACT chaperone complex picks up evicted H2A/H2B dimer [26]. Similarly Asf1 chaperone through its interaction with MCM complex takes up H3-H4 [27]. The existence of both chaperones at the replication fork is critical as FACT accelerates the unwinding activity of MCM and promotes formation of DNA replication origins [28]. Similarly, depletion of Asf1 has been shown to impair MCM helicase activity [27]. Once the DNA pol has passed, chaperones transfer parental histones back on to DNA and thus assembling nucleosomes. The Asf1-MCM interaction ensures accurate deposition of parental histones. Any inaccurate deposition may lead to loss of parental histone post-translational modifications (PTMs) involved in epigenetic silencing of gene expression [29]. In addition to parental histone transfer, histone chaperones promptly deposit newly synthesized histones onto nascent DNA. While deposition, chaperones also modulate, directly or indirectly, histone posttranslational modifications (PTMs). For example, the association between H3-H4 and Asf1 is required for acetylation of H3 lysine 56 (H3K56) by the Rtt109 acetyl transferase [30]. Following acetylation, the H3-H4 dimers are transferred to the next set of chaperones, CAF-1 and Rtt106, which then deposit the histones onto nascent DNA by their interaction with PCNA (proliferating cell nuclear antigen), known to be a processivity factor for DNA polymerases [31]. Thus, incorporation of new histones into nucleosomes is a carefully designed process carried out by a chain of histone chaperones.

There are no evidences of histone chaperones playing a dynamic role in chromatin disassembly process for the repair of double-strand break or a UV lesion. This is in disparity with DNA replication, where the lack of histone chaperones inhibits DNA replication. However, this does not exclude a role of histone chaperones as histone acceptors during the chromatin disassembly coupled to DNA repair. After nucleotide excision repair, the

nucleosome reassembly near the repair site is done by the human H3/H4 histone chaperones Asf1 and CAF-1 in a process similar to that of DNA replication [32].

## 3.2. Histone Chaperones: Role in DNA Transcription

A genome-wide loss of nucleosomes in the regulatory region is seen upon transcriptional activation suggesting that nucleosome depletion is a key factor involved in transcription [33]. Histone chaperones like FACT, also known as RNA polymerase II elongation complex, are involved in the rearrangement of histones H2A/H2B during transcriptional activation. How this disassembly and reassembly is regulated and coordinated with polymerase passage is still not very well understood. It is speculated that phosphorylation of the C-terminal domain (CTD) of the RNA polymerase (RNAP) II and posttranslational modifications of histones play a central role [34]. After the elongating polymerase has passed the promoter, it is phosphorylated by the Ctk1 kinase on Serine (Ser) 2 of the CTD [35]. This phosphorylated Ser 2 recruits the Set2 methyltransferase which then methylates H3 K36 (H3 K36Me), leading to the recruitment of the small Rpd3 (Rpd3S), a histonedeacetylase (HDAC) complex [36]. Once recruited, it leads to deacetylation of H3 and H4 thereby promoting chromatin reassembly and compaction. Throughout this process histone chaperones Nap-1 and Vsp75 interact with Ctk-1 kinase and Set2 [37]. This rapid reassembly is very important because any delay may lead to transcription from cryptic initiation sites present with ORFs, which may interfere with normal programming of the cell [38]. Another important prerequisite for rapid assembly is if long stretches of naked DNA are left out they may form R-loops, in which RNA transcripts are hybridized back to its template DNA strand, an important source of genomic instability [39]. Cells also have evolved a backup plan to avoid such deleterious effects. Histone chaperone HIRA deposits specialized histone variant H3.3 in the regions which are actively transcribed [40]. This in part is facilitated because ASF1 travels with the transcription machinery and/or rapidly fills in the gaps left in nucleosome arrays following passage of RNA polymerase by donating H3.3 to HIRA [41]. Therefore, in combination with reassembly of parental histones, incorporation of histone variants help to cover up DNA after transcription.

## 4. Histone Chaperones in Regulating Cellular Functions

The barcoding of genome with proper histone variants especially H3 variants safe guards the cellular memory of the transcriptional status of genes which can be inherited across generations [42]. In this regard, it can be considered that histone chaperones responsible for the deposition of histone variants, play an active role in the remodeling of the chromatin domains in accordance to cell-type specific gene expression patterns. Indeed, as expected HIRA, a histone chaperone of H3.3 along with depositing H3.3 in a replication independent manner at transcriptionally active loci also plays a role in cellular processes like skeletal myogenesis [43]. In response to differentiation signals, rapid accumulation of H3.3 is seen in enhancer regions and promotor regions of MyoD gene, leading to loss of H1, opening of chromatin, and eventual acceleration of transcription initiation at MyoD gene locus [44]. Upon their expression DNA binding transcription factors MyoD and Mef2, recruit ATP-dependent chromatin-remodeling complexes and histone-modifying enzymes for the activation of muscle genes [45]. The role of HIRA in muscle differentiation is more evident when HIRA-null mice die between embryonic days 10 and 11 with a wide range of phenotypes caused by defective mesendodermal tissues [46]. HIRA and H3.3 also play a major role in the early steps of osteoblastic differentiation [47]. Also, in response to angiogenic signal, levels of H3K56 acetylation is increased within endothelial cells, at the chromatin domains of *Vegfr*1, *Fgf*1 and *Pdgfa* (angiogenic genes) via a HIRA-mediated histone H3 exchange [48]. Not only in myogenesis and angiogenesis, recent genome-wide analysis of H3.3 has shown many upstream regulatory enhancers enriched with H3.3, signifying the site specific and regulated deposition of H3.3 by HIRA [14]. The assembly of histone variant H3.3, into nucleosomes by the replication-independent pathway is mediated by multiple histone chaperones, including HIRA (as discussed above), DAXX (death domain-associated protein) and DEK. H3.3 chaperones, DEK and DAXX are involved in the deposition and exchange of H3.3 at telomeres and regulatory elements [49]. DAXX along with the chromatin-remodeling factor ATRX (alpha thalassemia/mental retardation syndrome X-linked) regulates H3.3 deposition at telomeric heterochromatin regions [50]. DEK plays a major a role in maintaining heterochromatin integrity through its interaction with HP1$\alpha$ [51]. These facts conclude that H3.3 deposition at diverse chromatin regions occurs by distinct histone chaperones. Thus chaperones play an important role in gene expression by altering the chromatin environment locally by depositing their respective histone variants.

## 5. Histone Chaperones and Human Disease

Any mis-positioning of nucleosomes on to a stretch of DNA results in defect in gene expression and at times genome instability and cancer. Therefore, it is not incorrect to assume that mis-regulation of histone chaperones or histone-modifying enzymes regulating nucleosome assembly/disassembly may stimulate development of human disease (**Figure 1**). Here we discuss few reports highlighting the role of histone chaperones in disease pathogenesis and their potential to be used as a therapeutic marker. Proliferation is one of the key physiological characters of cancer. Indeed few of histone chaperones are known to be highly expressed in proliferating cells. For instance-Asf1b, an isoform of Asf1 in mammalian cells, is essential for cell proliferation as seen to be down regulated in senescent cells. When its levels were checked in various breast cancer cell lines a correlation was observed with a proliferative status of cells, with more expression in highly proliferative cells. The same association was seen with breast cancer patients and is related to increased metastasis and shorter survival of breast cancer patients [52]. Apart from Asf1b, CAF-1 is also known to be highly expressed in breast cancer tissues and in prostate cancers [53]. CAF-1 p60 levels also correlated significantly in many solid tumors with disease stage, especially in renal, endometrial and cervical cancer patients [54]. A splice variant of NASP, tNASP also has been shown to be expressed in high levels in cancer, germ, transformed, and embryonic cells. When its expression was reduced in prostate cancer cell line PC-3 and in HeLa, inhibition of proliferation, increased levels of p21 and apoptosis was seen [55].

FACT complex (H2A/H2B chaperone) is expressed at higher levels in tumor cell lines than in normal cells *in vitro* and its knockdown lead to reduced growth and survival of tumor cells [56]. In addition, FACT expression was found to be elevated during the development of mammary carcinomas in transgenic mice expressing the Her2/neu protooncogene [57]. Genome-wide analysis for FACT distribution in tumor cells has identified a subset of genes that have activities associated with malignancy and stem-like properties of tumor cells and cellular stress responses. Also FACT expression is seen to be elevated upon *in vitro* transformation of fibroblasts and epithelial cells by various agents indicating its requirement for transformation, but its overexpression cannot substitute for the requirement of H-Ras$^{V12}$. Therefore FACT cannot act as an oncogene but can still accelerate malignancy by providing certain chromatin changes which still needs to be elucidated. Moreover its expression can be significantly correlated with aggressiveness of cancers as elevated expression is seen during metastasis of
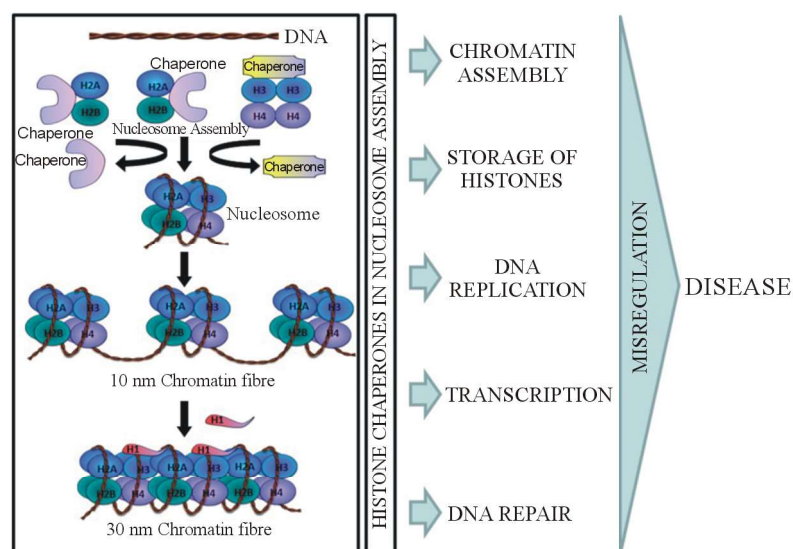


**Figure 1.** Chaperone and disease. Histone chaperones bind to their respective histone molecules and deposit them on to DNA template, leading to formation of nucleosome, repeating units of which join together to form a 10 nm chromatin fibre and upon H1 deposition a 30 nm chromatim structure is formed thus leading to compaction of DNA. By playing a major role in chromatin assembly, chaperones act as a central to DNA replication, repair and transcription. Thus, any misregulation in the levels of these proteins or any mutation in them leads to disease.

breast, renal, and prostate cancer [58]. Mutations in another H2A/H2B chaperone Nap-1 have also been associated with many human cancers. NPM1 (chaperone for H3/H4 and H1) play a role in ribosome assembly, inhibition of pro-apoptotic pathways, maintenance of genomic stability. It has also been known to interact with the tumor suppressor protein p53, Rb, and ARF and also many other viral proteins [59]. Also is significantly abundant in tumor and growing cells compared to normal cells, hence used as a tumor marker and also known to be a putative proto-oncogene [60]. NPM1 mutations are common in acute myeloid leukemia (AML) which is characterized by abnormal NPM1 accumulation in the cytoplasm [61]. Survival of NPM-negative colorectal cancer patients be likely to be better than those for patients with NPM-positive lesions [62].

Overexpression of the DEK, a histone chaperone for H3.3 has been reported in a number of cancers like glioblastoma, melanoma, colorectal and bladder carcinoma and is known to play major role in promoting epithelial transformation. DEK inhibits senescence and apoptosis via the destabilization of p53, hinting its role in carcinogenesis. In human promyelocytic HL-60 cells differentiation led to DEK down regulation [63]. Conversely, upon overexpression of the DEK, differentiation programs can be neutralized, favoring oncogenic transformation [63]. A direct proof of DEK as "oncogene" has developed when it was seen that papilloma formation was significantly decreased in DEK knockout mice compared to wild type animals and heterozygote controls [64]. It also forms a fusion protein with calcium-dependent phosphatase calcineurin (CAN) owing to chromosomal translocation which has been detected in acute myeloid leukemia (AML) [65]. This fusion results in reduced interactions of DEK with H3.3 aiding in the recruitment of HP1 and thus promoting leukemia progression through misregulation of transcriptional repression [51]. Amplifications and copy number increase of the DEK gene were also found in a variety of malignancies, particularly in bladder cancer, melanoma and retinoblastoma [66].

Apart from overexpression, certain mutations within chaperones and their associated proteins have also been related to cancer. Mutations in Daxx-ATRX–H3.3 pathway have been observed in pancreatic neuroendocrine tumors [67]. Such mutations have also been identified in pediatric glioblastoma tumor samples. Because of their high incidence these mutations are now called as the "driver mutations" for promoting cancers [68]. In addition to cancer, misregulation of histone chaperones has also been reported in other diseases. In DiGeorge syndrome (DGS), small region of six HIRA genes located on Chromosome 22 is frequently deleted resulting in reduced levels of HIRA production [69]. It has been reported that reduction of HIRA in animal model systems leads to persistent truncusarteriosus, a phenotypic change associated with DGS [70], suggesting that HIRA haploinsufficiency contributes to the development of DGS.

## 6. Concluding Remarks

Histone chaperones play a central role in governing many of the cellular functions and hence disease (specific chaperones are exemplified in **Table 1**). In this era of modern medicine where targeted therapies are being looked upon as the new ray of hope to win long fought battles against diseases like cancer, targeting histone

**Table 1.** Histone chaperones, functions and their implications in disease.

| Histone chaperone | Functions | Implication in disease | Reference number |
|---|---|---|---|
| Asf1 | Histone import, histone transfer to CAF-1 and HIRA, regulation of H3K56ac | Increased in breast cancer | 28, 31, 44, 58 |
| CAF-1 | H3.1-H4 deposition, heterochromatin formation, repair | Increased in renal, endometrial and cervical cancer | 12, 33, 46, 59 |
| DAXX | H3.3-H4 deposition at telomeric heterochromatin | Mutated in pancreatic neuroendocrine and glioblastoma | 55, 56, 68 |
| DEK | H3.3-H4 deposition, maintenance of heterochromatin | DEK-CAN fusion due to chromosomal translocation in AML | 55, 57, 66, 67 |
| NASP | H1 and H3/H4 supply and turnover | Increased in prostate cancer | 11, 60 |
| NPM | H1 and H3/H4 deposition, ribosome assembly, genomic stability | Mutated in AML patients | 18, 64, 65 |
| FACT | H2A/H2B deposition, Transcription | Increased during metastasis of breast, renal, and prostate cancer | 7, 61, 62, 63 |

chaperones may be a new weapon in the armory. Histone chaperones Asf1b, CAF-1p60 and tNASP are highly correlated with proliferating cells and with many cancers. Therefore these can be used as new proliferation markers of interest for early detection of a wide range of cancers, and can also be used as a powerful prognostic marker for occurrence of metastasis. Knockdown of tNASP resulted in inhibition of proliferation and apoptosis [55], leading us to consider them not only as prognostic markers, but also as a target of diagnostic importance. Another histone chaperone which has been in the limelight in recent years for its correlation with cancer is the FACT complex. Levels of FACT complex increase in certain cancers, based on which they can be divided into FACT positive and negative cancers. Survival of patients with FACT-positive tumors was significantly less than that of patients with FACT-negative tumors. Also, within these FACT-positive cancers, the levels of expression are very different; the more the expression of FACT, the more aggressive is the cancer. Link between FACT expression and metastasis is corroborated by the reports of levels of FACT to be significantly correlated with metastasis of breast, renal, and prostate cancer [58]. Hence it can act as a promising marker and target for those cancers characterized by high aggressiveness and poor prognosis. As FACT expression is absent/less in most normal cells/tissues, pharmacological inhibition of FACT could be a safe and operative strategy to treat those types of cancer for which there are very few treatment modalities.

Not only can the levels of chaperones, but also mutations in these proteins contribute towards disease progression. Using deep sequencing technology, mutations have been found in the H3.3/ATRX-DAXX pathway in pediatric glioblastoma tissue samples. As these mutations are very specific to cancer, drugs can be developed for targeting specifically such cancers. Even though many intricate details of how these mutations in chaperones and related proteins lead to human diseases are still in the dark, but with the advent of recent technologies it is hopefully just a matter of time for these to be revealed and targeted. However, before using them as therapeutic targets, further understanding is needed to determine whether the altered abundance of histone chaperones observed in human cancers is the consequence or the cause of tumorigenesis. Nonetheless, it leads us to hypothesize for the role of histone chaperones as a promising molecular target for therapies aiming to reverse epigenetic alterations in various diseases.

## Acknowledgements

## References

[1]   Luger, K., Mader, A.W., Richmond, R.K., Sargent, D.F. and Richmond, T.J. (1997) Crystal Structure of the Nucleosome Core Particle at 2.8 A Resolution. *Nature*, **389**, 251-260. http://dx.doi.org/10.1038/38444

[2]   Smith, S. and Stillman, B. (1991) Stepwise Assembly of Chromatin during DNA Replication *in Vitro*. *EMBO Journal*, **10**, 971-980.

[3]   Thoma, F., Koller, T. and Klug, A. (1979) Involvement of Histone H1 in the Organization of the Nucleosome and of the Salt-Dependent Superstructures of Chromatin. *Journal of Cell Biology*, **83**, 403-427. http://dx.doi.org/10.1083/jcb.83.2.403

[4]   Panetta, G., Buttinelli, M., Flaus, A., Richmond, T.J. and Rhodes, D. (1998) Differential Nucleosome Positioning on Xenopus Oocyte and Somatic 5 S RNA Genes Determines Both TFIIIA and H1 Binding: A Mechanism for Selective H1 Repression. *Journal of Cell Biology*, **282**, 683-697.

[5]   Lowary, P.T. and Widom, J. (1998) New DNA Sequence Rules for High Affinity Binding to Histone Octamer and Sequence-Directed Nucleosome Positioning. *Journal of Cell Biology*, **276**, 19-42.

[6]   Verreault, A. (2000) *De Novo* Nucleosome Assembly: New Pieces in an Old Puzzle. *Genes & Development*, **14**, 1430-1438.

[7]   Orphanides, G., LeRoy, G., Chang, C.H., Luse, D.S. and Reinberg, D. (1998) FACT, a Factor That Facilitates Transcript Elongation through Nucleosomes. *Cell*, **92**, 105-116. http://dx.doi.org/10.1016/S0092-8674(00)80903-4

[8]   Orphanides, G. and Reinberg, D. (2000) RNA Polymerase II Elongation through Chromatin. *Nature*, **407**, 471-475. http://dx.doi.org/10.1038/35035000

[9]   Smith, S. and Stillman, B. (1989) Purification and Characterization of CAF-I, a Human Cell Factor Required for Chromatin Assembly during DNA Replication *in Vitro*. *Cell*, **58**, 15-25. http://dx.doi.org/10.1016/0092-8674(89)90398-X

[10] De Robertis, E.M., Longthorne, R.F. and Gurdon, J.B. (1978) Intracellular Migration of Nuclear Proteins in Xenopus Oocytes. *Nature*, **272**, 254-256. http://dx.doi.org/10.1038/272254a0

[11] Tagami, H., Ray-Gallet, D., Almouzni, G. and Nakatani, Y. (2004) Histone H3.1 and H3.3 Complexes Mediate Nucleosome Assembly Pathways Dependent or Independent of DNA Synthesis. *Cell*, **116**, 51-61. http://dx.doi.org/10.1016/S0092-8674(03)01064-X

[12] Luk, E., Vu, N.D., Patteson, K., Mizuguchi, G., Wu, W.H., Ranjan, A., Backus, J., Sen, S., Lewis, M., Bai, Y. and Wu, C. (2007) Chz1, a Nuclear Chaperone for Histone H2AZ. *Molecular Cell*, **25**, 357-368. http://dx.doi.org/10.1016/j.molcel.2006.12.015

[13] Obri, A., Ouararhni, K., Papin, C., Diebold, M.L., Padmanabhan, K., Marek, M., Stoll, I., Roy, L., Reilly, P.T., Mak, T.W., Dimitrov, S., Romier, C. and Hamiche, A. (2014) ANP32E Is a Histone Chaperone That Removes H2A.Z from Chromatin. *Nature*, **505**, 648-653. http://dx.doi.org/10.1016/j.molcel.2006.12.015

[14] Goldberg, A.D., Banaszynski, L.A., Noh, K.M., Lewis, P.W., Elsaesser, S.J., Stadler, S., Dewell, S., Law, M., Guo, X., Li, X., Wen, D., Chapgier, A., DeKelver, R.C., Miller, J.C., Lee, Y.L., Boydston, E.A., Holmes, M.C., Gregory, P.D., Greally, J.M., Rafii, S., Yang, C., Scambler, P.J., Garrick, D., Gibbons, R.J., Higgs, D.R., Cristea, I.M., Urnov, F.D., Zheng, D. and Allis, C.D. (2010) Distinct Factors Control Histone Variant H3.3 Localization at Specific Genomic Regions. *Cell*, **140**, 678-691. http://dx.doi.org/10.1016/j.cell.2010.01.003

[15] Shintomi, K., Iwabuchi, M., Saeki, H., Ura, K., Kishimoto, T. and Ohsumi, K. (2005) Nucleosome Assembly Protein-1 Is a Linker Histone Chaperone in Xenopus Eggs. *Proceedings of the National Academy of Sciences of the United States of America*, **102**, 8210-8215. http://dx.doi.org/10.1073/pnas.0500822102

[16] Wade, P.A. and Kikyo, N. (2002) Chromatin Remodeling in Nuclear Cloning. *European Journal of Biochemistry*, **269**, 2284-2287. http://dx.doi.org/10.1046/j.1432-1033.2002.02887.x

[17] Gadad, S.S., Senapati, P., Syed, S.H., Rajan, R.E., Shandilya, J., Swaminathan, V., Chatterjee, S., Colombo, E., Dimitrov, S., Pelicci, P.G., Ranga, U. and Kundu, T.K. (2011) The Multifunctional Protein Nucleophosmin (NPM1) Is a Human Linker Histone H1 Chaperone. *Biochemistry*, **50**, 2780-2789. http://dx.doi.org/10.1021/bi101835j

[18] Angelov, D., Bondarenko, V.A., Almagro, S., Menoni, H., Mongelard, F., Hans, F., Mietton, F., Studitsky, V.M., Hamiche, A., Dimitrov, S. and Bouvet, P. (2006) Nucleolin Is a Histone Chaperone with FACT-Like Activity and Assists Remodeling of Nucleosomes. *EMBO Journal*, **25**, 1669-1679. http://dx.doi.org/10.1038/sj.emboj.7601046

[19] Park, Y.J. and Luger, K. (2006) The Structure of Nucleosome Assembly Protein 1. *Proceedings of the National Academy of Sciences of the United States of America*, **103**, 1248-1253. http://dx.doi.org/10.1073/pnas.0508002103

[20] van Dijk, J., Miro, J., Strub, J.M., Lacroix, B., van Dorsselaer, A., Edde, B. and Janke, C. (2008) Polyglutamylation Is a Post-Translational Modification with a Broad Range of Substrates. *Journal of Biological Chemistry*, **283**, 3915-3922. http://dx.doi.org/10.1074/jbc.M705813200

[21] Daganzo, S.M., Erzberger, J.P., Lam, W.M., Skordalakes, E., Zhang, R., Franco, A.A., Brill, S.J., Adams, P.D., Berger, J.M. and Kaufman, P.D. (2003) Structure and Function of the Conserved Core of Histone Deposition Protein Asf1. *Current Biology*, **13**, 2148-2158. http://dx.doi.org/10.1016/j.cub.2003.11.027

[22] DeSilva, H., Lee, K. and Osley, M.A. (1998) Functional Dissection of Yeast Hir1p, a WD Repeat-Containing Transcriptional Corepressor. *Genetics*, **148**, 657-667.

[23] Kaufman, P.D., Kobayashi, R., Kessler, N. and Stillman, B. (1995) The p150 and p60 Subunits of Chromatin Assembly Factor I: A Molecular Link between Newly Synthesized Histones and DNA Replication. *Cell*, **81**, 1105-1114. http://dx.doi.org/10.1016/S0092-8674(05)80015-7

[24] Muto, S., Senda, M., Akai, Y., Sato, L., Suzuki, T., Nagai, R., Senda, T. and Horikoshi, M. (2007) Relationship between the Structure of SET/TAF-Iβ/INHAT and Its Histone Chaperone Activity. *Proceedings of the National Academy of Sciences of the United States of America*, **104**, 4285-4290. http://dx.doi.org/10.1073/pnas.0603762104

[25] Park, Y.J. and Luger, K. (2008) Histone Chaperones in Nucleosome Eviction and Histone Exchange. *Current Opinion in Structural Biology*, **18**, 282-289. http://dx.doi.org/10.1016/j.sbi.2008.04.003

[26] Gambus, A., Jones, R.C., Sanchez-Diaz, A., Kanemaki, M., van Deursen, F., Edmondson, R.D. and Labib, K. (2006) GINS Maintains Association of Cdc45 with MCM in Replisome Progression Complexes at Eukaryotic DNA Replication Forks. *Nature Cell Biology*, **8**, 358-366.

[27] Groth, A., Corpet, A., Cook, A.J., Roche, D., Bartek, J., Lukas, J. and Almouzni, G. (2007) Regulation of Replication Fork Progression through Histone Supply and Demand. *Science*, **318**, 1928-1931. http://dx.doi.org/10.1126/science.1148992

[28] Tan, B.C., Chien, C.T., Hirose, S. and Lee, S.C. (2006) Functional Cooperation between FACT and MCM Helicase Facilitates Initiation of Chromatin DNA Replication. *EMBO Journal*, **25**, 3975-3985. http://dx.doi.org/10.1038/sj.emboj.7601271

[29] Jasencakova, Z., Scharf, A.N., Ask, K., Corpet, A., Imhof, A., Almouzni, G. and Groth, A. (2010) Replication Stress

Interferes with Histone Recycling and Predeposition Marking of New Histones. *Molecular Cell*, **37**, 736-743. http://dx.doi.org/10.1016/j.molcel.2010.01.033

[30] Adkins, M.W., Carson, J.J., English, C.M., Ramey, C.J. and Tyler, J.K. (2007) The Histone Chaperone Anti-Silencing Function 1 Stimulates the Acetylation of Newly Synthesized Histone H3 in S-Phase. *Journal of Biological Chemistry*, **282**, 1334-1340. http://dx.doi.org/10.1074/jbc.M608025200

[31] Rolef Ben-Shahar, T., Castillo, A.G., Osborne, M.J., Borden, K.L., Kornblatt, J. and Verreault, A. (2009) Two Fundamentally Distinct PCNA Interaction Peptides Contribute to Chromatin Assembly Factor 1 Function. *Molecular and Cellular Biology*, **29**, 6353-6365. http://dx.doi.org/10.1128/MCB.01051-09

[32] Mello, J.A., Sillje, H.H., Roche, D.M., Kirschner, D.B., Nigg, E.A. and Almouzni, G. (2002) Human Asf1 and CAF-1 Interact and Synergize in a Repair-Coupled Nucleosome Assembly Pathway. *EMBO Reports*, **3**, 329-334. http://dx.doi.org/10.1093/embo-reports/kvf068

[33] Lee, C.K., Shibata, Y., Rao, B., Strahl, B.D. and Lieb, J.D. (2004) Evidence for Nucleosome Depletion at Active Regulatory Regions Genome-Wide. *Nature Genetics*, **36**, 900-905. http://dx.doi.org/10.1038/ng1400

[34] Selth, L.A., Sigurdsson, S. and Svejstrup, J.Q. (2010) Transcript Elongation by RNA Polymerase II. *Annual Review of Biochemistry*, **79**, 271-293. http://dx.doi.org/10.1146/annurev.biochem.78.062807.091425

[35] Cho, E.J., Kobor, M.S., Kim, M., Greenblatt, J. and Buratowski, S. (2001) Opposing Effects of Ctk1 Kinase and Fcp1 Phosphatase at Ser 2 of the RNA Polymerase II C-Terminal Domain. *Genes & Development*, **15**, 3319-3329. http://dx.doi.org/10.1101/gad.935901

[36] Lee, J.S. and Shilatifard, A. (2007) A Site to Remember: H3K36 Methylation a Mark for Histone Deacetylation. *Mutation Research*, **618**, 130-134. http://dx.doi.org/10.1016/j.mrfmmm.2006.08.014

[37] Xue, Y.M., Kowalska, A.K., Grabowska, K., Przybyt, K., Cichewicz, M.A., Del Rosario, B.C. and Pemberton, L.F. (2013) Histone Chaperones Nap1 and Vps75 Regulate Histone Acetylation during Transcription Elongation. *Molecular and Cellular Biology*, **33**, 1645-1656. http://dx.doi.org/10.1128/MCB.01121-12

[38] Duina, A.A., Rufiange, A., Bracey, J., Hall, J., Nourani, A. and Winston, F. (2007) Evidence That the Localization of the Elongation Factor Spt16 across Transcribed Genes Is Dependent upon Histone H3 Integrity in *Saccharomyces cerevisiae*. *Genetics*, **177**, 101-112. http://dx.doi.org/10.1534/genetics.106.067140

[39] Aguilera, A. and Garcia-Muse, T. (2012) R Loops: From Transcription Byproducts to Threats to Genome Stability. *Molecular Cell*, **46**, 115-124. http://dx.doi.org/10.1016/j.molcel.2012.04.009

[40] Ahmad, K. and Henikoff, S. (2002) The Histone Variant H3.3 Marks Active Chromatin by Replication-Independent Nucleosome Assembly. *Molecular Cell*, **9**, 1191-1200. http://dx.doi.org/10.1016/S1097-2765(02)00542-7

[41] Schwabish, M.A. and Struhl, K. (2006) Asf1 Mediates Histone Eviction and Deposition during Elongation by RNA Polymerase II. *Molecular Cell*, **22**, 415-422. http://dx.doi.org/10.1016/j.molcel.2006.03.014

[42] Jenuwein, T. and Allis, C.D. (2001) Translating the Histone Code. *Science*, **293**, 1074-1080. http://dx.doi.org/10.1126/science.1063127

[43] Yang, J.H., Choi, J.H., Jang, H., Park, J.Y., Han, J.W., Youn, H.D. and Cho, E.J. (2011) Histone Chaperones Cooperate to Mediate Mef2-Targeted Transcriptional Regulation during Skeletal Myogenesis. *Biochemical and Biophysical Research Communications*, **407**, 541-547. http://dx.doi.org/10.1016/j.bbrc.2011.03.055

[44] Yang, J.H., Song, Y., Seol, J.H., Park, J.Y., Yang, Y.J., Han, J.W., Youn, H.D. and Cho, E.J. (2011) Myogenic Transcriptional Activation of *Myo*D Mediated by Replication-Independent Histone Deposition. *Proceedings of the National Academy of Sciences of the United States of America*, **108**, 85-90. http://dx.doi.org/10.1073/pnas.1009830108

[45] Black, B.L. and Olson, E.N. (1998) Transcriptional Control of Muscle Development by Myocyte Enhancer Factor-2 (MEF2) Proteins. *Annual Review of Cell and Developmental Biology*, **14**, 167-196. http://dx.doi.org/10.1146/annurev.cellbio.14.1.167

[46] Roberts, C., Sutherland, H.F., Farmer, H., Kimber, W., Halford, S., Carey, A., Brickman, J.M., Wynshaw-Boris, A. and Scambler, P.J. (2002) Targeted Mutagenesis of the *Hira* Gene Results in Gastrulation Defects and Patterning Abnormalities of Mesoendodermal Derivatives Prior to Early Embryonic Lethality. *Molecular and Cellular Biology*, **22**, 2318-2328. http://dx.doi.org/10.1128/MCB.22.7.2318-2328.2002

[47] Song, T.Y., Yang, J.H., Park, J.Y., Song, Y., Han, J.W., Youn, H.D. and Cho, E.J. (2012) The Role of Histone Chaperones in Osteoblastic Differentiation of C2C12 Myoblasts. *Biochemical and Biophysical Research Communications*, **423**, 726-732. http://dx.doi.org/10.1016/j.bbrc.2012.06.026

[48] Dutta, D., Ray, S., Home, P., Saha, B., Wang, S., Sheibani, N., Tawfik, O., Cheng, N. and Paul, S. (2010) Regulation of Angiogenesis by Histone Chaperone HIRA-Mediated Incorporation of Lysine 56-Acetylated Histone H3.3 at Chromatin Domains of Endothelial Genes. *Journal of Biological Chemistry*, **285**, 41567-41577. http://dx.doi.org/10.1074/jbc.M110.190025

[49] Drane, P., Ouararhni, K., Depaux, A., Shuaib, M. and Hamiche, A. (2010) The Death-Associated Protein DAXX Is a Novel Histone Chaperone Involved in the Replication-Independent Deposition of H3.3. *Genes & Development*, **24**, 1253-1265. http://dx.doi.org/10.1101/gad.566910

[50] Wong, L.H., McGhie, J.D., Sim, M., Anderson, M.A., Ahn, S., Hannan, R.D., George, A.J., Morgan, K.A., Mann, J.R. and Choo, K.H. (2010) ATRX Interacts with H3.3 in Maintaining Telomere Structural Integrity in Pluripotent Embryonic Stem Cells. *Genome Research*, **20**, 351-360. http://dx.doi.org/10.1101/gr.101477.109

[51] Kappes, F., Waldmann, T., Mathew, V., Yu, J., Zhang, L., Khodadoust, M.S., Chinnaiyan, A.M., Luger, K., Erhardt, S., Schneider, R. and Markovitz, D.M. (2011) The DEK Oncoprotein Is a Su(var) that Is Essential to Heterochromatin Integrity. *Genes & Development*, **25**, 673-678. http://dx.doi.org/10.1101/gad.2036411

[52] Corpet, A., De Koning, L., Toedling, J., Savignoni, A., Berger, F., Lemaitre, C., O'Sullivan, R.J., Karlseder, J., Barillot, E., Asselain, B., Sastre-Garau, X. and Almouzni, G. (2011) Asf1b, the Necessary Asf1 Isoform for Proliferation, Is Predictive of Outcome in Breast Cancer. *EMBO Journal*, **30**, 480-493. http://dx.doi.org/10.1038/emboj.2010.335

[53] Staibano, S., Mascolo, M., Mancini, F.P., Kisslinger, A., Salvatore, G., Di Benedetto, M., Chieffi, P., Altieri, V., Prezioso, D., Ilardi, G., De Rosa, G. and Tramontano, D. (2009) Overexpression of Chromatin Assembly Factor-1 (CAF-1) p60 Is Predictive of Adverse Behaviour of Prostatic Cancer. *Histopathology*, **54**, 580-589. http://dx.doi.org/10.1111/j.1365-2559.2009.03266.x

[54] Polo, S.E., Theocharis, S.E., Grandin, L., Gambotti, L., Antoni, G., Savignoni, A., Asselain, B., Patsouris, E. and Almouzni, G. (2010) Clinical Significance and Prognostic Value of Chromatin Assembly Factor-1 Overexpression in Human Solid Tumours. *Histopathology*, **57**, 716-724. http://dx.doi.org/10.1111/j.1365-2559.2010.03681.x

[55] Alekseev, O.M., Richardson, R.T., Tsuruta, J.K. and O'Rand, M.G. (2011) Depletion of the Histone Chaperone tNASP Inhibits Proliferation and Induces Apoptosis in Prostate Cancer PC-3 Cells. *Reproductive Biology and Endocrinology*, **9**, 50. http://dx.doi.org/10.1186/1477-7827-9-50

[56] Gasparian, A.V., Burkhart, C.A., Purmal, A.A., Brodsky, L., Pal, M., Saranadasa, M., Bosykh, D.A., Commane, M., Guryanova, O.A., Pal, S., Safina, A., Sviridov, S., Koman, I.E., Veith, J., Komar, A.A., Gudkov, A.V. and Gurova, K.V. (2011) Curaxins: Anticancer Compounds that Simultaneously Suppress NF-κB and Activate p53 by Targeting FACT. *Science Translational Medicine*, **3**, 95ra74. http://dx.doi.org/10.1126/scitranslmed.3002530

[57] Koman, I.E., Commane, M., Paszkiewicz, G., Hoonjan, B., Pal, S., Safina, A., Toshkov, I., Purmal, A.A., Wang, D., Liu, S., Morrison, C., Gudkov, A.V. and Gurova, K.V. (2012) Targeting FACT Complex Suppresses Mammary Tumorigenesis in *Her*2/*neu* Transgenic Mice. *Cancer Prevention Research*, **5**, 1025-1035. http://dx.doi.org/10.1158/1940-6207.CAPR-11-0529

[58] Garcia, H., Miecznikowski, J.C., Safina, A., Commane, M., Ruusulehto, A., Kilpinen, S., Leach, R.W., Attwood, K., Li, Y., Degan, S., Omilian, A.R., Guryanova, O., Papantonopoulou, O., Wang, J., Buck, M., Liu, S., Morrison, C. and Gurova, K.V. (2013) Facilitates Chromatin Transcription Complex Is an "Accelerator" of Tumor Transformation and Potential Marker and Target of Aggressive Cancers. *Cell Reports*, **4**, 159-173. http://dx.doi.org/10.1016/j.celrep.2013.06.013

[59] Kurki, S., Peltonen, K., Latonen, L., Kiviharju, T.M., Ojala, P.M., Meek, D. and Laiho, M. (2004) Nucleolar Protein NPM Interacts with HDM2 and Protects Tumor Suppressor Protein p53 from HDM2-Mediated Degradation. *Cancer Cell*, **5**, 465-475. http://dx.doi.org/10.1016/S1535-6108(04)00110-2

[60] Grisendi, S., Mecucci, C., Falini, B. and Pandolfi, P.P. (2006) Nucleophosmin and Cancer. *Nature Reviews Cancer*, **6**, 493-505. http://dx.doi.org/10.1038/nrc1885

[61] Haferlach, C., Mecucci, C., Schnittger, S., Kohlmann, A., Mancini, M., Cuneo, A., Testoni, N., Rege-Cambrin, G., Santucci, A., Vignetti, M., Fazi, P., Martelli, M.P., Haferlach, T. and Falini, B. (2009) AML with Mutated *NPM*1 Carrying a Normal or Aberrant Karyotype Show Overlapping Biologic, Pathologic, Immunophenotypic, and Prognostic Features. *Blood*, **114**, 3024-3032. http://dx.doi.org/10.1182/blood-2009-01-197871

[62] Yang, Y.F., Zhang, X.Y., Yang, M., He, Z.H., Peng, N.F., Xie, S.R. and Xie, Y.F. (2014) Prognostic Role of Nucleophosmin in Colorectal Carcinomas. *Asian Pacific Journal of Cancer Prevention*, **15**, 2021-2026.

[63] Wise-Draper, T.M., Morreale, R.J., Morris, T.A., Mintz-Cole, R.A., Hoskins, E.E., Balsitis, S.J., Husseinzadeh, N., Witte, D.P., Wikenheiser-Brokamp, K.A., Lambert, P.F. and Wells, S.I. (2009) DEK Proto-Oncogene Expression Interferes with the Normal Epithelial Differentiation Program. *American Journal of Pathology*, **174**, 71-81. http://dx.doi.org/10.2353/ajpath.2009.080330

[64] Wise-Draper, T.M., Mintz-Cole, R.A., Morris, T.A., Simpson, D.S., Wikenheiser-Brokamp, K.A., Currier, M.A., Cripe, T.P., Grosveld, G.C. and Wells, S.I. (2009) Overexpression of the Cellular DEK Protein Promotes Epithelial Transformation *in Vitro* and *in Vivo*. *Cancer Research*, **69**, 1792-1799. http://dx.doi.org/10.1158/0008-5472.CAN-08-2304

[65] Soekarman, D., von Lindern, M., Daenen, S., de Jong, B., Fonatsch, C., Heinze, B., Bartram, C., Hagemeijer, A. and Grosveld, G. (1992) The Translocation (6;9) (p23;q34) Shows Consistent Rearrangement of Two Genes and Defines a Myeloproliferative Disorder with Specific Clinical Features. *Blood*, **79**, 2990-2997.

[66] Riveiro-Falkenbach, E. and Soengas, M.S. (2010) Control of Tumorigenesis and Chemoresistance by the DEK Oncogene. *Clinical Cancer Research*, **16**, 2932-2938. http://dx.doi.org/10.1158/1078-0432.CCR-09-2330

[67] Jiao, Y., Shi, C., Edil, B.H., de Wilde, R.F., Klimstra, D.S., Maitra, A., Schulick, R.D., Tang, L.H., Wolfgang, C.L., Choti, M.A., Velculescu, V.E., Diaz Jr., L.A., Vogelstein, B., Kinzler, K.W., Hruban, R.H. and Papadopoulos, N. (2011) *DAXX/ATRX*, *MEN*1, and mTOR Pathway Genes Are Frequently Altered in Pancreatic Neuroendocrine Tumors. *Science*, **331**, 1199-1203. http://dx.doi.org/10.1126/science.1200609

[68] Schwartzentruber, J., Korshunov, A., Liu, X.Y., Jones, D.T., Pfaff, E., Jacob, K., Sturm, D., Fontebasso, A.M., Quang, D.A., Tonjes, M., Hovestadt, V., Albrecht, S., Kool, M., Nantel, A., Konermann, C., Lindroth, A., Jager, N., Rausch, T., Ryzhova, M., Korbel, J.O., Hielscher, T., Hauser, P., Garami, M., Klekner, A., Bognar, L., Ebinger, M., Schuhmann, M.U., Scheurlen, W., Pekrun, A., Fruhwald, M.C., Roggendorf, W., Kramm, C., Durken, M., Atkinson, J., Lepage, P., Montpetit, A., Zakrzewska, M., Zakrzewski, K., Liberski, P.P., Dong, Z., Siegel, P., Kulozik, A.E., Zapatka, M., Guha, A., Malkin, D., Felsberg, J., Reifenberger, G., von Deimling, A., Ichimura, K., Collins, V.P., Witt, H., Milde, T., Witt, O., Zhang, C., Castelo-Branco, P., Lichter, P., Faury, D., Tabori, U., Plass, C., Majewski, J., Pfister, S.M. and Jabado, N. (2012) Driver Mutations in Histone H3.3 and Chromatin Remodelling Genes in Paediatric Glioblastoma. *Nature*, **482**, 226-231. http://dx.doi.org/10.1038/nature10833

[69] Lorain, S., Demczuk, S., Lamour, V., Toth, S., Aurias, A., Roe, B.A. and Lipinski, M. (1996) Structural Organization of the WD Repeat Protein-Encoding Gene HIRA in the DiGeorge Syndrome Critical Region of Human Chromosome 22. *Genome Research*, **6**, 43-50. http://dx.doi.org/10.1101/gr.6.1.43

[70] Farrell, M.J., Stadt, H., Wallis, K.T., Scambler, P., Hixon, R.L., Wolfe, R., Leatherbury, L. and Kirby, M.L. (1999) HIRA, a DiGeorge Syndrome Candidate Gene, Is Required for Cardiac Outflow Tract Septation. *Circulation Research*, **84**, 127-135. http://dx.doi.org/10.1161/01.RES.84.2.127

# Review Article

# Histone Variant H3.3 and its Future Prospects in Cancer Clinic

*Divya Reddy[1,2], Sanjay Gupta[1,2]*

From the [1]Epigenetics and
Chromatin Biology Group,
Gupta Laboratory, Cancer
Research Institute, Advanced
Centre for Treatment
Research and Education
in Cancer, Tata Memorial
Centre, Navi Mumbai, [2]Homi
Bhabha National Institute,
Mumbai, Maharashtra, India

## Abstract

Histone variant, H3.3 has been a continuous subject of interest in the field of chromatin studies due to its two distinguishing features. First, its incorporation into chromatin is replication‑ independent, unlike the replication‑ coupled deposition of its canonical counterparts H3.1/3.2. Second, H3.3 has been consistently associated with an active state of chromatin. Apart from this function research in the past few years has also revealed that H3.3 has a central role to play in maintaining the somatic cell identity, for efficient ultraviolet induce DNA damage repair and proper segregation of chromosomes during cell division. Further, the discovery of "driver mutations" on this variant has bought it to limelight in cancer biology to the extent that "oncohistone," a new term has been coined for different mutants of H3.3. Here, we review the functional importance of H3.3 in the context of cancer.

**Key Words:** *Cancer, DNA damage, epigenome, mutation, oncohistone*

## Introduction

Nucleosome, a fundamental unit of chromatin, is made up of 147 bp of DNA wrapped a histone octamer. Histone octamer is formed by two copies each of the four core histones, H2A, H2B, H3, and H4.[1] Although the major functional role of histones is DNA compaction, recent evidence has bought to light that through modulation of the interaction between histones and DNA many cellular processes are governed. This modulation is largely brought about by a repertoire of posttranslational modifications occurring on N‑ terminal tails of histones.[2] However, histone variants the nonallelic subtypes of canonical histones are also known to modulate the chromatin dynamics and thus influencing the activity of the underlying DNA.[3]

## Histone H3 Variants

Replacement with histone variants/isoforms leads to the formation of a nucleosome having distinct functions compared to existing nucleosome with canonical histones inside the cell. For example, H2A.X nucleosome marks the site for recruitment of DNA damage proteins. Similarly, histone H3 variants have differential functions and have been under research focus since a long time. There are four major different H3 histones, H3.3 and CENPA (centromere‑ specific) being the replacement histones and H3.1 and H3.2 the canonical histones [Table 1]. Other than these, few tissue‑ specific H3 variants like H3t (testis‑ specific) and primate‑ specific variants H3.X and H3.Y are also been reported. In the current review, we focus on the histone H3.3 variant, its function in various cellular processes with special emphasis on its role as "oncohistone."

Canonical histone genes are organized into clusters containing multiple gene copies of each core as well as linker histones. In humans, three copies of genes encoding H3.2 are located within a histone cluster on chromosome 1, and ten copies of genes encoding H3.1 are clustered in the chromosome 6. These canonical H3‑ encoding genes are intronless, and their corresponding transcripts are not polyadenylated but rather have a conserved 26 bp stem‑ loop at their 3' ends.[4] The tandem organization of histone genes facilitates their simultaneous expression, thus aiding in the production of massive amounts of histone protein required for genome packaging during S phase. In contrast to the canonical histone H3, histone variant H3.3 genes, namely, H3F3A and H3F3B in humans, lie outside the histone gene clusters on chromosomes 1 and 17 respectively [Figure 1a]. They contain introns, and their mRNAs have poly (A) tails. Unlike canonical H3 which is expressed and incorporated into chromatin at S phase in a replication‑ dependent manner, variant H3.3 is expressed throughout the cell cycle.[5] In yeast, there is only one noncentromeric H3 gene, which encodes an H3.3‑ like protein, suggesting that H3.3 is more conserved than its canonical counterparts. At the protein level, H3.3 differs from the canonical histone H3 at only 4‑ 5 amino acids [Figure 1b]. In humans, H3.3 and H3 differ by residues 87, 89, 90, and 96 in the histone fold domain and residue 31 in the N‑ terminal tail. All these specific residues contribute to the distinct properties of variant H3.3. Amino acid residues 87–90 in H3.1‑ SAVM are replaced by AAIG in H3.3. These changes determine their unique deposition onto chromatin. At the N‑ terminus,

**How to cite this article:** Reddy D, Gupta S. Histone variant H3.3 and its future prospects in cancer clinic. J Radiat Cancer Res 2017;8:77-81.

### Access this article online

**Quick Response Code:**

**Website:** www.journalrcr.org

**DOI:** 10.4103/jrcr.jrcr_4_17

Ala 31 in H3.1 is replaced by Ser in H3.3, which undergoes phosphorylation in the pericentromeric region during mitosis.[6]

## Deposition and Functions of Histone H3.3

Incorporation of canonical H3 variants is mediated by the "histone chaperone" CAF‑1 chromatin assembly complex, and H3.3 is incorporated through a number of different pathways, including the CHD1 and ATRX chromatin remodeling complexes and the HIRA chaperone complex.[7] Ala 87 and Gly 90 in AAIG are important for the recognition of H3.3 by the variant‑specific chaperone death domain–associated protein (DAXX),[8] and G90 is also recognized by ubinuclein‑1, a subunit of the HIRA histone chaperone complex.[7] A study with mouse embryonic

### Table 1: Histone H3 variants: Differential histone chaperones, mutation, and role in cancer

| Mode of Deposition | Histone | Chaperone | Role In Cancer | Mutation |
|---|---|---|---|---|
| Replication Dependent | H3.1 | CAF‑1 | Mutated in pediatric glioma‑ DIPG, thalamic glioma and Chrondroblastoma | H3K27M H3G34V/R/W/L H3K36M |
| | H3.2 | CAF‑1 | NA | NA |
| Replication Independent | H3.3 | HIRA DAXX | Mutated in DIPG, Pediatric glioma and chrondroblastoma Decrease levels in adult glioma Elevated in lung cancer | H3K27M H3G34V/R/W/L H3K36M |
| Centromeric | CENPA | HJURP | Elevated in many cancers | NA |
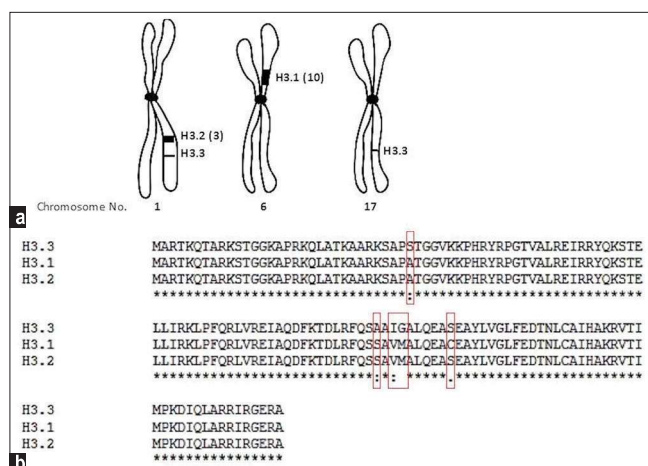


**Figure 1:** Genomic location and sequence differences in H3 variants. (a) Histone H3 variants H3.1, H3.2, and H3.3 are located on chromosomes 6, 1 and 17. H3.3 is encoded by two genes H3F3A and H3F3B located on chromosome 1 and 17, respectively. The numerical in the bracket indicates the number of genes present encoding the protein in the cluster. (b) Protein sequence alignment of H3 variants, H3.1, H3.2, and H3.3. Red highlights the changes amongst them

stem (ES) cells showed that the HIRA complex deposits H3.3 on transcribed genes, while the ATRX complex delivers H3.3 to telomeres and pericentromeric repeats.[9] When incorporated into a nucleosome, H3.3 amasses modifications associated with gene activation or open chromatin – including methylation on K4, K36, and K79 and acetylation on K9 and K14 – and is deprived of suppressive modifications, including K9 and K27 methylations.[2] H3.3‑containing nucleosomes are intrinsically unstable and promote gene activation, especially along with histone H2A.Z incorporation.[10]

H3.3 is highly conserved across metazoans, and its *in vivo* function has been studied in a number of different model organisms. In *Drosophila*, H3.3 is required only for fertility but is dispensable for both embryonic and postnatal. The fertility defects in H3.3‑ null flies can be rescued by ectopic expression of H3.2.[11] In *Xenopus*, HIRA‑ dependent H3.3 depositions are required for early gastrulation and mesodermal marker gene activation, and importantly, H3.2 overexpression cannot rescue the mutant phenotype. H3.3 maintains the somatic epigenetic memory in nuclear transferred *Xenopus* nuclei and supports differentiation of cultured murine muscle precursor cells.[12] In zebrafish, reduced levels of H3.3 in the nuclei leads to defects in cranial neural crest cell differentiation. H3f3b knockout mice also have reduced viability, and surviving adults are infertile.[13] In both ES cells and mouse embryonic fibroblasts, H3.3 loss caused a dramatic increase of mitotic defects indicative of chromosome structure dysfunctions, including anaphase bridges and lagging chromosomes.[14] Cells in which H3.3 has been knocked down are also susceptible to DNA damage.[15] This can be explained by the requirement for H3.3 in a gap‑ filling mechanism to ensure nucleosome replacement in transcriptionally active areas. H3.3 is incorporated at sites of ultraviolet (UV) damage, it protects against sensitivity to UV light and is required to maintain replication fork progression after UV damage.[16] H3.3 may also be important for the restart of transcription following DNA damage since knock down of the H3.3 chaperone HIRA resulted in an impaired recovery of RNA synthesis after UVC damage.[17]

Thus, HIRA‑ dependent incorporation of H3.3 is required for the reprogramming of nuclear transferred murine nuclei, transcriptional recovery after genomic DNA damage in human cancer cell lines, and also for polycomb‑ repressive complex 2 recruitment to bivalent loci in mouse ES cells.[18] Furthermore, somatic mutations in H3.3‑ encoding genes cause various types of cancer in humans, underscoring its role in maintaining tissue homeostasis.

## Role of Histone H3.3 in Genomic Stability and Cancer

With the aid of deep sequencing techniques, more and more mutations are being found in various chromatin‑ associated factors including histones. Histone H3 is found to be mutated at high frequency in several specific cancer types like pediatric high‑ grade glioblastoma (HGG), chondroblastoma and giant cell tumors of the bone.[19,20] The identified missense mutations K27M, G34V/R/W/L, and K36M were found predominantly in the genes encoding H3.3, H3F3A, and

H3F3B, and to a lesser extent in H3.1 genes, HIST1H3B and HIST1H3C. Due to such specificity and high frequency of these mutations they are defined as "Driver mutations" for tumorigenesis.[20]

Somatic mutation of H3 lysine 27 to methionine (K27M) was seen in □30% pediatric HGG tumors. The K27M mutation is most often found in H3F3A (>70%) with a few occurrences in HIST1H3B (□20%) and HIST1H3C. Diffuse intrinsic pontine glioma, a tumor of the pons, has an even higher incidence of K27M, with >70% of tumors sequenced containing the mutation and are particularly deadly, with an approximate age of onset of 8 years and overall survival rates of □10% postdiagnosis.[20,21] Sequencing of H3F3A and H3F3B in more than seventy chrondroblastomas revealed nearly 95% of the tumors harbor lysine 36 to methionine (K36M) substitutions, which mutate the target site for SETD2 and other K36 methyltransferases.[19] Unlike the K27M mutation of glioblastoma, nearly all of the K36M mutations were found in H3F3B (□90%) rather than in H3F3A. Interestingly, histone H3K36Me3 methyltransferase, SETD2 mutations, and H3.3 mutations are mutually exclusive. Giant cell tumors of the bone also have shown a high frequency of H3.3 mutations, with >90% of tumors sequenced containing substitutions of G34 to either tryptophan (G34W) or, in rare cases, leucine (G34 L).[22] Mutations of H3.3 were also observed at low frequency in osteosarcoma (2% containing G34R in H3F3A or H3F3B), conventional chondrosarcoma (1% containing K36M in H3F3A), and clear cell chondrosarcoma (7% containing K36M in H3F3B).[23] Interestingly, although highly prevalent in pediatric glioblastoma, to date, no K27M mutations have been observed in bone or cartilage tumors, and the K36M mutation has not been found in glioblastoma.

The occurrence of K27M, a dominant negative mutation leads to loss of H3K27Me3, a repressive mark and gain in H3K27Ac, an active enhancer associated mark thus leading to the activation of previously silenced genes and thus contributing to tumorigenesis.[24] Nucleosomes harboring either a G34R or G34V mutant H3.3 exhibit reduced H3K36Me2/Me3 levels on the same tail, but have no dominant effect on total cellular H3K36Me2/Me3 levels, however, it is linked to an altered transcriptional status of the cells, with quite widespread changes in RNA polymerase II association.[19] Chicken lymphoma DT40 cells either depleted for histone H3.3 or harboring H3.3 with G34R/V mutation are sensitive to UV due to loss of DNA repair mark H3K36Me3.[22] The presence of mutant H3.3 or aberrantly modified H3 proteins (due to dominant effects of K27M or local effects of G34 mutant H3.3) at key regulatory elements may be critical to alteration of transcriptional programs leading to tumor initiation or progression [Figure 2]. Not only mutations but deregulation of H3.3 levels has also been seen in certain cancers. MLL5 mediated decrease in H3.3 expression favors self-renewal properties of adult glioblastoma (glioblastoma multiforme [GBM]) cells and phenocopies pediatric GBM with H3.3 mutations, indicating potential therapeutic strategies for adult GBM.[25] Furthermore, a recent study has highlighted overexpression H3.3 is associated with lung cancer progression and promotes lung cancer cell migration by activating metastasis-related genes through the occupation of intronic regions.[26]

Histone H3 clipping has been observed in many cellular systems such as embryonic stem cells (hESCs), senescent fibroblasts, melanocytes, and hepatocytes. Analysis of the proteolytic clipping of histone H3 during the differentiation of hESCs revealed that the N-terminal tail of H3 can be cleaved at different sites and is mediated by a serine protease.[27] Notably, it has been suggested that cleaved products of H3 could contribute to regulate genes implicated in cell cycle promotion, DNA replication, cellular proliferation, apoptosis, and migration in senescence. Furthermore, a recent report claims a reduction in H3 clipping activity in cervical cancer cells.[28] However, what still remains a mystery is does this clipping activity has any variant specificity and what
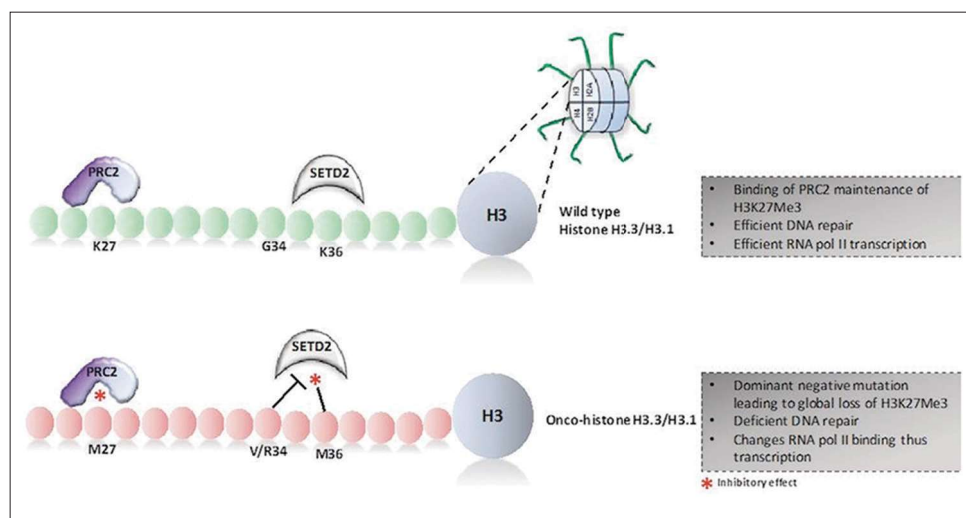


Figure 2: Effect of oncohistone on epigenome of cancer cells. Replacement of wild-type H3 (harboring K27, K36, and G34 residues) with oncohistones (harboring M27, M36, and V/R/W/L34 residues) leads to inhibitory effect on the activity of the writers, polycomb-repressive complex 2 and SETD2 enzymes, thus leading to alteration of epigenome in favor of oncogenesis

are the molecular mechanism through which they mediate oncogenesis.

H3.3 is incorporated into promoters of developmentally regulated genes, and these loci bear both H3K27Me3 and H3K4Me3 marks, marking these promoters as bivalent domains poised for transcriptional induction.[18] H3.3 is required for the establishment of the H3K27Me3 mark in these domains and it is easy to envisage that a switch to K27Ac or possibly K36Me3 either by recruitment of mutated H3.3 or global decrease in H3.3 may tip the balance to activation of aberrant developmental programs leading to tumorigenesis.

# Conclusions

Cancer epigenome as a target for better clinical management gives hope to us all, but more research is required to reveal exciting aspects in coming years. The deposition of H3.3 by HIRA is considered as a mark of transcriptional activity, and its deposition by DAXX at telomeric and a pericentromeric region marks heterochromatin state. Therefore, H3.3 has a bimodal functional role depending on the context, i.e., chromosomal location/chromatin environment. Conclusively, it can be said that H3.3 is a focal point of convergence for most of the epigenomic regulations in various cellular processes. Hence, it does not come as a surprise that H3.3 is mutated or deregulated in a disease like cancer. However, more in‑depth analysis is required before they can be used as a new diagnostic and therapeutic target for cancer.

## ConFlicts oF interest

There are no conflicts of interest.

# References

1. Luger K, Mäder AW, Richmond RK, Sargent DF, Richmond TJ. Crystal structure of the nucleosome core particle at 2.8 A resolution. Nature 1997;389:251‑60.
2. Hake SB, Allis CD. Histone H3 variants and their potential role in indexing mammalian genomes: The "H3 barcode hypothesis". Proc Natl Acad Sci U S A 2006;103:6428‑35.
3. Weber CM, Henikoff S. Histone variants: Dynamic punctuation in transcription. Genes Dev 2014;28:672‑82.
4. Whitfield ML, Zheng LX, Baldwin A, Ohta T, Hurt MM, Marzluff WF. Stem‑loop binding protein, the protein that binds the 3' end of histone mRNA, is cell cycle regulated by both translational and posttranslational mechanisms. Mol Cell Biol 2000;20:4188‑98.
5. Ahmad K, Henikoff S. The histone variant H3.3 marks active chromatin by replication‑independent nucleosome assembly. Mol Cell 2002;9:1191‑200.
6. Hake SB, Garcia BA, Kauer M, Baker SP, Shabanowitz J, Hunt DF, et al. Serine 31 phosphorylation of histone variant H3.3 is specific to regions bordering centromeres in metaphase chromosomes. Proc Natl Acad Sci U S A 2005;102:6344‑9.
7. Elasaesser SJ, Allis CD. Atp‑dependent. HIRA and Daxxconstitute two independent histone H3.3‑containingpredeposition complexes. Cold Spring Harb Symp Quant Biol2010;978‑1936113‑07‑1.
8. Wong LH, McGhie JD, Sim M, Anderson MA, Ahn S, Hannan RD, et al. ATRX interacts with H3.3 in maintaining telomere structural integrity in pluripotent embryonic stem cells. Genome Res 2010;20:351‑60.
9. Filipescu D, Müller S, Almouzni G. Histone H3 variants and their chaperones during development and disease: Contributing to epigenetic control. Annu Rev Cell Dev Biol 2014;30:615‑46.
10. Jin C, Felsenfeld G. Nucleosome stability mediated by histone variants H3.3 and H2A.Z. Genes Dev 2007;21:1519‑29.
11. Wen D, Banaszynski LA, Liu Y, Geng F, Noh KM, Xiang J, et al. Histone variant H3.3 is an essential maternal factor for oocyte reprogramming. Proc Natl Acad Sci U S A 2014;111:7325‑30.
12. Loppin B, Bonnefoy E, Anselme C, Laurençon A, Karr TL, Couble P. The histone H3.3 chaperone HIRA is essential for chromatin assembly in the male pronucleus. Nature 2005;437:1386‑90.
13. Yuen BT, Bush KM, Barrilleaux BL, Cotterman R, Knoepfler PS. Histone H3.3 regulates dynamic chromatin states during spermatogenesis. Development 2014;141:3483‑94.
14. Jang CW, Shibata Y, Starmer J, Yee D, Magnuson T. Histone H3.3 maintains genome integrity during mammalian development. Genes Dev 2015;29:1377‑92.
15. Ray‑Gallet D, Woolfe A, Vassias I, Pellentz C, Lacoste N, Puri A, et al. Dynamics of histone H3 deposition in vivo reveal a nucleosome gap‑filling mechanism for H3.3 to maintain chromatin integrity. Mol Cell 2011;44:928‑41.
16. Frey A, Listovsky T, Guilbaud G, Sarkies P, Sale JE. Histone H3.3 is required to maintain replication fork progression after UV damage. Curr Biol 2014;24:2195‑201.
17. Adam S, Polo SE, Almouzni G. Transcription recovery after DNA damage requires chromatin priming by the H3.3 histone chaperone HIRA. Cell 2013;155:94‑106.
18. Banaszynski, Wen D, Dewell S,Whitcomb S, Lin M, Diaz N, Elsasser S et al. Hira dependent histone H3.3 deposition facilitates PRC2 recruitment at developmental loci in ES cells. Cell 2013;155,107‑120.
19. Lu C, Jain SU, Hoelper D, Bechet D, Molden RC, Ran L, et al. Histone H3K36 mutations promote sarcomagenesis through altered histone methylation landscape.Science, 2016; 352(6287):844‑9.
20. Schwartzentruber J, Korshunov A, Liu XY, Jones DT, Pfaff E, Jacob K, et al. Driver mutations in histone H3.3 and chromatin remodelling genes in paediatric glioblastoma. Nature 2012;482:226‑31.
21. Chan KM, Fang D, Gan H, Hashizume R, Yu C, Schroeder M, et al. The histone H3.3K27M mutation in pediatric glioma reprograms H3K27 methylation and gene expression. Genes Dev 2013;27:985‑90.
22. Behjati S, Tarpey P, Presneau N, Scheipl S, Pillay N, Loo P, et al. Distinct H3F3A and H3F3B driver mutations define chrondroblastoma and giant cell tumor of bone. Nature Genetics,2013;45, 1479‑1482.
23. Joseph CG, Hwang H, Jiao Y, Wood LD, Kinde I, et al. Exomic analysis of myxoid liposarcomas, synovial sarcomas and osteosarcomas. Genes Chromosomes Cancer, 2014;53:15‑24.
24. Weinberg DN, Allis CD, Lu C. Oncogenic mechanisms of histone H3 mutations. Cold Spring Harb Perspect Med 2017;7. pii: A026443.

25. Gallo M, Coutinho FJ, Vanner RJ, Gayden T, Mack SC, Murison A, et al. MLL5 orchestrates a cancer self‑ renewal state by repressing the histone variant H3.3 and globally reorganizing chromatin. Cancer Cell, 2015;28:715‑ 29.

26. Park SM, Choi EY, Bae M, Kim S, Park JB, Yoo H, *et al*. Histone variant H3F3A promotes lung cancer cell migration through intronic regulation. Nat Commun 2016;7:12914.

27. Santos‑ Rosa H, Kirmizis A, Nelson C, Bartke T, Saksouk N, Cote J, *et al*. Histone H3 tail clipping regulates gene expression. Nat Struct Mol Biol 2009;16:17‑ 22.

28. Sandoval‑ Basilio J, Serafin‑ Higuera N, Reyes‑ Hernandez, Serafin‑ Hique ra I, Leija‑ Montoya G, Blanco‑ Morales M, *et al*. Low proteolytic clipping of histone H3 in cervical cancer. J Cancer 2016;7(13): 1856‑ 1860.